THE UNIVERSITY *of* EDINBURGH

Investigation of key non-coding and coding genes in cutaneous melanomagenesis

Yan Xu

Thesis presented for the degree of PhD

The University of Edinburgh

2011

Declaration

I hereby declare that this thesis has been composed by me and it has not been accepted in any previous applications for a degree at this time or at any other university. The work described has been performed by me, except where expressly indicated otherwise. All sources of information have been specifically acknowledged.

Acknowledgements

First and foremost, I would like to express my deepest and sincerest gratitude to my first supervisor, Professor David Melton, for his immense knowledge and enthusiasm. His great patience, understanding and encouragement have provided a good basis for the present thesis. I have also been touched for his all-out efforts to help me out of an unexpected circumstance. Moreover, I am truly grateful to my second supervisor, Jim Selfridge, for his short but unforgettable teaching for the first three months in my PhD life and for his constructive comments throughout this work. The financial support from CSC is also acknowledged.

I would also like to thank the following people that have given me help generously: Professor David Harrison and Susan Farrington who have given instructive suggestions in my committee meetings, Thomas Brenn who helped to identify and mark the specific area on FFPE samples which was very crucial for my PhD project, Bob Morris and Helen Caldwell who helped greatly in sample sectioning, coring and staining, Frances Rae for her experience in macrodissection, Rob Kitchen who helped me to use R language. I owe a big thanks to all those in the Melton lab past and present, particularly Ann-Marie Ritchie, Ewan Brown, Ewan McNeil, Liang Song and Weiling Li who have helped me greatly with too many things to mention.

It is also a pleasure to thank but apologize to other IGMM researchers and laboratory assistants not mentioned here specifically for their equally important help and contributions. My many thanks are given to PhD students and friends as well for making my life in Edinburgh more than colourful.

Finally, I am indebted to my family, especially to my beloved husband Kailai Yan and my parents. Without their continued love and self-sacrifices it would not have been possible for me to finish this thesis.

Table of contents

List of figures

List of tables

Abstract

Cutaneous melanoma is associated with significant morbidity and mortality representing the most significant cutaneous malignancy. As it is known that early diagnosis and treatment are the most efficient approaches to cure cutaneous melanoma, an improved understanding of the molecular pathogenesis of melanoma and exploration of more reliable molecular biomarkers are particularly essential. Two different types of molecular biomarker for melanoma have been investigated in this thesis.

microRNAs (miRNAs) are single-stranded RNA molecules of 20-23 nucleotides in length that are found in both animal and plant cells. miRNAs are involved in the RNA interference (RNAi) machinery to regulate gene expression posttranscriptionally. miRNAs have important roles in cancer: by controlling the expression level of their target genes they can affect cell signalling pathways and have been shown to have both prognostic and therapeutic potential. Importantly for melanoma research, reproducible miRNA expression profiles from formalin-fixed paraffin-embedded (FFPE) tissues can be obtained that are comparable to those from fresh-frozen samples.

The aims of the miRNA project were: first, to identify a melanoma-specific miRNA expression profile; secondly, to investigate roles of some of the melanoma-specific miRNAs identified in melanomagenesis. Using miRNA microarray on FFPE samples, I obtained a melanoma-specific miRNA expression profile. 9 of these differentially expressed miRNAs between benign naevi and melanomas (7 downregulated, 2 upregulated in malignancies) were verified by qRT-PCR and the functions of four of these miRNAs were studied. Ectopic overexpression of miR-200c and miR-205 in A375 melanoma cells inhibited colony forming ability in methylcellulose, an *in vitro* surrogate assay for tumourigenicity. Moreover, elevation of miR-200c resulted in increased expression levels of E-cadherin through negative regulation of the zinc finger E-box-binding homeobox 2 (ZEB2) gene. Ectopic overexpression of miR-211 in A375 melanoma cells repressed both colony formation

in methylcellulose and migratory ability in matrigel, an *in vitro* surrogate assay for invasiveness. These findings indicate that miR-200c, miR-205 and miR-211 act as tumour suppressors in melanomagenesis.

The second biomarker investigated, mutated BRAF, has been seen in 50-70% of spontaneous cutaneous melanoma. The commonest mutation in melanoma is a glutamic acid for valine substitution at position 600 (V600E). Oncogenic BRAF controls many aspects of melanoma cell biology. The aim of this part of the work was: firstly, to study BRAF V600E mutation status in our melanoma tissue microarray (TMA) panel; secondly, to correlate this mutation to various clinico-pathological features and evaluate its prognostic value through statistical analyses. BRAF V600E mutations were seen in 20% of the primary and 69% of the metastatic melanomas, respectively. More BRAF V600E mutations were seen in males relative to females. The mutation was also related to cell pigmentation, but not to age, ulceration or solar elastosis. Melanoma patients with the BRAF V600E mutation relapse earlier than patients without this mutation. However, no significant association between the BRAF V600E mutation and overall survival and melanoma specific survival was found.

Abbreviations

~	approximate
ºC	degrees Celsius
ml	millilitre
mg	milligram
mm	millimeter
ng	nanogram
ul	microlitre
ug	microgram
um	micrometer
v/v	volume against volume
w/v	weight against volume

6-4 PP	6-4 pyrimidone photoproducts
A	Adenosine
ACTH	Adrenocorticotropic hormone
ADARs	Adenosine deaminases acting on RNAs
Ago2	Argonaute-2
AJCC	American Joint Committee of Cancer
AM	Acral melanoma
AMO	Anti-miRNA oligonucleotides
AREs	AU-rich elements
ASIP	Agouti signalling peptide
bp	Base pair
BRN2	POU domain, class 3, transcription factor 2
B-CLL	B cell lymphocytic leukaemia
C	Cytidine
Cadherin	Calcium-dependent adhesion
CCND1	Cyclin D1
CD1	Cluster of differentiation 1
CDK2	Cyclin-dependent kinase 2

CDKN2A	Cyclin-dependent kinase inhibitor 2A
CKI	Cyclin-dependent kinase inhibitors
CPD	Cyclobutane pyrimidine dimers
CREB	cAMP response element-binding
DGCR8	DiGeorge critical region 8, or Pasha
dsRNA	Double-stranded RNA
E-cadherin	Epithelial cadherin
ECM	Extracellular matrix
EMT	Epithelial to mesenchymal transition
EORTC	European Organisation for Research and Treatment of Cancer
ERK	Extracellular-signal-regulated kinase
ET1	Endothelin-1
FACS	Fluorescence-activated Cell Sorting
FAK	Focal adhesion kinase
FC	Fold change
FDA	Food and Drug Administration
FFPE	Formalin fixed paraffin embeded
FRET	Förster Resonance Energy Transfer
FXR1	Fragile X mental retardation—related protein1
G	Guanosine
GIST	Gastrointestinal stromal tumours
GSK3	Glycogen synthase kinase-3
HCC	Hepatocellular carcinoma
HD-IL2	High dose interleukin-2
HIF-1α	Hypoxia inducible factor -1α
HOXD1	Homeobox protein Hox-D1
I	Inosine
IHC	Immunohistochemistry
ISH	*in-situ* hybridization
JAK/STAT	Janus kinase/signal transducer and activator of transcription
KEGG	Kyoto Encyclopaedia of Genes and Genomes
LATS2	Large tumour suppressor homolog 2

LDH	Lactate dehydrogenase
LMM	Lentigo maligna melanoma
LNA	Locked nucleic acid
lncRNA	Long non-coding RNA
LOX	Lysyl oxidase
MAPK	Mitogen-activated protein kinase
MART-1	Melan-A/Melanoma Antigen Recognised by T cells
MC1R	Melanocortin 1 receptor
MECP/MBD	Methyl-CpG-binding domain proteins
MEK	Mitogen-activated protein kinase kinase
MET	Mesenchymal to epithelial transition
metastamiR	Metastasis-related miRNA
MIB-1	Mindbomb homolog 1
miRNA	microRNA
MITF	Microphthalmia-associated transcription factor
MMP-2	Matrix metalloproteinase 2
MSH (R)	Melanocyte-stimulating hormone (receptor)
MSO	microRNA specific oligo
mTOR	mammalian target of rapamycin
ncRNA	non-coding RNA
N-cadherin	Neural-cadherin
NCCs	Neural crest cells
NER	Nucleotide excision repair
NFAT5	Nuclear factor of activated T-cells 5
NF- κB	Nuclear factor kappa B
NGS	Next generation sequencing
NM	Nodular melanoma
NO	Nitric oxide
NSCLC	Non-small cell lung cancer
nt	Nucleotide
Oct3/4	Octamer-binding transcription factor 3/4
oncomiR	Oncogenic miRNA

OS	Overall survival
PACT	Protein activator of PKR
PAP	Poly A polymerase
PASR	Promoter-associated small RNAs
P-Cadherin	Placental-cadherin
PCR	Polymerase chain reaction
PI3K	Phosphoinositide 3-kinase
piRNA	PIWI-interacting RNAs
PKB	Protein kinase B
pre-miRNA	Precursor microRNA
pri-miRNA	Primary microRNA
PPP2R2A	Protein phosphatase 2 regulatory subunit B alpha isoform
PTEN	Phosphatase and tensin homolog
RAS	Rat Sarcoma
RFLP	Restriction fragment length polymorphism
RHOC	RAS homolog gene family member C
RISC	RNA-induced silencing complex
RLC	RISC loading complex
RNASEN	RNase III enzyme Drosha
RNAi	RNA interference
ROS	Reactive oxygen species
SA-PMPs	Streptavidin-conjugated paramagnetic particles
SE	Solar elastosis
siRNA	Small-interfering RNA
SLITRK1	SLIT and NTRK-like protein 1
SMG	Scottish Melanoma Group
snoRNA	Small nucleolar RNA
SNP	Single nucleotide polymorphism
snRNA	Small nuclear RNA
SOX2	Sex determining region Y-box 2
SRB	Sulforhodamine B
SSM	Superficial spreading melanoma

ssRNA	Single-standed RNA
STDEV	Standard deviation
T	Thymidine
T-ALL	T cell acute lymphoblastic leukaemia
TCA	Trichloracetic acid
TGF-ß	Transforming growth factor beta
TIMPs	Tissue inhibitor of metalloproteinases
tiRNA	Transcription initiation RNAs
TMA	Tissure microarray
TNF- α	Tumour necrosis factor-α
TRBP	Tar RNA binding protein
TRPM1	Melastatin 1
TWIST1	Twist homolog 1
UTR	Untranslated region
UVR	Ultraviolet radiation
VEGF	Vascular endothelial growth factor
XP	Xeroderma pigmentosum
XPO5	Exportin-5
ZEB1/2	Zinc finger E-box binding homeobox 1/2

Chapter 1: Introduction

1.1 Cutaneous melanoma

Melanoma is a malignant tumour of melanocytes, which are pigment producing cells found predominantly in skin. Melanoma is one of the rare types of skin cancer, but causes the majority of skin cancer related deaths. The underlying mechanism of transformation of melanocytes to melanoma is a complex biological process involving a large number of genetic and environmental factors.

1.1.1 Introduction to melanocytes and effects of ultraviolet radiation

The skin of all mammals is pigmented, and while the intensity and hue of this pigmentation may vary with genetic and environmental factors, in all cases it results from the accumulation of heterogeneous polycyclic polymers known as melanins. The capacity to synthesize these compounds is restricted to ~5% of skin cells that have a common embryological origin and a distinct morphology and are thus considered to be a unique cell-type: the melanocytes [1]. During embryonic development, an epithelial- mesenchymal transition (EMT) involving epithelial cells of the neuroectoderm gives rise to migratory neural crest cells [2]. Neural crest cells (NCCs) are a transient, multipotent migratory cell population and are unique to vertebrates. The premigratory neural crest cells dissociate from the neural folds, become motile, and disperse to the different parts of the embryo, where they undergo further differentiation that gives rise to diverse cell lineages including melanocytes, craniofacial cartilage and bone, smooth muscle, peripheral and enteric neurons and glia. Melanocytes differentiate from their precursor cells—melanoblasts within the neural crest. By week 8 *in utero*, human melanocytes begin to migrate first to the dermis, and hence, to the stratum basale of the epidermis. Alternative paths also lead them to hair follicles or to the uveal tract of the eye and the retina. Melanocytes are relatively large, clear, dendritic cells that lack tonofilaments and desmosomes. They are distinguishable by their many dense, membrane-bound, spherical or ovoid organelles called melanosomes, occurring throughout the cytoplasm and associated

with a microtubule network extending into the dendritic arms. In some melanocytes, the melanosomes remain static within the cell. In other types of melanocyte, the cell can extend its surface as long pseudopodia carrying melanosomes away from the centre of the cell and increasing the cell's effectiveness in absorbing light. This extension happens slowly in dermal melanocytes in response to ultraviolet radiation (UVR) as well as in the production of new melanosomes and increased “donation” of melanosomes to adjacent keratinocytes. Keratinocytes may engulf the end of the melanocyte pseudopodia, which contains many melanosomes. Cytoplasmic dynein will carry the vesicles containing the melanin to the centre of the cell. This causes melanosomes to become sequestered around the keratinocyte's nucleus, providing optimal protection from UVR.

The skin relies on melanocytes to provide photoprotection and thermoregulation by producing melanin. There are two main types of melanin: yellow/red pheomelanin and brown/black eumelanin [3]. Both types of melanin derive from a common tyrosinase-dependent pathway with the same precursor, tyrosine. Individual melanocytes can produce both types of melanin with the ratio dependent on the expression of pigment enzymes and the availability of tyrosine and sulphydral-containing reducing agents in the cell [4]. Eumelanin is found in hair, areola, and skin, and colours hair grey, black, and brown. In humans, it is more abundant in people with dark skin. Pheomelanin is also found in hair and skin and is present in both lighter-skinned and darker skinned humans. Pheomelanin imparts a pink to red hue and, is found in particularly large quantities in red hair and freckled populations. Eumelanin and pheomelanin differ not only chemically but also in their physical properties. Pheomelanin is less efficient at protecting the skin against UVR-induced DNA damage. When UV irradiated, pheomelanin also produces more free radicals than those produced by eumelanin [5, 6]. Moreover, pheomelanin pigments have been suggested to enhance intrinsic DNA damage in cells, particularly in response to UVR [7, 8]. Therefore, pheomelanin may actually contribute to UV-induced skin damage rather than merely produce less protection against UVR [5, 6].

The melanocortin 1 receptor (MC1R), also known as melanocyte-stimulating hormone receptor (MSHR), melanin-activating peptide receptor, or melanotropin receptor, is a G protein-coupled receptor which binds to a class of pituitary peptide hormones known as the melanocortins, which include adrenocorticotropic hormone (ACTH) and the different forms of melanocyte-stimulating hormone (MSH). MC1R is one of the key proteins involved in regulating mammalian skin and hair colour. It is located on the plasma membrane of melanocytes. It works by controlling the type of melanin being produced and its activation causes the melanocyte to switch from generating the yellow/red pheomelanin by default to the brown/black eumelanin. When activated by one of the variants of MSH, typically α-MSH, MC1R initiates a complex signalling cascade that leads to the production of the brown/black pigment eumelanin. In contrast, the receptor can also be antagonized by agouti signalling peptide (ASIP), which reverts the cell back to producing the yellow/red pheomelanin. MC1R is a conserved and representative locus and major determinant of pigment phenotype [9]. MC1R variants are found related to increased risk of melanoma and non-melanoma skin cancer, independently of skin pigment [7, 10].

Although melanin absorbs much UVR, melanocytes can survive considerable genotoxic stress from UVR-induced DNA damage through DNA repair, by which a cell identifies and corrects damage to the DNA molecules that encode its genome. A cell that has accumulated a large amount of DNA damage, or one that no longer effectively repairs damage incurred to its DNA, can enter one of three possible states: senescence, apoptosis and unregulated cell division—carcinogenesis. Absorption of UVR produces two predominant types of DNA damage, cyclobutane pyrimidine dimers (CPD) and pyrimidine (6-4) pyrimidone photoproducts (6-4PP). Unrepaired UV-induced DNA damage can lead to transition mutations of cytidine-thymidine (C-T) and CC-TT [11], which are the most frequent mutations of p53 in both human and mouse skin cancers [12]. After UV exposure, cells activate p53 and stall the cell cycle for repair [13, 14]. If the damage is too severe, the cell will trigger apoptosis to get rid of a DNA damaged, potentially mutant cell [15]. The UVB-induced DNA lesions, CPD and 6-4PP, show differential biological effects with respect to the induction of apoptosis and cell cycle arrest. It was suggested that the 6-

4 PP lesion is more potent in the induction of UV-induced apoptosis while the CPD lesion appears to be more potent in the induction of cell cycle arrest [16]. Moreover, You *et al.* have documented that CPD lesions account for the majority of UV-induced mutations in mammalian cells. The more potent apoptosis-inducing activity of 6-4PP lesions may induce apoptosis and eradicate the damaged cell, thus removing its carcinogenic potential [17].

Nucleotide excision repair (NER) is one of the major repair systems for removal of DNA lesions. The NER pathway mainly repairs UV-induced DNA damage, and is also active against a broad range of endogenously generated oxidative lesions [18, 19]. Physiologically, the NER pathway excises damaged nucleotides, along with adjacent undamaged DNA. Studies on the human inherited disease, xeroderma pigmentosum (XP) identified NER deficiency as a dramatic genetic risk factor for melanoma [20], and NER-deficient XP patients develop numerous skin cancers under UV exposure, including a 2000-fold higher incidence of melanoma and non-melanoma skin cancer as compared to repair-proficient individuals [21, 22].

UVR causes genetic changes in the skin, impairs cutaneous immune function, increases the local production of growth factors, and induces the formation of DNA-damaging reactive oxygen species that influence keratinocytes and melanocytes [23, 24]. The initial detection of genomic damage that occurs within the melanocytes is termed direct sensitivity to DNA damage, while a response that is elicited from the melanocyte via paracrine messaging is indirect sensitivity. In response to UVR, keratinocytes produce larger amounts of endothelin-1 (ET1), α-MSH, and nitric oxide (NO). The first stimulates nearby melanocytes to proliferate, and all three stimulate melanogenesis [25-27]. NO also reduces the adhesion of melanocytes to the extracellular matrix, an effect that may bear on the increased dendriticity seen, and may also have implications for melanoma metastasis [28].

1.1.2 Melanoma epidemiology, classification, aetiology, and prevention

The incidence of cutaneous melanoma has continued to increase over the last 30 years in most white populations [29, 30]. In the UK in 2008, almost 11,800 cases of malignant melanoma were diagnosed and melanoma is the 6th most common cancer overall in the UK [31]. Within the UK, Scotland has the highest melanoma incidence, surpassing incidence rates in the US. Unlike most cancers, melanoma has a tendency for presentation at younger ages and is now the second most common malignancy in young people aged 15-34 in the UK [32].

The mean age of presentation with melanoma is about 55 years, but this may vary according to melanoma thickness and histological subtype [33]. Cutaneous melanoma is usually divided into four clinico-pathological subtypes: Acral melanoma (AM), Lentigo maligna melanoma (LMM), Nodular melanoma (NM) and Superficial spreading melanoma (SSM) [34]. AM tends to be found on the palms of the hands, the soles of the feet and in the nail bed and is not associated with UV exposure. NM and LMM tend to affect older individuals, whereas SSM, is by far the commonest form, is usually thinner and seen in younger individuals. The most common sites for women and men are the legs and the trunk, respectively. Site differences according to sex are likely to reflect genetic differences as naevi are also differently distributed between boys and girls from an early age [35].

The major risks for cutaneous melanoma are thought to be the interplay between the key environmental factor—sun exposure and genetic factors. To date, the risk factors have been identified as: history and pattern of sun exposure, hair and skin colour, multiple naevi, family history and hormonal factors.

Sunlight exposure represents the key environmental factor as described by the higher incidence of melanoma in Australia and other sunny parts of the US and Europe [30]. Interestingly, a meta-analysis of melanoma case-control studies found low relative risks associated with various measures of exposure to UVR, and the relation to sunshine was not dose dependent [36]. In contrast to non-melanoma skin cancer

which is linked to total lifetime sun exposure, melanoma development is most closely associated with intense, intermittent sun exposure [37]. Epidemiologic observations suggest that chronic or low-grade exposures to UV induce protection against DNA damage, whereas intense and intermittent exposures cause genetic damage [24]. Moreover, the incidence of sunburn during early childhood is particularly important [36]. Likewise, the link between sunbed usage and melanoma is controversial [38-41]. However, it is recommended to avoid sunbed use to protect against premature skin aging [41].

Light-skinned and red haired individuals exhibit higher risk of developing melanoma than those with darker skin and hair. Polymorphisms in the MC1R gene have been linked to fair skin and red hair and have been associated with an increased risk of melanoma [42, 43].

Moreover, it is found that an individual who has more than 100 common naevi or more than two atypical naevi has a 5-fold to 20-fold increased risk of melanoma [44], indicating that a most powerful genetic risk factor for melanoma is the number of naevi. 5% to 10% of melanoma patients have family history [45] and about 25%-40% of all families with melanoma have been linked to mutations in the cyclin-dependent kinase inhibitor, CDKN2A, gene on chromosome 9p21 [46].

Interestingly, women usually have thinner tumours and survive melanoma better than men even after adjustment for Breslow thickness (also Breslow depth, see Page 8) ulceration, and body site, which suggests that there may be X linked variable gene expression or hormonal factors affecting melanoma survival [45].

In the 1980's, health education campaigns aimed at primary prevention for melanoma by reducing sun exposure to people commenced in Australia and were soon adopted worldwide. There is as yet no direct evidence showing that reducing sun exposure has an effect on melanoma incidence. On the contrary, drastic reduction of sun exposure may be detrimental since it can prevent synthesis of adequate levels of vitamin D in the skin, which protects against inflammation,

cancer, psychiatric and autoimmune diseases [45]. So an important message for preventing melanoma would be to avoid sunburn and excessive sun exposure without protection instead of keeping away from the sun altogether. More importantly, secondary prevention—early identification and treatment, is a more efficient way, as tumours are highly visible with a good prognosis if detected early [45].

1.1.3 Melanoma diagnosis and staging

Guidelines written by Roberts *et al.* suggested that suspicious melanocytic lesions should be excised completely, with a clinical margin of 2mm of normal skin and a cuff of fat [47] so that accurate pathological diagnosis can be made from the examination of the entire lesion.

Primary melanoma staging is based on the histological features of the lesion. Accurate staging allows more precise classification, determines more appropriate treatment and improves the accuracy of predicting the likely prognosis and outcomes for melanoma patients. The updated American Joint Committee of Cancer (AJCC) staging (2010, 7th edition) for cutaneous melanoma (Table 1.1) considers localized melanoma, tumour thickness, the microscopic ulceration and rate of mitoses [48]. Breslow depth, used for describing tumour thickness, is used as a prognostic factor in melanoma of the skin (Also discussed in Chapter 1.1.4). It is a description of how deeply tumour cells have invaded. It is one of the cornerstones of the current AJCC TNM staging of malignant melanoma. A large study validated the importance of Breslow depth as one of the three most important prognostic factors in melanoma (the others being T stage and ulceration) [49]. Breslow depth is also used to predict the risk for lymph node metastasis, with deeper tumours being more likely to involve the nodes [50]. Ulceration is found in 20-25% of all melanomas and is more commonly seen in male patients. Mitotic rate was examined for the first time in the new staging system [48]. The Melanoma Staging Committee recommended that mitotic rate be determined by the “hot spot” approach and expressed as the number of mitoses per mm^2 of primary tumour [48].

Classification	Breslow Thickness	Ulceration Status/Mitoses
T		
Tis	N/A	N/A
T1	≤ 1.00	a: without ulceration and mitosis < 1/mm^2
		b: with ulceration or mitosis ≥ 1/mm^2
T2	1.01-2.00	a: without ulceration
		b: with ulceration
T3	2.01-4.00	a: without ulceration
		b: with ulceration
T4	> 4.00	a: without ulceration
		b: with ulceration
N	No. of Metastatic Nodes	Nodal Metastatic Burden
N0	0	N/A
N1	1	a: Micrometastasis
		b: Macrometastasis
N2	2-3	a: Micrometastasis
		b: Macrometastasis
		c: In transit metastases /satellites with metastatic nodes
N3	4+ metastatic nodes, Matted nodes, In transit metastases /satellites with metastatic nodes	
M	Site	Serum LDH
M0	No distant metastases	N/A
M1a	Distant skin, Subcutaneous, Nodal metastases	Normal
M1b	Lung metastases	Normal
M1c	All other visceral metastases	Normal
	Any distant metastases	Elevated

Table 1.1 AJCC TNM staging system 7th edition (2010): TNM categories. N/A: Not applicable. Micrometastasis: Diagnosed after sentinel lymph node biopsy. Macrometastasis: Defined as clinically detectable nodal metastasis. LDH: Lactate dehydrogenase.

There are some differences between the 6th (2002) edition and the 7th (2010) edition of the melanoma staging system. Comparisons in staging for localized melanoma (Stage I/ II), recommendations for using primary melanoma thickness and primary tumour ulceration in TNM categories and stage groupings in the 7th edition remain unchanged. Mitotic rate is first used in the new staging system. Multiple thresholds of mitotic rate were identified and the most significant correlation with survival was at a threshold of at least 1/mm^2 [48]. Data from the AJCC Melanoma Staging Database showed a highly significant correlation between increasing mitotic rate and declining survival rates. In a multifactorial analysis of 10,233 patients with clinically localized melanoma, mitotic rate was the second most powerful predictor of survival, after tumour thickness [48]. In staging for regional metastatic melanoma (stage III), immunohistochemical (IHC) detection of micrometastases is included in the new system as it is considered acceptable to classify nodal metastases solely on the basis of IHC staining of melanoma-associated markers (HMB-45, Melan-A/MART1). Finally, in staging for distant metastatic melanoma (stage IV), the updated AJCC staging system demonstrated that an elevated serum lactate dehydrogenase (LDH) level is an independent and highly significant outcome predictor for stage IV disease. A precise staging system is very important in melanoma diagnosis and prognosis since it determines any following treatment. The current overall survival rates for melanoma patients at the different TNM stages are shown in Table 1.2.

Stage	TNM Classification	5 Year OS (%)	10 Year OS (%)
IA	T1aN0M0	95.3	87.9
IB	T2aN0M0	90.9	83.1
	T1bN0M0		
IIA	T3aN0M0	78.7	63.8
	T2bN0M0		
IIB	T4aN0M0	67.4	53.9
	T3bN0M0		
IIC	T4bN0M0	45.1	32.3
IIIA	T1-4aN1aM0	69.5	63
	T1-4aN2aM0		
IIIB	T1-4aN1bM0	52.8	37.8
	T1-4aN2bM0		

	T1-4bN1aM0		
	T1-4bN2aM0		
	T1-4aN2cM0		
IIIC	T1-4bN1bM0	26.7	18.4
	T1-4bN2bM0		
	T1-4a/bN3M0		
IV	Any T any N M1a-1c	9.5	6.0

Table 1.2 AJCC TNM stages with 5 year and 10 year overall survival rates of melanoma patients. OS: Overall survival. Adapted from [49, 51].

1.1.4 Diagnostic and prognostic markers in melanoma

Histological examination of skin biopsies is still the gold standard for melanoma diagnosis [52]. However, it is a challenging task largely due to the wide morphological spectrum of cutaneous melanocytic tumours and lack of firm diagnostic criteria. In a recent study, there was only 55% agreement for difficult melanocytic lesions between two experts with significant, high level disagreement in 25% cases [53]. Under or over diagnosis can result in therapy failure or unnecessary melanoma treatment and large medical expenses.

The clinical prognostic markers identified so far include anatomical site, gender and age. Tumours located on the trunk, head or neck tend to be thicker indicating poorer outcomes. Survival rates are generally higher for females and the young. These clinical markers offer only rough prognostic estimation. The histological markers include depth of invasion and ulceration. Depth of invasion (Clark level) and tumour thickness (Breslow depth) are the most important parameters in melanoma prognosis. The Clark level describes how far a melanoma has penetrated into the skin. The Clark level of a melanoma uses a scale of I to V (with higher numbers indicating a deeper melanoma). The Breslow system is divided into four thickness integers: < 1mm, 1-2mm, 2-4mm, >4mm. Generally, the lower the Clark level and the thinner the melanoma is, the better the prognosis. It is found that much of the rise in melanoma incidence can be attributed to very thin melanoma lesions or melanomas

in situ, neither of which are easily diagnosed [45]. Moreover, the Clark level is no longer recommended as a staging criterion in the 7th AJCC staging system and has prognostic significance only in patients with very thin (Breslow depth <1 mm) melanomas [48]. No molecular biomarker is used in the 7th edition staging system.

Few biomarkers have been proven to have clinical significance in melanoma. Proliferation markers, such as Mindbomb homolog 1 (MIB-1) and Cyclin D1 (CCND1), and tumour suppressors, such as $p16^{INK4A}$ and p53, as well as anti-apoptotic proteins, such as Bcl-2, have been applied in the clinical setting [52]. However, these biomarkers have prognostic value rather than diagnostic benefit as abnormalities of these proteins are seen only in a subset of melanomas and are most pronounced only in advanced melanoma. Moreover, although most recently, the presence of specific gene copy number changes or mutations have proved useful in distinguishing between certain benign lesions and their malignant equivalents (e.g. Spitz naevi from spitzoid melanoma by 7p gain and HRAS mutation), no single genetic change has been informative over a wide range of lesion types [54]. Moreover, studies with such techniques are limited in their clinical application as they are technically challenging, costly and reliable interpretation requires experience and skill.

There is an urgent need for molecular biomarkers to assist histological diagnosis and provide accurate prognosis. To be clinically useful, these markers need to be technically easy and readily available for use on formalin-fixed and paraffin-embedded (FFPE) tissue using routine methods, such as immunohistochemistry (IHC) or *in situ* hybridization (ISH), which allow high throughput analysis.

1.1.5 Melanoma management

1.1.5.1 Sentinel lymph node biopsy

Sentinel lymph node biopsy is used in the staging of certain types of cancer to see if

they have spread to any lymph nodes, since lymph node metastasis is one of the most important prognostic signs. The procedure offers powerful prognostic information. Microscopic lymph node involvement is becoming an integral part of the AJCC staging system [55]. The AJCC Melanoma Staging Committee recommends that sentinel lymph node biopsy be performed as a staging procedure in patients for whom the information will be useful in planning subsequent treatments and follow-up regimens [48].

1.1.5.2 Current treatment

Treatment of melanoma that has not spread beyond the original area of growth (especially if it is thin and has not invaded the primary dermis) is highly effective, and most of these cancers can be cured mainly by surgery. However, therapy for distant metastatic melanoma is usually unsatisfactory, reinforcing the importance of early diagnosis and therapy.

By bearing in mind the clinical examination rules: Asymmetry of a lesion, Border irregularity, Colour change and Diameter greater than 6mm, also called the ABCD system of diagnosis [56], most melanomas can be identified from normal moles. Standard treatment for early melanoma (Stage I) patients is to remove the tumour tissue locally with or without wide local excision depending on the substage.

For medium melanoma (Stage II and III) patients with high risk of recurrence and distant metastatic potential, adjuvant treatments, a combination of surgery, chemo/radiotherapy and biological treatment, increase the chance of cure. However, the only drug that has been shown reproducibly to have some effect on patient outcome in large randomised trials is high dose intravenous interferon-α [57]. Preliminary results of the European Organisation for Research and Treatment of Cancer (EORTC) showed a significant improvement in relapse-free survival but not in distant metastasis-free survival or overall survival by interferon-α treatment for stage III melanoma patients [58]. There is currently no accepted standard adjuvant

treatment in the UK including high dose of interferon, so melanoma patients are referred instead to enter into clinical trials [59].

In the UK, only 7 to 19% patients whose melanoma has spread to distant lymph nodes or other parts of the body will live for more than 5 years [60]. Patients with metastases have a median survival of 6-9 months [55]. The treatment for these advanced melanoma (Stage IV) patients is inefficient. So far, no intervention has been shown to have significant effect on overall survival for these metastatic melanoma patients. Darcarbazine and high dose interleukin-2 (HD-IL2) are the only drugs approved by the Food and Drug Administration (FDA) in treating metastatic melanoma patients [61]. However, the clinical response rates are only ~10% and ~16%, respectively and both have high toxicity [62, 63]. The combinatorial approaches, including multiagent chemotherapy and bio/chemotherapy regimens, have failed to improve outcomes for advanced melanoma patients [64]. Surgery is used for treatment of local recurrences and for metastatic disease in regional lymph nodes and can also be helpful for patients with surgically resectable disease in up to 3 visceral sites.

Advances in understanding the molecular pathology of melanoma and in immunotherapeutics therefore provide hope for future enhancements in the treatment of advanced melanoma and in the adjuvant setting for patients at a high risk of recurrence.

1.1.6 Genetic and environmental interactions in melanoma progression

Although the tanning response to UVR appears dose-dependent, the nature of the exposure is also a factor that is relevant to induction of cutaneous melanoma. It has been interpreted that chronic and low-grade exposures to UVR induce protection against DNA damage, whereas intense, intermittent exposures causes genetic changes in melanoma pathogenesis [24]. The Clark model describes the histological changes that accompany the progression from normal melanocytes to malignant

melanoma [65], although it is losing its prognostic value. To better illustrate the alterations in molecular and environmental interactions, I show the Clark model along with the phenotypic and relevant molecular changes (Figure 1.1). Through Figure 1.1 it is clear that different biological activities and several key genetic changes occur relative to individual phases of the Clark model. The following discussions will focus on some of the key genes involved and their signalling pathways. Figure 1.3 (see Page 24) is a simple map of the key regulators and signalling pathways involved in melanomagenesis that offers a guide to the signalling networks of melanoma.

1.1.6.1 Mutations in the MAPK pathway

In the Clark model, the first phenotypic alteration in melanocytes is the development of benign naevi (Figure 1.1). The growth control in this stage is disrupted but growth of naevi is also limited—a naevus rarely develops to cancer [65]. Most naevi are growth arrested and express many markers of senescence. BRAF mutations (see next paragraphs) are often already present in benign naevi. These activated oncogenes are thought to trigger senescence (oncogene-induced senescence) [66]. The oncogene-induced senescence is probably the reason for the absence of progression from naevus to melanoma [67].

The RAS/RAF/MEK/ERK (the mitogen-activated protein kinase, MAPK) pathway regulates most important biological programmes, including proliferation, differentiation, angiogenesis and cell survival. In physiological situations, the MAPK pathway is stimulated after the interaction of growth factors with surface receptors and the transmission of these signals through the small GTPase, RAS [68]. RAS activates a number of downstream effectors, one of which is the RAF family of serine/threonine kinases. There are three isoforms of RAF, namely, ARAF, BRAF and CRAF. Once activated, RAF stimulates the MAPK cascade, resulting in the sequential activation of MEK1 and MEK2, which in turn activate ERK1 and ERK2

[69, 70]. The activated ERKs finally stimulate cytoplasmic targets or migrate to the nucleus, where they phosphorylate transcription factors.

In most melanoma cells, the situation is different. It has been shown that >90% of melanoma specimens have continuous hyperactivity of the MAPK pathway [71]. It is activated mainly by oncogenic mutations, although factors such as other autocrine growth factor stimulation [72], or N-cadherin (Neural-cadherin)-based homotypic cell-cell adhesion [73] can also be involved. The first such oncogenic mutation found to activate the MAPK pathway in melanoma was in NRAS [74]. Mutations have been identified in 15-25% of all melanomas [75] and most commonly result from substitution of leucine to glutamine at position 61 [76, 77]. The most common mutation to be reported in melanoma is in BRAF [77]. Although the reported frequency of the mutation varies in different studies, it seems that at least 60% of all melanomas harbour the BRAF mutation, which activates the MAPK pathway [78]. It has been identified that there are over 50 distinct mutations in BRAF [79]. Of these, the BRAF V600E mutation, a valine to glutamic acid substitution, is the most common and accounts for 80% of all reported BRAF mutations [77, 80].

Unlimited proliferation and apoptosis resistance are the two best-characterized roles for MAPK signalling in melanoma (Figure 1.2, Page 19). Constitutive MAPK activity enhances cyclin D1 and downregulates p27 expression in melanoma cells [81]. A pharmacological study showed that inhibition of either MEK or BRAF in melanoma cell lines led to a profound G1-phase cell cycle arrest. Moreover, constitutive MAPK activation can suppress apoptosis through the release of Smac/DIABLO from mitochondria [82] and through the ribosomal S6 kinase-mediated inactivation of the pro-apoptotic protein BAD [83]. More recent experiments have shown that the BRAF V600E mutation can decrease the levels of the pro-apoptotic Bcl-2 family member, BIM through a MAPK-mediated mechanism [84].

The constitutive MAPK activity is also involved in melanoma cell metastasis through activation of angiogenesis, adhesion disruption and immunosuppression. The

activated MAPK pathway may regulate angiogenesis through the control of hypoxia inducible factor -1α (HIF-1α) expression [85]. In addition, downregulation of V600E BRAF with small-interfering RNA (siRNA) resulted in significant reduction of vascular endothelial growth factor (VEGF) produced by melanoma cells, implicating that melanoma-associated angiogenesis is partially mediated by the MAPK pathway. There is also evidence that BRAF/MAPK signalling activity may contribute to metastasis of melanoma through regulating ß3 integrins and matrix metalloproteinase expression [86-89]. Finally, it has also been suggested that BRAF/MAPK may allow melanoma cells to escape from immune surveillance through suppression of their highly immunogenic melanocytic antigens, including Melan-A/Melanoma antigen recognised by T cells (MART-1), gp-100 and tyrosinase [90].

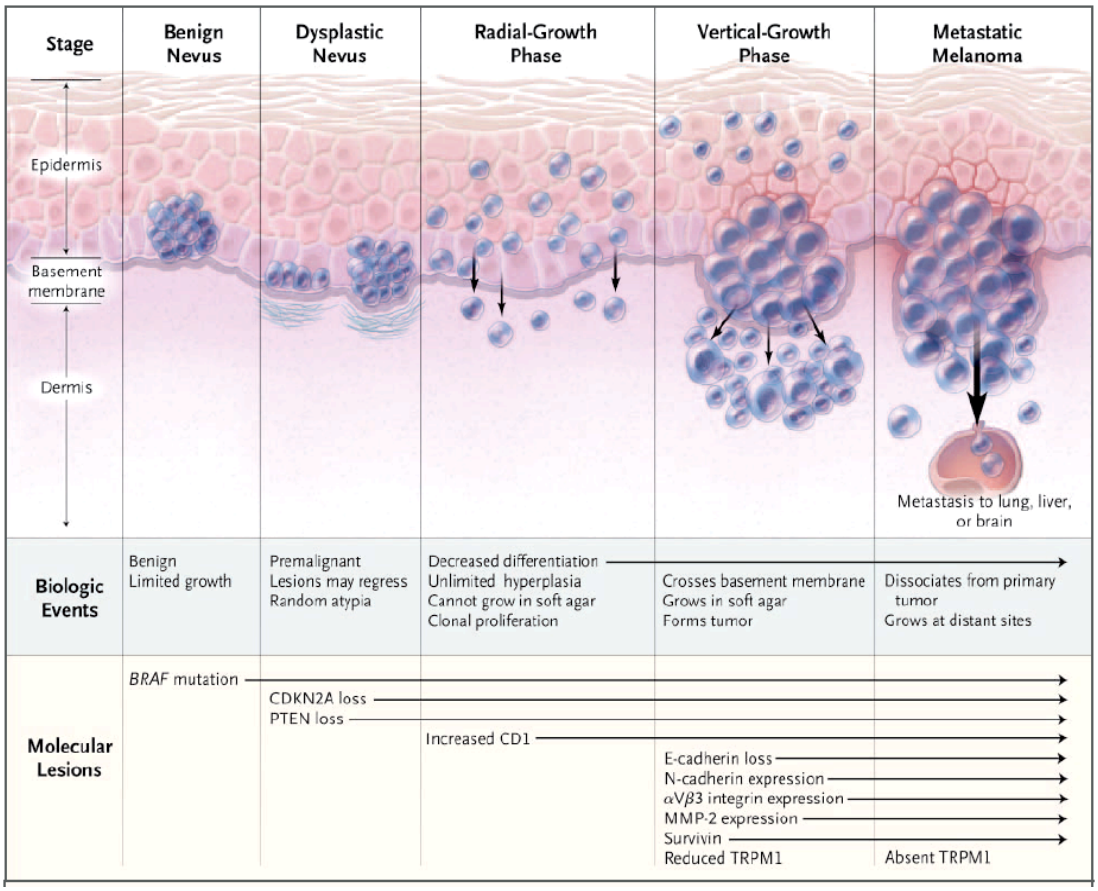

Figure 1.1 The Clark model along with the relevant biological events and molecular changes in melanoma progression. CDKN2A: Cyclin-dependent kinase inhibitor 2A. PTEN: Phosphatase and tensin homologue. CD1: Cluster of differentiation 1. MMP-2: Matrix metalloproteinase 2. TRPM1: Melastatin 1. Adapted from [91].

1.1.6.2 PI3K/AKT pathway

Besides activation of the MAPK pathway, other signalling pathways may be equally important in melanoma progression. The phosphoinositide 3-kinase (PI3K)/ protein kinase B (PKB/AKT) pathway is one of the widely explored signalling pathways [92, 93]. PI3K plays a crucial role in effecting alterations in a broad range of cellular functions in response to extracellular signals. A key downstream effector of PI3K is the serine-threonine kinase AKT, which in response to PI3K activation, phosphorylates and regulates the activity of a number of targets including kinases, transcription factors and other regulatory molecules. Activation of the PI3K/AKT pathway in melanoma is induced through either paracrine/autocrine growth factors, or the loss of expression and/or mutation of negative pathway regulators. This subsequently affects cell proliferation and apoptosis and intersects with the MAPK pathway [78] (Figure 1.2). For example, the insulin-like growth factor-1 is known to stimulate growth of early-stage melanoma cells, at least partially through activating PI3K/AKT pathway.

One of the most vital regulators of AKT is the phosphatase and tensin homolog (PTEN). The PTEN locus on chromosome 10 is a second chromosomal region that is frequently affected by homozygous deletion in melanoma and other cancers [94-96]. In physiological situations, PTEN can prevent AKT activation through degrading the products of PI3K. Although how the PI3K pathway is activated in melanoma is not fully understood, loss of expression and function of PTEN and PTEN mutation activate AKT. Loss of PTEN expression occurs in up to 30% of melanoma cell lines and 10% of melanoma tissues [97].

There are three AKT members, AKT1-3 [98]. Different AKT members exhibit different expression levels dependent on the cell type. 43-50% of melanomas have selective constitutive activity of AKT3 [92]. AKT has critical roles in cancer development in regulating apoptosis through the inhibition of BAD (pro-apoptotic protein) and increasing cell proliferation by elevating CCND1 expression, and activating the mammalian target of rapamycin (mTOR) pathway [78, 99, 100].

Stimulation of the mTOR pathway leads to increased protein translation and cell proliferation [78]. Moreover, AKT effects many other pathways including the stimulation of ribosomal S6 kinase, the suppression of forkhead signalling, and inhibition of glycogen synthase kinase-3 (GSK3) [101, 102]. Other studies demonstrated that AKT transformed melanocytes under hypoxic conditions through the Notch signalling [103, 104].

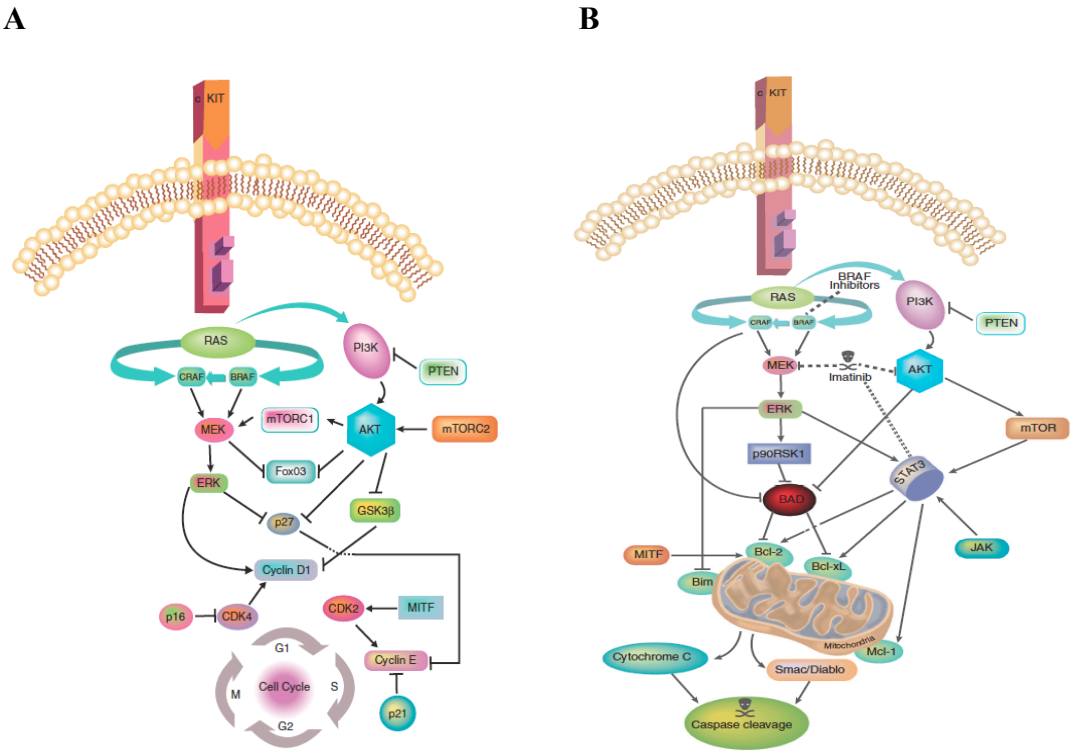

Figure 1.2 Intersected functions of MAPK and PI3K signalling pathways. A, In regulating cell proliferation; B, In regulating apoptosis. Adapted from [78].

1.1.6.3 MITF and melanocyte differentiation

Clark proposed that many naevi could regress through differentiation and that the failure of this differentiation is necessary for dysplasia [65]. The microphthalmia-associated transcription factor (MITF) is the key regulator in the development and differentiation of melanocytes [105] and maintains melanocyte progenitor cells in adults [106, 107]. However, the relationship between MITF and melanoma

development is complex.

On the one hand, MITF contributes to melanocyte differentiation by triggering cell cycle exit through induction of the cell cycle inhibitors $p16^{INK4a}$ and $p21^{Cip}$ [108, 109]. High levels of MITF have differentiation and anti-proliferation functions in melanoma cells, while low levels of MITF are found in invasive melanoma cells [110, 111]. All the above evidence suggests that MITF must be downregulated for melanoma progression.

On the other hand, MITF contributes to melanocyte survival by increasing the expression of an anti-apoptotic gene, Bcl-2 [112] and cyclin-dependent kinase 2 (CDK2) [113]. In animal models, deficiencies of both MITF and Bcl-2 caused grey hair because of a loss of differentiated melanocytes. The loss of melanocytes is due to the apoptosis of melanocyte progenitor cells in the hair follicles [106]. In a melanoma cell study, it was found that survival of malignant melanocytes was dependent on Bcl-2 as decreased Bcl-2 induced cell death. Moreover, MITF also functions in melanocyte pigmentation. α-MSH induced intracellular signalling via MC1R subsequently elevates MITF expression, which in turn increases the transcription of genes underlying melanin synthesis [114]. Furthermore, the MITF gene is amplified in 10–15% of melanomas in which BRAF is mutated and overexpression of both MITF and BRAF could transform primary cultures of human melanocytes, indicating that MITF is an oncogene [115]. These studies support the view that continued expression of MITF is essential in melanoma cells.

Marais' group proposed that in melanoma cells oncogenic BRAF exerts exquisite control over MITF on two levels: oncogenic BRAF downregulates MITF protein by targeting it for degradation in an ERK-dependent manner and then counteracts this by elevating MITF transcription through an octamer-binding transcription factor BRN2-dependent manner [116]. Through these opposing mechanisms, oncogenic BRAF ensures that the protein levels are permissive for melanoma cell survival and proliferation.

1.1.6.4 Cell adhesion and invasion

In the Clark model, invasion commences in the vertical-growth phase when melanoma cells grow intradermally as an expanding nodule (Figure 1.1). Whereas, when tumour cells dissociate from the primary lesion, migrate through the surrounding stroma, and invade blood vessels and lymphatics to form a tumour at a distant site, the tumour is then called metastatic melanoma [117]. Apparently, the formation of metastatic melanoma is also related to environmental alterations surrounding primary melanoma cells. Cell adhesion is one of the major environmental processes. Normally, it controls cell migration, tissue organization, and organogenesis [118]. Disturbances in cell adhesion contribute to tumour invasion, tumour-stroma interactions and tumour-cell signalling. Cadherins and integrins are the most important structural protein superfamilies involved in cell adhesion.

Cadherins (named for "calcium-dependent adhesion") are a class of type-1 transmembrane proteins that sustain cell-to cell contacts, form connections with the actin cytoskeleton, and influence intracellular signalling. The extracellular domain of cadherins binds to like cadherins on other cells in regions of cell contact called adhesion junctions. There are three subtypes of cadherins, N-cadherin (Neural-cadherin), E-cadherin (Epithelial-cadherin) and P-cadherin (Placental-cadherin). The intracellular domain is associated with a larger protein complex that includes ß-catenin and forms structural links with bundles of actin filaments. Progression from radial-growth phase to vertical-growth phase of melanoma is marked by the loss of E-cadherin and presence of N-cadherin [119, 120]. Additionally, besides the changes in cell adhesion, decreased E-cadherin expression and aberrant N-cadherin expression increase the survival of melanoma cells by stimulating ß-catenin signalling [73, 121, 122].

The integrins are the cell membrane receptors of extracellular matrix (ECM) proteins. Transition from radial to vertical-growth of melanoma is related to the expression of

αVß3 integrin [123], which induces expression of matrix metalloproteinase 2, an enzyme that degrades the collagen in basement membrane [124-126].

1.1.6.5 Other genes and signalling networks involved in melanoma

CDKN2A (also called p16) is a tumour suppressor protein, which in humans is encoded by the CDKN2A gene. CDKN2A plays an important role in regulating the cell cycle, and mutations in CDKN2A increase the risk of developing a variety of cancers, especially melanoma. This gene generates several transcript variants, which differ in their first exons. Alternative splicing of various exons within CDKN2A produces two distinct tumour suppressors: INK4A and alternate reading frame protein (ARF, also called p14). These tumour suppressor proteins $p16^{INK4A}$ and $p14^{ARF}$ are encoded by overlapping frames at the CDKN2A locus on chromosome 9p21. $p16^{INK4A}$ (an inhibitor of CDK4) blocks the cell cycle at the G1-S checkpoint by inhibiting cyclin-dependent kinases, suppressing the proliferation of cells with damaged DNA or activated oncogenes [127]. $p14^{ARF}$ acts as a tumour suppressor by restraining the cell cycle or promoting cell death after DNA damage or aberrant proliferation stimulated by various oncogenes. ARF participates in the key regulatory process that controls the p53 protein level. Moreover, the studies done *in vitro* and *in vivo* also suggest the low frequency of p53 mutations observed in melanoma is a consequence of the frequent loss of CDKN2A (and ARF) [128-130], which inactivates the p53 pathway [127].

In some melanoma samples with a low prevalence of BRAF mutation, DNA copy number gains and mutations in c-KIT gene were characterized [131]. c-KIT, a transmembrane tyrosine growth factor receptor, acts on a downstream signalling cascade leading to key intracellular signals that control cellular proliferation and survival. Three crucial pathways, MAPK, PI3K and STAT signalling, were initiated by KIT activation [132]. c-KIT mutation frequency is very high in gastrointestinal stromal tumours (GIST). In melanoma, c-KIT mutations were identified in 17% of chronic sun-damaged cutaneous, 11% of acral and 21% of mucosal melanomas

[131]. In addition, KIT gene amplification was found in 6% of chronic sun-damaged, 7% of acral lentiginous and 8% of mucosal melanomas. *In vitro* studies demonstrated that point mutations of c-KIT resulted in activation of c-KIT protein in melanoma cells and therefore stimulated downstream proliferation and pro-survival signalling pathways [132, 133].

Melanomas also exhibit constitutive activity in multiple other pathways, including nuclear factor kappa B (NF- κB), Src, Janus kinase/signal transducer and activator of transcription (JAK/STAT3), Wnt, Hedgehog and Notch [134-137]. Although most studies have focused on the role of individual signalling pathways, these different pathways in melanoma comprise a highly interconnected network. Multiple feedback loops in the intercrossed network would increase the difficulty in treatment of melanoma as inhibition of one pathway may activate a parallel pathway. For example, inhibition of mTOR leads to a rebound increase in the MAPK pathway through a PI3K-mediated mechanism [138]. These reciprocal interactions between the signalling pathways active in melanoma require strongly combined targeted therapy strategies.

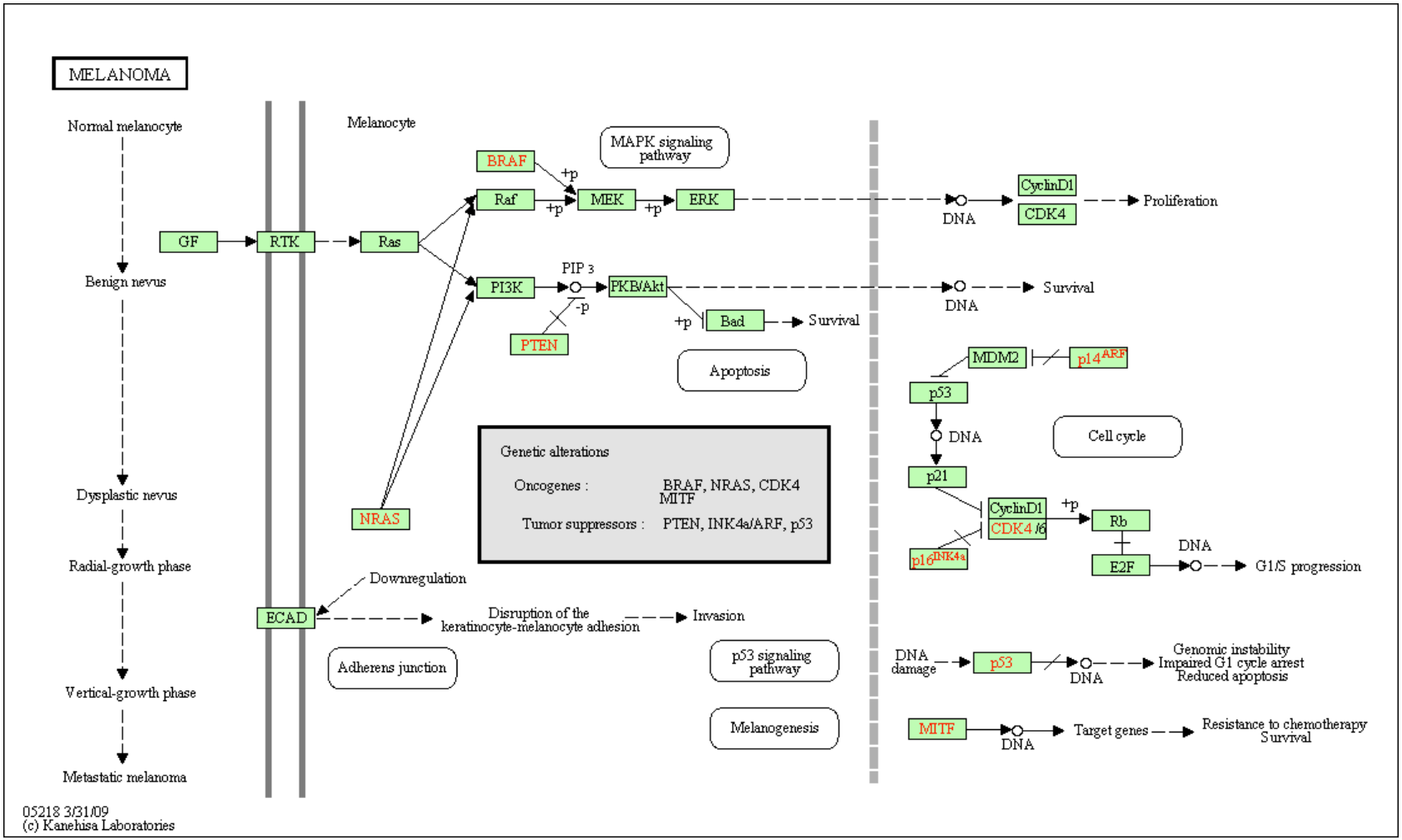

Figure 1.3 Key signalling pathways in human melanoma pathogenesis. Adapted from the Kyoto Encyclopaedia of Genes and Genomes (KEGG) pathway database (http://www.genome.jp/kegg/pathway/hsa/hsa05218.html). Genes in red represent the most important genes involved in this disease, which are framed together in a grey box. GF: Growth factor. ECAD: E-cadherin. RTK: Receptor tyrosine kinase.

1.1.7 Prospects for new therapies

Given the continuous rising incidence of cutaneous melanoma and inefficient conventional treatments, especially for advanced and recurrent melanoma patients, a wide range of studies are trying to find better molecular biomarkers and novel therapeutic strategies. Cancer treatment is entering into a "targeted therapy" era and this approach has shown extraordinary clinical benefits in several cancers. Specific kinase inhibitors are now used as the standard treatments for chronic myelogenous leukaemia, HER2/neu-amplified breast cancer, clear-cell renal cell carcinoma and GIST [139]. However, the precondition to the success of using these approaches is dependent on the identification of genetic aberrations in these diseases. Accumulating evidence showed melanoma harbours genetic changes in key protein kinase signalling pathways.

Sorafenib is a small molecule inhibitor of tyrosine kinase receptors, including wild type BRAF, V600E BRAF and CRAF. Sorafenib inhibited the growth and survival of BRAF-mutant human melanoma cells and slowed down the growth of melanoma xenografts [140]. However, a randomized Phase III trial of sorafenib did not increase the clinical response or disease control rate achieved by the chemotherapy agents alone [141], although a nonrandomized trial of sorafenib in combination with paclitaxel and carboplatin showed promising activity, with 26% clinical response rate [142]. More excitingly, a V600E-mutant-specific BRAF inhibitor, PLX4032, shows great effects on BRAF V600E positive melanoma patients. In the dose escalation portion of the Phase I clinical trial in metastatic melanoma, 56% of patients with the BRAF V600E mutation had a partial response and an additional 31% had a minor response. No responses were seen in patients without a BRAF V600E mutation [142]. Preliminary results from a dose expansion cohort of an extra 31 patients with V600E-mutant BRAF reported that 70% achieved a clinical response [143].

There are also several case reports of individual melanoma patients with c-KIT mutations who have achieved remarkable clinical responses to c-KIT small molecule inhibitors, such as imatinib, sorafenib and dasatinib [144-147]. For example,

imatinib showed a 50% clinical response rate among 10 melanoma patients with c-KIT mutations, but in none of the 10 patients with c-KIT amplification of the wild type gene [143].

The promising results with PLX4032 and c-KIT inhibitors in melanoma patients with BRAF and c-KIT mutations, respectively, add to the growing list of successful clinical strategies targeting specific activating genetic events in cancer. Although such studies to date have focused on the treatment of advanced melanoma, in the future these molecular insights may lead to improved early diagnosis of the disease. Personalized strategies of targeted therapies are likely the hope for melanoma patients. Moreover, a novel class of non-coding genes—microRNAs (miRNAs), are becoming a "hotspot" for cancer research including melanoma (Chapter 1.2). Numerous studies have shown their potential not only act as biomarkers, but they also play an important role in cancer therapy, including anti-drug resistance which is also a common issue for targeted therapy.

1.2 microRNAs

1.2.1 General introduction to non-coding genes

Over the past decade an explosion in the number of genome-wide studies has challenged the traditional view that most genes are protein-coding. Although counter-intuitive it is now clear that the number of protein-coding genes of humans and mice are close to those in the 1mm long *Caenorhabditis elegans* (*C. elegans*), and that all multicellular organisms have fewer protein-coding genes than some simple unicellar eukaryotes [148]. An explanation for the apparent paradox involves non-protein-coding genes: whilst only 2% of the mammalian genome encodes mRNAs the vast majority of the genome is transcribed as short and long non-coding RNAs (ncRNAs) which contribute to biological complexity [149]. In the expanding RNA world, the importance of thousands of regulatory ncRNAs including miRNAs, small interfering RNAs (siRNAs), PIWI-interacting RNAs (piRNAs, PIWI originally

from P-element induced wimpy testis in *Drosophila*) [150] and various classes of long ncRNAs (lncRNAs) is being increasingly recognized while new short transcripts, such as promoter-associated small RNAs (PASRs) and transcription initiation RNAs (tiRNAs) have recently been described [151, 152] .

The earliest demonstration of fundamental and general functions for regulatory RNA in eukaryotic biology was the finding that double-stranded RNA (dsRNA) introduced into *C. elegans* is cleaved into ~22 nucleotide (nt) small RNAs which cause widespread and heritable gene silencing [153-155]. Although it was originally thought to be restricted to exogenous dsRNAs, it is now clear that plants and animals produce endogenous siRNAs, miRNAs and piRNAs [156-161]. Small regulatory RNAs (siRNAs, miRNAs and piRNAs) guide effector Argonaute proteins to genomic loci or target RNAs in a sequence specific manner. Unlike siRNAs and miRNAs which are found ubiquitously, the longest small RNA class, piRNAs, which are 25-30nt in length, are first produced by successive waves of Argonaute-cleavage of long-non-coding transcripts arising from a Dicer-independent pathway and are largely restricted to the germline [157, 158, 162]. For lncRNAs, it is known that at least 80% of the transcription in the mammalian genome is exclusively in association with lncRNAs [151]. They are frequently long, spliced and contain canonical polyadenylation signals. lncRNA promoters are bound and regulated by transcription factors, including octamer-binding transcription factor 3/4 (Oct3/4), cAMP response element-binding (CREB), c-MYC, sex determining region Y-box 2 (Sox2), NF- κB, p53 [163-166]. Interestingly, ncRNAs are pervasive in all complex genetic phenomena in the eukaryotes (See Table 1.2). ncRNAs facilitate normal development and physiology and, when dysfunctional, underpin disease. Many intergenic regions associated with complex diseases express ncRNAs. Despite their potential use as diagnostic markers and therapeutic targets, and although there has been a near-exponential growth of manuscripts devoted to regulatory RNAs, their precise mechanisms of biogenesis and roles in signalling are not fully understood because of their natural complexity and diversification. Within the existing ncRNAs, the miRNA family is the best-characterized class both in terms of its biogenesis and

function. In my thesis the introduction to non-coding genes mainly focuses on miRNAs, since they are the main subjects of my project.

	Length	VD	TR	Post-TR	GI/TD	EM
endo-siRNA	~21-22nt	√	√	√	√	
miRNA	~22nt	√	√	√		
piRNA	~26-30nt				√	√
snoRNA	ND			√		
sdRNA	ND			√		
tiRNA	ND		√			√
lncRNA	>~200nt					√

Table 1.3 Summary of simplified representation of regulatory ncRNAs and their roles VD: Viral defence, TR: Transcriptional regulation, GI: Genome integrity, TD: Transposon defence, EM: Epigenetic modification; endo-siRNA: Endogenous siRNA, miRNA: microRNA, piRNA: PIWI RNA, snoRNA: Small nucleolar RNA, sdRNA: sno-derived RNA, tiRNA: Transcription initiation RNA, lncRNA: Long non-coding RNA. ND: Not described, √ : Specific function described. Adapted from [167].

1.2.2 History and biogenesis of microRNAs

The first miRNA to be discovered, *lin-4* was found in 1993 in the nematode *C. elegans* and functioned as a regulator in development [168]. The exact nature of this RNA was a mystery at that time, though there was evidence showing that *lin-4* negatively regulated *lin-14* protein expression by a novel antisense mechanism. In 2000, the second miRNA, *let-7*, was discovered [169]. *let-7* was evolutionarily conserved among animal species including vertebrates, ascidian, hemichordate and mollusk, indicating that these small molecules are important to many biological and pathological processes [169]. *let-7* targets well-established cell-cycle regulators, such as CDK6 and RAS [170, 171]. Since the first two miRNAs were identified, the miRNA field has grown tremendously and has become an integral component of the way we think gene expression is regulated. Many other miRNA genes have been

discovered in different species. In the latest release of miRBase 16, more than 1,100 mature miRNAs have been confirmed in human [172].

During the past few years studies on basic mechanisms of miRNA biogenesis and functions have seen some surprising new discoveries in miRNA processing and post-transcriptional regulation and the different processes between plants and animals. Mammalian miRNAs are short and highly conserved molecules [173, 174] that seem to have evolved independently of plant miRNAs as their sequences and biogenesis pathways differ substantially [175]. The introduction to the biogenesis of miRNA here focuses predominantly on the mammalian system and related information is also cited from model systems, including the fruitfly *Drosophila melanogaster* and nematode *C. elegans*.

Biogenesis can be divided into two major steps: miRNA processing in the nucleus and subsequent miRNA maturation in the cytoplasm (Figure 1.4, Page 32).

1. miRNA processing in the nucleus (Figure 1.4-A)

1) Transcription of the pri-miRNA

A miRNA is processed from a primary miRNA (pri-miRNA), which is either transcribed by RNA polymerase II or RNA polymerase III [176-178]. Because both polymerases are regulated differently and can recognize specific promoters and terminators, there exists a wide range of regulatory options [179]. Furthermore, each miRNA located in the same genomic cluster can be transcribed and regulated independently [180]. An average human pri-miRNA is usually composed of a 33 base pair (bp) hairpin stem, a terminal loop, and two single-stranded (ss) flanking regions of several kilobases [181].

2) pri-miRNA cleavage by the Drosha-DGCR8 microprocessor complex

After transcription, the nuclear microprocessor complex formed by the RNase III enzyme Drosha (RNASEN) and the DGCR8 (DiGeorge critical region 8, also known as Pasha, Partner of Drosha) protein cut the pri-miRNA. 5' and 3' arms of the pri-miRNA hairpin are cleaved by the two RNase domains of Drosha [182], whereas

Pasha interacts with the pri-miRNA and acts as a molecular ruler to determine the precise cleavage site [183] that is located ~11bp away from the ssRNA/dsRNA junction at the base of the hairpin stem. The resulting pre-miRNA (precursor miRNA) is now generated comprising of a ~22bp stem and a terminal loop.

3) Pre-miRNA export mediated by Exportin-5-Ran-GTP

Thereafter, Exportin-5 (XPO5), a Ran-GTP-dependent dsRNA-binding protein, transports the pre-miRNA from nucleus into cytoplasm [184]. XPO5 can also protect the pre-miRNAs against nuclear degradation because knockdown of XPO5 only induces a decrease of mature miRNAs but not nuclear accumulation of pre-miRNAs [184-186]. XPO5 binding to a defined length of double-stranded stem and the 3' overhangs ensures the export of only correctly processed pre-miRNAs [186-188].

2. miRNA maturation in the cytoplasm (Figure 1.4-B)

1) The RISC loading complex (RLC): Dicer, TRBP and PACT join Ago2

Prior to Dicer cleavage, the RISC (RNA-induced silencing complex) loading complex (RLC) needs to be generated to provide a platform for RISC assembly and cytoplasmic processing. RLC is composed of the RNase Dicer, the double-stranded RNA-binding domain proteins TRBP (Tar RNA binding protein) and PACT (protein activator of PKR) and associates to form a complex that is subsequently replenished by the core component Argonaute-2 (Ago2) [189-193]. RISC contains a single-stranded miRNA guiding it to its target mRNA while Ago2 also mediates RISC effects on mRNA targets. Neither TRBP nor PACT is essential for Dicer-mediated cleavage of pre-miRNA but they enhance RISC formation and participate in the recruitment of Ago2 [191-193].

2) Two fates after nuclear export: Ago-2-mediated ac-pre-miRNA cleavage and Dicer-mediated pre-miRNA cleavage

An additional endonucleolytic cleavage step occurs before Dicer-mediated cleavage: for some highly complementary miRNAs, Ago2 cuts the 3' arm in the middle of the hairpin to generate a nicked hairpin termed the ac-pre-miRNA, also regarded as the prospective passenger strand [194]. Dicer can process this precursor as efficiently as

noncleaved pre-miRNAs. This additional step might explain the early association of Ago2 with RLC, even before pre-miRNA [189-193]. Once the RLC is formed, the RNase III Dicer cleaves off the loop of the pre-miRNA or the nicked ac-pre-miRNA and generates a roughly ~22nt miRNA duplex [195]. One mature miRNA end in the duplex is already determined by Drosha, Dicer cleavage defines the other mature miRNA end with 2nt protruding overhangs [196, 197].

3) Unwinding the miRNA duplex into guide and passenger strand

Following Dicer cleavage, the miRNA duplex is separated into the functional guide strand and the subsequently degraded passenger strand, while the ternary complex of Dicer, TRBP and Ago2 dissociates [190].

4) Guide strand selection and passenger strand degradation

Both strands of the miRNA duplex could have given rise to two different mature miRNAs. In fact, in a similar manner to siRNA duplexes, only one strand is usually incorporated into the RISC and the other is degraded [198]. In mammals, thermodynamic stability of the two terminal base pairs determines the functional asymmetry: the miRNA strand with the less stable base pair at its 5' end in the duplex is loaded into RISC, whereas the miRNA strand with the more stable base pair is typically degraded [198, 199].

5) Silencing the target gene with help from Argonaute proteins

Finally, the mature miRNA incorporated into RISC triggers the target gene silencing step with help from Argonaute proteins. At least three independent mechanisms of miRNA-mediated mRNA silencing have been discovered so far: target cleavage, translation repression, and mRNA decay [200, 201]. In situations of perfect complementarity between mature miRNA and its target transcripts, the Ago2-RISC cleaves the mRNA [202]. Translational inhibition is achieved via various mechanisms: CAP structure dissociation with elongation factor, translation-elongation blockage, or ribosome drop-off promoting premature dissociation of the mRNA [203-205]. In addition, miRNAs trigger deadenylation and subsequent decapping to initiate degradation of the mRNA target.

A

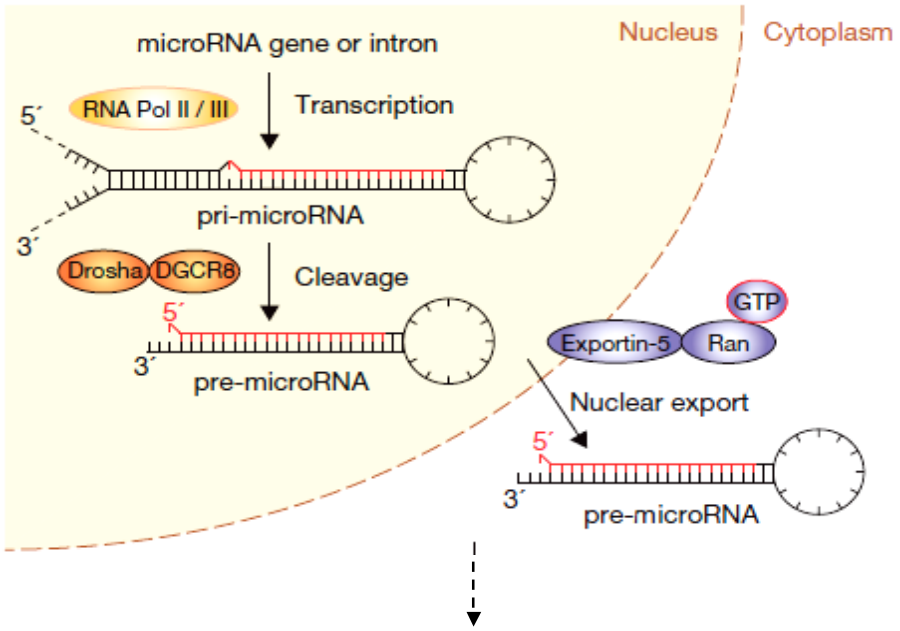

B

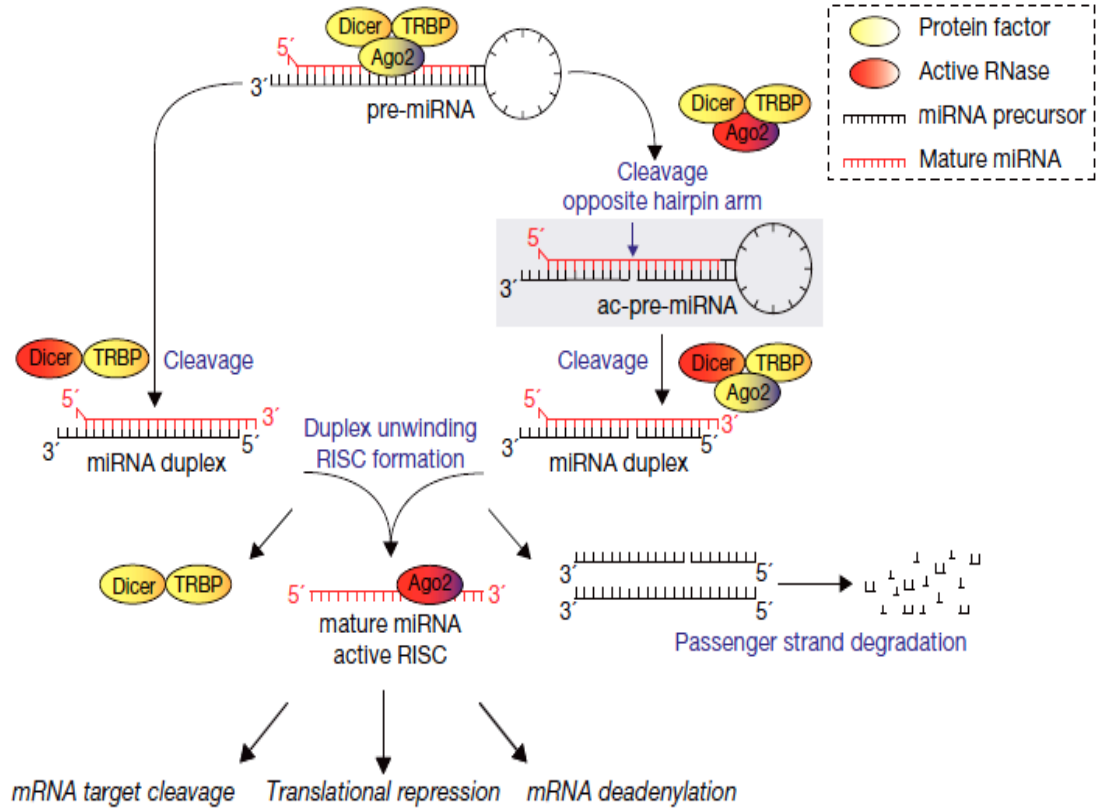

Figure 1.4 Biogenesis of miRNAs. The figure describes the key steps of microRNA biogenesis. Adapted from [179].

1.2.3 Regulation of microRNAs

As described above, biogenesis of miRNA has been intensively studied and well described. However, the regulation of miRNA expression remains largely unclear. In early studies, promoter regions had been determined for only a small portion of miRNAs [206]. Most of the predicted miRNA promoters were not confirmed in wet-laboratory experiments [172], although several *in silico* studies predicted the promoter regions of miRNAs [207-209]. According to whether the miRNA is localized in a transcribed genome region (for a protein coding gene) or not, miRNAs can be classified as 'intragenic' and 'intergenic'. Localization of promoters for intergenic and inversely-directed intragenic miRNAs is largely unknown, whereas promoters for overlapping primary genes are considered to be promoters for the intragenic miRNAs that are localized in the same direction as the primary gene. However, the means by which miRNA expression is regulated appears complicated and needs to be answered.

There is no single pathway universal to mature miRNA processing and it actually appears to be a well-organized and regulated process. There are many common or specific regulatory mechanisms operating throughout the whole activity to facilitate and supervise the processing of individual miRNAs by regulation in both transcriptional and posttranscriptional pathways. Here I discuss some common regulatory mechanisms including miRNA editing, miRNA-related single nucleotide polymorphism (SNP) and epigenetic regulation.

1.2.3.1 microRNA editing

RNA editing is an important process defined as a post-transcriptional change of RNA sequences by deamination of adenosine (A) to inosine (I). It takes place either in the nucleus or in the cytoplasm. The A to I editing of primary transcripts by ADARs (adenosine deaminases acting on RNAs) was first described for miR-22 [210], followed by a lot of other miRNAs such as miR-151, miR-197, mi-223, miR-376a,

miR-142 and miR-143 [211, 212]. Many pri-miRNAs and pre-miRNAs are targeted by ADARs at different stages in their processing, and the modifications can affect both Drosha-mediated and Dicer-mediated cleavage, and also prevent the export of pre-miRNAs. For instance, in pri-miR-142, A to I editing inhibits its cleavage by Drosha and contributes to its degradation by the nuclease Tudor-SN, which has affinity for dsRNA containing inosine-uracil pairs [213]. For another example, editing of pre-miR-151 prevents Dicer processing in the cytoplasm and results in accumulation of pre-miR-151 [214]. However, whether miRNA editing is predominantly in the nucleus (on the pri-miRNAs) or in the cytoplasm (on the pre-miRNAs) needs to be established. In addition to alterations of miRNA processing, miRNA editing can also have impact on miRNA target specificity. A single A to I change in the seed sequence of miR-376-5p precursor redirects the mature miRNA to a new target, resulting in altered protein expression in mice [215].

1.2.3.2 microRNA and SNPs

The first miRNA related SNP was found in the miR-189 binding site of SLIT and NTRK-like protein 1 (SLITRK1), which was associated with Tourette's syndrome [216]. Since then, several other studies have identified SNPs in miRNA genes (pri-miRNA, pre-miRNA and mature miRNA) using systematic sequencing and *in silico* methods. Catalogues of SNPs in miRNAs have been created and made public [217-219]. An example, a G-U SNP in miR-125a results in processing blockage and consequently reduces the levels of mature miR-125a [218]. Most studies have tried to associate SNP occurrence with susceptibility to cancer. (More information about miRNAs and SNPs in cancer is discussed later in this Chapter—section 1.2.7.2.)

1.2.3.3 microRNA and epigenetics

Recently, many studies have focused on identification of the relationship between regulation of miRNAs and epigenetics. The first study of this type established that

the expression of miR-127 is regulated epigenetically. In this study, pharmacological unmasking of epigenetically silenced miRNAs activated 17 of 313 miRNAs investigated in the bladder cancer cell line T24 and the normal fibroblast cell line LD419 [220]. DNA methylation level and histone modification status at identified promoter regions of miR-127 correlated significantly with mature miR-127 expression. Subsequent to this initial report, studies on the epigenetic regulation of miRNAs have increased dramatically. Epigenetic mechanisms, including DNA methylation and histone modification, not only regulate the expression of protein-encoding genes, but also miRNAs. Conversely, another subset of miRNAs controls the expression of important epigenetic regulators, including DNA methyltransferases, histone deacetylases and polycomb group genes. This complicated network of feedback between miRNAs and epigenetic pathways appears to form an epigenetics–miRNA regulatory circuit (Figure 1.4), and to organize the whole gene expression profile [172]. When this regulatory circuit is disrupted, normal physiological functions are interfered with, contributing to various disease processes. (More information about miRNAs and epigenetics in cancer is discussed later in this Chapter—section 1.2.7.3.)

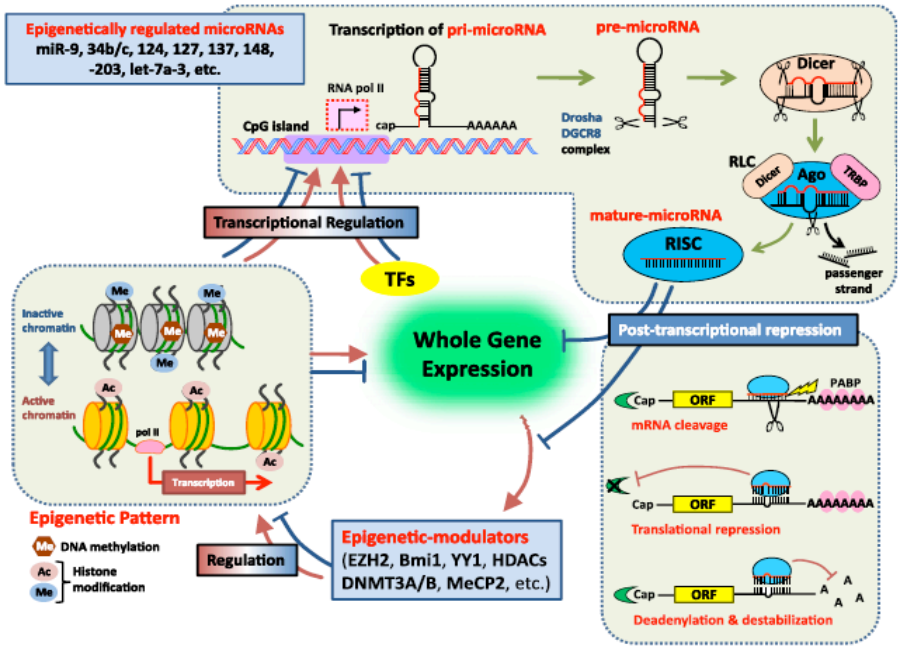

Figure 1.5 Epigenetic-microRNA regulatory circuit. PABP: poly (A) binding proteins. TF: Transcriptional factors. TRBP: Tar binding protein. Adapted from [172].

1.2.4 Functions of microRNAs

Besides perfectly matched sequence complementarity only between the "seed" region of the miRNA (~2-7nt of mature sequence) and its target gene, the miRNA binds to the 3' UTR of its targets through imperfect base pairing [221]. Depending on the precise nature of the binding, this induces degradation, destabilization, or translational repression of the mRNA and consequently silences gene expression [200]. Additionally, because of the imperfect complementarity of binding, a single miRNA can influence a broad range of mRNAs and a whole miRNA family may regulate thousands of target genes [222, 223]. The estimation that more than 30% of protein-coding genes are regulated by miRNAs at the posttranscriptional or translational level [224] indicates that almost all cellular pathways are directly or indirectly affected by miRNAs. So far miRNAs are reported to have been involved in 94 diseases [225], ranging from psychiatric disorders [226], through diabetes [227], to cancer [228] (More miRNA functions related to cancer are discussed in this Chapter—section 1.2.7.).

Notably, there was a unique study that defined a novel role for miRNA that can upregulate mRNA translation [229]. AU-rich elements (AREs) bind specific proteins to regulate mRNA stability or translation in response to external and internal stimuli. In a previous study, the same authors had already demonstrated that upon cell cycle arrest, the ARE in the tumour necrosis factor-α (TNF-α) mRNA is transformed by serum starvation into a translation activation signal, recruiting Ago and fragile X mental retardation—related protein1 (FXR1). They found that the expression of miR-369-3 is necessary for translation up-regulation of the ARE-containing reporter. A siRNA directed against the loop region of pre-miR-369-3 prevented this translation up-regulation under serum-starved conditions. The knockdown cell line was rescued with synthetic miR-369-3 resistant to siRNA and the translation efficiency of the ARE-containing receptor was increased five-fold. All the above results indicate that miR-369-3 is specifically required for TNF-α ARE-mediated translation activation under growth arrest conditions. Similarly, they also found *let-7* and a synthetic miRNA miRcxcr4 induced translation upregulation of target mRNAs on cell arrest,

although they repressed translation in proliferating cells. Therefore, they thought that there is miRNA oscillation between repression and activation in coordination with the cell cycle: in proliferating cells they repress translation, whereas in G1/G0 arrest they activate translation.

1.2.5 Detection of microRNAs

The first method to quantify miRNA was northern blotting. However, it requires a relatively large amount of RNA and is insensitive, especially for those miRNAs with low expression levels. Thereafter, reflecting the need for greater precision and higher throughput, miRNA real-time RT-PCR and miRNA microarray methods are commonly used.

The real-time RT-PCR makes use of a stem loop reverse transcription primer to generate cDNA templates, which are then amplified using specific primers and tested with specific fluorescent probes. Currently four different chemistries, TaqMan®, Molecular Beacons, Scorpions® and SYBR® Green, are available for real-time PCR. All of these chemistries allow detection of PCR products via the generation of a fluorescent signal. TaqMan probes, Molecular Beacons and Scorpions depend on Förster Resonance Energy Transfer (FRET) to generate the fluorescence signal via the coupling of a fluorogenic dye molecule and a quencher moiety to the same or different oligonucleotide substrates. SYBR Green is a fluorogenic dye that exhibits little fluorescence when in solution, but emits a strong fluorescent signal upon binding to double-stranded DNA. The choice should be made according to individual situation as each different chemistry method has its own advantages and disadvantages.

Microarray for quantifying miRNA is optimal for the simultaneous analysis of hundreds of miRNAs present in one sample or multiple samples. Recently, for better understanding of miRNA roles in different diseases, determination of miRNA expression in FFPE tissues has become of interest to researchers. Therefore, methods have been developed to profile miRNAs from FFPE specimens and to localize

miRNA expression at the cellular and subcellular levels by *in situ* hybridization (ISH). Although it is challenging to perform ISH with miRNAs because of their very small size, introduction of locked nucleic acid (LNA) probes has greatly improved the performance of this technique. For specific detection of miRNA the use of the nucleic acid analogues LNA, in which the ribose ring is locked into a C3' -endo conformation by a 2' -O, 4' -C methylene bridge (Figure 1.5), have shown great advantages for ISH [230]. LNA exhibits higher base pairing affinity than DNA and RNA as measured by UV melting analyses [231], and as also observed by ISH [230]. In addition, the design of LNA oligos can be optimized to enable increased mis-match discrimination and thereby enable specific identification of highly similar sequences such as miRNA family members [231] and single mutations [232]. Several groups have used this technique successfully for different miRNAs on both tissues and cells [233, 234].

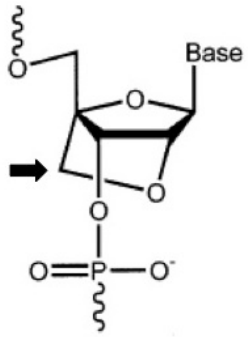

Figure 1.6 Structure of locked nucleic acid. The black arrow indicates the bridge.

1.2.6 Identification of microRNA targets

Precise target prediction of miRNAs is a challenging task in miRNA research, especially for those newly identified miRNAs implicated in specific diseases but with little help from previous literature. To assist this task a variety of computer-aided prediction algorithms have become available. These algorithms are trained by well known miRNA-mRNA interaction rules gained from microarray data in order to identify novel miRNA targets. Among algorithms, miRanda [235] is one of the most popular and others include TargetScan [236], PicTar [237], PITA [238] and RNA22

[239]. However, most of them suffer from either high false positive or false negative rates due to insufficient specificity and sensitivity. To overcome these disadvantages, other approaches have been developed. DIANA-microT [240] and DIANA-miRPath [241] are gene set analysis based approaches. DIANA-miRPath software performs an enriched analysis of multiple miRNA target genes comparing each set of miRNA targets to all known Kyoto Encyclopaedia of Genes and Genomes (KEGG) pathways [242, 243] and therefore it becomes a valuable tool for interpreting targets which are affected by deregulated miRNAs. Since the prediction algorithms do not always offer identical targets, using the intersected target lists from multiple algorithms serves to narrow down the candidate targets with higher confidence. However, computationally predicted targets still need to be verified through biochemical identification to understand the mode of action of miRNAs and their functions.

1.2.7 microRNA and cancer

Given the fundamental role of miRNAs, it is no surprise that miRNAs have been shown to be involved in a great spectrum of diseases, including cardiovascular [244], infectious [245], neurologic [246] and metabolic diseases [247, 248]. Equally interesting, miRNAs have been found important in tumourigenesis with more than 3,000 publications associating miRNAs with cancer to date. To further understanding of the miRNA functions in malignancies, the following sections focus on miRNAs in genomic organization, tumourigenic behaviours and pathways, epigenetics and clinical applications.

1.2.7.1 Association with genomic alterations

Approximately 50% of annotated miRNA genes are located in cancer-associated regions or fragile sites [249-251]. For example, the miRNA cluster 15a/16-1 is located on 13q14, a frequently deleted genomic locus in chronic B cell lymphocytic leukaemia (B-CLL) [249]. Other examples include deletion of *let-7g*/miR-135-1 in a

variety of human malignancies [250], amplification of the miR-17-92 cluster in lymphoma [252], translocation of miR-17-92 in T cell acute lymphoblastic leukaemia (T-ALL) [253] and amplification of miR-26a in glioblastoma [254]. In a study with higher genomic resolution, 283 miRNA genes in 227 human ovarian, breast, and melanoma cancer specimens were analyzed for copy number changes [255]. Of all the analyzed miRNAs, 37.1% in ovarian cancer, 72.8% in breast cancer and 85.9% in melanoma were located in genomic regions with gene copy number changes. In all three cancers, the copy number of 26 particular miRNA genes increased, whereas 15 decreased. This indicates that some miRNAs participate in the generation of a "common" tumour phenotype while others are specific to a particular cancer type.

1.2.7.2 microRNA related SNPs

miRNA related SNPs can occur in miRNA genes (specifically in "seed regions") , miRNA binding sites of target genes and in miRNA-processing machinery.

SNPs in miRNA genes are thought to influence miRNA functions through the transcription of primary transcript, through pri-miRNA and pre-miRNA processing, and thirdly through effects on miRNA-mRNA interactions [256]. The first evidence that point mutation in miRNA genes can have a functional effect and confer cancer susceptibility comes from a seminal study by Carlo Croce's group. A germline mutation (C to T) in pri-miR-16-1 was found in familial chronic lymphocytic leukaemia (CLL) and resulted in decreased miR-16-1 expression. A SNP in the terminal loop of pre-miR-27a was associated with lessened advanced breast cancer risk in families with a history of non-BRCA-related disease [257]. A unique example of a functional miRNA SNP in pre-miR-146a (C to G), led to altered processing, lower expression of mature sequence and susceptibility to papillary thyroid carcinoma [258]. Individuals with a heterozygous genotype have a higher risk of developing papillary thyroid carcinoma than homozygous populations.

The disruptive action of SNPs in the miRNA binding site of target mRNAs is similar to seed region SNPs for altered gene expression in cancer. *let-7* binds to the 3' UTR of KRAS and negatively regulates KRAS's expression [171]. Very low expression of *let-7* and elevated KRAS were found in lung cancer. Chin *et al.* sequenced the 3' UTR of KRAS and identified ten *let-7* complementarity sites. A new SNP (T to G) in LCS6 was present in 20% of lung cancer cases and 5% of the control populations [259].

Recent studies suggest that SNPs in the biogenesis machinery are also associated with cancer risk, drug response and prognosis [256]. Low level of Drosha was related to poor ovarian cancer survival [260]. XPO5 was decreased in bronchioloalveolar carcinoma and stage I lung cancer [261] but increased in high-grade prostate cancer [262].

1.2.7.3 In epigenetics

Genetic lesions cannot solely explain the complexity of the abnormalities that arise in a cancer cell. Epigenetics offers an additional and equally important explanation that, along with genetics, contributes to a better understanding of the whole malignant process. It is now defined as the inheritance of changes in gene activity that is independent of DNA sequence [263]. DNA methylation and histone modifications are the two major events of epigenetics. Likewise for miRNA, not only genetic alterations might cause the deregulation of subsets of miRNAs, but epigenetic changes can also have an effect on miRNA expression.

It was hypothesized that miRNA genes with tumour suppressor features could be hypermethylated in cancer in the same way as classic protein-coding genes [264, 265]. Two tumour-suppressor miRNAs, miR-127 and miR-124a that negatively regulate the expression of oncogenes CDK6 and Bcl-6 were methylated in various cancers [220, 265]. Some recent papers have demonstrated that the presence of CpG island hypermethylation of miRNA genes is a widespread phenomenon in cancer, as

shown for miR-9-1, miR-193a, miR-137, miR-342, miR-203, miR-34b/c and miR-1 [266]. In addition, global DNA hypomethylation events can also affect miRNAs. The human *let-7a-3* gene is located on chromosome 22q13.31 and is embedded in a CpG island. *let-7a-3* was found hypomethylated in lung cancer cells relative to normal lung cells [267]. For miRNA genes with histone modifications, DNA hypermethylation interacts with histone modifications through precise crosstalk mediated by the transcriptional repressor methyl-CpG-binding domain proteins (MeCP/MBDs) [268]. miR-124 silencing by DNA methylation was accompanied by the presence of the transcriptional repressors MeCP2 and MBD2, and absence of active histone marks, such as acetylation of histone H3 and H4 [265].

Since more hypermethylated protein-coding genes and miRNA genes have been discovered in cancer that are involved in invasion and metastasis, novel therapeutic opportunities targeting such hypermethylation will present themselves in the future.

1.2.7.4 Dysregulation in tumourigenic pathways

Expression changes in miRNAs could drive tumourigenesis, through their roles as tumour suppressors or oncogenes. Upregulated or downregulated miRNAs involved in malignancies are respectively referred to as oncogenic miRNAs (also called "oncomiRs") or tumour-suppressor miRNAs. Functional studies performed in cancer cell lines or mouse models of various cancers through overexpression or knockdown of miRNAs have supported these different roles for miRNAs in tumourigenesis. For example, the expression cluster miR-17-92 was increased in lung cancer, especially in small-cell lung cancer [269]. Lung cancer cell growth was also increased by miR-17-92 expression. In contrast to miR-17-92, Takamizawa *et al.* found that expression levels of *let-7* were often reduced in both *in vivo* and *in vitro* lung cancer studies [270]. They also observed that overexpression of *let-7* in A549 lung adenocarcinoma cell lines inhibited cell growth. *let-7* negatively regulates its target genes: RAS and MYC [171]. It was also shown that lung tumour tissues display decreased levels of *let-7* and increased levels of RAS protein relative to normal lung tissue.

In both solid and haematological malignancies, many other miRNAs have expression changes indicating that they function as oncogenes or tumour suppressors. The MYC oncoprotein family has crucial roles in the pathogenesis of many human neoplastic diseases through deregulating both cell growth and death check points and, in a permissive environment, rapidly accelerating the affected clone through the carcinogenic process. miR-155 expression has been correlated to MYC over-expression in B-cell cancers, suggesting it may be playing a role in the regulation of this oncogene [271]. Other studies showed that expression of miR-155 was upregulated in pediatric Burkitt's lymphoma, in Hodgkin's lymphoma and large B-cell lymphomas [272, 273] and also in breast, lung, colon, and thyroid cancers [274, 275]. The oncomiR, miR-221 is increased in glioblastoma [276], and tumour suppressors like the miR-34 family in breast cancer [277], and miR-143/145 in colorectal neoplasia are reduced relative to normal tissues [278].

Additionally, some miRNAs have been regarded as metastasis-related miRNAs (also termed as "metastamiRs") through cell line and xenograft experiments. For instance, breast cancer related examples include miR-10b, miR-9, miR-31 and miR-335, either as pro-metastatic regulators (the former two), or anti-metastatic effectors (the latter two) [279].

The observed global deregulation of miRNA expression on tumour initiation, maintenance or metastasis can be explained through studying miRNA targeted genes and the pathways that they regulate. It is difficult to assign an individual miRNA or miRNA cluster to a single or a certain type of tumourigenic pathway because there are many hundreds of miRNAs and each miRNA can have hundreds of targets and there are also signalling crosslinks between different pathways. As noted, miRNA regulation is pervasive in almost all biological transductions in tumour-stromal ecosystems involving cell adhesion, angiogenesis, proteolysis and cell signalling.

Metastasis of malignancies requires the loss of expression or function of E-cadherin. E-cadherin regulates the actin cytoskeleton via its association with ß-catenin, which is also a transcription factor involved in the Wnt signalling pathway. The E-cadherin/

ß-catenin system acts as a tumour suppressor of invasion and low E-cadherin expression level is correlated to inverse patient survival and advanced histological grade in colorectal cancer [280]. Interestingly, both E-cadherin and ß-catenin mRNAs contain potential miRNA binding sites: miR-9 in E-cadherin and miR-139 and miR-200a in ß-catenin. Upregulated miR-9 has been reported in breast cancer relative to normal tissues [281]. Integrins perform essential roles in cell adhesion to the ECM. αVß3 integrin is upregulated in tumour cells at the invasion front as well as acting as a marker of neovessels following activation of the angiogenic switch [282]. The mRNAs for both integrin αV and ß3 subunits contain binding sites for miRNA, such as miR-32 for integrin αV and *let-7*/miR-98 for integrin ß3 [283]. As mentioned above altered expression of *let-7* might contribute to the development of lung cancer through regulating RAS [171]. Moreover, integrin ß1 was downregulated on overexpression of miR-124 [284]. Similar to integrins, transcripts encoding the cytoskeletal proteins paxillin and focal adhesion kinase (FAK) that are downregulated in cancer have potential miRNA binding sites [285]. For FAK, miR-32/92 binding sites are present, just as in integrins αV and α5. FAK also shares a miR-199 site in common with fibronectin. Lysyl oxidase (LOX), involved in the crosslinking of collagen and elastin, is one of the important regulators in the tumour cell microenvironment. Elevated LOX expression is related to poor survival and promotes tumour cell invasion via increased formation of focal adhesions. LOX contains a binding site for miR-145, which is reduced in many cancers and has been reported to be deleted in prostate cancer [281].

Tumour angiogenesis requires tumour cell factors, such as VEGF and is driven by multiple mechanisms. The four tissue inhibitor of metalloproteinases (TIMPs) are intriguing molecules for their having both pro- and anti-tumourigenic functions [286]. TIMP3 is also antiangiogenic by blocking VEGF binding to VEGFR2 [287]. TIMP3 mRNA contains a large number of potential target sites for miRNA, including miR-21 and miR-17/20/106 that are upregulated and strongly related to a poor prognosis signature [275, 288]. Moreover, TIMP3 also has a site for miR-221/222, which are upregulated in papillary thyroid cancer. All the above evidence

indicates deregulated miRNA expression could influence both angiogenesis and proteolysis pathways, resulting in dysregulation in tumour invasion and metastasis.

1.2.7.5 In stem cell activation

Several studies have shown miRNAs are associated with the self-renewal of stem cells. In mice and zebrafish, the absence of *Dicer-1* results in lethality early in development and loss of stem cell populations [289, 290]. Shcherbata *et al* reported that in Drosophila melanogaster, the *Dicer-1* mutation affects germline stem cells showing delay in the G_1 to S transition and indicating an important role of miRNAs in the division of stem cells [291]. This suggests that miRNAs might be involved in stem cell activation. However, which set of miRNAs are the crucial players for normal stem cell maintenance and whether they are involved in cancer stem cells needs to be elucidated.

1.2.7.6 Clinical applications

The miRNA family can be very useful in clinical applications since their expression is specifically altered in different cancers, or between normal and malignant tissues. miRNA expression profiling studies suggest miRNAs are superior biomarkers for cancer subtype classification and prognostication [292-294]. On the other hand, changing miRNA expression back to normal could be a potential therapeutic strategy.

Two of the earliest reports have shown the utility of miRNAs expression profiles to distinguish tumour from normal samples, identify tissue of origin for tumours of unknown origin or in poorly differentiated tumours and to distinguish different types/subtypes of tumours [295, 296]. Moreover, it is also elucidated that certain alterations of miRNAs occur in patients at an early stage of cancer and thus may be helpful for early detection. The availability of FFPE specimens for miRNA detection

[297] makes it feasible to use miRNAs for diagnostic purposes as biomarkers. More excitingly, some new studies have also shown that miRNAs can be detected in serum [298, 299]. Beyond the realm of diagnosis, a series of publications has shown that miRNAs can act as useful indicators of clinical outcome [283, 300, 301] and can be used for estimation of treatment efficiency [302].

General therapeutic strategies involving antisense-mediated inhibition of oncogenic miRNAs and miRNA replacements with miRNA mimics or viral vector-encoded miRNAs have been generated.

Application of 2'-O-methyl anti-miRNA oligonucleotides (AMOs) targeting the oncomiR, miR-21 has been found to inhibit glioblastoma and breast cancer cell growth *in vitro* and in an MCF-7 breast cancer xenograft mouse model [288, 303]. In another AMO application, modified AMOs conjugated with cholesterol termed "antagomiRs" were systematically delivered through intravenous injection to target the liver-specific miR-122 in mice [247, 248]. Other miRNA reduction strategies include miRNA sponges and construction of lentiviral vectors as anti-miRNA decoys [304].

For overexpressing miRNA, viral or liposomal delivery mechanisms have been used [305, 306]. Using adenovirus-associated virus in a hepatocellular carcinoma (HCC) animal model, a successful elevation of a tumour suppressive miRNA, miR-26 in HCC occurred and resulted in inhibition of cell proliferation and tumour-specific apoptosis [307]. It is also thought that cationic liposomes or polymer-based nanoparticle formulations can be developed to achieve the delivery of miRNA mimics and tested for therapeutic efficacy [308]. Absence of vector-based toxicity is the advantage of these mimics, indicating that these approaches might be promising tools for future tumour therapy.

Finally, it has been reported that miRNA therapy can also enhance the response and suppress resistance to anticancer chemo-/radio-therapy. miR-200c levels were extremely low in poorly differentiated cancer cells and restoration of miR-200c

increases their sensitivity to microtubule-targeting agents by 85% [309]. Weidhaas *et al.* showed that the *let-7* family can radiosensitize A549 lung cancer cells, while reducing let-7 levels causes radioresistance [310].

1.3 Summary and aims

Cutaneous melanoma is likely to become an increasingly important public issue due to its continuous increase of incidence over the last 30 years. Inaccurate diagnosis and prognosis, and extremely low efficiencies for therapy of metastatic melanoma constitute the major barriers to curing melanoma. The objective of the studies in this thesis is to lower these barriers by identifying key non-coding genes and coding genes involved in melanomagenesis.

As has been explained miRNAs are crucial factors in almost all biological progresses such as development, cell differentiation, proliferation, apoptosis and chemo-resistance, so that any abnormality of functional miRNAs may affect the development of organisms, lead to disease and influence therapeutic efficiency. Moreover, miRNA analysis has a number of advantages compared to conventional mRNA analysis. First, owing to its small size, it is less susceptible to degradation and has been successfully extracted from 10 years old FFPE specimens [311]. Secondly, the quality of miRNA expression data from FFPE specimens is equivalent to that from fresh frozen ones [312]. Furthermore, an indication of the potential of miRNAs in cancer diagnosis demonstrated that miRNA expression profiles can distinguish between tumour and normal tissue and can also define the tissue of origin in tumours of diagnostic uncertainty [313].

Given the unsolved issues of melanoma and the importance and advantages of miRNA analysis, the objectives of Chapter 3 and Chapter 4 are:

1) To identify melanoma-specific miRNA diagnostic and prognostic markers.
2) To establish functional miRNAs in melanomagenesis and by connecting to their downstream signalling pathways to begin to identify potential miRNA treatments.

Oncogenic BRAF mutations are frequent in cutaneous melanoma occurring at sites with little or moderate, as opposed to high levels of sun-induced damage. BRAF is a vital coding-gene in the MAPK pathway and a mutant BRAF inhibitor has shown effective therapeutic function in melanoma. In our group we have melanoma Tissue Microarray (TMA) samples available with full clinical records, from both sun-exposed and non-exposed sites and at all pathological stages from naevus to metastasis, as well as a mature method to genotype the V600E BRAF mutation. Therefore, the aims of Chapter 5 are:

1) To genotype BRAF V600E mutation status in melanoma TMA samples.
2) To investigate possible correlation between BRAF mutation status and clinicopathological features.
3) To evaluate whether the BRAF mutation has prognostic value.

Chapter 2: Materials and Methods

2.1 Materials

2.1.1 General reagents and plastic consumables

General laboratory chemicals were purchased from Fisher Scientific (absolute alcohol, methanol, phenol, isopropanol, chloroform, xylene, Na_2EDTA, isoamyl alcohol, potassium acetate, sodium hydroxide, glycerol). Some commonly used solutions were obtained from Medical Research Council, Human Genetics Unit stock, including Dulbecco PBS, dH_2O, 1M Tris pH7.5 and pH8.0, 5M NaCl, 20x TBE, 0.5M EDTA, 5M NaOH. All the general reagents were stored at room temperature unless otherwise indicated.

General plastic consumables were purchased from Greiner Bio One.

2.1.2 DNA isolation reagents

For mammalian cells:
Tail buffer: 10mM Tris-HCl pH8.0, 400mM NaCl, 3mM Na_2EDTA, 1% (w/v) SDS. Stored at 4°C.
Proteinase K stock solution: 2mg/ml proteinase K (Sigma-Aldrich, P2308), 100mM Na_2EDTA, pH 7.5, 2% (w/v) SDS. Stored at -20°C.
PCA: 25 parts redistilled phenol, 24 parts chloroform, 1 part isoamyl alcohol. Stored at 4°C.
CA: 24 parts chloroform, 1 part isoamyl alcohol. Stored at 4°C.

For FFPE samples:
QIAamp® DNA Micro isolation kit and QIAamp Mini Elute column (QIAGEN, 56304). Stored at room temperature/4°C.

2.1.3 RNA isolation reagents

For mammalian cells:
RNA-Bee (AMSBIO, CS-1048-100ml). Stored at 4°C.

For formalin fixed paraffin embedded (FFPE) samples:
RecoverAll™ Total Nucleic Acid Isolation Kit (Applied Biosystems, AM1975). Stored at room temperature/4°C.

2.1.4 PCR reagents and oligonucleotides

Nested PCR and restriction digestion reagents

Polymerase chain reaction (PCR) stock reagents: 5x Clear PCR buffer (Promega, M890A), 25mM $MgCl_2$ (Promega, A351H), 100mM dNTP set (GE Healthcare, 27-203501), GoTaq Flexi DNA Polymerase (Promega, M8305). 5x Green GoTaq® Flexi buffer (Promega, M891A). XbaI (New England Biolabs, R0145S). All stored at -20 °C.

PCR Primers for genotyping BRAF V600E mutation

Custom oligonucleotides were purchased from Sigma-Genosys. Lyophilised oligonucleotides were resuspended in sterile dH_2O to 100pmol/ul stock solution and stored at -20 °C. Working stocks were diluted to 25pmol/ul and stored at -20 °C. Primer details are shown in the following.

Primer	Sequence (5'-3')	Description
BRAF TAQ	CTACTGTTTTCCTTTACTTACTACAC CTCAGA	First round PCR forward primer
BRAF Rev5	CTGATTTTTGTGAATACTGGGAA	First round PCR reverse primer
BRAF XbaI	TAAAAATAGGTGATTTTGGTCTAGC TCTAG	Nested PCR forward primer
BRAF REV	GGCCAAAAATTTAATCAGTGGA	Nested PCR reverse primer

TaqMan® real time reverse transcription-PCR (real time RT-PCR)

For RT-PCR:
TaqMan® MicroRNA Reverse Transcription Kit (Applied Biosystems, PN4366596/4366597). Stored at -20°C.

High Capacity RNA to cDNA Master Mix (Applied Biosystems, PN4390712/4390713). Stored at -20°C.

For real time PCR:
TaqMan® 2X Universal PCR Master Mix, No AmpErase® UNG (Applied Biosystems, PN4324018). Stored at 4°C.

TaqMan® microRNA expression assays and gene expression assays

All the human microRNA expression assays and gene expression assays were purchased from Applied Biosystems. The details are shown in the following table.

TaqMan® Assay name	Applied Biosystems Assay ID	Mature Sequence
miR-92	00430	UAUUGCACUUGUCCCGGCCUG
RNU6B	001093	CGCAAGGATGACACGCAAATTCGTGAAGCG TTCCATATTTTT
miR-200a	000502	UAACACUGUCUGGUAACGAUGU
miR-200b	002251	UAAUACUGCCUGGUAAUGAUGA
miR-200c	002300	UAAUACUGCCGGGUAAUGAUGGA
miR-141	000463	UAACACUGUCUGGUAAAGAUGG
miR-205	000509	UCCUUCAUUCCACCGGAGUCUG
miR-203	000507	GUGAAAUGUUUAGGACCACUAG
miR-20b	001014	CAAAGUGCUCAUAGUGCAGGUAG
miR-675	002005	UGGUGCGGAGAGGGCCCACAGUG
miR-211	000514	UUCCCUUUGUCAUCCUUCGCCU
miR-10b	002218	UACCCUGUAGAACCGAAUUUGUG
miR-214	002306	ACAGCAGGCACAGACAGGCAGU
miR-373	000561	GAAGUGCUUCGAUUUUGGGGUGU
miR-137	000593	UAUUGCUUAAGAAUACGCGUAG
miR-335	000546	UCAAGAGCAAUAACGAAAAAUGU
miR-199a	000498	CCCAGUGUUCAGACUACCUGUUC
let-7b	002619	UGAGGUAGUAGGUUGUGUGGUU
ß-actin	4352935	N/A
E-cadherin	Hs01023894_m1	N/A
Zeb2	Hs00207691_m1	N/A

N/A: Not applicable.

2.1.5 Gel electrophoresis reagents

TBE buffer: 90mM Tris-HCl, 90mM boric acid, 2mM Na_2EDTA, pH8.3.

TBE gel: 3% (w/v) agarose gel, 0.5x TBE buffer, 0.5ug/ml ethidium bromide.

HyperLadder I/V (Bioline, BIO-33025/33031). Stored at 4°C.

2.1.6 Illumina microRNA microarray

Illumina microRNA microarray (Illumina, Catalog # MI 501-1001, Part # 11297743).

2.1.7 Protein detection reagents and antibodies

RIPA buffer: 150mM NaCl, 25mM Tris-HCl pH7.2, 0.1% SDS, 1% Triton X-100, 1% deoxycholate, 1mM Na_2EDTA, 1x Protease inhibitor cocktail tablet (Roche Complete)/25-50ml, 20mM NaF, 100uM orthovanadate.

Bicinchoninic acid (BCA) Assay Kit (Pierce Biotechnology, 23227).

Resolving buffer: 390mM Tris-HCl pH 8.8.

Resolving gel (8-12%): 8-12% acrylamide (40% stock, Severn Biotech Ltd, 2-2400-05. Stored at 4°C.), 1x resolving buffer, 0.1% SDS (20% stock, National Diagnostics, EC-874), 0.1% Ammonium persulphate (APS) (Sigma-Aldrich, 3678), 0.08% TEMED (Sigma-Aldrich, T2281-25ML). Prepared immediately prior to use.

Stacking buffer: 123mM Tris-HCl pH6.8.

Stacking gel (4-8%): 5% acrylamide, 1x stacking buffer, 0.1% SDS, 0.1% APS, 0.1% TEMED. Prepared immediately prior to use.

Running buffer: 192mM Glycine, 25mM Tris, 0.1% SDS pH8.3.

Transfer buffer: 192mM Glycine, 25mM Tris, pH 8.3.

5x Protein Sample buffer: 225mM Tris-HCl pH6.8, 5% SDS, 20% Glycerol, 0.05% (w/v) Bromophenol Blue (Sigma-Aldrich, B-5525).

Dithiothreitol (DTT) (Sigma-Aldrich, D0632). Stored at -20 °C.

TBS: 5mM Tris-HCl, 75mM NaCl, pH7.4.

TBST: 5mM Tris-HCl, 75mM NaCl, 0.05-0.1% (v/v) Tween-20, pH7.4.
Blocking buffer: 5% (w/v) dried skimmed milk, 1x TBST.

Immobilon-P PVDF transfer membrane (Millipore, Billerica, Massachusetts).

Page Ruler™ Plus Prestained Protein Ladder (Fermentas, SM1811), stored at -20°C.

Enhanced chemiluminescence Plus solution (Amersham Biosciences, Buckinghamshire, UK).

Antibodies

Primary antibody				**Secondary antibody**		
Type	**Supplier**	**kDa**	**Dilution**	**Type**	**Supplier**	**Dilution**
Mouse Anti-E-cadherin	BD, 610181	120	1:2500	Rabbit Anti-Mouse	Dako, P0260	1:2000
Mouse Anti-ß-actin	Sigma, 015K-4821	42	1:5000	Rabbit Anti-Mouse	Dako, P0260	1:2000

2.1.8 Mammalian cell lines and cell culture reagents

Mammalian cell lines

Human immortalised melanocyte lines: Hermes1 and Hermes4a immortalised with a telomerase expressing retrovirus [314].

Human malignant melanoma cell lines: A375, C32, G361 and WM115 were obtained from the European Collection of Cell Cultures (ECACC). HBL was obtained from Gentaur (Brussels, Belgium). EDMEL3 was isolated by Ewan Brown from a metastasis removed from a melanoma patient. EDMEL3 early passage cell line (passage 2) and four EDMEL3 subclones and two EDMEL3 xenograft cell lines were obtained and cultured in David Melton's group.

Human ovarian cancer cell lines: PEA2, PEO1, PEO14 and PEO23 were donated by Dr Grant Sellar, Cancer Research Centre, the University of Edinburgh. PEA2: Cisplatin-resistant derivative of human ovarian cancer cell line—PEA1. PEO1: Human ovarian cancer cell line. PEO14: Human ovarian cancer cell line. PEO23: Cisplatin-resistant derivative of PEO14 [315].

General Mammalian cell culture media and reagents

Dulbecco's Modified Eagle Medium (DMEM) (Invitrogen, GIBCO®, 41965). Stored at 4°C.

Fetal Calf Serum (FCS) (Invitrogen, GIBCO®, 16170)

100x Non Essential Amino Acid (NEAA) (Invitrogen, GIBCO®, 11140). Stored at 4°C.

100mM Sodium Pyruvate (Invitrogen, GIBCO®, 11360). Stored at 4°C.

Penicillin-Streptomycin (P/S) liquid (Invitrogen, GIBCO®, 15070-063). Working solution: 50U/ml Penicillin and 50ug/ml Streptomycin. Stored at -20°C.

200mM L-glutamine (100x) (Invitrogen, GIBCO®, 21051-040). Stored at -20°C.

The working media were made according to the requirement of the specific experiments.

PBS: 140mM NaCl, 3mM KCl, 2mM KH_2PO_4, 10nM Na_2HPO_4 pH7.4.

Trypsin-EDTA: 10x trypsin-EDTA (Invitrogen) diluted in PBS to 0.25% (w/v) trypsin, 1mM Na_2EDTA. Stored at -20°C.

Reverse transfection reagents

Opti-MEM® I Reduced Serum Medium (Invitrogen, GIBCO®, 31985-054). Stored at 4°C.

siPORT™ NeoFX™ (Applied Biosystems, AM4510/4511). Stored at 4°C.

Ambion® Pre-miR™ microRNA precursors: hsa-miR-205 (Applied Biosystems, PM11015), hsa-miR-200c (Applied Biosystems, PM11714), hsa-miR-211 (Applied Biosystems, PM10168). Stored at -20°C.

Ambion® Anti-miR™ microRNA inhibitor: hsa-miR-20b (Applied Biosystems, AM10975). Stored at -20°C.

FAM™ dye-labeled Anti-miR™ Negative Control #1 (Applied Biosystems, AM17012). Stored at -70°C.

FAM™ dye-labeled Pre-miR™ Negative Control #1 (Applied Biosystems, AM17121). Stored at -70°C.

Cell cycle assay reagents

Citrate buffer stock solution: 2000mg trisodium citrate (BDH Laboratory Supplies, 301287F), 121mg Tris Base (Sigma-Aldrich, T1378), 1044mg spermine tetrahydrochloride (Sigma-Aldrich, S2876), and 2ml nonidet NP40 (Sigma-Aldrich, N3516), pH 7.6, in 2000ml dH_2O. Stored at 4°C.

Solution A: 10mg trypsin type IX-S (Sigma-Aldrich, T0303) in 500ml dH_2O, pH7.6. Stored at 4°C.

Solution B: 250mg trypsin inhibitor (Sigma-Aldrich, T9253) and 50mg RNase A (Sigma-Aldrich, R4875) in 500ml dH_2O, pH 7.6. Stored at 4°C.

Solution C: 208mg propidium iodide (Sigma-Aldrich, 81845) and 500mg spermine tetrahydrochloride (Sigma-Aldrich, S2876) in 500ml dH_2O, pH 7.6. Stored at 4°C.

Sulforhodamine B (SRB) assay reagents

25% Trichloracetic acid (TCA) solution: by dilution of 100% TCA solution (Sigma-Aldrich, T4885-500G). Stored at 4°C.

1% acetic acid solution: by dilution of 20ml of Glacial Acetic Acid (BDH, 10001 6x) into distilled water to a final volume of 2 litre.

0.4% SRB solution: by dissolution of 2g of SRB (Sigma-Aldrich, S9012-5G) in 1% acetic acid solution to a final volume of 500ml. Stored at 4°C.

10mM Tris solution pH 10.5: by dissolution of 1.21g of Tris base in water to a final volume of 1 litre with addition of HCl to pH 10.5. Stored at 4°C.

Cisplatin (Faulding DBL, 100mg/100ml).

Transwell migration assay materials

Matrigel™ Basement Membrane Matrix (BD Biosciences, 354234). Stored at -20°C.

Transwell inserts (Corning Inc, 3422).

Calcein-AM (Biotium, 30026). Stored at -20°C.

Colony formation assay reagents

2x Minimum Essential Medium (MEM) (Invitrogen, GIBCO®, 21935). Stored at 4°C.

2.8% (w/v) Methylcellulose (RD system, HSC001). Stored at -20°C.

UltraPure™ Agarose (Invitrogen, 15510-027).

2.1.9 Human tissue samples

For Chapter 3, 18 benign naevi (archived between 2005 and 2006) and 21 metastatic melanoma samples (archived between 1993-1997) were cored (∅2mm cores) from Formalin Fixed Paraffin Embedded (FFPE) blocks by Bob Morris. Primary melanoma tissues (archived between 1992-1997) were obtained from macrodissection of 10μm sections of FFPE blocks. All the tissue blocks were marked by pathologist, Thomas Brenn.

For Chapter 5, 115 primary and 29 metastatic melanoma FFPE samples with complete clinical records were obtained from Ewan Brown's tissue microarray (TMA) panel. Cores from the above sample blocks are ∅0.6mm.

Clinicopathological data were collected using the Scottish Melanoma Group (SMG) database. FFPE benign naevi, primary and metastatic melanoma specimens were obtained with local ethics committee approval from the Pathology Department, Royal Infirmary, Edinburgh.

2.1.10 Macrodissection reagents and materials

Plain glass slides without any charge or adhesive (VWR International).

Nuclear Fast Red stain (Sigma-Aldrich, N3030-100ml, 0.1% solution in 5% aluminium sulphate).

Razor blades (Swann-Morton, Ref 0505).

RNaseZap (Applied Biosystems, AM-9780/9784).

Digestion buffer (Applied Biosystems, AM1975).

2.1.11 Equipment and software

Equipment

Bio-Rad PCR Thermal Cycler DNA Engine TETRAD2.

Stuart Orbital Shaker SSL1.

Whirlmixer™ Fisons SGP-202-010J.

Sanyo CO_2 Incubator MCO-17A.

Centrifuges: Eppendorf Germany 5415R and 5702, Hettich Mikro 20, Heraeus Multifuge 3S-R, Sorvall® Microspin 24S.

Labtech Thermo Nanodrop 2000 spectrophotometer.

Grant Instrument (Cambridge) Ltd. Water Bath, TYPE JB1.

Grant Instrument (Cambridge) Ltd. Heat block, BT3.

Microscope: Leica TYPE 090-135.001 (Cell culture), Nikon Eclipse Ti.

HYBAID Oven, MINI 10.

SCIE-PLAS Electrophoresis system.

Bio-Rad Gel Doc 2000.

Bio-Rad Protein Mini-PROTEAN3™ electrophoresis system.

Beckman Coulter Counter Z series.

Thermo ELECTRON CORPORATION Multiskan Spectrum.

Fisher Scientific Bio-TEK plate reader, synergy HT.

Applied Biosystems HT7900.

Confocal Leica SP5 with Laser lines: 488nm, Objectives: 10x 0.4 N.A (ECRC).

GE Image Quant LAS 4000.

Heraeus HERAsafe Biological Safety Cabinet HS 12.

Software

SDS 2.3/RQ manager 1.2 for real time PCR data analysis.

GenomeStudio™ Gene Expression Module v1.0 and R 2.9.2 for microarray data analysis.

Cluster 3.0/TreeView for Hierarchical Clustering analysis.

Flow Jo 7.6.1 for cell cycle analysis.

Image J 1.43u for methylcellulose assay, transwell migration assay and western immunoblotting quantification.

GraphPad Prism Version 4.0b for general statistics.

2.2 Methods

2.2.1 DNA isolation and DNA based experiments

DNA isolation from mammalian cell lines

Genomic DNA of all cultured mammalian cells was isolated using the same method. Cells were plated in a 60-100mm dish prior to DNA isolation. When cells were ready, the medium was discarded and cells were washed once with 10ml of PBS. Cells were scraped from the dish in another 3ml of PBS and were transferred to two 2ml-eppendorf tubes and cells were pelleted. Then 750ul of tail buffer and 15ul of proteinase K (20mg/ml) were added to each tube and the mixture was incubated overnight at 37°C. Protein and lipid were removed from the DNA solution by two extractions with 750ul PCA, followed by a 750ul CA extraction. In each case the phases were mixed by vigorous shaking, separated by centrifugation and the aqueous

phase was transferred to a fresh tube without disturbing the interphase. The genomic DNA was precipitated by adding 750ul of isopropanol and centrifuged at top speed for 6 minutes. The DNA pellet was then washed twice with 70% ethanol, air-dried, resuspended in sterile dH_2O and stored at -20°C.

DNA isolation from FFPE samples

Primary and metastatic melanoma FFPE sample cores (2-3 cores/tube) were de-paraffinised with 1ml xylene. Following centrifugation, the xylene was discarded and the samples were washed with absolute alcohol and air-dried. DNA was extracted from the deparaffinised tissue using the QIAamp® DNA Micro isolation kit and following the manufacturer's protocol. Briefly, samples were resuspended in 15ul ATL (a buffer with proteinase K to lyse samples) buffer and 10ul proteinase K solution supplied from the kit, mixed thoroughly and incubated at 56°C overnight. 25ul of ATL and 50ul of buffer AL (a buffer to allow optimal binding of DNA to the membrane), followed with 50ul of absolute alcohol were added and after incubation at room temperature for 5 minutes the samples were added to QIAamp MiniElute columns and centrifuged at 6,000g for 60 seconds. The columns were washed by 500ul AW1 (washing buffer 1 for clean up of genomic DNA) and 500ul AW2 (washing buffer 2 for clean up of genomic DNA) buffers respectively and centrifuged at 6,000g for 60 seconds again. DNA was eluted in 25ul sterile dH_2O by centrifugation at 20,000g for 60 seconds. (ATL, AL, AW1, AW2 supplied from the kit).

Measurement of DNA concentration

DNA samples were measured using the Thermo Nanodrop spectrophotometer. Sterile dH_2O was used to blank the Nanodrop spectrophotometer and the DNA50 parameter was chosen. Then 1.5-2.0ul of each sample was added to the Nanodrop spectrophotometer and the software gave the concentration of each sample and the

OD260/280 ratio. The OD260/280 ratio provides a measure of the purity of nucleic acid solutions and the extent of protein contamination. Ratios between 1.75 and 1.9 are regarded as acceptable for DNA. DNA50: for double stranded DNA, when OD260=1, DNA concentration is 50ug/ml.

Nested PCR and restriction digestion for genotyping BRAF V600E mutation

Routine PCRs were prepared in a 50ul volume containing 5x PCR buffer, 25mM $MgCl_2$, 5mM dNTP, 1U Taq DNA polymerase, 25pmol/ul forward and reverse primers and ~100ng genomic DNA template. A negative control containing no DNA template was present each time. Nested PCR is a modification of the basic PCR procedure intended to reduce the contamination in low abundance products due to the amplification of unexpected primer binding sites. The specific nested PCR programmes were as follows:

	First round		Second Round (nested)	
Step1:	1x	94°C 4 minutes	1x	94°C 4 minutes
Step2:	35x	94°C 30seconds	35x	94°C 30seconds
		61°C 30seconds		58°C 30seconds
		72°C 30seconds		72°C 30seconds
Step3:	1x	72°C 5minutes	1x	72°C 5minutes
Step4:		10°C ∞		10°C ∞
	Product: 275bp		Product: 134bp	

XbaI restriction fragment length polymorphism (RFLP) analysis

Restriction digests contained 2-4U restriction enzyme per 1ug DNA and the XbaI reaction buffer supplemented with 100ug/ml BSA. Restriction digests were incubated at 37°C for a minimum of 2 hours.

Cut control		Uncut control	
PCR DNA	15ul	PCR DNA	15ul
10X Buffer	3ul	10X Buffer	3ul
XbaI	2ul	dH_2O	12ul
dH_2O	10ul		

Incubate at 37°C for 2 hours
Product: 105bp if BRAF V600E mutation is present.

Digests, cut control (positive control) and uncut control (negative control) samples were loaded onto a 2-3% agarose gel.

Assessment of sensitivity of genotyping method

A heterozygous BRAF V600E mutation positive melanoma cell line—G361 (mutant) and a BRAF mutation negative ovarian cancer cell line—PEO1 (wild type) were used to test the sensitivity of the assay. First, 1, 2 and 3ul of the two genomic DNAs were run on a gel to confirm their relative DNA concentrations. Secondly, DNA solutions of the two cell lines were diluted until they were at a similar concentration to the DNA concentrations of the FFPE samples. Thirdly, different amount of DNA from the BRAF V600E wild type cell line and from thr BRAF mutant cell line were mixed in ratios 100:0, 90:10, 80:20, 50:50, 0:100 so that the total amount of DNA in each mixture was the same. Finally, the nested PCR and restriction digestion assays were run to see what was the lowest ratio of BRAF V600E containing DNA that could be detected in the presence of wild type DNA.

Gel electrophoresis

DNA fragments were separated on 2-3% (w/v) agarose gels containing 0.5ug/ml ethidium bromide and 0.5x TBE. DNA samples were mixed with sample buffer prior to loading. Electrophoresis was carried out at 30-100V in 0.5x TBE buffer. DNA was visualized by UV illumination and Hyperladder I/V^{TM} was used as a size marker.

2.2.2 RNA isolation and RNA based experiments

RNA isolation from mammalian cell lines

Prior to total RNA isolation, cells in plates/dishes were washed with PBS twice. Total RNA was then isolated from cultured mammalian cell lines using the reagent RNAzol^{TM}B. Cultured cells were lysed directly in the culture dish by the addition of RNAzol^{TM}B (0.2ml/10^6 cells) and lysate was mixed by pipetting several times. The RNA was extracted by the addition of 0.2ml chloroform/ml of RNAzol^{TM}B followed by vigorous shaking of the mixture for 30 seconds. The emulsion was then centrifuged at 12,000g for 15 minutes at 4°C. The aqueous phase was transferred to a fresh tube and an equal volume of isopropanol was added. RNA was allowed to precipitate at room temperature for 10 minutes and was then pelleted by centrifugation at 12,000g for 5 minutes. The RNA pellet was then washed in 70% ethanol and centrifuged at 7500g for 5 minutes. The pellet was allowed to air dry before being resuspended in 100-150ul of sterile dH_2O for storage either at -20°C in the short term, or at -70°C for longer periods.

Macrodissection

All the sections for macrodissection were cut, mounted and stained by Helen Caldwell. The first three 3um sections were discarded from each block. Then 15 10um sections were cut with a 3um section between every three 10um sections. The 3um sections were used for H&E staining. 10um sections were stained using Nuclear Fast Red for dissection. After sections were cut and mounted on glass slides and stained either using H&E or Nuclear Fast Red, all slides were dried in an oven.

The specific area for dissection was marked by Thomas Brenn on the H&E slides. The Nuclear Fast Red stained slides were placed on the microscope stage and the melanocytic cells were scraped with a razor blade that had been slightly moistened with Digestion buffer. Non-tumour elements, such as lymphocytes, blood vessels

and connective tissues were avoided. The scrapings were removed with a fine sterile pipette tip, and placed in a microfuge tube containing 100-200ul Digestion buffer. The above scraping steps were repeated from additional 10um sections until the Digestion buffer in the tube became pink in colour with the stained scrapings.

RNA isolation from melanocytic tissue samples

Melanocytic FFPE samples were isolated using the RecoverAll™ Total Nucleic Acid Isolation Kit with the guidance of the protocol. The recovered nucleic acids with this kit are suitable for downstream applications such as microarray analysis, quantitative real-time RT-PCR, and mutation screening. Briefly, the FFPE samples (3-4 cores or scrapings from 15 sections per tube) were de-paraffinised with 1ml 100% xylene, mixed and incubated at 50°C for 3 minutes. Xylene was then discarded after centrifugation at top speed for 2 minutes. The sample pellet was washed twice with 1ml absolute alcohol and air-dried. Digestion buffer and protease were added to the pellet and incubated at 50°C for 15 minutes and then 80°C for 15 minutes. Isolation additive/ethanol mixture was then added and mixed. The whole mixture was passed through a Filter Cartridge and washed with 700ul of Wash1 and 500ul of Wash2/3. After centrifugation to remove residual fluid, DNase solution was added to each Filter Cartridge and incubated for 30 minutes at room temperature. The Cartridge was then washed with Wash1 and Wash2/3 again and RNA was eluted in sterile dH_2O for storage either at -20°C in the short term, or at -70°C for longer periods.

Measurement of RNA concentration

RNA samples were measured using the Thermo Nanodrop spectrophotometer. Sterile dH_2O was used to blank the Nanodrop spectrophotometer and the RNA40 parameter was chosen. Then 1.5-2.0ul of each sample was added to the Nanodrop spectrophotometer and the software gave the concentration of each sample and the OD260/280 ratio. The OD260/280 ratio provides a measure of the purity of nucleic

acid solutions and the extent of protein contamination. Ratios between 1.8 and 2.0 are regarded as acceptable for RNA. RNA40: for single stranded RNA, when OD260=1, RNA concentration is 40ug/ml.

TaqMan real time reverse transcription PCR (real time RT-PCR)

I used 10-100ng of total RNA per 15ul RT Reaction. All kit components and RNA samples were allowed to thaw on ice.

1) RT-PCR

Each 15ul reaction consists of 7ul RT master mix (including 0.15ul dNTP, 1.00ul reverse transcriptase, 1.50ul reverse transcriptase buffer, 0.19ul RNase inhibitor, 4.16ul Nuclease-free water), 3ul primer, and 5ul RNA sample. After the above components were added into a 0.2ml polypropylene tube, the tube was sealed and mixed gently. The solution was spun down to the bottom of the tube. Then the tube was incubated on ice for 5mins and kept on ice until it was ready to load the thermal cycler. The RT-PCR programme was as follows:

Step1: 16°C 30 minutes
Step2: 42°C 30 minutes
Step3: 85°C 5 minutes
Step4: 4°C ∞

2) Real time PCR

Each 20ul mixture consists of 1.00ul 20X TaqMan® MicroRNA and mRNA Assay, 1.33ul of RT product, 10.00ul of TaqMan® 2X Universal PCR Master Mix-No AmpErase® UNG, 7.67ul of Nuclease-free water. To avoid pipetting many small amount of components, a master mix sufficient for triplicate assays on all samples was prepared, including 10% extra volume to account for pipetting losses, in the same tube. The solution was mixed gently and centrifuged to the bottom of the tube. Then the whole mixture, including primer and RT products, was added into a plate

and sealed with an optical adhesive cover (Bio-Rad Microseal® 'B' Film, MSO1001) followed with brief centrifugation of the plate and elimination of any air bubbles. The plate was then loaded onto the real time PCR instrument (Applied Biosystems HT7900). The real time PCR programme was as follows:

Step1: 1x 95°C 10 minutes
Step2: 40x 95°C 15 seconds
60°C 1 minutes

qPCR quantification method

There are two major methods to quantify changes in RNA levels using real time PCR. One is absolute quantification and the other is relative quantification. The former is better to accurately determine an unknown gene's absolute amount. Relative quantification is more suitable to compare expression of the same gene between different samples.

In relative quantification, the standard curve method and comparative Ct method (ΔΔCt method) are two commonly used strategies. In relative quantification, for quantification normalized to an endogenous control, standard curves are prepared for both the target and the endogenous reference. For each experimental sample, the amount of target and endogenous reference is determined from the appropriate standard curve. Then, the target amount is divided by the endogenous reference amount to obtain a normalized target value. Again, one of the experimental samples is the calibrator. Each of the normalized target values is divided by the calibrator normalized target value to generate the relative expression levels. The standard curve method is a time-consuming process and dilution must be accurate.

The comparative Ct method, another quantification approach, involves comparing the Ct values of the samples of interest with a control or calibrator such as a non-treated sample or RNA from normal tissue. The Ct values of both the calibrator and

the samples of interest are normalized to an appropriate endogenous housekeeping gene. The comparative Ct method is also known as the $2^{-\Delta\Delta Ct}$ method, where $\Delta\Delta Ct = \Delta Ct_{sample} - \Delta Ct_{reference}$. Here, ΔCt_{sample} is the Ct value for any sample normalized to the endogenous housekeeping gene and $\Delta Ct_{reference}$ is the Ct value for the calibrator also normalized to the endogenous housekeeping gene.

Validation of amplification efficiency for the ΔΔCt calculation

For the ΔΔCt calculation to be valid, the amplification efficiencies of the target and the endogenous reference must be approximately equal. This can be established by looking at how ΔCt varies with template dilution. If the plot of cDNA dilution versus delta Ct is close to zero, it implies that the efficiencies of the target and endogenous control genes are very similar. A slope in the plot of log input amount (RNA/DNA dilution factor) versus ΔCt <0.1 passes this equivalent efficiency test [316]. This method increases throughput and eliminates dilution errors. However, if an endogenous control gene cannot be found whose amplification efficiency is similar to the target, then the standard curve method is preferred.

In my study, amplification efficiency of various target miRNAs and mRNAs were validated using the standard curve method with dilution factors of 2 and 4, respectively.

Illumina microRNA microarray

The microRNA microarray was done in the Genetics Core of the Wellcome Trust Clinical Research Facility, Western General Hospital by Lee Murphy. A brief workflow is shown in Chapter 3.2.2.1.

2.2.3 Protein extraction and protein detection

Protein extraction

Cells were first washed with cold PBS and then scraped into 1ml of cold PBS in a 1.5ml eppendorf tube, followed by centrifugation at 3,000rpm for 3 minutes to form a pellet. The cell pellet was resuspended in 50-200ul RIPA lysis buffer and maintained on ice for 15-30 minutes. The suspension was centrifuged at 13,000rpm for 15 minutes at 4°C and the supernatant was collected and stored at -70°C.

Measurement of protein concentration

Protein concentrations were determined using the BCA™ Assay Kit in a 96-well plate. The original lysates were diluted 10-fold in dH_2O to a final volume of 25ul. dH_2O was used as a blank control. 200ul of working reagent from the kit was added to each sample and incubated at 37°C for 30 minutes. The plate was then scanned using a plate Spectrophotometer at 562nm. Concentrations of samples were calculated using the standard curve generated from known BSA standards and the dilution factor.

SDS polyacrylamide gel electrophoresis (SDS-PAGE)

Proteins with different molecular weight were separated by discontinuous SDS-PAGE. The concentration of polyacrylamide in the resolving gel was determined by the molecular weight of proteins. First, a 10-12% resolving gel (used for protein weights between 30kDa-200kDa) was made to separate the proteins. The resolving gel was overlaid with isopropanol to remove air bubbles and give an even gel surface prior to polymerisation at room temperature. After the isopropanol was discarded the stacking gel was added and a comb was inserted. The comb was removed after the stacking gel was set and the gel cassette was assembled into the Mini-PROTEAN3™

electrophoresis module and immersed in the running buffer. Appropriate amounts of protein samples were mixed with 4x sample buffer and were heated at 95°C for 5 minutes before loading onto the gel along with a Prestained Protein Ladder. Proteins were separated by electrophoresis at 80V for the stacking gel and 150V for the resolving gel.

Western immunoblotting

Proteins were electrophoretically transferred onto an Immobilon-P PVDF transfer membrane in transfer buffer according to the method of Towbin [317]. The transfer was completed by using a Mini Trans-Blot system (Bio-Rad) at 100V, constant voltage at 4°C with an ice block for 1 hour. Then the membrane was taken out and rinsed in TBST for 5 minutes and subsequently was blocked in the blocking buffer for 1 hour. The membrane was incubated overnight at 4°C with primary antibody that had been diluted in the blocking buffer. After washing 3 times (5-10 minutes/wash) in TBST, the filter was incubated with secondary antibody at room temperature for 1 hour. Unbound antibodies were washed away by 3 TBST rinses. Finally, the membrane was overlaid with ECL Plus for 1 minute. Immunoreactive bands were visualized either by autoradiography or using the ImageQuant LAS 4000 system (GE, ImageQuant) to make an electronic record.

2.2.4 Cell culture and cell based experiments

General culture conditions for mammalian cell lines

The cell culture medium was pre-warmed to 37°C before frozen stocks of mammalian cells were defrosted. The frozen cell stock was then quickly thawed in a 37°C water bath. 5ml medium was added and mixed with a cell suspension. A cell pellet was then formed by centrifugation at 1,300 rpm for 5 minutes. A single cell

suspension was prepared in fresh medium and transferred to appropriate flasks for culture. Flasks were incubated at 37°C in 5% CO_2.

When the cells were confluent, the medium was removed and trypsin-EDTA was added to the flasks (1ml/25cm^2 flask) for 5 minutes. Trypsin is a serine protease that can make adhesive cells detach from the culture surface. 4ml fresh medium was added to the cell-trypsin suspension and the mixture was then centrifuged at 1,300 rpm for 5 minutes to form a cell pellet. The cell pellet was resuspended in an appropriate volume of fresh medium, either for a future culture or for downstream work. As commonly used mammalian adherent cell lines divide approximately once every 24 hours, the cells were passaged to 12.5-25% confluency. Passaging was routinely carried out once every 2-4 days.

Cryopreservation of cell lines

Cells were trypsinised and a cell pellet was made by centrifugation at 1,300 rpm for 5 minutes and was then resuspended in cell culture medium containing 10% (v/v) DMSO and 20% FCS (cells from a 10cm diameter area were resuspended in 1ml total volume). The use of DMSO increases the survival of cells during freezing and thawing by minimising the formation of ice crystals within the cells. Prior to transferring cell stocks to a liquid N_2 cryostore for indefinite storage, the cell stocks were stored at -20°C for 1 hour and then at -70°C overnight.

Cell counting

Cells were diluted 1:100 in isoton (Coulter Isoton® II dilents) and counted using the Coulter Counter Z series.

Lipid-based reverse transfection

In traditional transfection of adherent cells, the amount of exposed cell surface, and not the number of transfection complexes, is the limiting factor to transfection efficiency [318]. Reverse transfection is believed to increase cell exposure to transfection complexes, often leading to greater transfection efficiency.

Reverse transfection (also called Neofection), developed by Ambion, is a more streamlined transfection method. Reverse transfection involves simultaneously transfecting and plating cells, much like products used for transfecting suspension cells. siPORT NeoFX Transfection Agent and RNA are mixed, incubated, distributed to culture wells, and overlaid with cells. The method produces equivalent or improved transfection efficiency over the standard pre-plated method for many of the cell types tested and saves an entire day in the process [318]. siPORT NeoFX Transfection Agent is a lipid-based formulation that provides extremely high levels of transfection without inducing cellular stresses common to other transfection agents.

Prior to the specific experiments, the best transfection efficiency was assessed using mixtures of different volumes of siPORT NeoFX and the negative control small RNA. Assessment of transfection efficiency is described in the next section.

The brief procedure for the specific transfections in my project was as follows: I used two types of tissue culture plate for transfection, 12-well and 6-well. First, melanoma cells were trypsinised and diluted in normal growth medium to 10^5 cells/ml. Cells were set aside at 37°C in the incubator while the transfection complexes were prepared. Appropriate volumes of siPORT NeoFX were diluted in OPTI-MEM I medium and incubated for 10 minutes at room temperature. Then appropriate amounts of small RNAs (precursors and inhibitors of specific microRNAs) were diluted into OPTI-MEM I medium. Diluted siPORT NeoFX and diluted small RNA were mixed and incubated for 10 minutes at room temperature and dispensed into a culture plate. Finally, the prepared cell suspensions were placed onto the siPORT

NeoFX/small RNA complexes and the plates were put into the incubator. The medium in each well was replaced daily with fresh normal culture medium.

Assessment of transfection efficiency

FAM™ dye-labeled Pre-miR™ Negative Control is a carboxyfluorescein (FAM™)-labeled double-stranded RNA oligonucleotide designed for monitoring uptake of Pre-miR™ microRNA precursors by fluorescence microscopy or flow cytometry.

FAM™ dye-labeled Anti-miR™ Negative Control is a carboxyfluorescein (FAM™)-labeled RNA oligonucleotide designed for monitoring uptake of Anti- miR™ microRNA inhibitors by fluorescence microscopy or flow cytometry.

Different volumes for siPORT NeoFX and FAM dye negative control were sequentially mixed and transfected to melanoma cells. Cells were examined using Fluorescence-activated Cell Sorting (FACS) at several times (24-hour, 48-hour and 72-hour) after transfection to obtain the best match of siPORT NeoFX and small RNA that produced the highest transfection efficiency. Results are shown in Chapter 4.2.1.

Final concentration of the small RNA used: 30nM for precursors, 150nM for inhibitors. Final volumes of siPORT NeoFX: 8ul/well in 12-well plates, 16ul/well in 6-well plates.

Cells were transfected with small RNAs for 16-18 hours prior to the downstream experiments, including cell proliferation, cisplatin sensitivity, methylcellulose formation and transwell migration assay.

Cell cycle

Cells were trypsinised and harvested as described above. The cell pellet was washed with PBS and centrifuged. The new cell pellet was then resuspended in 100ul citrate buffer and stored at -20°C until the day of the FACS assay. Prior to doing FACS, the cell suspension in citrate buffer was first treated with an appropriate volume of solution A for 2 minutes to lyse the cell membrane and then treated with an appropriate volume of solution B for 10 minutes to stop the effect of solution A. After a further 10 minutes of solution C treatment, the samples were ready for flow cytometry. All the FACS assays were done by Elizabeth Freyer and I analysed the data using Flow Jo software. 24-hour, 48-hour and 72-hour time courses were examined after transfection.

Cell proliferation (SRB assay)

Cells were plated at a density of 1,000-1,500 cells/well in 96-well plates in normal growth medium. Each experimental group had 16 replicates. The plates were assayed over four days at 24-hour, 48-hour, 72-hour and 96-hour. For the assay, 50ul of 25% (v/v) TCA was added to each well of the plates and incubated at 4°C for at least 1 hour. Plates were washed with slow-running tap water for 10 times and air-dried. Then 50ul of 0.057% (w/v) SRB solution was added to the plates and incubated at room temperature for 30 minutes, and then rinsed for four times with 1% (v/v) 150ul of acetic acid to remove unbound dye and air-dried. 150ul of 10mM Tris solution (pH 10.5) was then added to each well and the plates were incubated at room temperature for 60 minutes with agitation to solubilise the protein-bound dye. Plates were read using a plate reader at OD 510nm.

Cisplatin sensitivity assay (SRB assay)

Prior to seeding cells to 96-well plates, different amounts of cisplatin were prepared to make final concentrations at 0uM, 0.1uM, 0.3uM, 0.6uM, 1uM and 3uM. The following procedures were the same as described in the cell proliferation SRB assay. Cells were fixed at Day 5.

Transwell migration assay

An inverse invasion assay was used to test cell migration ability. The method is a modified version of the one devised [319] by Margaret Frame's group at the Edinburgh Cancer Research Centre. In brief, an aliquot of Matrigel was thawed slowly on ice. Ice-cold PBS and the Matrigel were mixed 1:1 and 100ul of the mixture was added to each Transwell that was later inserted into a 24-well plate. The plate was incubated for at least 30 minutes at 37°C to allow the Matrigel to set. During this time, 10^5-$4x10^5$/ml cell suspensions were prepared in their normal growth medium. When the Matrigel was set, the Transwells were inverted on the lid of the plate and 100ul of cell suspension were added onto the underside of the filter of the each Transwell. The Transwells were carefully covered with the base of the plate such that it contacted the droplet of the cell suspension. The inverted plate was put into the incubator for 2-4 hours to allow the cells to attach to the filter. The plate was turned right-side-up after incubation. Each Transwell was dipped sequentially into 3x1ml serum free medium to wash away the unattached cells. The Transwells were left in the third change of serum free medium and 100ul of normal growth medium with serum were added into each Transwell on top of the Matrigel. (In this case, there was DMEM with serum only in the Transwell not in the well-chamber. Therefore, cells should migrate through the Matrigel towards the serum.) The plate was then put back to the incubator for 5 days.

After 5 days of incubation, fixation and staining of the Transwells were done prior to confocal microscope scanning. The procedure was as follows: For n Transwells,

(n+1) ml of serum free medium was put into a universal and (n+1) ul of Calcein-AM was added [320]. 0.5ml of this mixed solution was added to each of the n wells of the plate. The n Transwells were put into the n wells of the plate. Another 0.5ml of the mixture was then added into the top of each Transwell. The plate was put into the incubator for at least 1 hour and then examined immediately on the confocal microscope.

Horizontal z-sections through the Matrigel were examined at 10-15μm intervals using a Leica confocal microscope to assess how far the cells had migrated from the bottom layer of the Matrigel towards the top layer (Figure 2.1). The bottom layer is adjacent to the filter of the Transwell. Therefore, it contains the most cells and has the brightest fluorescence. The middle layer contains less cells compared to the bottom layer so that it has less fluorescence. The top layer indicates the layer that has no cells and so no fluorescence. The further and the more cells that migrate, the stronger the invasive ability the cells have. For each Transwell, 3-5 different fields at each layer were randomly picked and scanned as replicates of each group. Data were analysed using Image J to quantify cell invasive ability through both distance of migration and number of migrated cells.

3D confocal microscope scanning model

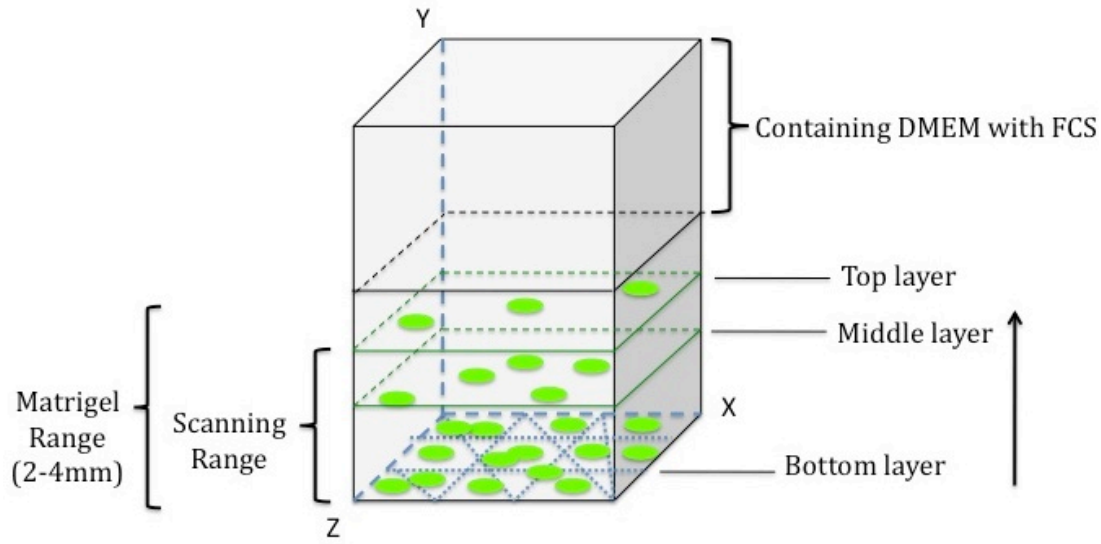

Figure 2.1 The 3D confocal microscope scanning model. The cube represents a Transwell. X, Y, Z represent the three dimensions respectively. The green round circles represent cells at different layers. Bottom layer: lots of fluorescent cells; Middle layer: reduced number of fluorescent cells; Top layer: very few fluorescent cells. Black arrow represents the scanning direction from bottom to top.

Colony formation assay

The methylcellulose assay was used to test the colony formation ability of tumour cells. This is a recognised *in vitro* surrogate assay for *in vivo* tumourigenicity and has been described to support colony formation of various human tumours [321]. In brief, 1.8% (w/v) agarose solution was made and boiled. The melted agarose solution was diluted 1:1 in fresh 2x MEM medium supplemented with 10% FCS, NEAA, Sodium Pyruvate, P/S and L-glutamine. 2ml of the mixture was then quickly poured into each well of a 6-well plate and left aside until solid. During this time, 2.8% Methylcellulose solution was prepared in MEM medium using 2x MEM with the same supplements. An appropriate number of cells were mixed with the methylcellulose solution and 2ml of the mixture was poured onto the bottom agarose base. $5x10^3$-10^4 cells were seeded in each well. The 6-well tissue culture plates were incubated at 37°C in 5% CO_2 for 9-12 days.

Images of colonies were taken at Day1, Day3, Day6, Day9, Day12. About 30 colonies of each experimental group were used in calculation of colony size. Data were analysed using Image J. Images of entire wells were also taken on the Gel Doc so that colony number could be determined.

2.2.5 Statistics

All the statistical analysis was done using Prism except for analysis of microarray results. T-test and One-way ANOVA for Chapters 3 and 4. Chi-square, Fisher's exact and Kaplan Meier survival for Chapter 5. P=0.05 was used as the significance

level, except where the Bonferroni correction was applied. All the statistical tests are two-sided.

Data analysis of microarray was done using R language and Cluster 3.0 and TreeView. More information on statistical analysis of the microarray data is described in Chapter 3.2.2.3.

Chapter 3: Expression screen for melanoma-specific microRNAs in FFPE tissues

3.1 Introduction

A study by Rosenfeld *et al.* showed that microRNAs (miRNAs) can accurately identify cancer tissue origin [322], indicating that miRNA profiling in cancer diagnosis may be superior to mRNA gene signatures. Besides its diagnostic advantages, the miRNA expression profile is found to correlate with survival in cancer patients. Given the tremendous regulatory potential of miRNAs and their often tissue-specific and disease-specific expression patterns [295, 323], several unique miRNA expression profiles have been found to be associated with bio-molecular and prognostic characteristics of human lung cancer, chronic lymphocytic leukemia and ovarian cancer [283, 293, 324], indicating that miRNA signatures could be used to define biological or clinical features of human cancers.

When this study started there were only a very limited number of studies investigating melanoma-specific miRNA expression patterns and their role in cutaneous melanoma. The first two expression profiling studies identified a set of 17 miRNAs that were expressed significantly differently in eight melanoma cell lines compared to other cancer cell lines [325, 326]. A following microarray-based miRNA profiling studied, carried out only on melanocytes and melanoma cell lines derived from either primary or metastatic melanomas, discovered a number of miRNAs differentially expressed in melanoma cells compared to melanocytes [327]. However, the above differentially expressed miRNAs from the literature were obtained from cell-based microarray, not from tissue profiling. Moreover, there was no miRNA expression profile available based on tissue samples to interpret the roles of these miRNAs in the progression of melanoma systematically and investigate their prognostic value using different stages of melanocytic lesions. Therefore, the main aims of this chapter are: first, to identify a melanoma-specific miRNA expression profile on tissues; secondly, to obtain miRNA candidates as biomarkers of melanoma; thirdly, to pinpoint potential miRNAs which might be acting in the key regulatory pathways in the pathogenesis of cutaneous melanoma.

What is the best way to detect miRNA expression? What type of samples can bring

the most benefits for this study? These are the initial questions to be answered. As described in Chapter 1, there are different methods to detect miRNA expression such as northern blotting, quantitative RT-PCR (qRT-PCR or real time RT-PCR), and microarray. Microarray has the advantage in detecting expression of thousands of miRNAs in multiple samples, making it ideal for large screening experiments. The Illumina miRNA expression profiling assay uses human- and mouse- specific panels containing the most current content for profiling miRNA expression in a highly multiplexed assay with flexible multi-sample readout formats. It has several advantages, such as its high sensitivity, low sample input (100-200ng of total RNA which is very important due to the low harvest of total RNA from FFPE samples), robust nature and high specificity. The human miRNA panel contains 1,146 assays including seven types of built-in control probes, for detecting more than 97% of the miRNAs described in the miRBase database [328]. This assay takes advantage of enzymatic primer extension in addition to hybridization to achieve high mismatch discrimination. It has been reported that the Illumina BeadArray platform has the highest built-in feature redundancy of any currently available array, which further increases reproducibility and improves the signal-to-noise ratio [329]. The methodology of the Illumina Beadarray panel is a modification of an assay developed previously for high-throughput gene expression profiling, the DASL_ Assay (cDNA-mediated annealing, selection, extension and ligation) [329]. This assay could distinguish between individual miRNAs within families and could analyze the expression of 735 human miRNAs from the miRBase. The 735 target miRNAs included 470 well-annotated human miRNA sequences (miRBase: http://microrna.sanger.ac.uk/, version 9.1, February 2007 Release) and 265 miRNAs identified later [330, 331]. Expression profiles obtained by the method are highly comparable to that obtained by qRT-PCR and direct sequencing [332]. Finally, this method, in conjunction with the 96-sample array matrix should prove useful for high-throughput expression profiling of miRNAs in large numbers of tissue samples simultaneously [332].

However, microarray technology is only semi-quantitative and cannot distinguish between highly homologous mature miRNAs within a family accurately because of

its inability to optimize hybridization conditions for all miRNAs [333], although the use of locked nucleic acid-modified [334] probes has improved specificity [335]. qRT-PCR is the "gold standard" for validating microarray data and is an invaluable tool for highly sensitive and accurate profiling of miRNA population subsets. TaqMan MicroRNA Assays offer several distinct advantages over conventional miRNA-detection methods:

High-quality quantitative data – the assays can detect and quantify miRNA over more than six logs of dynamic range.

Sensitivity – the assays can detect miRNAs in as little as 1 to 10ng of total RNA, allowing conservation of limited samples.
High specificity – the assays claim to detect only mature miRNA, not its precursor, with single-base discrimination.

Fast and simple methodology – the two-step protocol takes less than four hours.

The real time RT-PCR for determining miRNA expression uses a stem-loop reverse transcription primer to generate cDNA templates, which are then amplified using specific primers and detected with specific fluorescent probes (Figure 3.1). In TaqMan real-time PCR assays, the assay probe carries a fluorogenic reporter dye at its 5' end and a quencher at its 3' end. The quencher absorbs the fluorescence emission of the reporter while the two are close to each other as part of the probe, which means there is no fluorescent signal detected. During each cycle of PCR, the physical separation of the reporter and quencher dyes caused by the action of Taq DNA polymerase results in an increase in fluorescent signal. The Ct (cycle threshold) value is defined as the number of cycles required for the fluorescent signal to cross the threshold (ie exceed background level). Ct levels are inversely proportional to the amount of target nucleic acid in the sample (ie the lower the Ct level the greater the amount of target nucleic acid in the sample). Generally, when real time assays undergo 40 cycles of amplification, Cts < 29 are strong positive reactions indicative of abundant target nucleic acid in the sample, Cts of 30-37 are positive reactions

indicative of moderate amounts of target nucleic acid, Cts of 38-40 are weak reactions indicative of minimal amounts of target nucleic acid which could represent environmental contamination. Whether the Ct value is high or low mainly depends on the starting amount of target nucleic acid and quality (purity) of samples.

(A)

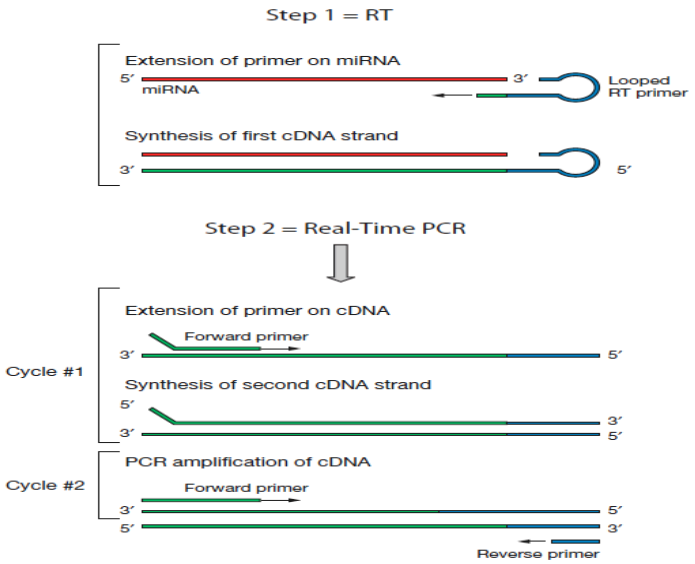

(B)

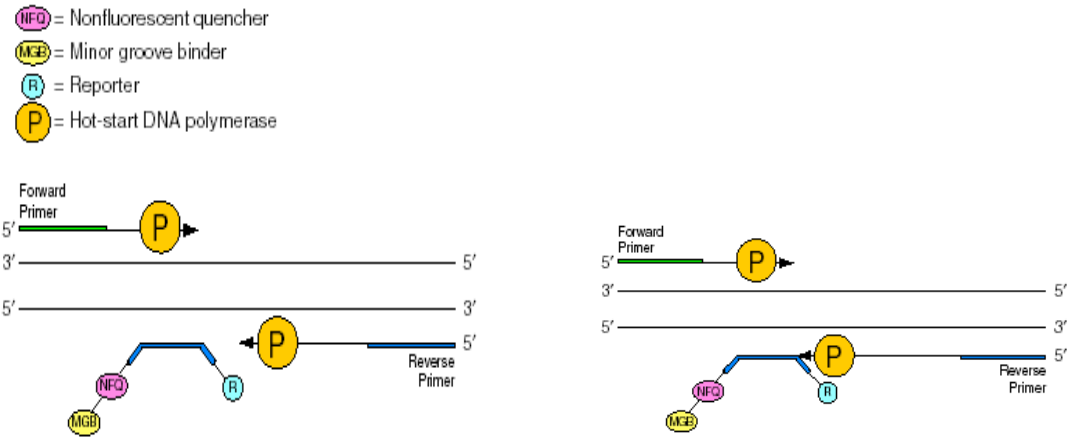

Step 1 Polymerization **Step 2 Strand Displacement**

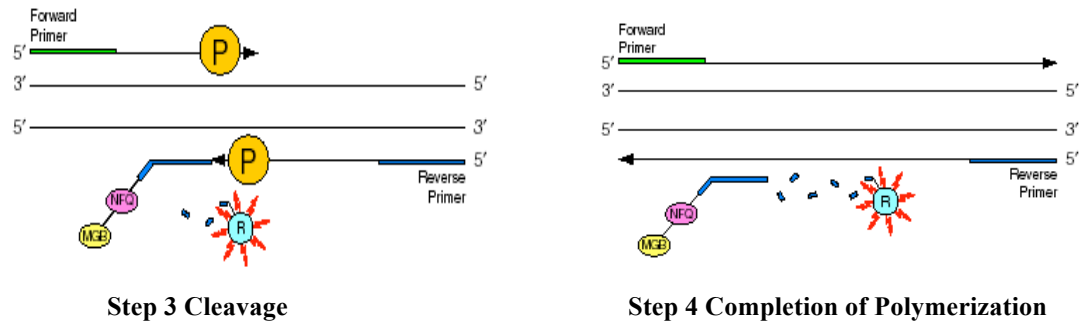

Step 3 Cleavage **Step 4 Completion of Polymerization**

Figure 3.1 The workflow of TaqMan qRT-PCR. (A) Two-step RT-PCR. (B) TaqMan MGB Probes and their detection system in Real Time RT-PCR. Adapted from [336].

Fresh-frozen tissue has traditionally been the standard source for miRNA expression profiling studies. Given the enormous amount of physiological information stored in archived FFPE tissue and the abundance of clinical data retrievable in association with it, it will prove invaluable if miRNA expression levels could be routinely and systematically analyzed in FFPE tissues. Moreover, unlike the situation in other tumours, the study of the molecular biology of melanomagenesis has been constrained by a combination of small tumour specimens and unavailability of fresh tissue. Numerous studies have documented that it is feasible and informative to characterize miRNA from FFPE samples with qRT-PCR [311, 312], as well as microarrays [322, 337, 338]. For melanocytic lesions, a study by Glud *et al.* showed that high-quality miRNA can be extracted from FFPE naevi and that reproducible and comparable miRNA expression profiles can be obtained from FFPE and fresh frozen samples [339].

Taken together, Illumina miRNA Expression Profiling Human microarray (Version2) and TaqMan MicroRNA Real Time PCR Assays were chosen to detect miRNA expression in both cultured cells and FFPE samples. It was expected that the miRNA candidates from archival FFPE tissues rather than cultured melanoma cells would be the better source of miRNA biomarkers and miRNAs involved in melanomagenesis.

In melanoma research, morphological separation is particularly difficult for certain types of melanocytic lesion such as dysplastic naevus, naevus of special sites, naevus

with dermal regression, recurrent naevus and Spitz naevus, as well as for specific types of melanoma. Blue naevus and Spitz naevus are two types of melanocytic naevus, which are uncommon and generally benign. Dysplastic naevus is an atypical melanocytic naevus, a mole whose appearance is different from that of common moles. Generally, it is believed that individuals with multiple dysplastic naevi are at much higher risk for developing melanomas. However, whether the dysplastic naevus represents a transition between benign naevus and melanoma is still controversial.

The most difficult diagnostic problems in separating naevi from melanomas are benign naevi showing clinical and/or histological features of malignancy and melanomas mimicking benign naevi [340-342]. Superficial spreading melanoma is the commonest melanoma subtype in adults, but it has significant clinical as well as histological overlap with dysplastic naevi. Therefore, reliable separation is difficult to make and is impossible in some cases. Benign acquired melanocytic naevi may also show specific changes more classically associated with melanoma. Spitz naevi are characterized by distinct cytological features, as well as atypia and mitotic activity more usually associated with melanoma and distinction from melanoma is notoriously difficult. These tumours most frequently present in childhood and adolescence and misdiagnosis as childhood melanoma or underdiagnosis can result in disastrous consequences for the patient. Similarly, naevi at special anatomical sites may show an atypical clinical presentation and share many histological features with invasive melanoma despite their benign behaviour. The most important sites include the vulva, acral locations as well as the ear, areas where extensive surgery is difficult and potentially mutilating. Finally, naevoid melanoma is characterized by histological features reminiscent of a banal melanocytic naevus. This represents one of the most challenging diagnoses in Dermatopathology and most cited cases have only been diagnosed retrospectively following melanoma recurrence [342]. In conclusion, there is an urgent need for adjuvant molecular markers to precisely separate benign from malignant melanocytic disease.

In this Chapter, I obtained a melanoma-specific miRNA expression profile based on FFPE samples by using miRNA microarray. 23 miRNAs with higher functional potential were selected as candidates from more than two hundred differentially expressed miRNAs between benign naevi and malignancies. Furthermore, nine specific miRNAs from the 23 candidates were verified by qRT-PCR and some of them were taken on into functional assays, which are described in Chapter 4. Finally, expression of five miRNAs from the nine verified miRNAs was determined using qRT-PCR in additional melanocytic lesions, including Blue naevus, Spitz naevus and dysplastic naevus FFPE samples.

3.2 Results

3.2.1 Pilot qRT-PCR in cultured cells and FFPE tissues

In order to test the feasibility of quantifying expression of miRNAs in melanoma FFPE samples by TaqMan qRT-PCR and look for appropriate endogenous control RNAs for the assay, a series of pilot experiments were first carried out in both human cell lines and FFPE samples.

Ten miRNAs were selected and their expression was determined in seven human cell lines including two immortalized melanocytes (HER1 and HER4), four malignant melanoma cell lines (EDMEL3, G361, C32 and A375) and one ovarian cancer cell line (PEO1) by TaqMan qRT-PCR (Table 3.1). RNU6B is commonly used as an endogenous control in qRT-PCR assays. However, from my results I considered it unsuitable for this purpose since the amount of RNU6B was low in each sample (the majority of Ct values were higher than 29) and there were considerable variations between the cell lines. miR-92 was a better endogenous control and was chosen instead since it was abundant in all cell lines and its Ct value was much more constant between cell lines than that of RNU6B. The remaining eight miRNAs were selected from unpublished and published reports describing their relevance to melanoma [325, 326, 343-345]. Expression of all eight miRNAs was detected in

melanocytes or melanoma cell lines (Table 3.1). There were variations in both the level of the same miRNA between cell lines and of the different miRNAs in the same cell line. In general, expression of miR-211, miR-10b and *let-7b* was much more abundant compared to miR-214, miR-373, miR-335, miR-199a and miR-137. More interestingly, expression of miR-211 was much lower (10^{3-4}-fold) in all tumour cell lines (except G361) than in the immortalized melanocytes.

In FFPE specimens, using the same input amount of total RNA (10ng), expression of three miRNAs in six old primary melanoma tissues was quantified by the same qRT-PCR assays used on the cultured cells (Table 3.2). All three miRNAs were successfully detected in the FFPE samples, although the Ct values for the miR-92 control were around five cycles higher than in cultured cells and showed more variation between samples. Ct values for miR-214 were actually smaller in FFPE tissues than in most of the cultured cell samples. I conclude that it is realistic to investigate miRNA levels in FFPE melanoma tissues.

miRNA	HER1	HER4	EDMEL3	G361	C32	A375	PEO1
miR-92	22.6±0.3	22.8±0.2	21.6±0.2	22.1±0.1	22.6±0.2	22.2±0.2	21.6±0.2
RNU6B	30.0±0.4	29.6±0.2	32.8±0.5	30.5±0.7	31.2±0.5	34.9±0.3	31.2±0.2
miR-211	22.2±0.5	23.6±0.3	32.3±0.1	24.8±0.1	32.6±0.1	36.2±0.5	37.9±0.7
miR-10b	26.6±0.5	26.7±0.4	27.0±0.4	27.8±0.5	27.1±0.3	31.4±0.3	28.0±0.5
miR-214	35.5±0.5	37.5±0.2	23.1±0.2	35.6±0.1	36.4±0.4	34.6±0.3	34.5±0.6
let-7b	25.8±0.2	26.3±0.2	23.1±0.3	25.4±0.5	24.0±0.2	26.9±0.1	22.6±0.3
miR-373	37.7±0.7	N/A	38.3±0.2	37.7±0.7	N/A	38.3±0.5	N/A
miR-335	35.3±0.1	N/A	31.4±0.6	N/A	N/A	36.9±0.4	30.8±0.1
miR-199a	N/A	N/A	29.3±0.5	N/A	N/A	N/A	N/A
miR-137	N/A	N/A	N/A	34.7±0.6	37.8±0.2	37.5±0.7	N/A

Table 3.1 Expression of microRNAs in cultured cells. Expression of 10 small RNAs was determined by TaqMan qRT-PCR on seven human cell lines: two immortalized melanocytes (HER1 and HER4), four malignant melanoma cell lines (EDMEL3, G361, C32 and A375) and one ovarian cancer cell line (PEO1). Results represent average Ct values ± STDEV of once in a triplicate repeat using 10ng of total RNA. N/A indicates that the Ct value was higher than 40 and so was not determined.

miRNA	No.4	No.5	No.6	No.7	No.8	No.9
miR-92	25.7±0.1	26.3±0.6	26.0±0.3	28.5±0.4	26.3±0.3	29.2±0.4
miR-211	31.7±0.2	31.6±0.2	30.1±0.6	32.4±0.4	32.4±0.6	34.9±0.3
miR-214	30.6±0.4	32.5±0.4	33.0±0.6	33.3±0.5	34.3±0.2	33.8±0.4

Table 3.2 Expression of microRNAs in primary FFPE melanoma tissues. Expression of miR-92, -211 and -214 was determined by TaqMan qRT-PCR in six primary FFPE melanoma tissues (No.4-9). Results represent average Ct values ± STDEV of once in a triplicate repeat using 10ng total RNA.

3.2.2 High throughput screen of melanoma-specific microRNAs

3.2.2.1 Sample preparation and processing of Illumina microRNA microarray

My array contained 80 samples, including 19 cell lines and 61 FFPE tissues. There were two immortalized human melanocytes (HER1 and HER4), 13 human melanoma cells (A375, C32, G361, WM115, HBL and the EDMEL3 series) and four ovarian cancer cell lines (PEA2, PEO1, PEO14 and PEO23). The EDMEL3 malignant melanoma cell line was isolated from a late-recurring distal metastasis of a primary melanoma. Early and late passage samples of the cell line, as well as subclones with different morphologies (epithelial, spindle cell, mixed) were available. In addition cells retrieved back into culture from successful xenografts of EDMEL3 into mice were also included. For FFPE tissues, there were 11 benign naevi (archived between 2005 and 2006), 29 primary (15 recurrent and 14 non-recurrent age and sex-matched pairs) and 21 metastatic archival cutaneous melanoma tissues (archived between 1993-1997). Samples of benign naevi and metastatic melanomas were obtained from ∅2mm cores of FFPE blocks by Bob Morris. For the much smaller primary melanomas, tumour samples were separated from adjacent non-tumour tissues by macrodissection of 10µm sections of FFPE blocks. Suitable areas on all the tissue blocks were marked by the pathologist, Thomas Brenn.

To perform Illumina miRNA Microarray, 100-200ng of total RNA were required. Total RNA of FFPE samples were isolated using RecoverAll™ Total Nucleic Acid

Isolation Kit specialised for FFPE. Up to four 10um sections, or up to 35 mg of unsectioned core samples, can be processed per reaction. It is optimized for isolation of total nucleic acids, including miRNAs from FFPE tissue. Recovered nucleic acids are suitable for qRT-PCR and microarray analyses. The yields of total RNA of the FFPE samples were between 400ng and 9,000ng. The 260/280 ratios were 1.58-2.07. The full total RNA yields and the ratio of 260/280 are shown in Appendix 1.

80 total RNA (200ng) samples were sent to the Genetics Core of the Wellcome Trust Clinical Research Facility, Western General Hospital. Illumina miRNA microarrays were performed using the Illumina 96-sample Universal Array Matrix by Lee Murphy. This involves a 3-day programme, containing several steps. First, the assay starts by polyadenylating 200ng total RNA with a Poly-A-Polymerase (PAP). The polyadenylated RNA is converted to cDNA using a biotinylated oligo-dT primer with a universal PCR sequence at its 5'-end. The miRNA assay monitors miRNA expression by targeting sequences with chimeric oligos containing universal PCR amplification primer sites. One miRNA-specific oligo is used to assay each miRNA. In this process, the biotinylated cDNA is annealed to the query oligos (microRNA specific oligos, MSOs). The mixture is bound to streptavidin-conjugated paramagnetic particles (SA-PMPs) to select the cDNA/oligo complexes. cDNA templates are hybridized with the set of MSOs that corresponds to all the targeted miRNAs. After oligo annealing, mis-hybridized and non-hybridized oligos are washed way. A polymerase is then added, causing the MSO to undergo extension. Then a universal PCR is followed. The primer on the strand that is complementary to the array is fluorescently labelled. After PCR amplification, the labelled, single-stranded product is prepared for hybridization to the bead on the array containing the complementary address sequence. The BeadArray Reader measures fluorescence intensity at each addressed bead location. The intensity of the signal corresponds to the quantity of respective miRNA in the original samples. Finally, the miRNA expression data are obtained from the scanned microarray images collected from the Illumina BeadArray Reader. The workflow scheme is shown in Figure 3.2.

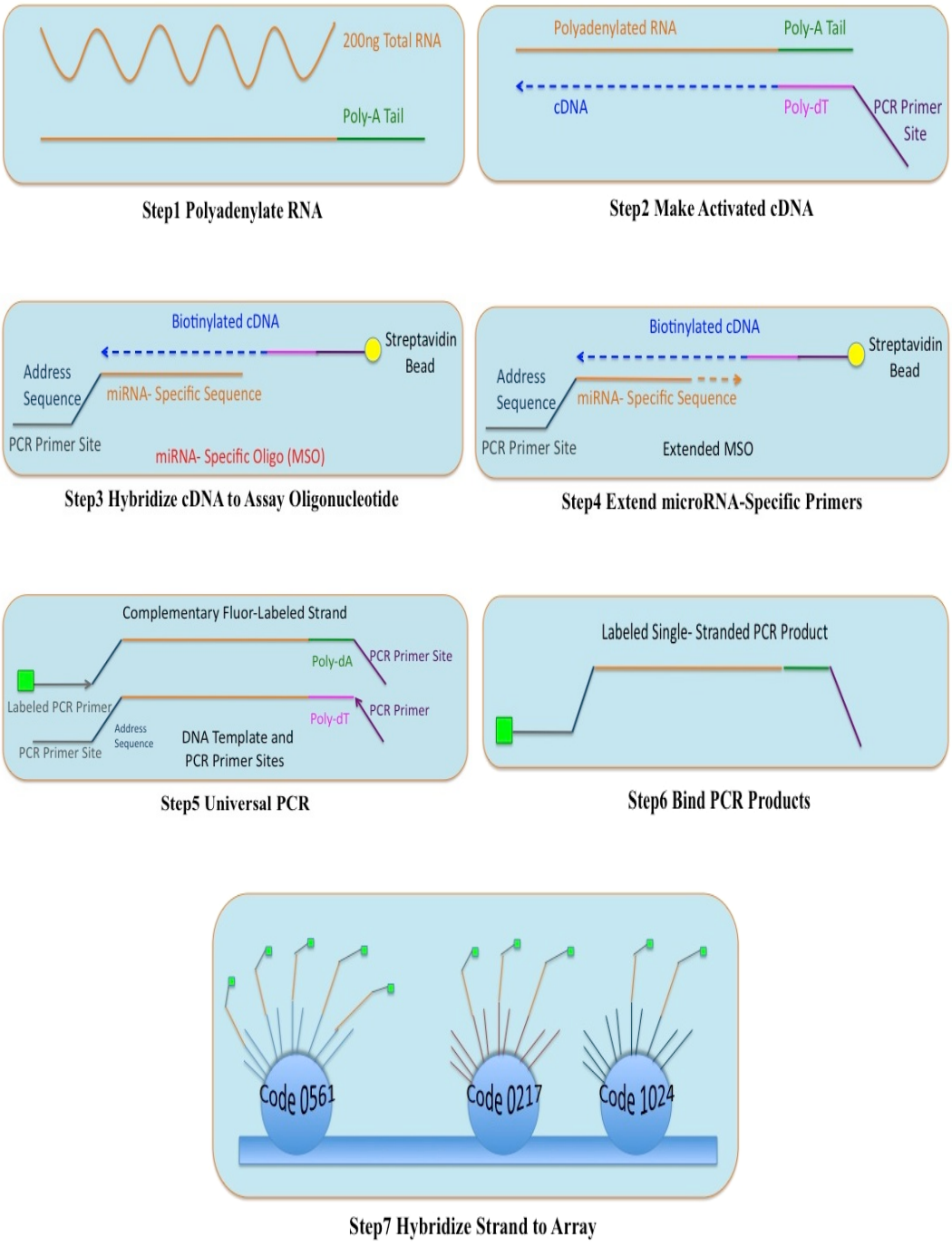

Figure 3.2 The workflow of the microRNA microarray. Adapted from [346].

3.2.2.2 Quality control of Illumina microRNA microarray

The built-in control set on the microarray showed that my array data were of good quality (Figure 3.3). The figure shows the signals for the seven built-in controls and

the average miRNA signal intensity. The negative controls consist of query oligos targeting 15 random sequences that do not appear in the human genome. Generally, the mean signal intensity of these probes defines the system background. The background is represented by both the imaging system background and by any signal resulting from cross-hybridization or non-specific binding of dye. The BeadStudio application uses the signals and signal standard deviation (STDEV) of these probes to establish gene expression detection limits. The average miRNA signal intensity of array samples was about ten times higher than that of the negative controls in my array, which indicated that the array was well probed and emitted strong fluorescent signals compared to the negative controls. Polyadenylation control oligos detect transcripts of a set of highly expressed housekeeping genes that already contain a stretch of poly-A sequence. These target sequences do not need a polyadenylation process to add poly-A sequence to their 3'-ends. Therefore, even without the polyadenylation process, these target sequences will show strong signals on the array. In contrast, microRNA target sequences need a successful polyadenylation process to add the poly-A sequence. If the polyadenylation process is ineffective, they will not be amplified and will not show signal. In my polyadenylation step (PAP) control, it was clear that successful polyadenylation of miRNA target sequences occurred yielding decent miRNA signals. Annealing controls test the efficiency of annealing MSOs with different melting temperatures (T_ms) to the same cDNA target. The MSO with higher T_m should always have a higher signal than the MSO with lower T_m. My array annealing controls were consistent with this. The internal single mismatch controls measure the specificity of extension in the second- strand cDNA synthesis step by comparing the signal intensity of perfectly matched oligos versus oligos with an internal mismatch. The extension controls (3' -mismatch) measure the specificity of extension in the second-strand cDNA synthesis step by comparing the signal intensity of perfectly matched oligos versus oligos with mismatch at the 3'-end. As expected, my mismatch controls and extension controls both showed that the perfectly matched query oligo had high signal while the mismatched oligo had dramatically decreased signal. The intensity of the positive control was much higher than that of the negative control in the contamination controls meaning my array wasn't contaminated with mouse miRNA (Illumina has human and mouse miRNA

profiling panels). Hybridization controls are the positive controls for hybridizing PCR product to capture probes on the universal arrays. Both of my hybridization controls showed the expected strong signals.

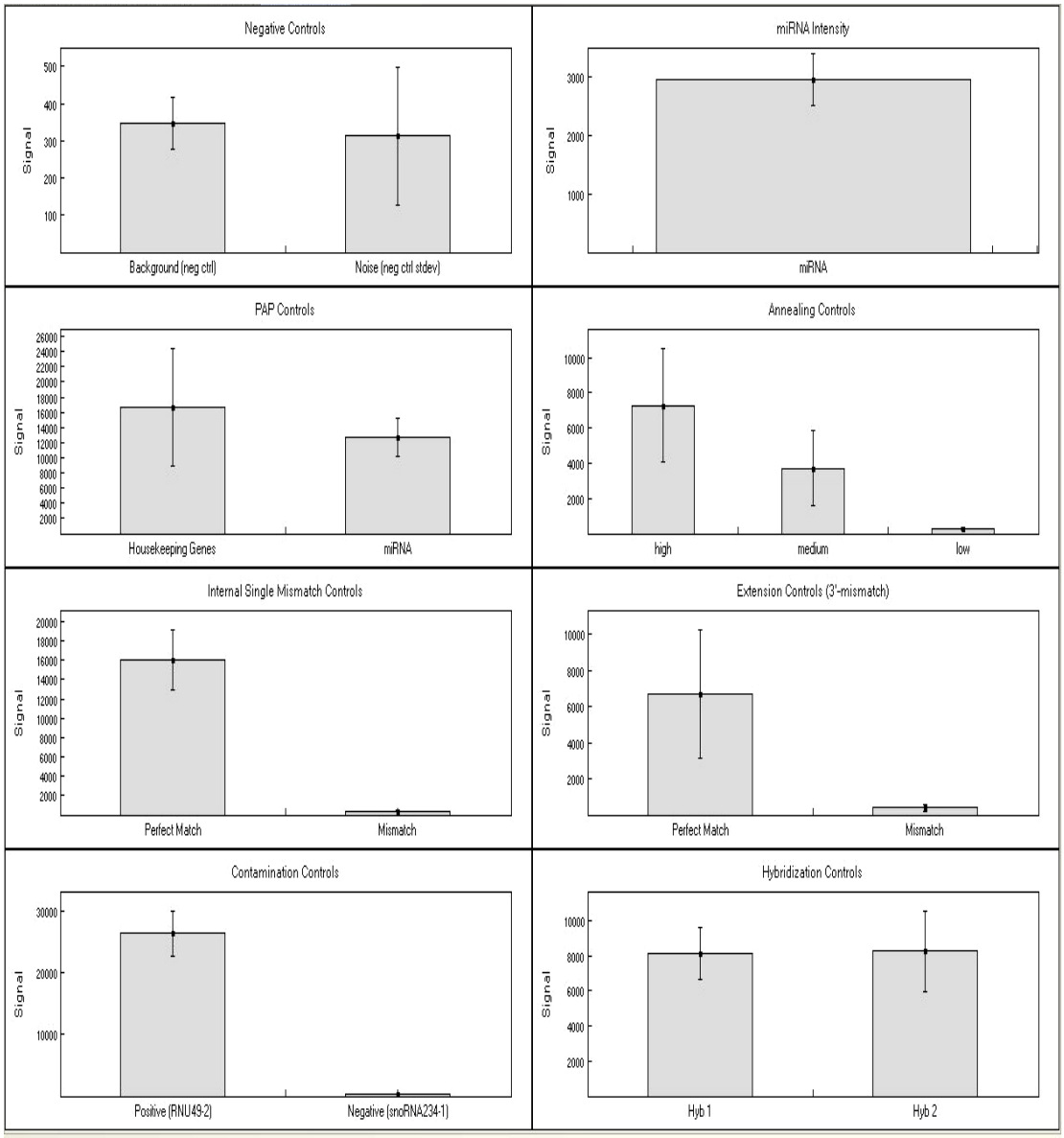

Figure 3.3 Summary of Illumina microRNA microarray control data. Negative Control: Determination of background signal; PAP Control: Control for polyadenylation step; Annealing Control: Control for MSO (miRNA specific oligo); Internal Single Mismatch: Stringency control; Extension Control: Positive and negative control for extension reaction; Contamination Control: Control for PCR contamination; Hybridization Control: Positive control for hybridization; miRNA Intensity: Average signal intensity of miRNA samples.

3.2.2.3 Data analysis of Illumina microRNA microarray

The fundamental goal of microarray experiments is to identify genes that are differentially expressed in the conditions being studied. Comparison statistics can be used to help identify differential gene expression and cluster analysis can be used to identify patterns of gene expression and to segregate a subset of genes based on these patterns.

Illumina miRNA microarray was used as a preliminary screen for differentially expressed miRNAs in certain stages of melanoma. To preserve as many differential miRNAs as possible my miRNA microarray raw data were not background subtracted and for calculation convenience it was also $\log_2$ transformed. The results of many DNA microarray experiments are fluorescence ratios. Ratio measurements are most naturally processed in log space. In log space ($\log_2$ for simplicity) the data points become 0, 1.0, -1.0. With these values, 2-fold up and 2-fold down expression changes are symmetric about 0. Although the raw data were not background subtracted, a filter [Detection P Value <0.01 in at least 80% of samples for each probe] was applied. Detection P Value is a statistical calculation that provides the probability that the signal from a given probe is greater than the average signal from the negative controls. The reason for using this filter instead of background subtraction is because there may be some miRNA signals lower than the background but still showing differences from negative controls. Among a total of 1,146 probes, 862 (75.2%) passed through the filter. Thereafter, operated data were analyzed using R version 2.8.1 software and normalized using the Quantile method which is recommended to normalize miRNA data as it works best in reducing non-biological variations in miRNA expression values between array samples [347]. Quantile normalization is a method used to make the distribution, median and mean of probe intensities the same for every sample. Hierarchical clustering was performed using Cluster 3.0 software and the TreeView programme was used to give interactive graphical analysis of clustering results. In clustering array results, City block distance (Manhattan distance) and complete linkage clustering methods were selected to analyze $\log_2$-transformed data.

From the miRNA detection pilot experiment, miR-92 was chosen to be the internal control for the qRT-PCR assay because of its abundant and relatively constant expression in both melanoma cells and tissues. In the microarray, the summary of miR-92 average signal in different types of cell and FFPE samples is shown in Figure 3.4. The miR-92 average signal ranged between 19000 and 25000 for both cells and FFPE. Importantly, all but one group (Primary*) of FFPE samples showed equivalent average miR-92 signal intensities to the cell samples. The average signal of the Primary* group was 40% lower than the other FFPE groups. All nine samples in this group were prepared 2 years earlier and isolated with a different method relative to all the other samples. They were used in the pilot experiments (the six samples in Table 3.2 were from this group) and appeared in the microarray experimental quality control data. However, the data from this group were finally excluded from the data analysis because they were the source of many outliers in the boxplot of raw data for many other miRNAs in addition to miR-92.

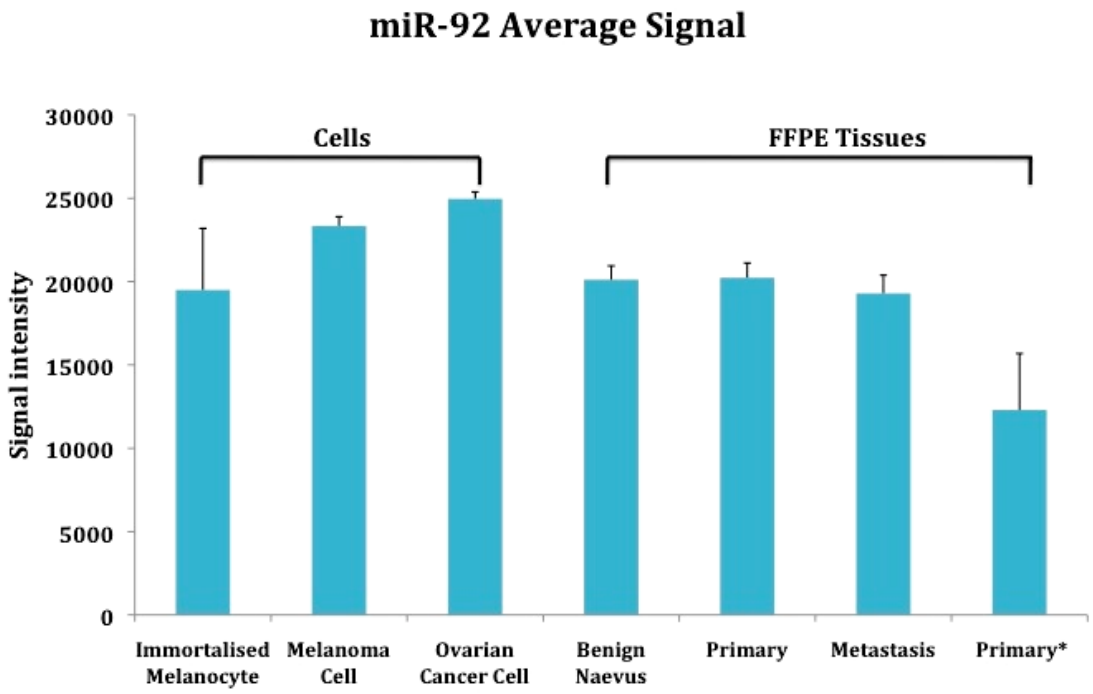

Figure 3.4 miR-92 average signal intensities of all groups of cell and tissue samples on the microarray. The histogram shows the average fluorescent signal intensities ± SEM of miR-92 of all samples groups on the array. Group Primary* represents nine old primary melanoma FFPE tissues where RNA was prepared by a different method.

3.2.2.4 Overview of hierarchical clustering

miRNAs can be highly tissue-specific biomarkers [348-350] and have been linked to the development of specific malignancies [351]. Previous studies have shown them as promising candidates for the construction of a biologically driven classification algorithm for identifying cancer tissue of origin [275, 313, 322]. Although specimens in my array do not contain many different cancer types compared to the published studies, it was still of great interest to explore the internal relationships between cells and tissues of the same cancer, in particular the miRNA expression changes between melanocytic benign lesions and malignancies, comparisons between different melanoma cell lines and between derivatives of the same cell line.

To identify patterns of miRNA expression, a cluster analysis was done on both cell lines and fixed tissues, except for the Primary* melanoma group. The entire clustering heatmap is shown in Appendix 2. Describing the miRNA based tissue classification on the whole data set is too complicated. Therefore, a simple example is shown here to make the main points. The selected part of the heatmap shows differentially expressed miRNAs in the EDMEL3 cell series relative to other samples (Figure 3.5). Basically, the shorter the distance between the samples in the analysis, the closer is their relationship. It is encouraging that the whole EDMEL3 cell series were close to each other in the same cluster. Figure 3.5 shows the best illustration of the EDMEL3 series cluster where the very high expression (yellow in the heatmap) of these 22 miRNAs in this cluster is easily distinguished from the lower expression in the other samples on the array. Generally, samples of the same origin were found in the same cluster or in closely related clusters: First, cell lines were clustered separately to FFPE tissues. Secondly, the EDMEL3 series were solely grouped in the same cluster and close to the other metastatic melanoma cell lines. Ovarian cancer cell lines were grouped in the same cluster, along with one metastatic melanoma cell line. The remaining melanoma cell lines were adjacent to the EDMEL3 cell series, but intermingled with two immortalised melanocytes lines. For tissues, the cluster patterns were more complicated. Benign naevi were all grouped together, except N5 and N6, and were mixed with primary and metastatic melanomas. Moreover, the

metastatic melanoma tissue sample, ME (from where the EDMEL3 cell line was isolated), was clustered with other metastases rather than with the EDMEL3 cell series. However, it is clear from Figure 3.5 that expression in this group of 22 miRNAs is high in the ME metastasis as well as in the EDMEL3 cell series.

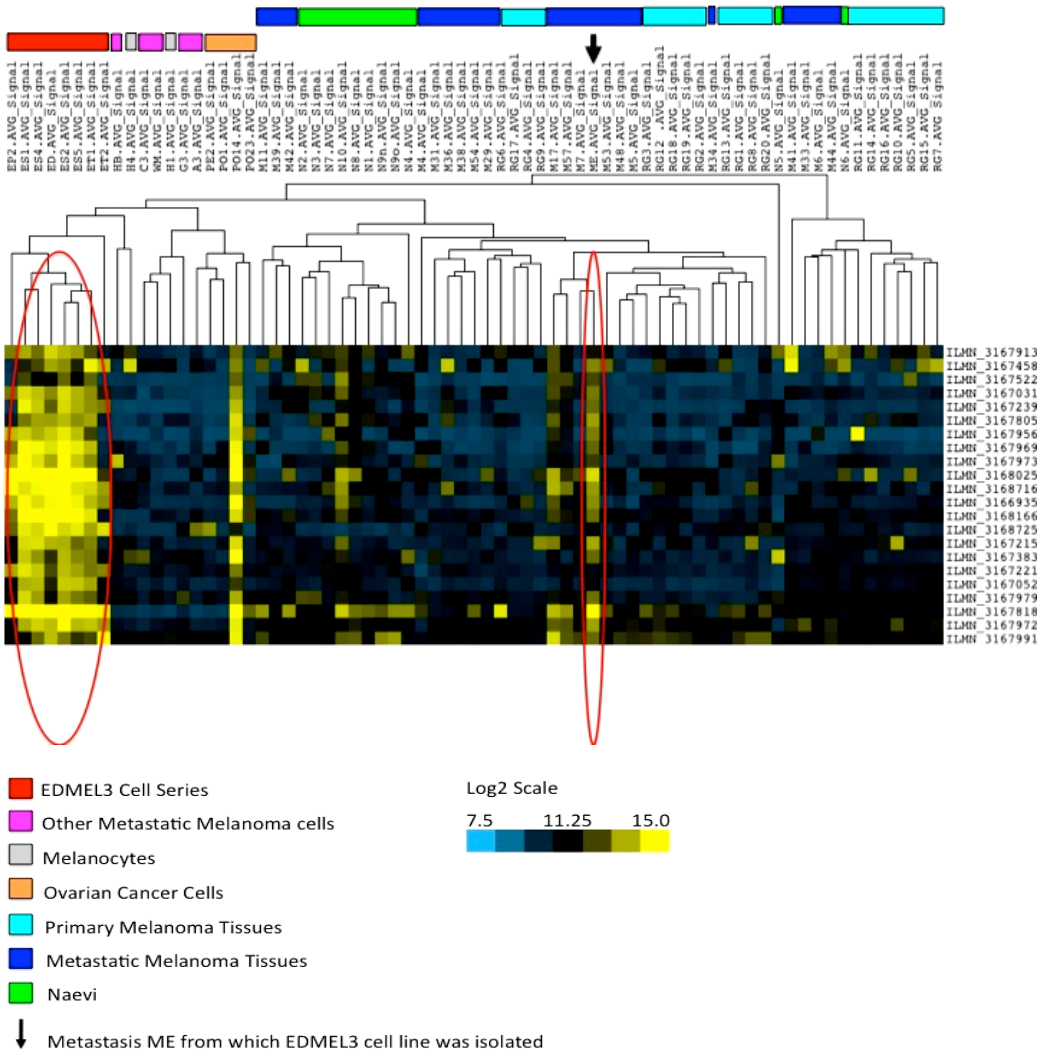

Figure 3.5 Hierarchical clustering of microRNA expression patterns in the microarray. The clustering obtained for all 71 samples (19 cell lines and 52 FFPE specimens) is illustrated with 22 selected miRNAs in the array expressed above the threshold level. A colour key is shown above each sample to identify the type of cell line or tissue sample. The selected heatmap of expression data for the 22 miRNAs is shown vertically below each sample. The red ellipses illustrate the similarity between the different members of the EDMEL3 melanoma cell line series and the ME metastasis from which the EDMEL3 cell line was derived. The bottom two keys: Coloured squares and a black arrow identify the types of sample. The blue-yellow colour log2 scale (0.0-14.0) depicts log2 expression level of the miRNAs on the heatmap. Naevi: Benign naevi.

3.2.2.5 Melanoma-specific microRNA expression profile

It was impossible to do statistical analysis of cell lines to compare the miRNA expression differences between melanocytes and melanoma cell lines because only two immortalised melanocytes were available to go on the array. Moreover, since I have shown that robust expression profiles can be generated with miRNAs isolated from FFPE tissues and my clustering indicated major differences in expression patterns between FFPE samples and cultured cells, I concluded that it was preferable to analyze the FFPE data. Therefore, the following data analysis is only based on FFPE samples. Differential expression analysis between benign naevus, primary melanoma and metastatic melanoma groups was accomplished using R language. Single miRNA comparisons between groups were done using the t-test (P value) error model with adjusted P value used for multiple comparisons. The array contains 470 well-annotated human miRNA sequences denoted with hsa-miR-# and 265 new identified miRNAs termed HS_ #. The rest are termed solexa-# as putative but as yet unconfirmed miRNAs.

There were 82 well-annotated miRNAs (including HS and solexas the total was 113 miRNAs) differentially expressed in the comparison between primary melanomas and benign naevi (adjusted P value <0.05). 28 of the 82 miRNAs were upregulated in primary melanomas.

Comparing metastatic melanomas and benign naevi, 74 miRNAs (including HS and solexas the total was 97 miRNAs) were differentially expressed (adjusted P value <0.05). 30 of the 74 miRNAs were upregulated in metastatic melanomas.

In the comparison between metastatic and primary melanomas, 22 miRNAs (including HS and solexas the total was 25 miRNAs) were differentially expressed (adjusted P value <0.05). The expression of 12 miRNAs was increased in the metastatic melanoma group. The full lists of the differentially expressed miRNAs in the three comparisons are shown in Appendix 3.

In the above comparisons, there were too many differentially expressed candidates to investigate further using qRT-PCR verification. Moreover, to investigate which miRNAs are essential to melanomagenesis through functional studies and by looking for miRNA target genes with the miRBase targets database is a big challenge because each miRNA potentially has hundreds of targets. So to narrow the candidate list, the more stringent criteria [log2 FC (fold change)>|2| and adjusted P value< 0.001] were added. 20 miRNAs were now selected in the primary melanoma versus naevi comparison, 19 in the metastatic melanoma versus naevi comparison and only two miRNAs (miR-203, miR-205) remained in the metastatic versus primary melanoma comparison (Table 3.3 A-C). There was considerable overlap between these three selected miRNA candidate lists (Figure 3.6). In the primary melanoma versus benign naevi comparison, 7 miRNAs were increased and 13 miRNAs were reduced in the primary melanoma. In the metastatic melanoma versus benign naevus comparison, 7 miRNAs were upregulated and 12 miRNAs were downregulated in the metastatic melanoma.

Only two miRNAs, miR-205 and miR-203 were present in all three comparisons and both were downregulated in melanomas. Their expression was decreased from the naevus through the primary melanoma and then to the metastatic melanoma group.

All five members of miR-200 family, miR-200a, b, c and 141, 429 were decreased in the metastatic melanoma versus the benign naevus group and three of them (miR-200a, b and 141) were also downregulated in the primary melanoma versus benign naevus group. Expression of miR-20b and miR-675 was increased in the melanomas in comparison of primary vs. benign naevi and metastatic vs. benign naevi. miR-211 was differentially downregulated in metastatic melanomas relative to benign naevi, but was not in the top candidate lists (adjusted P value = 0.0087, $\log_2$FC = -2.4). Although it did not pass through the adjusted P value < 0.001 filter, it was also chosen for qPCR verification because of the huge expression difference detected between melanocytes and most melanoma cells in the pilot qRT-PCR study.

The signal intensity summary for miR-211 and eight of the above miRNAs (miR-429 was not included because of its differential expression similarity but lower overall expression level compared to other miR-200 family members) is shown in Figure 3.7 A-C. These nine miRNAs were then subjected to the qPCR verification.

The limitations of the best current prognostic markers for melanoma, Breslow thickness and Clark level, drive the search for better molecular markers. I also looked to see whether there were any differentially expressed miRNAs between recurrent and non-recurrent primary melanomas. However, there were no significant differences of miRNA expression in the comparison of 10 pairs of age and sex matched recurrent and non-recurrent primary melanomas (adjusted P value> 0.05).

(A) Primary melanoma vs. benign naevus

	ID	Adjusted P	P value	Log_2 FC	Log_2 Average Intensity	Average Intensity
1	miR-603	1.45E-12	5.06E-15	2.79	11.71	3342.96
2	miR-663b	7.04E-10	4.90E-12	3.43	12.22	4759.02
3	miR-1826	8.69E-10	7.06E-12	2.23	13.60	12453.11
4	miR -200b*	1.26E-09	1.17E-11	-3.52	9.32	639.23
5	miR -183	2.47E-09	3.15E-11	-3.06	8.96	497.90
6	miR -149	5.13E-07	7.15E-09	-2.41	9.12	556.74
7	miR -200a	1.55E-06	2.34E-08	-2.79	9.52	735.01
8	miR -205	2.49E-06	4.05E-08	-2.44	11.34	2597.07
9	miR -675	4.87E-06	9.04E-08	3.06	11.11	2203.52
10	miR -99a	6.97E-06	1.39E-07	-2.03	11.84	3675.38
11	miR -200b	6.97E-06	1.46E-07	-3.04	11.83	3636.42
12	miR -455-5p	8.39E-06	1.95E-07	-2.45	9.60	774.70
13	miR -182	1.76E-05	4.48E-07	-2.82	9.69	825.12
14	miR -203	2.91E-05	7.75E-07	-2.62	10.88	1880.62
15	miR -494	4.99E-05	1.39E-06	2.91	11.36	2636.98
16	miR -455-3p	1.93E-04	6.03E-06	-2.13	12.51	5813.25
17	miR -20b	2.55E-04	8.28E-06	2.43	11.16	2281.88
18	miR -141	5.14E-04	1.91E-05	-2.16	10.03	1048.34
19	miR -198	7.98E-04	3.15E-05	2.45	9.09	544.99
20	miR -224	9.86E-04	4.23E-05	-2.54	10.13	1123.36

(B) Metastatic melanoma vs. benign naevus

	ID	Adjusted P	P value	Log_2 FC	Log_2 Average Intensity	Average Intensity
1	miR -205	3.88E-16	4.50E-19	-5.23	11.34	2597.07
2	miR -203	2.06E-15	7.18E-18	-6.00	10.88	1880.62
3	miR -183	6.41E-11	2.98E-13	-3.52	8.96	497.90
4	miR -200b*	1.27E-10	9.28E-13	-3.78	9.32	639.23
5	miR -200c	1.27E-10	1.03E-12	-3.13	13.04	8393.22
6	miR -603	1.26E-09	1.17E-11	2.20	11.71	3342.96
7	miR -200b	8.86E-08	1.14E-09	-3.67	11.83	3636.42
8	miR -200a	8.86E-08	1.23E-09	-3.11	9.52	735.01
9	miR -663b	9.07E-08	1.37E-09	2.81	12.22	4759.02
10	miR -141	2.24E-06	4.42E-08	-2.92	10.03	1048.34
11	miR -149	4.38E-06	9.14E-08	-2.15	9.12	556.74
12	miR -429	1.91E-05	4.66E-07	-2.53	9.14	564.22
13	miR -21*	2.42E-05	6.17E-07	2.12	9.86	927.24
14	miR -224	3.06E-05	8.23E-07	-3.16	10.13	1123.36
15	miR -182	3.06E-05	8.52E-07	-2.71	9.69	825.12
16	miR -142-5p	1.02E-04	2.96E-06	2.26	9.50	723.46
17	miR -20b	2.26E-04	7.09E-06	2.43	11.16	2281.88
18	miR -675	2.90E-04	9.43E-06	2.40	11.11	2203.52
19	miR -9	5.51E-04	1.98E-05	2.88	10.76	1729.62

(C) Metastatic vs. primary melanoma

	ID	Adjusted P	P value	Log_2 FC	Log_2 Average Intensity	Average Intensity
1	miR -205	4.42E-09	6.64E-12	-2.79	11.34	2597.07
2	miR -203	4.42E-09	1.03E-11	-3.38	10.88	1880.62

Table 3.3 Differentially expressed microRNAs in benign naevi, primary and metastatic melanoma FFPE tissues. (A) Top 20 differentially expressed miRNAs in primary melanoma vs. naevi comparison. (B) Top 19 differentially expressed miRNAs in metastatic melanoma vs. naevi comparison. (C) Top 2 differentially expressed miRNAs in metastatic vs. primary melanoma comparison. ID: miRNA. P value: from t-test. Adjusted P: adjusted P value is the way to correct for multiple testing. Log_2 FC: Log_2 fold change (In X vs. Y comparison, when Y>X, log_2 FC is negative, when Y<X, log_2 FC is positive. Only miRNAs with Log2 FC >|2| and adjusted P value< 0.001 are shown. Average Intensity: stands for the average signal intensity of all samples on the array for the particular miRNA.

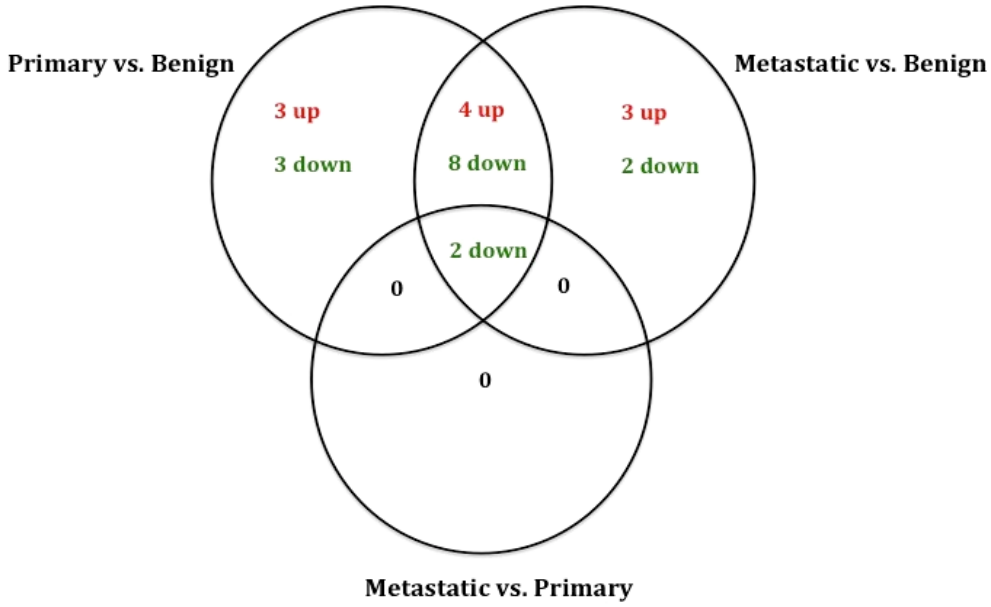

Figure 3.6 Relationship between differentially expressed microRNAs shown in Table 3.3. For each circle (X vs. Y comparison) a red number means upregulated miRNAs in X while a green number means downregulated miRNAs in X.

(A)

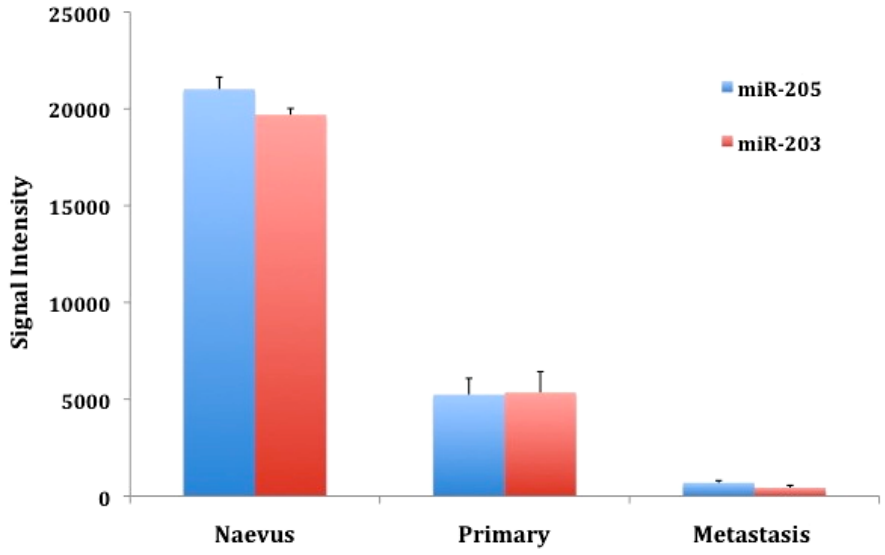

(B)

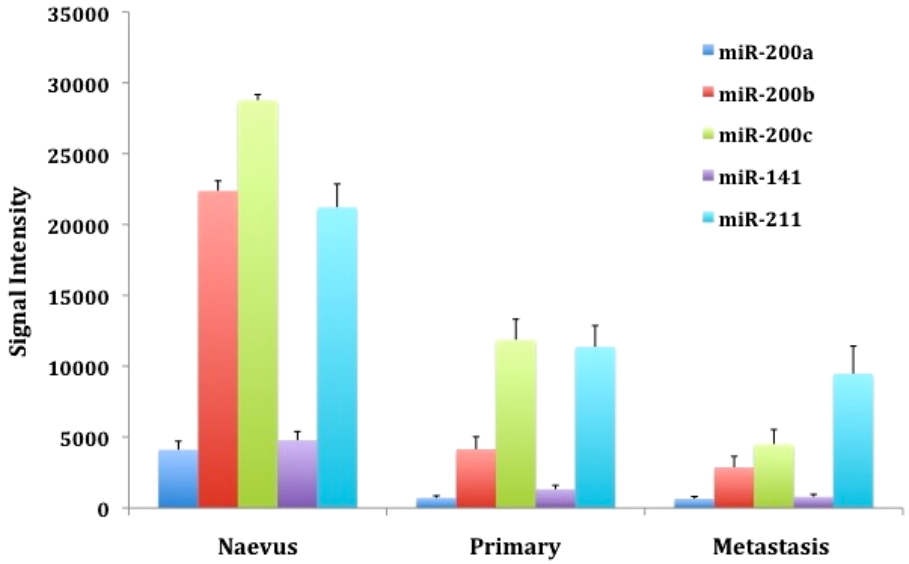

(C)

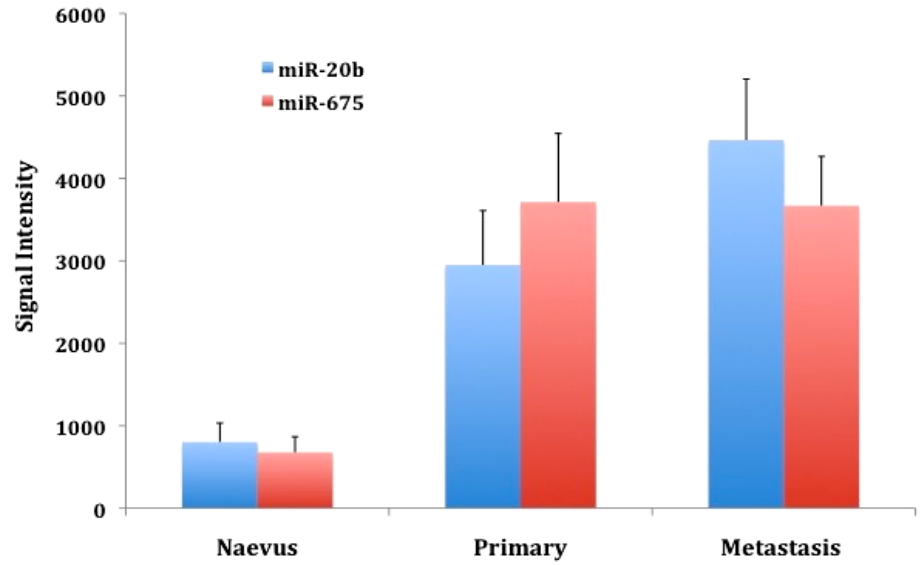

Figure 3.7 Expression of microRNAs in FFPE samples on the microarray. The histograms (A-C) show the average fluorescent signal intensities ± SEM for the top selected miRNAs in the microarray. (A) Expression of miR-203 and miR-205. (B) Expression of miR-200a, miR-200b, miR-200c, miR-141 and miR-211. (C) Expression of miR-20b and miR-675. Group size: Naevus (n=11), Primary (n=20), Metastasis (n=21). Here the Naevus group represents benign naevus.

3.2.3 TaqMan qRT-PCR verification

3.2.3.1 Amplification efficiency of target microRNAs

As described in Chapter 2, there are two major methods to quantify miRNA expression using qRT-PCR. I compared the standard curve method and the ΔΔCt method for determining the expression of a target miRNA relative to an internal control in a number of cell lines. An example comparison between reference gene miR-92 and target gene miR-211 gave excellent agreement (Table 3.4). Moreover, the validation of the ΔΔCt method for miRNA expression relative to miR-92 as endogenous control showed that the slopes of the relative efficiency plot between each individual target miRNA and reference miRNA miR-92 were all below 0.1, indicating that the ΔΔCt method was valid for comparing the expression of these miRNAs between sample groups. The amplification efficiency plots are shown in Appendix 4. Therefore, I decided to proceed using the ΔΔCt method. (Details of the standard curve and the ΔΔCt method were introduced in Chapter 2, Page 69-70.)

		HER1	HER4	A375	EDMEL3
Ct	miR-92	22.6±0.3	22.8±0.2	22.2±0.2	21.6±0.2
	miR-211	22.2±0.5	23.6±0.3	36.2±0.5	32.3±0.1
Standard Curve	miR-211/92	0.95	0.46	0.000044	0.00046
	RQ	1.00	0.48	0.000046	0.00048
ΔΔCt	RQ	1.00	0.48	0.000032	0.00069

Table 3.4 Comparison of the standard curve and the ΔΔCt method. To quantify miRNA expression, Ct values for miR-211 and the endogenous control miR-92 were determined by qRT-PCR on HER1, HER4, A375 and EDMEL3 cell lines. Ct results show average Ct values ± STDEV of once in a triplicate repeat. For the standard curve method, the absolute ratio of miR-211/miR-92 expression is shown along with expression normalized to HER1. For the ΔΔCt method the expression is shown normalized to HER1. RQ: relative quantity.

3.2.3.2 Verification of target microRNAs in FFPE melanocytic specimens

Nine differentially expressed target miRNAs identified from the microarray have been verified by qRT-PCR. Another eight new benign naevi were added to the verification experiments to increase the sample set. In each case the qRT-PCR results were in accordance with that of the microarray. Seven miRNAs were downregulated while two were upregulated in melanoma compared to benign naevi (Figure 3.8). Four members of the miR-200 family (miR-200a, 200b, 200c, 141) showed significant decreased expression between benign and malignant tissues of between 15 and 200 fold (Figure 3.8-A). However, except for miR-141 ($p< 0.01$), there was no significant decrease between primaries and metastases. Expression of miR-211 was decreased in both primary (4-fold) and metastatic melanoma (6-fold) compared to benign naevi ($p<0.001$), but again there was no significant difference between primaries and metastases. For both miR-203 and miR-205 there was a greater than 10-fold decrease from benign naevi to primary melanomas and a greater than 2000-fold decrease from benign naevi to metastatic melanomas. All the expression differences between groups were significant (Figure 3.8-B). The remaining two miRNAs, miR-20b and miR-675, were both significantly upregulated in tumours. Expression was 10-fold higher in malignancies than benign naevi for miR-20b and 20-fold higher for miR-675, although in each case there was no significant difference between primary and metastatic melanomas (Figure 3.8-C).

Expression of these nine miRNAs between recurrent and non-recurrent primary melanomas was also compared. All seven miRNAs that were downregulated in metastatic compared to primary melanomas show a lower level trend in the recurrent compared to the non-recurrent samples. miR-20b which was upregulated in the metastatic melanomas compared to primary melanomas, seems present at higher level in recurrent than in the non-recurrent primary tumours. However, none of the differences were significant ($P>0.05$) (Figure 3.9).

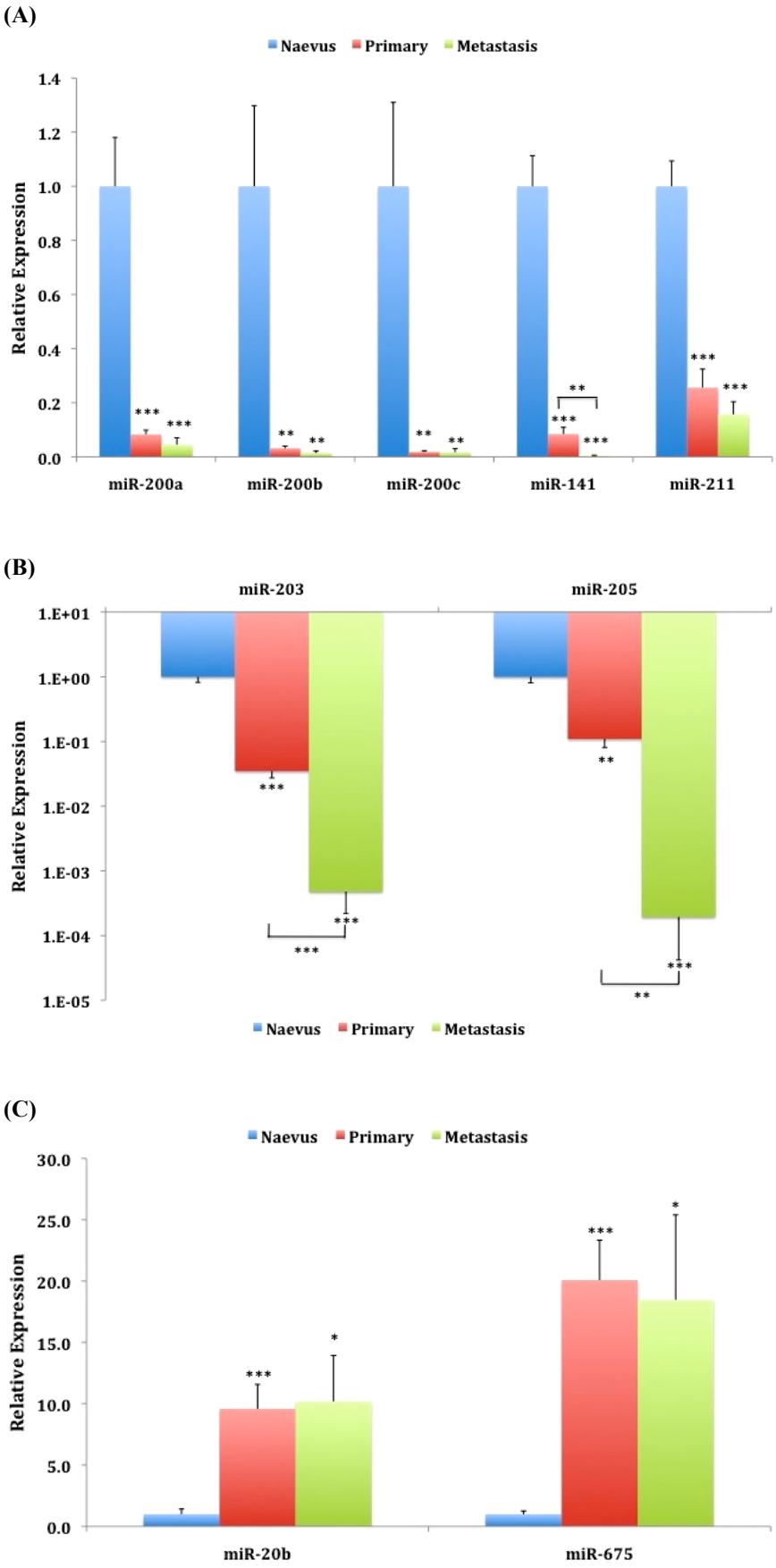
(A)
Naevus
Primary
Metastasis
Relative Expression
1.4
1.2
1.0
0.8
0.6
0.4
0.2
0.0
miR-200a
miR-200b
miR-200c
miR-141
miR-211
(B)
miR-203
miR-205
1.E+01
1.E+00
1.E-01
1.E-02
1.E-03
1.E-04
1.E-05
Relative Expression
Naevus
Primary
Metastasis
(C)
Naevus
Primary
Metastasis
30.0
25.0
20.0
15.0
10.0
5.0
0.0
Relative Expression
miR-20b
miR-675

Figure 3.8 Different microRNA expression levels during melanoma progression. (A) Downregulated miRNAs miR-200a, miR-200b, miR-200c, miR-141 and miR-211. (B) Downregulated miRNAs miR-203 and miR-205. (C) Upregulated miRNAs miR-20b and miR-675. Expression was determined by qRT-PCR using the ΔΔCt method. Expression of each miRNA relative to miR-92 and normalized to the mean of the Naevus group is shown. Results represent average relative expression ± SEM. Group size: Naevus (n=12-17), Primary (n=20), Metastasis (n=14). Here the Naevus group represents benign naevus. Y-axis in (B) is log10 scale. One-asterisk $p<0.05$, two-asterisk $p<0.01$, three-asterisk $p<0.001$.

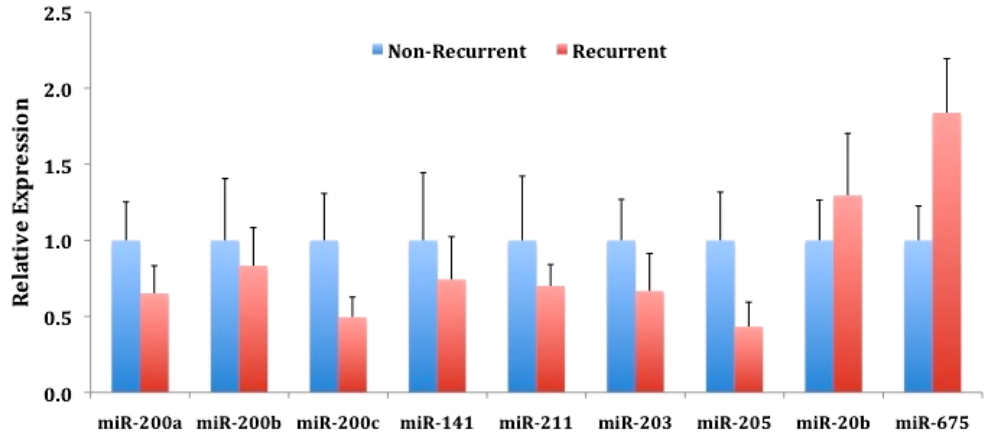

Figure 3.9 microRNA expression levels between non-recurrent and recurrent primary melanoma samples. Expression was determined by qRT-PCR using the ΔΔCt method. Expression of each miRNA relative to miR-92 and normalized to the mean of the Non-recurrent group is shown. Results represent average relative expression ± SEM. Group size: non-recurrent (n=10), Recurrent (n=10).

3.2.3.3 Expression of microRNAs in additional classes of melanocytic lesions

Based around the miRNA expression differences that I had seen between benign naevi and melanomas I decided to investigate the ability of these miRNAs to distinguish between some of more complex types of melanocytic lesions. I used the TaqMan assay because of its ability to detect miRNAs in as little as 1ng of RNA, as such it is much more sensitive than microarray.

Previously, samples of benign naevi and metastatic melanomas were obtained from Ø2mm cores of FFPE tissue blocks, while macrodissection on 10µm sections was required to isolate the much smaller primary melanomas from adjacent non-tumour tissues. The smaller size of the Blue, Spitz and dysplastic naevi available meant that samples for RNA isolation were also obtained by macrodissection of 10µm sections. Total RNA of these FFPE samples was isolated using the same kit as for previous FFPE samples. In general, the yields of scrapings from macrodissection were smaller than that from the cores. The 260/280 ratios of these total RNAs were similar to the RNAs from the cores. The full yields and 260/280 ratios are shown in Appendix 1.

TaqMan qPCR expression data for five miRNAs in the original benign naevi, primary and metastatic melanoma comparisons is shown in Figure 3.10, along with the new data on Blue, Spitz and dysplastic naevi. Interpretation is compromised by the small number of new samples assayed. However, for miR-203, miR-205 and miR-200c the Blue, Spitz and dysplastic naevi appeared to group with the tumour samples rather than with benign naevi. Expression of miR-203, 205 and 200c in Blues was significantly lower than that in benign naevi ($p<0.05$), while the expression difference between Blues and primary melanomas was not significant. For miR-211 the Blue naevi had higher expression and grouped with the benign naevi, while the Spitz and dysplastic naevi had lower expression closer to the melanomas. Expression of miR-20b in the Spitz and dysplastic naevi was closer to that in benign naevi than in melanomas. miR-20b expression was significantly higher in Blues than that in benign naevi, while the expression difference between Blues and primary melanomas was not significant.

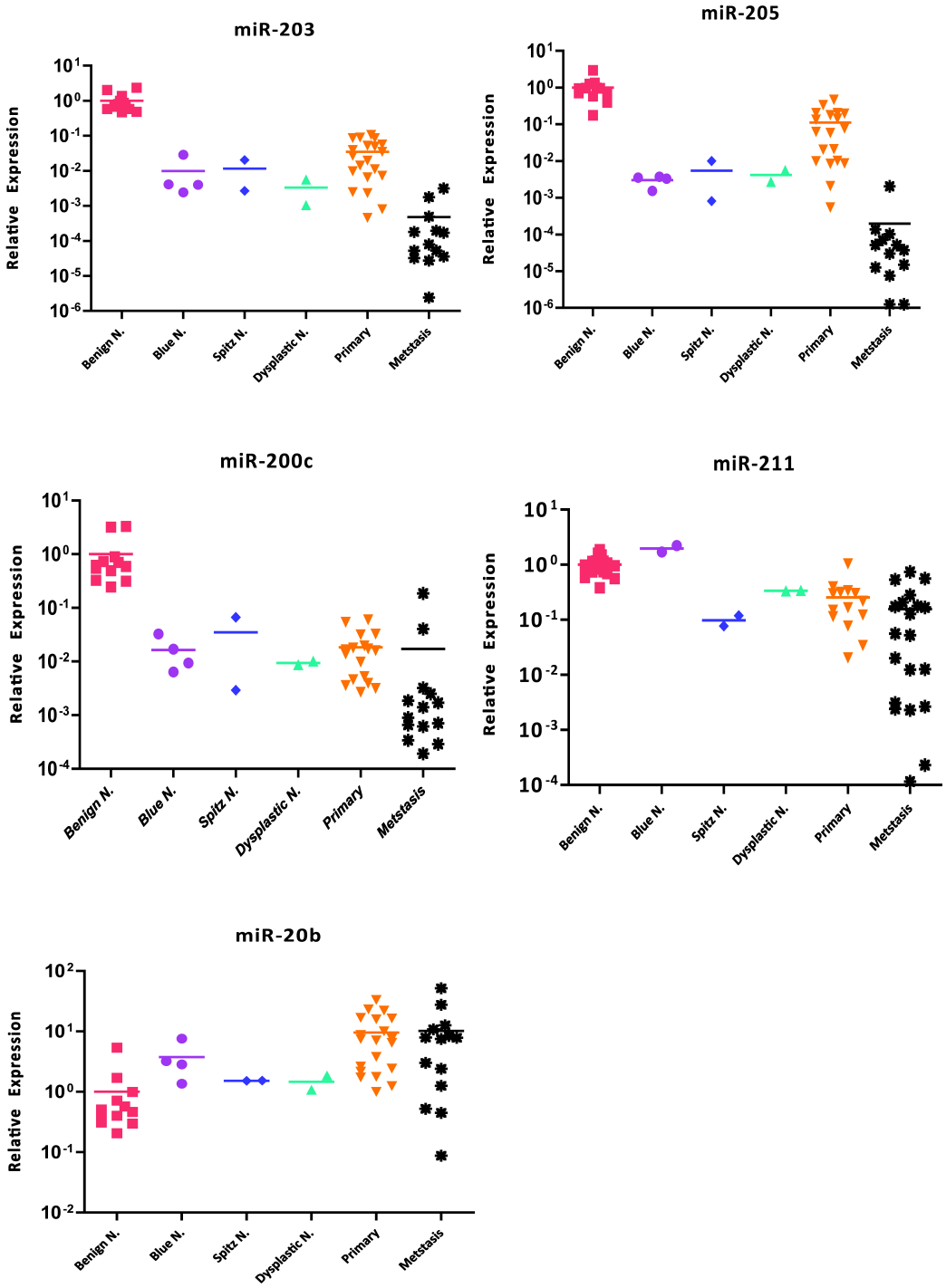

Figure 3.10 Expression of microRNAs in various melanocytic lesions. Expression of miR-203, miR-205, miR-200c, miR-211 and miR-20b was determined by qRT-PCR using the ΔΔCt method. Expression of each miRNA relative to miR-92 and normalized to the mean of the Benign Naevus group is shown on a log10 scale. Horizontal lines in all graphs indicate the means for each lesion group. Individual data points for each sample in the group are also shown. Group size: Benign Naevus (n=12-17), Blue Naevus (n=2-4), Spitz Naevus (n=2), Dysplastic Naevus (n=2), Primary (n=20) and Metastasis (n=14).

3.3 Discussion

To date, three principal methods have been used to measure expression levels of miRNAs: microarray hybridization, real-time PCR and next generation sequencing (NGS) [352]. Northern blotting analysis was also adopted to study the expression of miRNA genes [168, 353] and was used as a method for detecting miRNA expression in cancer cells [269]. Due to the increasing demands for high-throughput analyses, NGS, also known as high-throughput sequencing, is coming into wider use than Northern blotting. All three methods comprehensively analyze miRNA expression, with each option having advantages and disadvantages. The clear merit of NGS is its ability to identify novel miRNAs, while qPCR is better used as a validation rather than a discovery tool [352]. As with genomic DNA and RNA analysis, microarrays are still the best choice for a standarized genome-wide assay that is amenable to high-throughput applications. I believe the experimental strategy adopted in this chapter—a combination of microarray and qRT-PCR—is most appropriate to identify a reliable melanoma-specific miRNA expression profile.

In performing experiments for miRNA quantification, variation in the amount of starting material, sample collection, RNA preparation and quality, and reverse transcription (RT) efficiency can all contribute to quantification errors. Normalization to an endogenous control is currently the most accurate method to correct for potential RNA input or RT efficiency biases. For TaqMan MicroRNA Assays, the chosen endogenous controls should share similar properties, such as RNA stability and size. Small nuclear RNA (snRNA) and small nucleolar RNA (snoRNA) are good choices as internal controls because their size is close to miRNAs and they show constitutive and abundant expression across a large number of tissues and cell lines. Undoubtedly, the consistency of expression should be confirmed under the specific conditions of the experiment. In addition to use of snRNA or snoRNA, some specific miRNAs themselves (including miR-92, especially in tissue samples) that demonstrate the least variability can be an alternative choice [354]. Therefore, given the evaluation of my pilot qRT-PCR experiments and of my microarray, miR-92 was regarded as a better endogenous

control than the commonly used snRNA, RNU6B, for its stability of expression across different types of melanocytic samples.

An early miRNA expression study revealed that 129 miRNAs were able to classify human cancers into their tissue of origin solely on the basis of their miRNA expression profile [313]. In addition, the miRNA profile can also reflect the developmental lineage and differentiation state of tumours [355]. Analysing the cluster patterns of my array work without sophisticated raw-data correction, the cell lines and tissues were well separated although the classification within cell lines or tissues was not ideal. The closely related EDMEL3 series of melanoma cell lines were all classified in the same cluster and were adjacent to other metastatic melanoma cell lines. Naevus tissues were also mostly grouped together in the same cluster. However, the rest of the melanoma cell lines were intermingled with two melanocytes lines. For another example, primary and metastatic melanoma tissues did not cluster separately, but were mixed together along with some naevus tissues. It seems that the cluster analysis of my miRNA microarray data here is more useful as a tool in classifying tissue origin rather than in distinguishing melanomas from benign melanocytic lesions, or primary tumours from metastatses. To obtain better expression profiles, the following factors should be taken into account: tissue heterogeneity, quantity and quality of total RNA input, quality control of the array, heterozygosity of melanoma and using a panel containing all known and uncharacterised miRNAs. I think tissue hererogeneity is the most crucial factor that affects profiling results. Even under close supervision to ensure pure sample collection, tumour tissues still contain multiple cell types, each with its specific gene expression programme. Disease not only changes the expression programme of the affected cell type but also its cell type composition. Therefore, to best separate these effects in the profiling of heterogeneous tumour samples, it may be useful to profile tumour cell lines and individual cell types that may be present in one tumour sample, or define miRNA cellular localization by performing *in situ* hybridization (ISH). However, my Illumina microarray has still identified a number of miRNAs whose expression changes during melanoma progression. This conclusion is supported by

the verification results for the selected miRNAs from qRT-PCR, which were entirely consistent with the Illumina array data.

The existence of unique miRNA expression profiles for different tumour histology types and subtypes, due largely to the tissue specificity of miRNAs, appears to be a useful adjuvant diagnostic tool when tumours cannot be accurately classified by morphology and immunophenotype. Besides the diagnostic value of miRNA, emerging evidence also manifests their role in cancer prognosis. Reduced *let-7* and high expression of miR-155 in human lung cancers was associated with poor survival [270]. Aberrant miRNA expression features may reflect a tendency for early disease relapse. Tong *et al*. looked for differentially expressed miRNAs through miRNA expression profiling and qRT-PCR of 40 prostatectomy specimens from stage T2a/b, early relapse and non-relapse cancer patients, to better understand the relationship between miRNA dysregulation and prostate oncogenesis [356]. A > 40% difference in expression between the relapse and non-relapse subsets was observed for miR-135b and miR-194, although this trend of differential expression did not attain statistical significance for the limited number of patients analyzed. I also looked for any differentially expressed miRNAs between recurrent and non-recurrent primary melanoma tissues. However, there were no miRNAs with significantly different expression between the two categories of primary melanoma. Considering the small number of highly differentially expressed miRNAs in the metastatic versus primary melanoma comparison, I realize that it may be unrealistic to expect to see differences between recurrent and non-recurrent primary melanomas in such a relatively small sample set. Interestingly, the reduction in seven downregulated miRNAs and elevation in two upregulated miRNAs verified by qRT-PCR (Figure 3.9) in recurrent compared to non-recurrent primaries is compatible with the sequential transition observed from benign naevus through primary to metastatic melanoma. It is possible that the number of samples was not big enough to reveal a significant difference between recurrent and non-recurrent primary melanomas. Looking for miRNAs with prognostic value should ideally consider the actual length of survival and not just whether or not the patients relapse. Some patients may still live a very long time with recurrent tumours. This was not accomplishable with my data because the full

clinical records of the cases were not readily available. Two research groups have studied melanoma survival associated with miRNA expression profiles. Segura's group identified 18 miRNAs (See Table 3.5, Page 116) whose overexpression in melanoma metastases was significantly correlated with longer survival (≥ 18 months post-recurrence survival) compared to shorter survival (< 18 months post-recurrence survival) [357], such as miR-155 and miR-142-5p, which are upregulated in malignancies in my differentially expressed miRNA candidates. Furthermore, low expression of miR-191 and high expression of miR-193b in melanomas compared to melanocyte cells were associated with poor melanoma-specific survival [358].

Firm diagnostic criteria based on histological features alone are difficult to establish owing to the wide morphological range of melanocytic naevi and significant morphological overlap of benign lesions and malignant melanoma leading to both over-treatment as well as delayed treatment. Therefore, I decided to extend my study of miRNA expression changes during melanoma progression to an additional set of melanocytic lesions: Blue, Spitz and dysplastic naevi. However, the preliminary study using five of my candidate miRNAs on a very small set did not allow me to make any clear conclusions about miRNA expression patterns in these naevi. Analysis of more samples would be required before differences of any useful diagnostic miRNA between these expanded groups of melanocytic lesions could be estimated. However, such an approach could still be helpful diagnostically if large sample number could be linked to miRNA ISH to eliminate the need for RNA extraction from very small lesions such as *in-situ* melanoma.

Up to ~60% of human genes are putative targets of one or more miRNAs [359]. miRNAs play a role in all major biomolecular processes, including metabolism [360], cell proliferation [361], apoptosis [362], development and morphogenesis [363, 364], stem cell maintenance and tissue differentiation [365]. So any abnormality occurring in the above programmes could induce diseases including cancer. Therefore, when searching for biomarkers or looking for new treatment for cancers, it is important to look for tumour-specific miRNA candidates, especially if they can be linked to one or more key signalling pathway(s) in the cancer. Some miRNAs identified from my

array results have already been studied in some other cancers. For instance in breast cancer, miR-9 promotes metastases by directly targeting E-cadherin [366] and miR-155 regulates cell survival, growth and chemosensitivity by targeting FOXO3a [367]. In another instance in hepatocellular carcinoma, *let-7c* induces apoptosis through inhibiting Bcl-xL [368] and miR-224 represses apoptosis by targeting the apoptosis inhibitor-5 [369].

In melanoma miRNA research, besides my data other melanoma-specific miRNA expression patterns have now been identified, based on both cell lines and tissues. Table 3.5 summarises the miRNAs that are differentially expressed, either in melanoma cells relative to other cancer cells, or between normal and malignant cells/tissue samples from microarray profiling. The first two papers discussing miRNA profiles on the NCI-60 cell panel identified 17 significantly differentially expressed miRNAs in melanoma cell lines versus other cancer cell lines. 11 of these miRNAs (miR-182, 183, 203, 224, 200b*, 200a, 200c, 141, 211, 204, 335) overlapped with my full list of FFPE differentially expressed miRNAs and 8 of 11 appear in the refined lists. In Mueller's study, an overview of differentially expressed miRNAs with validated target genes and their impact on cellular functions in malignant melanoma was summarized. Five miRNAs (miR-137 and miR-182, miR-141, miR-183 and miR-200c) discussed were differentially expressed in my FFPE array work. However, the above differentially expressed miRNAs from the literature were obtained either from cell-based microarray or from tissue analysis, but not from tissue profiling. Very few studies have systematically interpreted full miRNA expression profiles by microarray on melanocytic FFPE samples. Among the above profiles, only two studies (the last two in Table 3.5) included the different stages of melanocytic lesions between naevi and malignant melanomas as in my array samples. One of these two papers described 31 miRNAs (13 upregulated, 18 downregulated) that were differentially expressed in metastatic melanomas relative to benign naevi and 15 of them were verified by qRT-PCR [370]. The sample panel of this study contained only 8 benign naevi and 8 metastatic melanomas, but no primary melanomas. Another study correlating cell line-derived miRNA expression patterns with melanoma patients included 3 benign naevi, 5 primary and 7 metastatic

melanoma samples [371]. It was found that expression of selected miRNAs was inconsistent when comparing cell line–derived and patient-derived data. Some discrepancies were also detected when miRNA microarray data were correlated with qPCR-measured expression levels. Furthermore, they identified miRNA-200c to be consistently downregulated in melanocytes, melanoma cell lines, and patient samples, whereas miRNA-205 and miRNA-23b were markedly reduced only in patient samples. In contrast, miR-146a and miR-155 were upregulated in all analyzed patients but none of the cell lines. Both of these two papers used far fewer samples than mine. Comparing these two papers with my array results, some common differentially expressed miRNAs emerge including: some (not all) members of the miR-200 family, miR-203, miR-205, miR-193b, miR-125b, miR-211, miR-204, miR-20b, miR-183, miR-196a, *let-7c*. I conclude that my miRNA profiling study is the best melanoma-specific miRNA profile so far because it uses the most miRNA probes, has the most FFPE samples, contains complete stages in melanoma progression and is verified by qPCR.

Literature	Number	Type	Overlapping miRNAs in my array
Gaur/ Blower, 2007	17	Cell	miR-182, miR-183, mir-203, miR-224, miR-200b*, miR-200a, miR-200c, miR-141, miR-211, miR-204, miR-335 (11)
Mueller, 2009	22	Cell	miR-141, miR-182, miR-183, miR-200c, miR-137 (5)
Segura, 2010	18	Tissue	miR-455-3p, miR-145, miR-497, miR-155, miR-342-5p, miR-193b, miR-142-5p (7)
Caramuta, 2010	32	Cell	let-7c, miR-211, miR-9, miR-196a (4)
Chen, 2010	31	Tissue	miR-193b, miR-211, miR-149, miR-200c, miR-205, miR-203, miR-200b, miR-141, miR-204 (9)
Philippidou, 2010	/	Cell/ Tissue	miR-155, miR-142-5p, miR-200c, miR-183, miR-193b, miR-205, miR-203, miR-125b, miR-20b, miR-196a, *let-7c* (11)

Table 3.5 Summary of overlapping miRNAs between the literature and my array results. Number represents differentially expressed miRNAs in the particular paper.

I considered two different approaches before moving on to study the functional role

in melanoma of some of the differentially expressed miRNAs that I identified: choose miRNAs that have never been studied and explore their targets blindly, or select miRNAs with established connections in other cancers and with some known human targets. After studying the top selected miRNA candidates, I found that about 10 have been shown to have roles in other cancers and so I chose the latter approach. First, all five members of the miRNA-200 family (miR-200a, 200b, 200c, 141, and 429) were present in my refined lists of differentially expressed candidates. The miRNA-200 family regulates PDGF-δ-mediated epithelial to mesenchymal transition (EMT) in prostate cancer cells [372]. EMT facilitates tissue remodelling during embryonic development and is viewed as an essential early step in tumour metastasis. The role of the miRNA-200 family and miR-205 in EMT has been studied [373, 374] (For more information see Chapter 4.1.2 and 4.1.3). Decreased expression of miR-203 was identified in prostate, bladder, gastric, and colorectal cancers [375-377]. Li et al. found overexpression of miR-203 significantly reduced cell proliferation and survival, and induced cell apoptosis in the p53-mutated colon cancer cells. Moreover, overexpressing miR-203 could increase the cytotoxic role of paclitaxel in the p53-mutated colon cancer cells, but not in the p53 wild type cells [378]. Given the fact that miR-205 and miR-203, two downregulated miRNAs, appeared in all three of my comparisons, I verified them using qPCR as preparation for future functional study. miR-20b and miR-675 were found to be functional in modulating c-MYC and RB genes respectively [379, 380]. All the above miRNAs appear at the top of my selected comparisons.

However, this doesn't mean that the other differentially expressed miRNAs not in the top lists can be ignored. One such is miR-211 with its large expression difference between immortalised melanocytes and most of the malignant melanoma cell lines I examined. Other published papers also showed that miR-211 was downregulated in both melanoma tissues and melanoma cell lines compared to normal melanocytes [381-383]. However, overexpression of miR-211 was found to be involved in poor survival of oral carcinoma patients [384], indicating that there may be an oncogenic potential for miR-211 in some tissue-specific functions. This seems quite common with other miRNAs also having opposite expression patterns in different cancers.

There are also reports of the same miRNA having opposite expression patterns in the same cancer. For example, miR-182 was found downregulated in melanoma samples from my array results, whereas it was reported upregulated in other melanoma samples [385].

The few functional studies reported on the role of these miRNAs in cutaneous melanoma are discussed in detail in Chapter 4 where I go on to describe the results of my own functional studies.

Chapter 4: Functional studies of microRNAs in melanoma cells

4.1 Introduction

Besides the use of miRNA as diagnostic and prognostic markers in cancer, they have important functional roles through their ability to regulate the expression of target genes by binding with perfect or imperfect complementarity to the 3' UTRs of their target mRNAs. About 61% of miRNA genes are located within intronic regions of protein-coding genes, but they are also found in exons themselves and in intergenic regions [355]. Moreover, more than 50% of miRNA genes can be found in cancer-associated genomic regions or in fragile sites, suggesting that miRNAs play an extremely important role in the pathogenesis of neoplasias [250]. This has been confirmed by a great number of functional studies in various cancers. Generally, dysregulated miRNAs participate in carcinogenesis through altered expression of their targets, which are involved in cell proliferation, apoptosis and metastasis.

4.1.1 Roles of microRNAs in cell proliferation and apoptosis

Members of the Cip/Kip family of cyclin-dependent kinase inhibitors (CKIs) are well characterized for their role as negative regulators of G_1-phase cell-cycle progression [386]. p21, p27 and p57 are members of this family. In gastric carcinogenesis, several miRNAs have been found to be involved in altering the expression of CDK inhibitors. Two clusters of miRNAs, miR-106b/93/25 and miR-221/222, are upregulated in gastric cancer tissues and have been reported to inhibit CKIs [387]. miR-25 directly targets p57, and miR-106b/93 target p21. They both control their targets through the 3' UTR, and subsequently induce cell proliferation. miR-221/222 have been reported to suppress both p27 and p57. Ectopic expression of these two miRNAs enhances CDK2 activity and assists the G1-S transition. Enforced expression of the miR-221/222 cluster also promotes the growth of gastric cancer xenografts in nude mice. Furthermore, aberrant miRNAs have been shown to regulate apoptosis by changing the expression of Bcl-2 family members in gastric cancer as well. miR-15b, miR-16, miR-34 and miR-181b all directly target the

antiapoptotic protein Bcl-2. They are downregulated in gastric cancer cells and thus reduce apoptosis [388, 389].

Knockdown of miR-31 repressed lung cancer cell clonal growth and *in vivo* tumourigenicity. miR-31 could function as an oncomiR by directly repressing the tumour suppressors, large tumour suppressor homolog 2 (LATS2) and protein phosphatase 2 regulatory subunit B alpha isoform (PPP2R2A) [390]. miR-122, which accounts for 70% of the total liver miRNA population, was found to be frequently downregulated in hepatocellular carcinoma (HCC) and in all HCC-derived cell lines. miR-122 can suppress HCC cell growth by directly targeting cyclin G1 expression [391], as well as reducing the invasive capability of HCC-derived cells [392].

Figure 4.1 is adapted from a review that discusses the role of miRNAs in liver cancer. Interestingly, the figure represents an interacting network of the most common aberrant miRNAs and their target genes in a variety of different cancers. For example, similar functions of miR-106 and miR-93 mentioned above in gastric cancer also have been observed in liver cancer. p21 is also a direct target of miR-106b and miR-93 [393] that are overexpressed in HCC and may have critical roles in cell proliferation by regulating the G1-to-S cell cycle transition. Likewise, miR-221/miR-222 can function as oncogenes in HCC by binding to target sites in the 3' UTR of p27 [394] and as well as directly interacting with p57 [395] at the post-transcriptional level. By controlling these two CDK inhibitors, miR-221/222 promotes HCC cell growth by increasing the number of cells in S-phase.

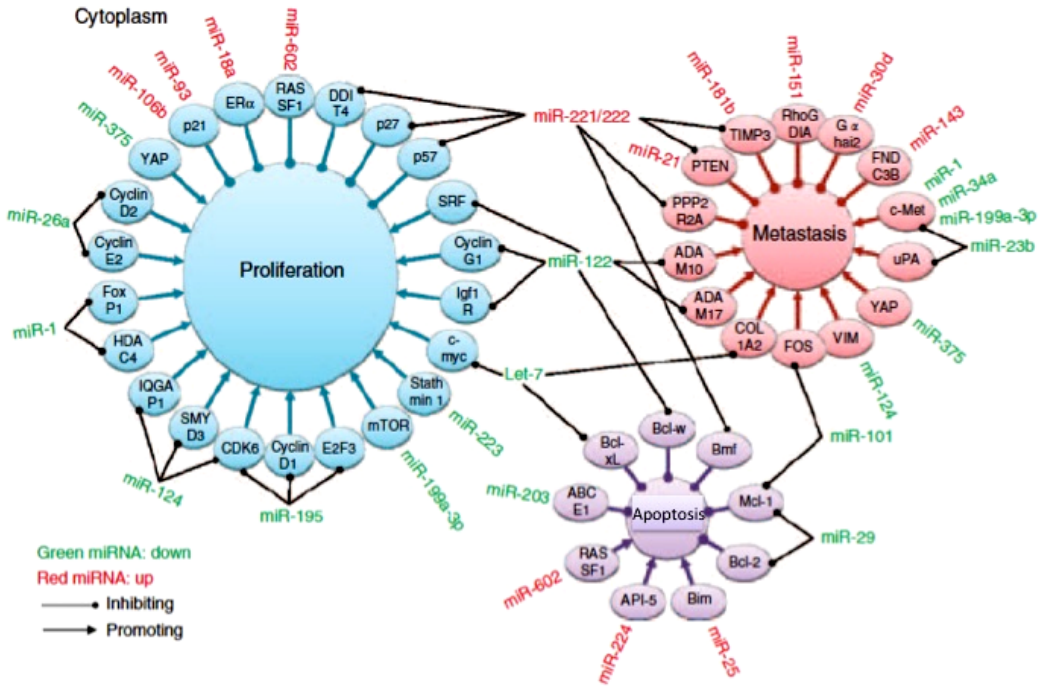

Figure 4.1 The network of aberrant microRNAs and their target genes in cancer. Green miRNA: Downregulated in cancer. Red miRNA: Upregulated in cancer. Adapted from [396].

4.1.2 Roles of microRNAs in tumour metastasis

The above examples are mostly relevant to roles of miRNAs in cell growth and apoptosis. A great number of miRNAs are also involved in tumour metastasis. Metastasis from primary tumours involves multiple steps and genes. Neoplastic cells need to dissociate from primary tumours and enter body cavities or more commonly, circulatory systems (lymphatics and/or blood vasculature), and survive during transportation until they arrest at discontiguous sites, exit the circulation and finally proliferate at ectopic sites (colonization) in response to local growth factors [397]. Although primary tumour formation is a prerequisite to metastasis, tumourigenicity and metastasis are distinct phenotypes. Therefore, the question is whether there exist specific metastasis-regulatory miRNAs (metastamiRs). Many studies have found both metastasis-suppressing and metastasis-promoting metastamiRs, which have

been discovered in the metastatic cascade including cell growth, EMT, adhesion, migration, invasion, apoptosis and/or angiogenesis [279]. miR-10b was the first metastasis-promoting miRNA described that was highly expressed only in metastatic breast cancer cell lines [398]. miR-10b was found to enhance migration and invasion *in vitro* and metastasis *in vivo*. miR-10b expression was elevated by Twist homolog 1 (TWIST1) and it directly targeted Homeobox protein Hox-D1 (HOXD1), leading to increased expression of RAS homolog gene family member C (RHOC).

Members of the miR-200 family are very important metastasis-suppressing metastamiRs that particularly aroused my attention, as they were all present in my differentially expressed miRNA list. The miR-200 family was found to reverse the EMT process needed for metastasis by driving a mesenchymal to epithelial transition (MET) through directly targeting E-cadherin (CDH1) transcription repressors Zinc finger E-box binding homeobox1/2—ZEB1 (δEF1)/ ZEB2 (SIP1) in various cancers (Figure 4.2), including breast, pancreatic, colorectal and ovarian [399-404]. Moreover, miR-205, which also directly targeted both ZEB1 and ZEB2, was found downregulated in cancer cells that had undergone EMT. In addition, upregulation of the miR-200 family and miR-205 in EMT cell lines caused morphological change from a spindle-shaped, mesenchymal form to a rounded, epithelial-like form [399].

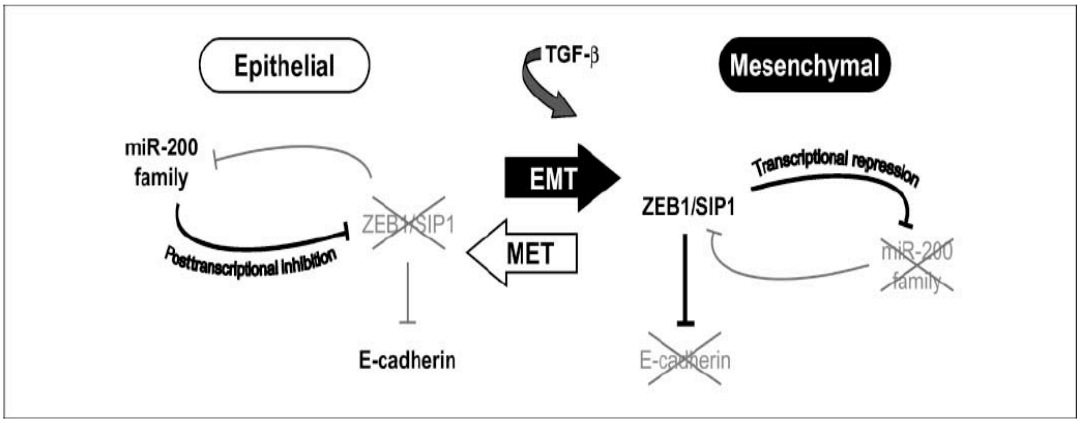

Figure 4.2 The schematic model for feedback loop between the miR-200 family and ZEB1/ZEB2 in switching the EMT-MET process. In epithelial cells, a stable state is maintained by high levels of miR-200, which inhibits ZEB1/SIP1 and increases the expression of ZEB-repressed epithelial genes such as E-cadherin. The switch to a mesenchymal state can be induced by TGF-ß, which increases ZEB1-SIP1 levels. This in turn triggers and maintains a mesenchymal state through ZEB1-SIP1

binding to ZEB-type E-boxes within the miR-200 family promoter and repressing miR-200 transcription. Together, this system forms a double-negative feedback loop, maintaining stable cellular states depending upon the relative levels of ZEB1-SIP1 and miR-200, yet retaining the ability to switch between these states, as exemplified by TGF-ß induced EMT. Figure is adapted from [401].

4.1.3 The miR-200 family, EMT and melanoma

The miR-200 family comprises five members: miR-200a, b, c, 141 and 429, which are generated from two transcripts. Human miR-200a/b/429 are located on chromosome 1 and miR-200c/141 are located on chromosome 12. The members of this family are highly related in sequence, especially in the nucleotide 2-8 seed region (Table 4.1 and Figure 4.3) that determines target specification, indicating that they likely target a similar complement of mRNAs. Within the five members, miR-200a and miR-141 have the same seed region, while the other three group together with a different common seed region (Table 4.1).

EMT-like processes take place during embryonic development and wound healing [405] and in carcinogenesis, as well as when cancer cells undergo a change from a differentiated to a more invasive undifferentiated tumour [405, 406]. When an EMT-like process is triggered, cells lose epithelial features and acquire mesenchymal signatures. Cells become more invasive by expressing proteases that allow them to pass through basement membrane and migrate. During EMT, cancer cells can express various transcription factors in response to stimulation with soluble factors that are present in the tumour environment, such as TGF-ß. The two E-box-binding transcription factors—ZEB1 and ZEB2 are important regulators because they negatively regulate the expression of E-cadherin and assist the EMT process [407-409]. Figure 4.4 shows a schematic model of ZEB1 3' UTR regions with the miR-200c stem-loop.

miR-200	Sequence
miR-200a	5' UAACACUGUCUGGUAACGAUGU 3'
miR-200b	5' UAAUACUGCCUGGUAAUGAUGA 3'
miR-429	5' UAAUACUGUCUGGUAAAACCGU 3'
miR-200c	5' UAAUACUGCCGGGUAAUGAUGG 3'
miR-141	5' UAACACUGUCUGGUAAAGAUGG 3'

Table 4.1 Sequence alignment of microRNAs of the miR-200 family. The seven –nucleotide seed regions are underlined. There are two subgroups: miR-200a and miR141; miR-200b, c and 429.

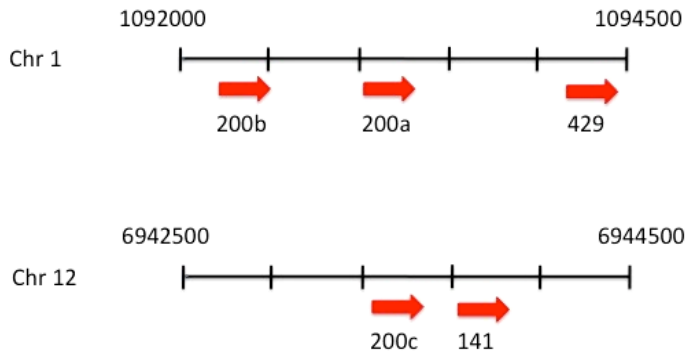

Figure 4.3 Chromosomal locations of the members in the miR-200 family in the human genome. Chr: Chromosome.

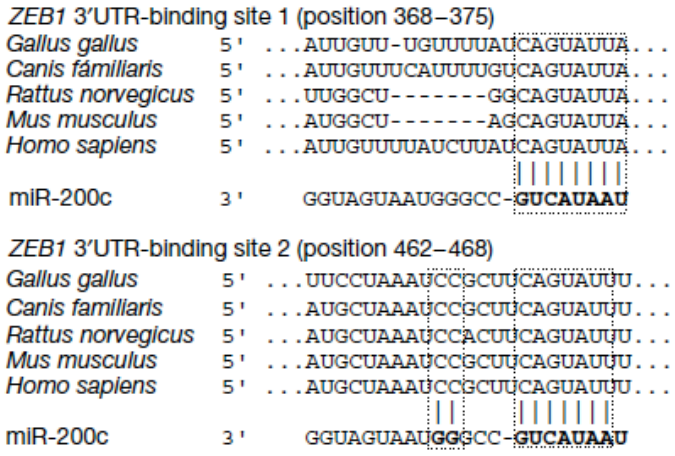

Figure 4.4 The schematic model of ZEB1 binding sites for the miR-200c stem loop. The figure shows two ZEB1 binding sites to the miR-200c stem loop. The putative recognition sites are highly conserved among various species. Adapted from [403].

The NCI-60 panel contains nine different cancers that can be genetically divided into two major branches: subcluster 1 (SC1) cells have a mesenchymal gene signature and subcluster 2 (SC2) cells have an epithelial gene signature [410]. As it is known that E-cadherin is lost during cancer progression, Park *et al.* sorted all NCI-60 panel cell lines from highest to lowest E-cadherin/Vimentin ratio using western blot analysis [404]. Thus, NCI-60 cell lines were grouped into three: epithelial group (with high E-cadherin, low Vimentin), undefined (either equal expression or no expression of both) and mesenchymal group (with low E-cadherin, high Vimentin). Expression of the miR-200 family was positively correlated with E-cadherin, suggesting that the miR-200 family is a powerful marker for cell lines with an epithelial nature. More interestingly, seven of eight melanoma cell lines in the NCI-60 panel belonged to the mesenchymal group and one was in the undefined group. This, combined with my microarray results, led me to ask whether the miR-200 family plays the same role in melanoma metastasis.

First, the question, whether EMT is relevant in melanoma needs, to be answered. Looking back to EMT during embryonic development, primary EMT (that which occurs in tissues that have never undergone a previous EMT) not only occurs at gastrulation but also at neural crest formation. This is the cell lineage that gives rise to melanocytes and changes in cadherin expression and cell-cell adhesion are crucial to neural crest delamination. Besides the roles of EMT in the origin of melanocytes, studies also identified a close relationship between EMT and melanoma. Melanoma constitutively produces TGF-ß and its expression may be related to tumour progression [411]. TGF-ß is involved in downregulation of E-cadherin in melanoma [412]. It was also found that N-cadherin was directly regulated by E-cadherin and loss of E-cadherin could induce NF-κB activity and N-cadherin expression in tumourigenic EMT [413]. A high-throughput study using cutaneous melanoma tissues suggested that EMT-related genes, including N-cadherin, contributed to the promotion of the metastatic phenotype by supporting specific adhesive, invasive and migratory properties [414]. In their study, increased N-cadherin was matched by loss of cadherin 10 expression, a type II cadherin with near-equivalent binding strength to that of E-cadherin [415]. To determine whether human melanoma cells have

decreased levels of E-cadherin, Tang *et al*. stained nine melanoma cell lines. Six of them showed negative staining and the remaining three (SK-MEL-1, 2 and 28) showed positive staining [416]. However, only SK-MEL-1 had E-cadherin at a similar level to normal melanocytes, while the other two showed decreased E-cadherin levels. Another study also showed the loss of E-cadherin expression and high mesenchymal protein expression (N-cadherin, Vimentin and Fibronectin) in melanoma cell lines. Moreover, after cytokine treatment, these mesenchymal proteins were elevated further, indicating that malignant melanoma cell lines are susceptible to EMT after cytokine treatment [417]. However, there has been no report yet that focused on studying the relationship between the miR-200 family and EMT in melanoma metastasis.

Chemotherapy-resistance is often observed in platinum-based chemotherapy, currently the main regimen in non-small cell lung cancer (NSCLC) treatment [418], and is a key cause of chemotherapeutic failure. A recent study investigated the expression of miR-200c in a panel of NSCLC cell lines and a strong inverse correlation with invasion was detected. Reintroduction of miR-200c into highly invasive/aggressive NSCLC cells induced a loss of the mesenchymal phenotype by restoring E-cadherin and reducing N-cadherin expression, and inhibited *in vitro* cell invasion as well as *in vivo* metastasis formation. Moreover, they found overexpression of miR-200c sensitized NCI-H1299 NSCLC cells to cisplatin and cetuximab treatment [419]. This study indicates that the loss of miR-200c expression can induce an aggressive, invasive, and chemoresistant phenotype. Therefore, increasing miR-200c expression level might contribute to anti-carcinogenesis and sensitize to chemotherapy.

4.1.4 Roles of microRNAs in melanoma

So far, studies of miRNAs related to melanoma have mainly involved two aspects: expression and functions of miRNAs, impacts of epigenetic regulation of miRNAs. The majority of the studies have focused on investigating aberrant miRNAs in

melanoma and their functions in melanomagenesis through studying their targets, because it is the most direct approach to identify potential biomarkers that have diagnostic and prognostic values, as well as to discover novel therapeutic targets. A small number of aberrant miRNAs that play a crucial role in melanoma pathogenesis have been identified through functional studies. These miRNAs were identified either from cell based work or tissue study, with or without a microarray screen. I summarise these human melanoma related miRNAs in Table 4.2. This summary does not consider epigenetic regulation of miRNAs or the subsequent impact on melanomagenesis.

miR	Function	Target	Sample type	miRNA Array	Reference
miR-137	Tumour suppressor	MITF α-MSH[1]	Cell	(-)	Bemis LT, 2008
miR-221/222	OncomiR	cKIT	Cell	(-)	Felicetti F, 2008; Igoucheva O, 2009
miR-34	Tumour suppressor	MET	Cell	(-)	Migliore C, 2008
miR-340	Tumour suppressor	MITF	Cell	(-)	Goswami S, 2010
miR-196a	Tumour suppressor	HOX-B7	Cell	(-)	Braig M, 2010
miR-148	Tumour suppressor	MITF	Cell	(-)	Benedikta S, 2010
miR-200	Tumour suppressor	MARCKS, MLC2	Cell	(-)	Elson-Schwab I, 2010
miR-205	Tumour suppressor	E2F1, E2F5	Cell	(-)	Dar AA, 2011
miR-155	Tumour suppressor	SKI	Cell	(-)	Levati L, 2011
miR-125b[2]	Prognostic marker	NA	Tissue	(-)	Glud M, 2010/11
miR-182	OncomiR	FOXO3,	Cell+Tissue	(-)	Segura MF,

		MITF			2009
miR-15b[2]	Prognostic marker	NA	Cell+Tissue	(-)	Satzger I, 2010
miR-193b	Tumour suppressor	CCND1	Cell+Tissue	Tissue (+)	Chen J, 2010
miR-214	OncomiR	TFAP2C	Cell+Tissue	(-)	Penna E, 2011
miR-211	Tumour suppressor	1. KCNMA1	Cell+Tissue	Cell (+)	Mazar J, 2010;
		2. TGFBR2, NFAT5	Cell	(-)	Levy C, 2010;
		3. BRN2	Cell	Cell (+)	Boyle GM, 2011

Table 4.2 Summary of melanoma related microRNAs. MET: MNNG HOS Transforming gene, HOX-B7: Homeobox B7, MARCKS: Myristoylated alanine-rich C-kinase substrate, MLC2: Myosin light chain 2, SKI: V-ski sarcoma viral oncogene homolog, FOXO3: Forkhead box O3, CCND1: Cyclin D1, TFAP2C: Transcription factor AP-2 gamma, KCNMA1: potassium large conductance calcium-activated channel, subfamily M, alpha, TGFBR2: transforming growth factor receptor II, NFAT5: nuclear factor of activated T-cells 5, BRN2: POU domain, class 3, transcription factor 2. NA: Not applicable. In the miRNA Array column, Tissue (+)/Cell (+) means miRNA microarray data based on tissues or cells. α-MSH[1] was found to regulate miR-137. miR-125b[2]/miR-15b[2] act as prognostic markers involved in melanoma progression.

In this Chapter, a series of assays have been performed to investigate potential functions of four miRNAs (miR-200c, 205, 211 and 20b) through manipulating their expression in a human malignant melanoma cell line—A375. To assay for functional miRNAs in melanomagenesis from the set of miRNA candidates identified in Chapter 3, transient transfection was used as it has been proved effective in many functional studies.

4.2 Results

4.2.1 Physiological expression levels of microRNAs in cell lines

As described in Chapter 3, miR-200c, 205 and 211 were significantly decreased while miR-20b was significantly increased in melanoma FFPE samples compared to benign naevi. The expression levels of miR-200c, miR-205 and miR-211 in immortalised melanocytes and several melanoma cell lines are shown in Figure 4.5. The expression levels of miR-200c and miR-205 were generally higher in melanoma cell lines (Figure 4.5-A) than in immortalised melanocytes. However, the expression of miR-211 was greatly decreased in melanoma cell lines relative to immortalised melanocytes (Figure 4.5-B).

(A)

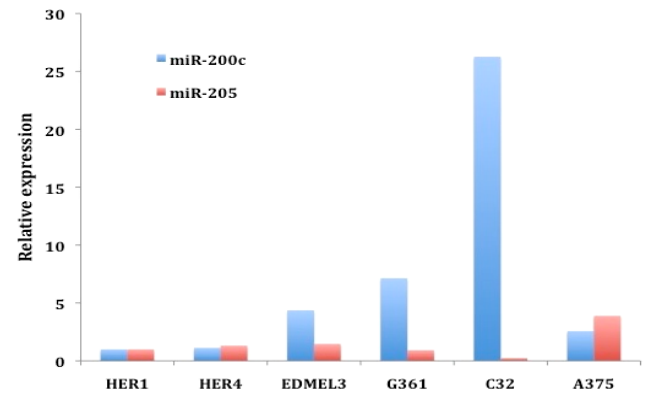

(B)

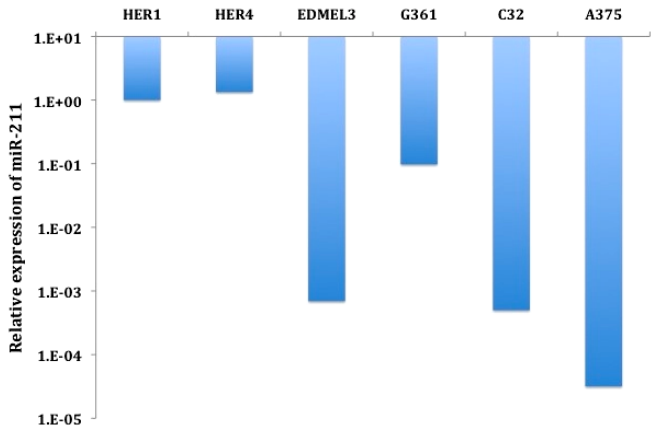

Figure 4.5 Expression levels of selected miRNAs in cell lines. Histograms show the expression of three miRNAs (A) miR-200c, miRNA-205 and (B) miR-211 that were downregulated in human melanoma samples. The expression levels were calculated using the ΔΔCt method relative to miR-92 and were normalized to the HER1 group. The qRT-PCR results represent the average of two individual experiments.

From Figure 4.5, it is clear that expression of miR-211 is downregulated in both melanoma samples and melanoma cell lines, whereas the expression patterns of miR-200c and miR-205 are more complicated. In retrospect, it may have been preferable to compare normal rather than immortalised melanocytes with melanoma cells *in vitro* when considering the role of miRNA expression differences between benign naevi and malignant melanomas. However, neither normal nor immortalised melanocytes are appropriate *in vitro* representatives of the benign naevus *in vivo* as the some genetic features of melanocytes and naevi are not the same. For example, many naevi have mutated BRAF and may experience senescence, while normal and immortalised melanocytes do not show all of these features. Therefore, I think it is valid to overexpress levels of these miRNAs in melanoma cells to mimic the naevus-like situation *in vivo*. I artificially increased miR-200c, 205 and 211 levels in A375 to study their function by comparing cell proliferation, apoptosis, colony formation in methylcellulose and invasion in the miRNA-transfected cells relative to controls. FACS cell cycle analysis, SRB cell proliferation assay, transwell migration assay and methylcellulose colony formation assay were all used. I also used the same assays to see whether there was any functional change after I decreased the expression of miR-20b in A375 cells. For each assay, a negative control group (non-transfected A375 cells), a scramble miRNA control group (A375 cells transfected with scrambled miRNA precursor or inhibitor) and an experimental group (A375 cells transfected with precursor miR-200c, miR-205, miR-211 and inhibitor miR-20b) were included.

4.2.2 Optimization of transfection efficiency

Prior to functional studies, to obtain the highest transfection efficiency various amount of transfection agents and fluorescently labelled small RNA oligos (precursor/ inhibitor scramble miRNA controls) were mixed and after 24 hours the successfully transfected fluorescently labelled cells were detected using FACS (Table. 4.3). Conditions G1 and G3 in Table 4.3-A showed the highest two efficiencies where about 50% of cells in the populations were transfected successfully with miRNA precursors. In Table 4.3-B, conditions G2, G3 and G6 gave very high efficiencies (>90% of the cell populations) in miRNA inhibitor transfection assays. Given the need to obtain the best transfection efficiency with the least transfection agent, I chose condition G3 for gain-of-function experiments (Table 4.3-A), and condition G3 for the knockdown experiments (Table 4.3-B).

(A)

	Control	G1	G2	G3	G4	G5
NeoFx (ul)	0	4	4	8	12	16
Pre-scramble (nM)	0	50	30	30	30	30
Efficiency (%)	0.3	47.8	29.1	56.3	41.1	29.2

(B)

	Control	G1	G2	G3	G4	G5	G6
NeoFx (ul)	0	4	4	4	8	8	8
Anti-scramble (nM)	0	10	50	100	10	50	100
Efficiency (%)	0.3	11.8	91.9	95.2	39.2	89.6	97.8

Table 4.3 Optimization of transfection conditions. The tables show the transfection efficiency with different input amounts of transfection agents and small RNA oligos after 24 hours as assessed using FACS to measure fluorescence from the labelled oligo. (A) Optimization in miRNA gain-of-function experiments. Pre-scramble represents a negative control for a miRNA precursor. (B) Optimization in inhibiting endogenous miRNA molecule experiments. Anti-scramble represents a negative control for a miRNA inhibitor. G: Group. NeoFx: Transfection agent. Pre-scramble/Anti-scramble (nM) represents final concentration of both small oligos.

4.2.3 Time course

To confirm how long transfected miRNAs remain in the cells, the fluorescently labelled cell assay was assessed over a 3-day time course (Table 4.4). In the transfecting precursor assay (Table 4.4-A), the transfection efficiency was higher at 24 hours (84%) compared to the optimization experiment (Table 4.3-A). For both precursor and inhibitor transfection, the frequencies of labelled cells dropped rapidly on subsequent days (Table 4.4). However, the reduction was more rapid in the inhibitor transfection group than in the precursor transfection group.

(A)

		Control	G
NeoFx (ul)		0	8
pre-scramble (nM)		0	30
Frequency (%)	**24hr**	1.9	83.9
	48hr	0.2	43.9
	72hr	0.1	12.5

(B)

		Control	G
NeoFx (ul)		0	4
anti-scramble (nM)		0	100
Frequency (%)	**24hr**	0.8	97.4
	48hr	0.4	23.9
	72hr	0.5	3.6

Table 4.4 Decay of transfected microRNAs over a three-day time course. The tables show the reduction in fluorescent signal from the transfected miRNA over 3 days. (A) Frequencies of labelled cells in miRNA gain-of-function experiments. Pre-scramble represents a negative control for a miRNA precursor. (B) Frequencies of labelled cells in inhibiting endogenous miRNA molecule experiments. Anti-scramble represents a negative control for a miRNA inhibitor. G: Group. NeoFx: Transfection agent. Pre-scramble/Anti-scramble (nM) represents final concentration of both small oligos.

4.2.4 Functional studies for miR-200c and miR-205

4.2.4.1 Expression level changes following transfection of miR-200c and miR-205 precursors

Expression of miR-200c and miR-205 were significantly reduced in melanomas compared to benign naevi as described in Chapter 3. Thus, precursors of both miR-200c and miR-205 were transfected into A375 melanoma cells for functional studies. Expression of miR-200c and miR-205 were assayed daily for 3 days using qPCR (the same method as used in Chapter 3) after precursors of miR-200c and miR-205 were transfected. Levels of both miR-200c and miR-205 were dramatically increased in precursor transfected cell groups (pre-200c group and pre-205 group) on all three days compared to non-treated negative control and scramble control groups (Table 4.5). The levels were highest at 24 hours and then dropped rapidly over the time course. Phenotypic changes were not seen among the various groups of transfected and control cells (Figure 4.6).

Because miRNA expression 24 hours after transfection was more than 10^6 fold increased relative to controls for miR-205, an extra experiment was carried out to investigate the possibility that the qRT-PCR assay was detecting the precursors themselves in addition to their mature miRNA products.

0.015nmoles of miR-205 precursor were used per well of A375 cells transfected and the yield of total RNA recovered 24hours later was typically 1ug. 100ng of total RNA was used for cDNA synthesis in the qRT-PCR assay. Thus, if the transfection was 100% efficient, 100ng of input RNA in the qRT-PCR assay would contain 0.0015nmoles of miR-205 precursor. When 100ng of non-transfected A375 cell RNA was spiked with 0.0015nmoles of miR-205 precursor and used in the same qPCR assay for quantifying miR-205, the miR-205 signal was $4x10^4$-fold the A375 control level. The equivalent signal for A375 cells transfected with miR-205 precursor was > 10^6-fold the A375 control level. Therefore, although the qRT-PCR

assay does detect the miR-205 precursor, the great majority of the signal obtained is from mature miR-205 rather than its precursor.

(A) Expression of miR-200c

	Negative	Scramble	pre-200c
24hr	1.00±0.23	3.71±2.33	21752±7810
48hr	1.00±0.12	0.92±0.11	5983±2225
72hr	1.00±0.25	0.88±0.19	2187±817

(B) Expression of miR-205

	Negative	Scramble	pre-205
24hr	1.00±0.48	1.42±0.51	1392245±552660
48hr	1.00±0.56	0.97±0.10	521964±142580
72hr	1.00±0.34	1.50±0.59	179269±61807

Table 4.5 Comparison of microRNA expression in negative control, scramble and miR-200c and miR-205 precursor transfected A375 melanoma cells. The two tables compare target miRNA expression changes in negative control, scramble and miR-200c precursor (A) and miR-205 precursor (B) treated A375 cells over 3 days by qRT-PCR using the ΔΔCt method. Expression of each miRNA is shown relative to miR-92 and normalized to the mean of negative control group. Results represent average relative expression ± SEM from three independent determinations, each with triplicate samples. pre-200c: miR-200c precursor treated group, pre-205: miR-205 precursor treated group. The abbreviated terms are used throughout the chapter.

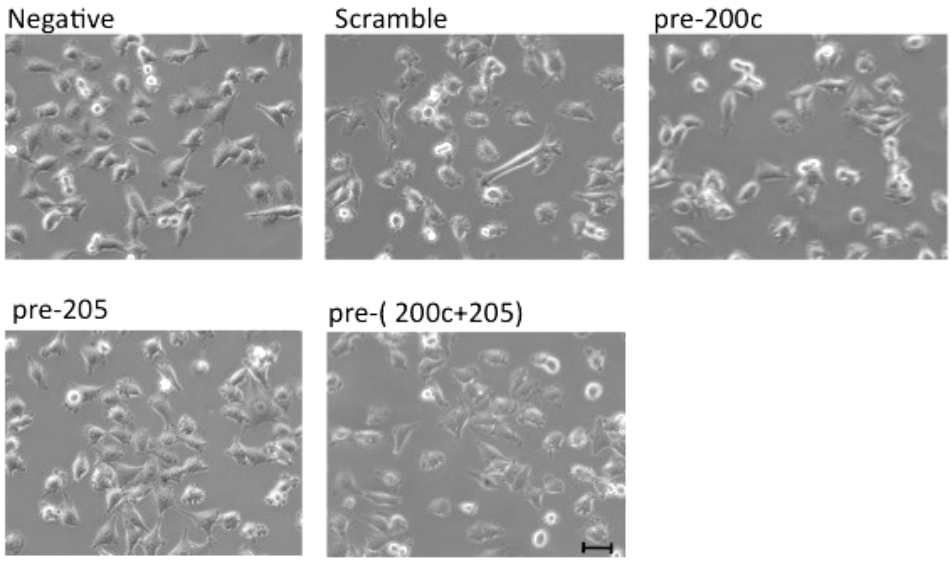

Figure 4.6 Phenotypic comparison of negative control, scramble and miR-200c and miR-205 precursor transfected A375 melanoma cells. The pictures show no phenotypic changes in precursor treated A375 melanoma cells. Magnification: 200x. The black scale bar in picture pre-(200c+205) represents 20um.

4.2.4.2 Cell cycle assay

The cell cycle status of miRNA precursor transfected and control cells was determined post-transfection at 24-, 48- and 72-hours. No changes were seen between the groups for the pre-200c (Table 4.6-A), or the pre-205 (Table 4.6-B) experiments.

(A) miR-200c

	24hr (%)			48hr (%)			72hr (%)		
	(-)	Sr	pre-200c	(-)	Sr	pre-200c	(-)	Sr	pre-200c
Sub G1	1.9	2.2	2.4	2.8	4.1	3.9	4.2	6.5	5.5
G1	50.7	52.3	49.8	52.5	53.1	54.0	63.6	62.3	62.7
S	23.3	22.4	24.3	21.9	22.5	20.3	16.8	16.3	17.3
G2	24.1	23.1	23.5	22.8	20.3	21.8	15.4	14.9	14.5

(B) miR-205

	24hr (%)			48hr (%)			72hr (%)		
	(-)	Sr	pre-205	(-)	Sr	pre-205	(-)	Sr	pre-205
Sub G1	2.1	2.4	2.8	3.0	2.8	3.5	4.2	5.2	3.4
G1	59.3	59.7	60.7	55.9	55.3	52.5	54.8	52.9	52.8
S	20.0	20.1	18.8	22.1	21.8	22.3	20.8	21.6	22.6
G2	18.6	17.8	17.7	19.0	20.1	21.7	20.2	20.3	21.2

Table 4.6 Cell cycle comparison in negative control, scramble and miR-200c and miR-205 precursor transfected A375 melanoma cells. Results represent percentage of cells in each phase of the cell cycle at 24 hours, 48 hours and 72 hours post-transfection determined by FACS from two individual experiments. (A) miR-200c precursor treatment and (B) miR-205 precursor treatment. (-), negative control; Sr, scramble. The above data are the mean results of the two individual experiments.

4.2.4.3 Cell proliferation assay

The SRB cell growth assay was used to assess cell proliferation of miRNA precursor transfected and control cells over a 4-day time course. The assay started immediately post-transfection of precursors of miR-200c and miR-205 (Day0). The same timing was used for migration and colony formation assays. The results were consistent with the cell cycle assay in that no changes were observed between the pre-200c and pre-205 transfected groups and their control groups (Figure 4.7).

(A) miR-200c

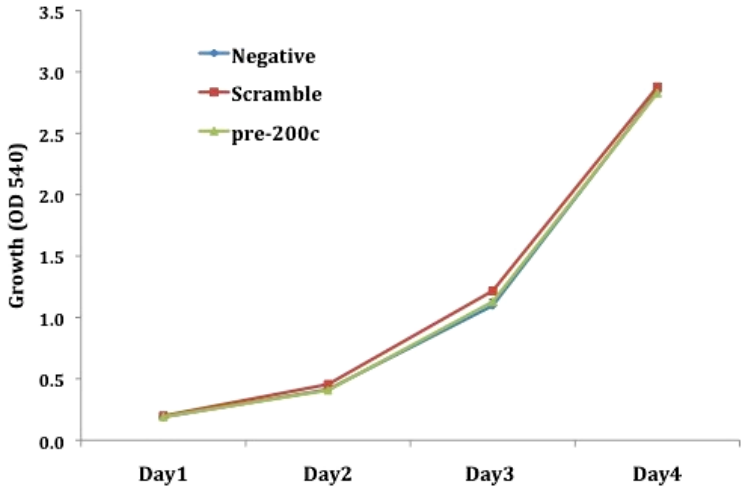

(B) miR-205

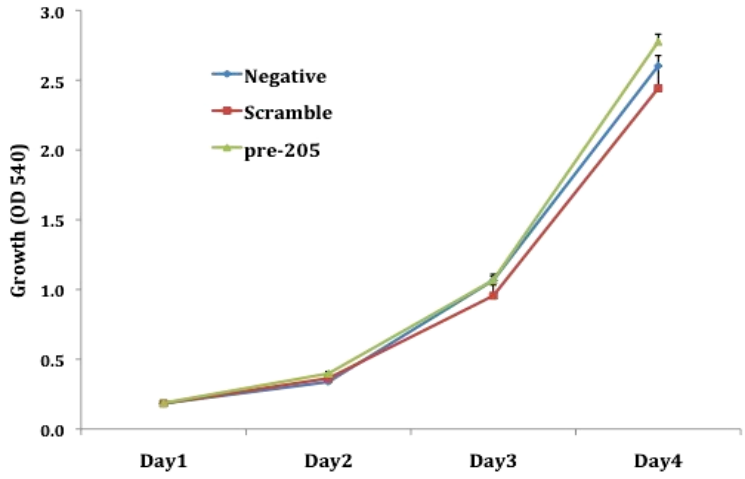

Figure 4.7 Comparison of cell growth in negative control, scramble and miR-200c and miR-205 precursor transfected A375 melanoma cells. The graphs compare cell growth over 4 days. Y-axis represents OD 540 for SRB dye extracted from stained wells as an indirect measure of cell number. Results show average OD values ± SEM of once in a 16-replicate for each time point. (A) miR-200c precursor treatment and (B) miR-205 precursor treatment. Note that error bars are present for all data points, but are often too small to be visible. This experiment was repeated two times with the same result. The above result is from one individual experiment.

4.2.4.4 Transwell migration assay

To determine whether elevated levels of miR-200c and miR-205 influence invasive ability of A375 melanoma cells, the transwell migration assay was performed and migration was analysed on Day 5. For all three experimental groups, pre-200c, pre-205 and pre (200c+205), relative cell numbers at the 40um-layer seem lower than those of both scramble and negative controls (Figure 4.8). However, the differences were not significant (Figure 4.8-A) because of variation between experiments.

(A)

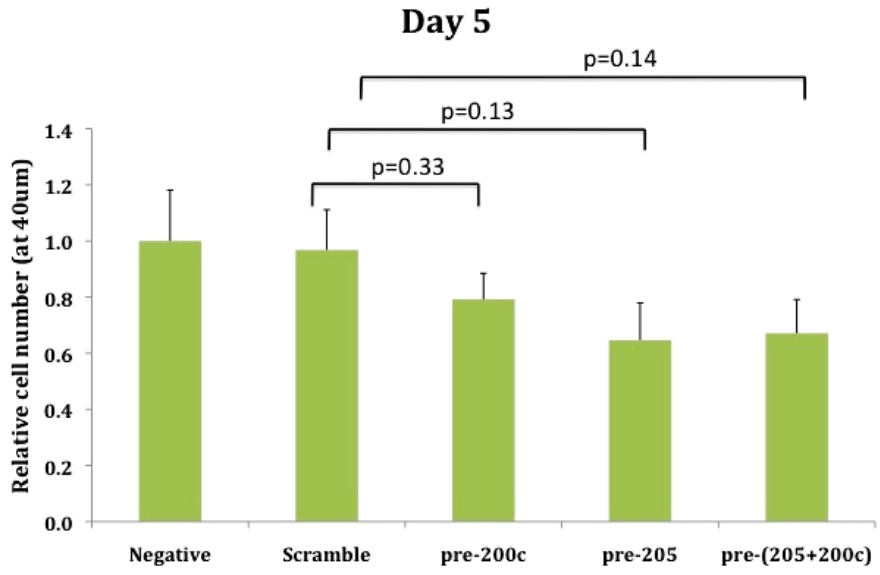

(B)

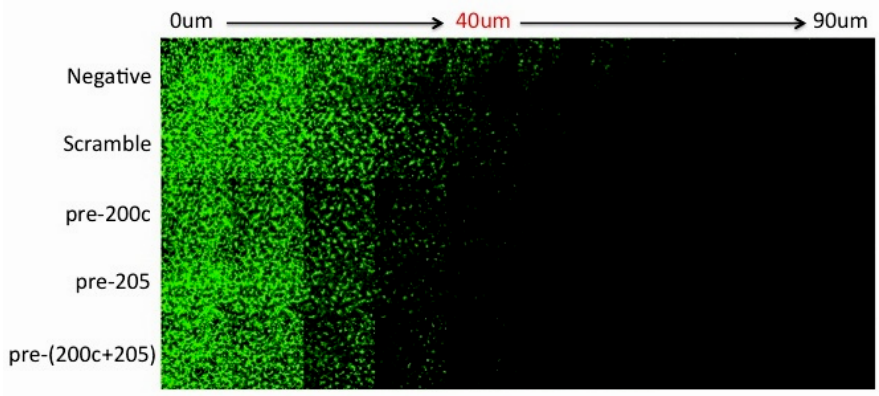

Figure 4.8 Comparison of invasive ability in negative control, scramble and miR-200c and miR-205 precursor transfected A375 melanoma cells. The two figures compare the invasive ability using the transwell inverse invasive assay. (A) Cells migrating through matrigel after 5 days were quantified at the 40um-layer. The relative cell number was measured for each group using the ratio of the cell number at the 40um-layer/ that at bottom layer (0um). Results represent average ratios ± SEM of five microscope fields of one individual experiment. The ratio for each group was normalized to the negative control group. (B) Stacked pictures are confocal microscopic pictures from the bottom layer (0um) to the tenth layer (90um). Each layer is 10um thick. The 40um-layer indicated in red was used to quantify relative cell number. This experiment was repeated three times. The above result is from one individual experiment.

4.2.4.5 Methylcellulose colony formation assay

To determine whether elevated levels of miR-200c and miR-205 affect tumourigenicity of A375 cells, the colony forming ability in methylcellulose was assayed. Colony size was used to evaluate the capacity for colony formation and was measured on Day1, Day3, Day6. Images of entire wells were taken on Day12 and the colony number was counted using Gel doc software with a size threshold parameter set at 3.1 to exclude single cells and very small colonies.

Colony size measured on Day 1, Day 3 and Day 6 is shown in Figure 4.9 (A-C). It is clear from Figure 4.9-A, where each group on Day 1 contains predominantly single cells that all groups were equivalent at the start. There was no difference of colony size on Day 3 between the groups (Figure 4.9-B). However, the colony size was

significantly smaller on Day 6 for all the experimental groups compared to their controls (Figure 4.9- C). The pre-200c group showed a smaller colony size than the pre-205 group, but there was no indication of an additive effect in the pre-(200c+205) group.

Colony numbers on Day12 for negative control, scramble control, pre-200c, pre-205 and pre-(200c+205) were 433, 492, 341, 396 and 315. In Figure 4.9-D, a decreased colony number was observed in each experimental group compared to the controls, and the colony size also looked smaller in experimental groups, consistent with the measurements made on Day6. The colony size was not measured at this stage because the colonies were much bigger on Day12 and difficult to image with the microscope.

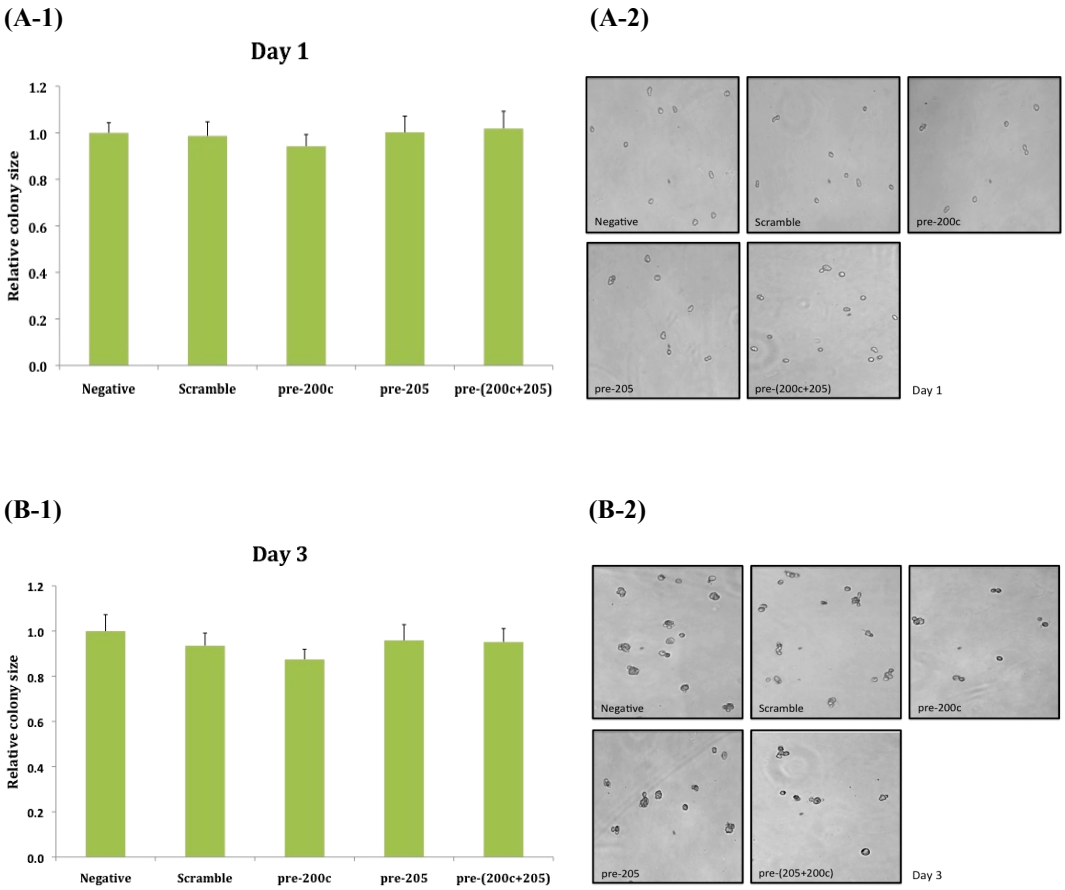

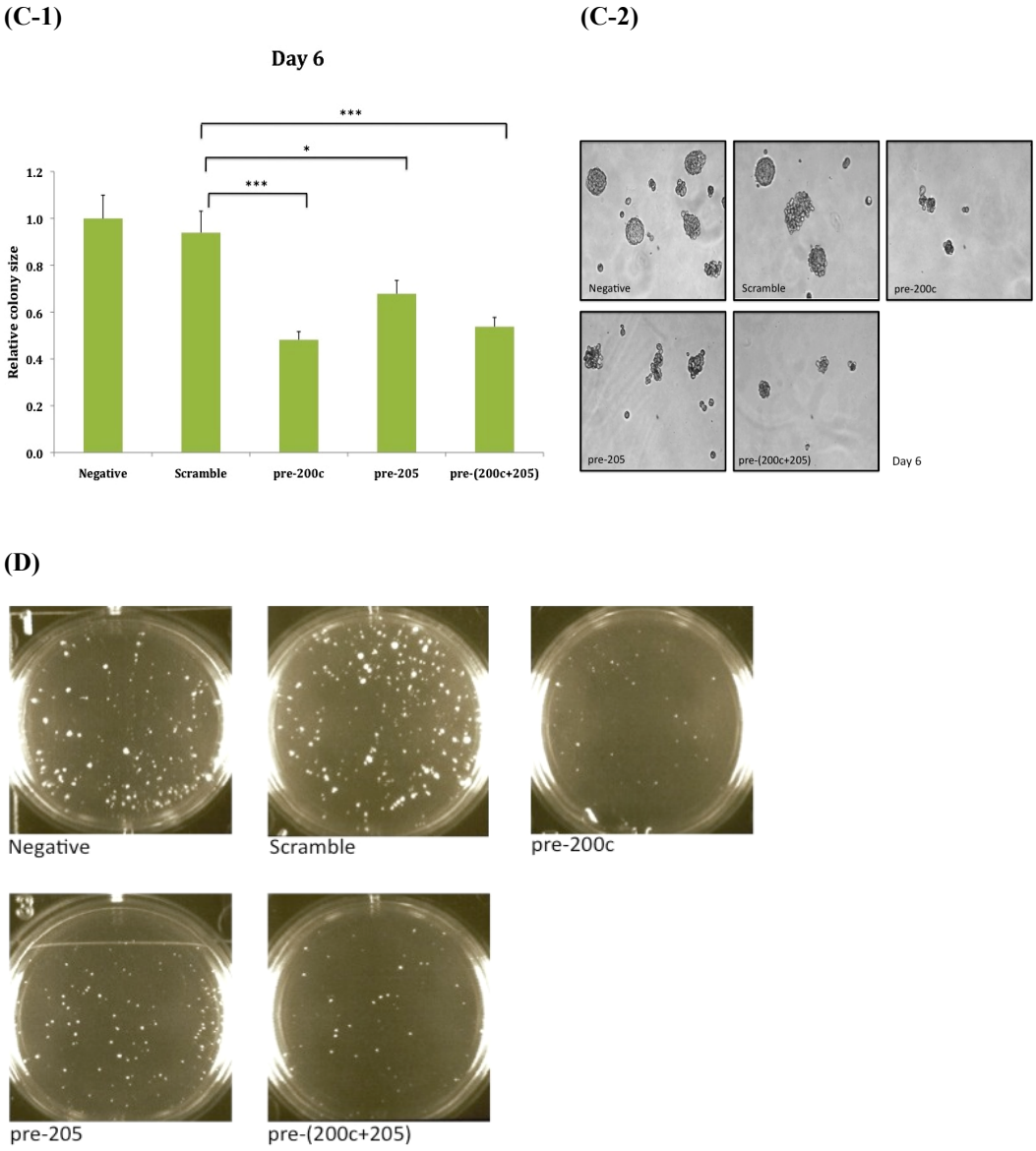

Figure 4.9 Comparison of colony formation in negative control, scramble and miR-200c and miR-205 precursor transfected A375 melanoma cells. The three histograms compare the average colony size in the methylcellulose assay on Day 1, Day 3 and Day 6 (A-1, B-1, C-1). Results represent the average colony size ± SEM of 30 colonies and each group was normalized to the negative control group. Images of colony size of each group are also shown (A-2, B-2, C-2). (C-1) One asterisk: $p<0.05$, three asterisks: $p<0.001$. (D) Images show the colony number in each entire well of a plate on Day12. The assay was repeated three times. The above results were from one individual experiment.

4.2.4.6 Study of miR-200c and miR-205 target genes

ZEB1 and ZEB2 are predicted targets of both miR-200c and miR-205 and this has been demonstrated experimentally in some epithelial cell cancers such as breast and prostate cancer [399, 420]. On the Diana Lab webpage for miRNA target prediction, ZEB2 ranks as the No.1 target of miR-200c (http://diana.cslab.ece.ntua.gr/microT/). Moreover, as described in Section 4.1, E-cadherin is negatively regulated by ZEB2. Therefore, mRNA and protein levels of ZEB2 and E-cadherin were detected using qPCR and western blotting in transfected A375 melanoma cells with elevated levels of miR-200c and miR-205. N-cadherin expression was also detected due to the inverse correlation of E-cadherin and N-cadherin expression in the EMT process.

4.2.4.6.1 Validation experiment on qPCR assays for ZEB2, E-cadherin and N-cadherin mRNAs

As described in Chapter 2, when analyzing qPCR results using the ΔΔCt method, validation experiments first need to be done to evaluate whether the amplification efficiencies of target and reference are equal. For mRNA qPCR, beta-actin was used as the internal control. The slopes of the relative efficiency plots between each individual target mRNA and reference mRNA, beta-actin, were all below 0.1 (Figures are shown in Appendix 5), indicating that the ΔΔCt method was valid.

4.2.4.6.2 ZEB2, E-cadherin and N-cadherin mRNA levels changes

mRNA level changes of ZEB2, E-cadherin and N-cadherin were assayed daily in A375 cells for a 3-day time course post-transfection. ZEB2 expression was downregulated in the pre-200c group for all 3 days, and the reduction was significant on Day1 (4.5-fold) and Day2 (2-fold) compared to the scramble control, indicating that the inhibitory effect was reduced over the time course (Figure 4.10-A). The expression level of ZEB2 was also reduced in the pre-205 group on Day1 but the reduction was not significant (p=0.066) compared to the scramble control (Figure

4.10-B). ZEB2 expression was also decreased in the pre-(200c+205) group on Day1 and Day2, and was significant at Day2 compared to the scramble control (Figure 4.10-C). Consistent with the results of the methylcellulose colony formation assay, there was no indication of an additive effect in the pre-(200c+205) group on the reduction of ZEB2 mRNA levels. Again, in line with the rapid decline of miR-200c and miR-205 levels post-transfection, their effect on ZEB2 mRNA was most marked 24 hours post-transfection.

Subsequently, E-cadherin gene expression was only assayed in miR-200c elevated cells as ZEB2 expression was significantly reduced by miR-200c, but not by miR-205 overexpression. E-cadherin gene expression was increased in the pre-200c group on all three days compared to the controls and the elevation effect was significant on Day1 (3-fold) and Day2 (4-fold) (Figure 4.11-A). This was compatible with the observed reduction in ZEB2 mRNA on the same days. However, there were no N-cadherin gene expression changes in the pre-200c group relative to the controls (Figure 4.11-B), suggesting that expression changes of ZEB2 and E-cadherin caused by miR-200c overexpression failed to trigger the expected subsequent reduction of N-cadherin expression (See discussion).

(A)

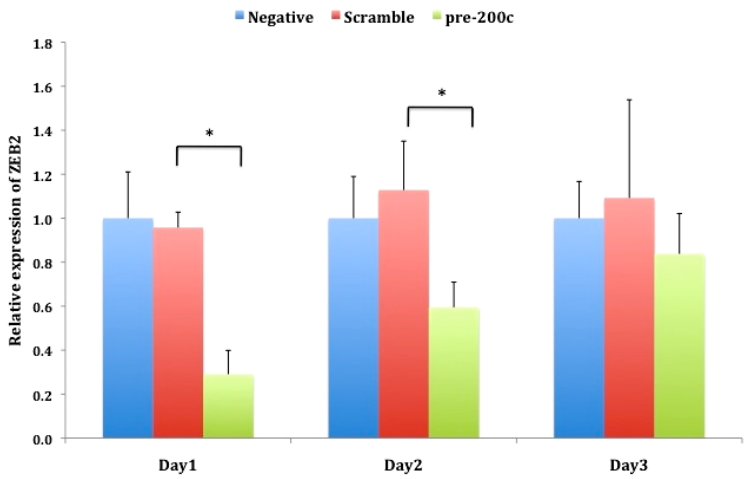

(B)

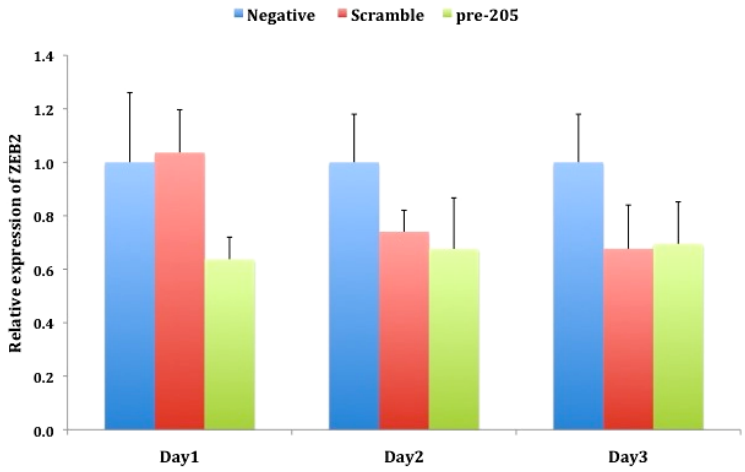

(C)

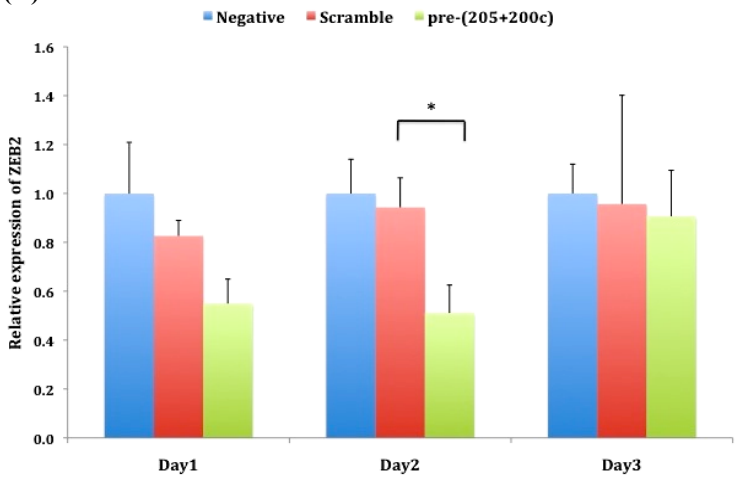

Figure 4.10 Comparison of ZEB2 expression in negative control, scramble and miR-200c and miR-205 precursor transfected A375 melanoma cells. The series of histograms compare the expression of ZEB2 mRNA in negative control, scramble and miR-200c precursor (A), miR-205 precursor (B) and miR-(200c+205) precursors (C) treated A375 cells by qRT-PCR using the ΔΔCt method. Expression of ZEB2 mRNA relative to beta-actin is shown and is normalized to the mean of the negative control group. (A-C) Data represent average relative expression of ZEB2 ± SEM from three individual experiments. One-asterisk: $p<0.05$.

(A)

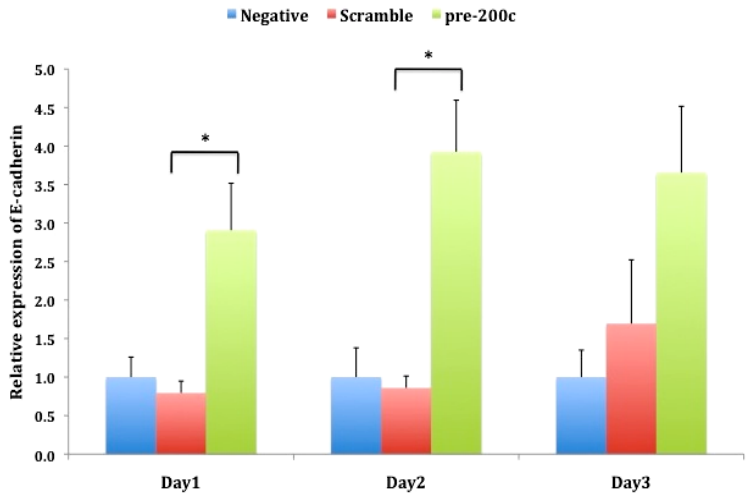

(B)

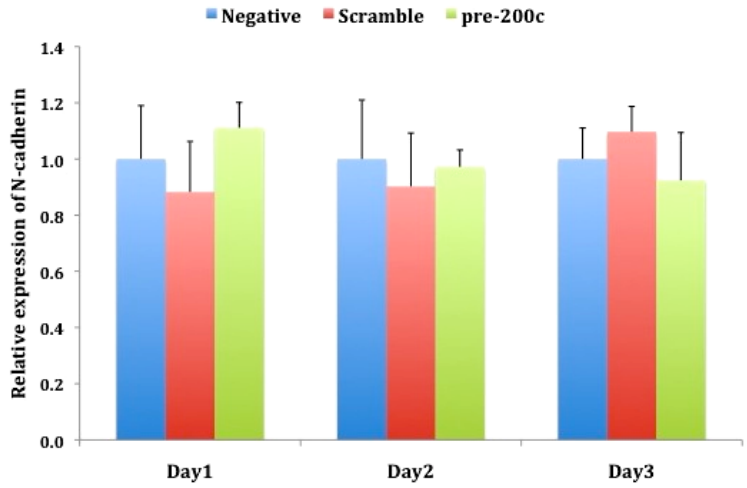

Figure 4.11 Comparison of E-cadherin and N-cadherin expression in negative control, scramble and miR-200c precursor transfected A375 melanoma cells. The histograms compare the expression of E-cadherin and N-cadherin relative to beta-actin in A375 melanoma cells by qRT-PCR using the ΔΔCt method. (A) E-cadherin expression results were normalized to the mean of the negative control group. Data represent average relative expression ± SEM from three individual experiments. One-asterisk: $p<0.05$. (B) N-cadherin expression results were also normalized to the mean of the negative control group. Data represent average relative expression ± SEM from three individual experiments.

4.2.4.6.3 E-cadherin protein level changes

Upregulation of miR-200c in A375 melanoma cells negatively regulated ZEB2 gene expression, resulting in upregulation of E-cadherin gene expression. Thus, western blotting was used to establish whether there were corresponding E-cadherin protein level changes. E-cadherin protein was not detectable in any of the A375 samples tested (negative control, scramble or pre-200c groups), but it was detectable in the immortalised melanocyte cell line, HER1 (Figure 4.12-A). As the mRNA level of E-cadherin in melanocytes (average Ct value was 27.3) was much higher (~100 fold) than that in untreated A375 melanoma cells (average Ct value was higher than 34), any upregulation of E-cadherin protein level in the pre-200c group, equivalent to the observed 4-fold increase in mRNA levels, would probably not to be detectable. I considered using another melanoma cell line instead of A375 for these experiments. Of the five other melanoma cell lines assayed, it turned out that E-cadherin protein was only detectable in G361 (Figure 4.12-A). However, the E-cadherin protein level in G361 was higher than that in HER1 (Figure 4.12, B and C). For this reason G361 was considered unsuitable to demonstrate increased levels of E-cadherin proteins through transfection to elevate miR-200c levels.

(A)

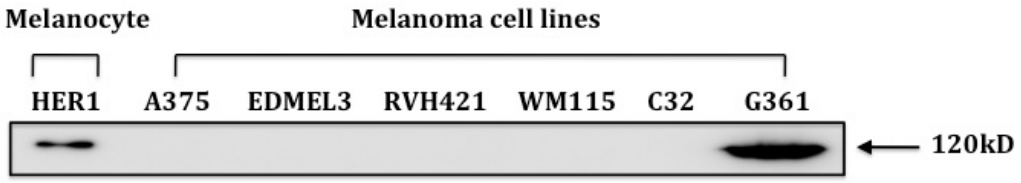

(B)

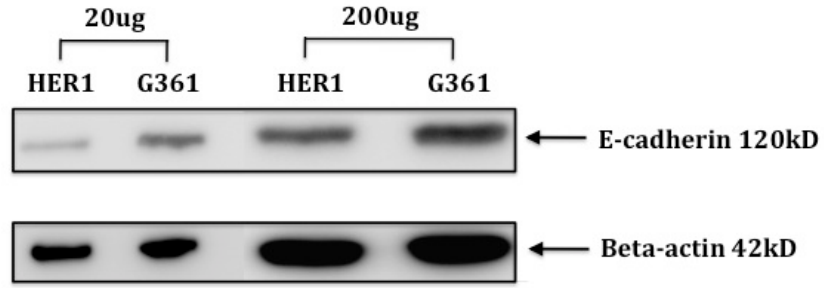

(C)

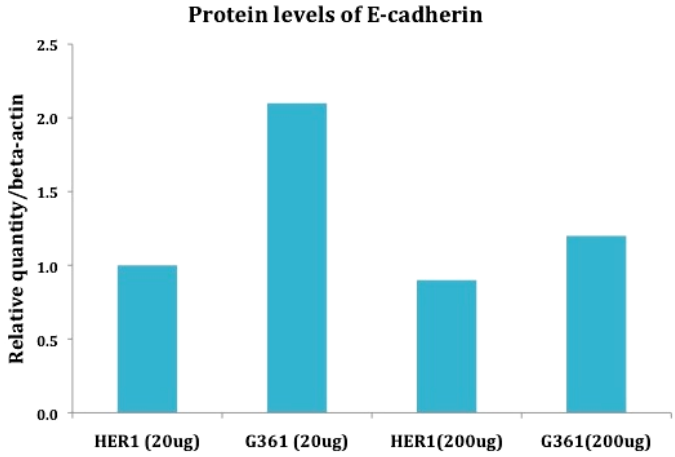

Figure 4.12 E-cadherin protein levels in melanoma cells and melanocytes. (A) Detection of E-cadherin protein in various melanoma cell lines. HER1: an immortalised melanocyte cell line taken as the positive control. (B) E-cadherin protein level changes in two input amounts of cell proteins (20ug and 200ug). (C) The histogram shows the relative protein quantity of E-cadherin over beta-actin for the western blotting shown in (B). Each group was normalised to the HER1 (20ug) group. The western blot experiment was repeated twice with the same result.

4.2.4.7 Effects of miR-200c overexpression on sensitivity of melanoma cells to cisplatin

To assess whether upregulated miR-200c could sensitize A375 melanoma cells to cisplatin, five concentrations of cisplatin were added to negative, scramble and pre-200c groups and cell survival data were obtained at Day 5 post-transfection. Cells with increased miR-200c levels showed a slightly reduced survival rate compared to control groups when treated with 0.1uM and 0.3uM cisplatin (Figure 4.13). However, when cisplatin was increased to more toxic concentrations, the cell survival rate was indistinguishable between the groups with an IC50 for cisplatin in all three groups of 0.44uM.

	0 uM	0.1uM	0.3uM	0.6uM	1uM	3uM
Negative (%)	100±8.3	97.9±4.1	74.5±6.5	31.9±7.0	12.3±1.4	4.6±0.9
Scramble (%)	100±1.1	92.3±2.0	71.7±4.1	28.7±1.3	13.2±0.2	5.4±1.2
pre-200c (%)	100±1.2	88.5±0.7	65.9±0.2	31.1±1.9	14.0±0.4	5.7±1.5

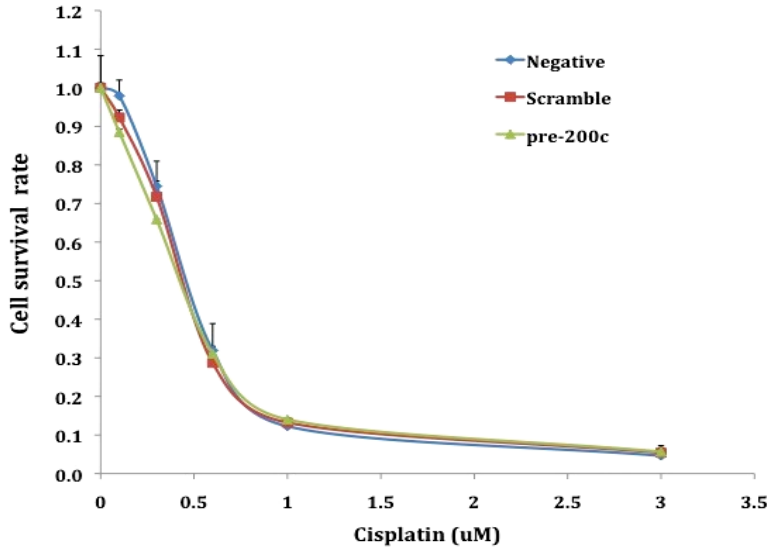

Figure 4.13 Cisplatin sensitivity of negative control, scramble and miR-200c precursor transfected A375 melanoma cells. The table shows cell survival rate of different groups treated with various concentrations of cisplatin for 5 days. Results were normalized to untreated controls and represent average cell survival ± SEM from two individual experiments. Every group of each experiment contained 8 replicates. X-axis: Concentration of cisplatin. Y-axis: Cell survival rate. Note that error bars are present for all data points, but are often too small to be visible.

4.2.5 Functional studies for miR-211

4.2.5.1 Expression level changes following transfection of miR-211 precursor

The expression of miR-211 was significantly reduced in melanoma cells as described in Chapter 3. Therefore, miR-211 precursor was used to increase its expression in A375 melanoma cells for miR-211 functional studies. The expression of miR-211 was tremendously increased compared to negative and scramble controls for the 3 days assayed following transfection of precursor miR-211 (Table 4.7). The increasing level is comparable to the difference between immortalised melanocytes and melanoma cell lines (see Figure 4.5B), which suggests that the miR-211 expression level manipulation *in vitro* may well reflect the situation *in vivo*. miR-211 levels decreased over time, but not so rapidly as for miR-200c and miR-205.

	Negative	Scramble	pre-211
24hr	1.00±0.26	0.71±0.22	1828710±665240
48hr	1.00±0.24	1.72±0.67	1597780±108000
72hr	1.00±0.11	0.99±0.47	934060±270440

Table 4.7 Comparison of microRNA expression in negative control, scramble and miR-211 precursor transfected A375 melanoma cells. The table compares expression changes of miR-211 in negative control, scramble and miR-211 precursor treated A375 cells over 3 days by qRT-PCR using the ΔΔCt method. Expression of each miRNA is shown relative to miR-92 and normalized to the mean of the negative control group. Results represent average relative expression ± SEM two times in a triplicate repeat. pre-211: miR-211 precursor treated group.

4.2.5.2 Cell cycle assay

The cell cycle status of miRNA precursor transfected and control cells was determined post-transfection at 24-, 48- and 72-hours. No changes were seen between the groups for the pre-211 experiment (Table 4.8).

	24hr (%)			48hr (%)			72hr (%)		
	(-)	Sr	pre-211	(-)	Sr	pre-211	(-)	Sr	pre-211
Sub G1	2.4	4.7	4.3	6.8	6.9	6.7	1.3	1.4	1.8
G1	49.4	48.7	48.3	52.6	53.6	51.1	68.1	64.2	65.9
S	26.5	25.8	25.8	19.0	18.2	18.5	15.0	17.5	16.9
G2	21.7	20.8	21.6	21.6	21.3	23.7	15.6	16.9	15.4

Table 4.8 Cell cycle comparison in negative control, scramble and miR-211 precursor transfected A375 melanoma cells. Results represent percentage of cells in each phase of the cell cycle at 24 hours, 48 hours and 72 hours post-transfection determined by FACS. The above data are the average results of two individual experiments.

4.2.5.3 Cell proliferation assay

The SRB cell growth assay was used to assess cell proliferation of miR-211 precursor transfected and control cells over a 4-day time course. The assay started immediately post-transfection of the miR-211 precursor (Day0). The same timing was used for migration and colony formation assay. The results were consistent with

the cell cycle assay in that no changes were observed between the pre-211 transfected group and their control groups (Figure 4.14).

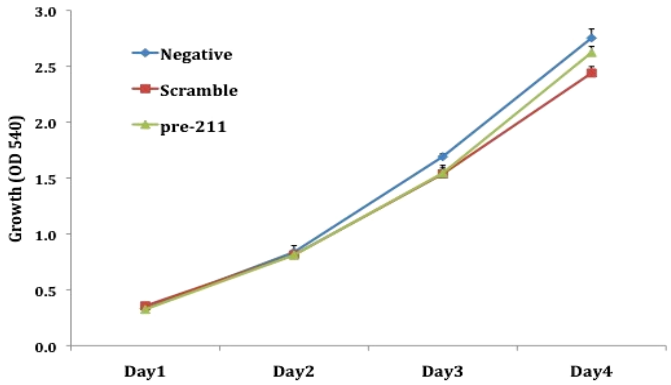

Figure 4.14 Comparison of cell growth in negative control, scramble and miR-211 precursor transfected A375 melanoma cells. The graphs compare cell growth over 4 days. Y-axis represents OD 540 for SRB dye extracted from stained wells as an indirect measure of cell number. Results show average OD values ± SEM of once in a 16-replicate for each time point. Note that error bars are present for all data points, but are often too small to be visible. The experiment was repeated twice with the same result. The above result is from one experiment.

4.2.5.4 Transwell migration assay

Transwell migration assays were performed and migration was analysed on Day 5 in order to determine whether elevated levels of miR-211 influence invasive ability of A375 melanoma cells. The relative cell number of the pre-211 group was significantly lower than both the scramble and negative control groups at the 40um-layer (Figure 4.15-A). The reduced invasion of the pre-211 group compared to the other two showed up clearly in the stacked pictures taken through the matrigel (Figure 4.15-B), and particularly in the enlarged images of the bottom layer and 60um-layer shown in Figure 4.15-C.

(A)

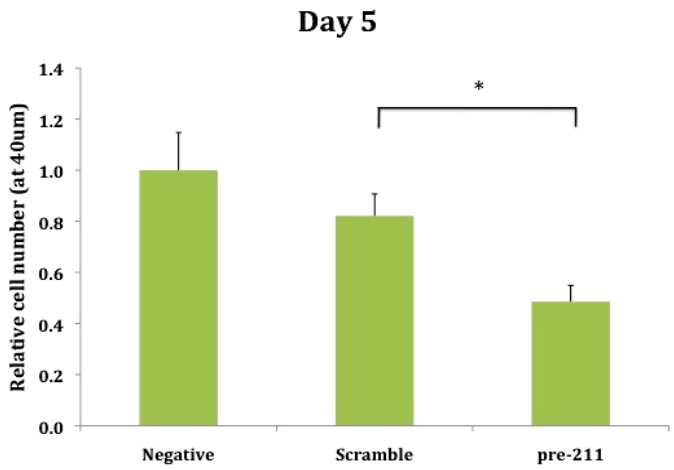

(B)

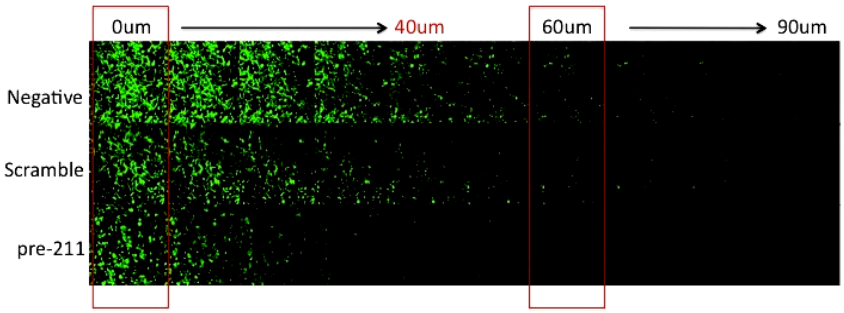

(C)

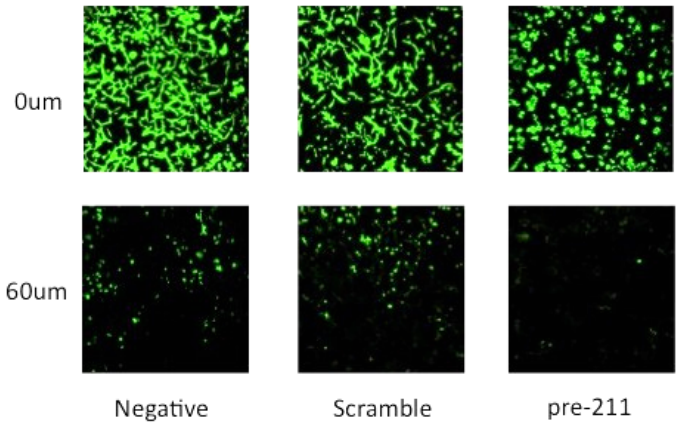

Figure 4.15 Comparison of invasive ability in negative control, scramble and miR-211 precursor transfected A375 melanoma cells. The three figures compare the invasive ability using the transwell inverse invasive assay. (A) Cells migrating through matrigel after 5 days were quantified at the 40um-layer. The relative cell number was measured for each group using the ratio of the cell number at the 40um-layer/ that at the bottom layer (0um). Results represent average ratios ± SEM of six microscope fields of one individual experiment. The ratio for each group was normalized to the negative control

group. (B) Stacked pictures are confocal microscopic pictures from the bottom layer (0um) to the tenth layer (90um). Each layer is 10um thick. The 40um-layer indicated in red was used to quantify relative cell number. The 60um-layer indicated in red is illustrated in enlarged images in (C). (C) Three images (Upper row—0um) represent the bottom layers for the three groups, another three images (Lower row—60um) represent the sixth layers for the three groups. The experiment was repeated three times with the same result. The above result is from one individual experiment.

4.2.5.5 Methylcellulose colony formation assay

To determine whether elevated levels of miR-211 affect tumourigenicity of A375 cells, the colony forming ability in methylcellulose was assayed after transfection. Colony size was used to evaluate the capacity of colony formation and was measured on Day1, Day3, Day6. Images of entire wells were taken on Day12 and colony number was counted using Gel doc software with a threshold parameter set at 3.1 to exclude single cells and very small colonies.

Colony size measured on Day1, Day3 and Day6 is shown in Figure 4.16 (A-C). It is clear from Figure 4.16-A, where each group on Day1 contains mainly single cells that all groups were equivalent at the start. There was no difference of colony size on Day3 between the groups (Figure 4.16-B). However, the colony size was significantly smaller on Day6 for all the experimental groups compared to their controls (Figure 4.16-C). The difference between negative and scramble was not significant ($P > 0.05$).

Colony numbers on Day12 for negative control, scramble control, pre-211 were 770, 547 and 305, respectively. In Figure 4.16-D, a decreased colony number was observed in each experimental group compared to the controls. The colony size was not measured at this stage because the colonies were much bigger on Day12 and difficult to image with the microscope.

(A-1)

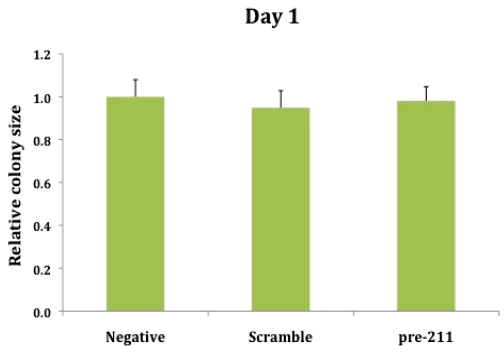

(A-2)

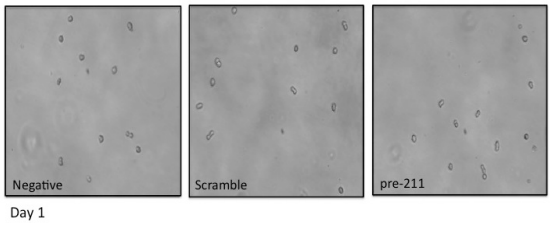

(B-1)

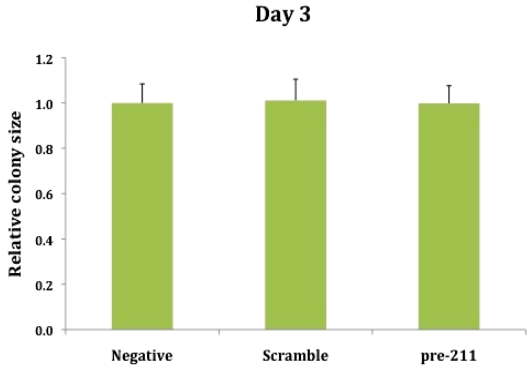

(B-2)

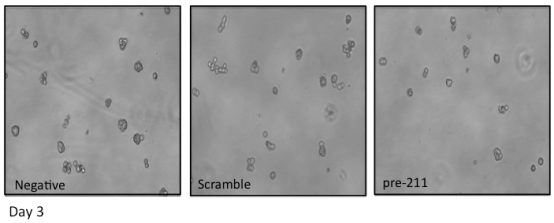

(C-1)

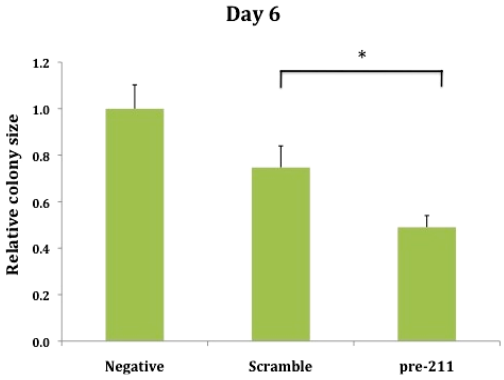

(C-2)

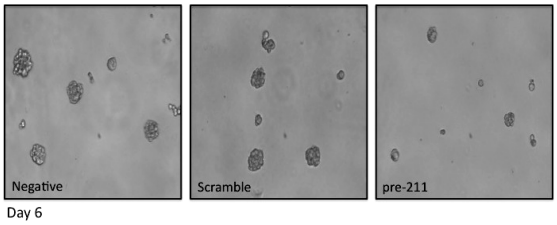

(D)

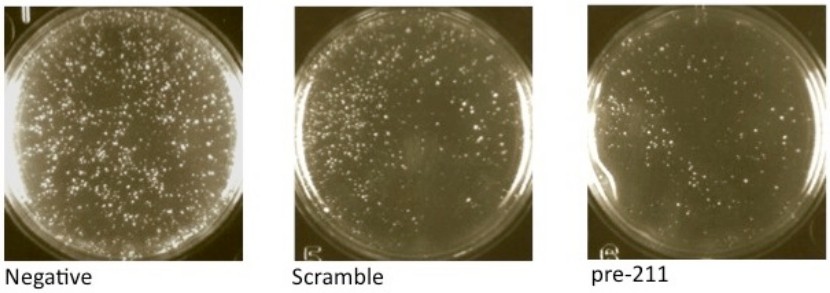

Figure 4.16 Comparison of colony formation in negative control, scramble and miR-211 precursor transfected A375 melanoma cells. The three histograms compare the average colony size in the methylcellulose assay on Day 1, Day 3 and Day 6 (A-1, B-1, C-1). Results represent the average colony size ± SEM of 30 colonies and each group was normalized to the negative control group. Images of colony size of each group are also shown (A-2, B-2, C-2). (C-1) One asterisk: $p<0.05$. (D) Images show the colony number in each entire well of a plate on Day12. The experiment was repeated three times. The above result is from one individual experiment.

4.2.6 Functional studies for miR-20b

4.2.6.1 Expression level changes following transfection of miR-20b inhibitor

Expression of miR-20b was significantly increased in melanomas compared to benign naevi as described in Chapter 3. Therefore, miR-20b inhibitor was transfected into A375 melanoma cells to decrease its expression for functional studies.

Expression of miR-20b was significantly decreased at 24 hours (5 fold) and 48 hours (2 fold) compared to the scramble controls ($p<0.05$) (Table 4.9). The reduction effect diminished rapidly over time. It is also clear that inhibiting expression of miRNAs using inhibitors is not as efficient as increasing expression of miRNAs using precursors, as the inhibitory effect on miR-20b was much smaller than the elevating effect observed earlier on miR-200c, miR-205 and miR-211.

	Negative	Scramble	anti-20b
24hr	1.00±0.14	1.21±0.30	0.23±0.04
48hr	1.00±0.20	0.91±0.06	0.45±0.06
72hr	1.00±0.20	0.91±0.28	0.96±0.19

Table 4.9 Comparison of microRNA expression in negative control, scramble and miR-20b inhibitor transfected A375 melanoma cells. The table compares miR-20b expression changes in negative control, scramble and miR-20b inhibitor treated A375 cells by qRT-PCR using the ΔΔCt method. Expression of miR-20b relative to miR-92 is shown and is normalized to the mean of the negative control group. Results represent average relative expression ± SEM three times in a triplicate repeat. Anti-20b: miR-20b inhibitor treated group.

4.2.6.2 Cell cycle assay

The cell cycle status of miRNA inhibitor transfected and control cells was determined post-transfection at 24-, 48- and 72-hours. No changes were seen between the groups for the anti-20b experiment (Table 4.10).

	24hr (%)			48hr (%)			72hr (%)		
	(-)	Sr	anti-20b	(-)	Sr	anti-20b	(-)	Sr	anti-20b
Sub G1	3.3	4.0	3.9	3.2	2.9	3.2	2.2	1.9	2.1
G1	52.2	53.7	53.5	59.3	59.8	59.4	59.4	58.3	59.2
S	24.3	23.8	23.4	21.4	20.7	20.0	20.4	21.0	20.4
G2	20.2	18.5	19.2	16.1	16.6	17.4	18.0	18.8	18.3

Table 4.10 Cell cycle comparison in negative control, scramble and miR-20b inhibitor transfected A375 melanoma cells. Results represent percentage of cells in each phase of the cell cycle at 24 hours, 48 hours and 72 hours post-transfection determined by FACS. The above data are the average results of two individual experiments.

4.2.6.3 Cell proliferation assay

The SRB cell growth assay was used to assess cell proliferation of miR-20b inhibitor transfected and control cells over a 4-day time course. The assay started immediately post-transfection of the miR-20b inhibitor (Day0). The same timing was also used for the migration and colony formation assays. The results were consistent with the cell

cycle assay in that no changes were observed between the anti-20b group and their control groups (Figure 4.17).

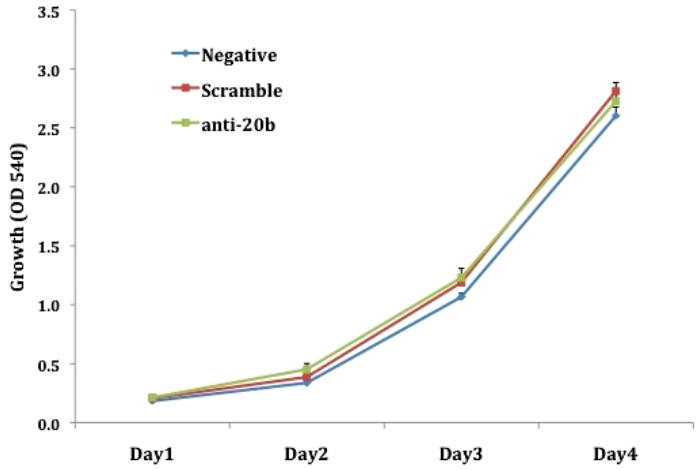

Figure 4.17 Comparison of cell growth in negative control, scramble and miR-20b inhibitor transfected A375 melanoma cells. The graphs compare cell growth over 4 days. Y-axis represents OD 540 for SRB dye extracted from stained wells as an indirect measure of cell number. Results show average OD values ± SEM of once in a 16-replicate for each time point. Note that error bars are present for all data points, but are often too small to be visible. The experiment was repeated twice with the same result. The above figure shows one of the individual experments.

4.2.6.4 Transwell migration assay

Transwell migration assays were also performed for the miR-20b experiment and migration was analysed on Day 5 in order to determine whether decreased levels of miR-20b influence invasive ability of A375 melanoma cells. There was no difference seen for the relative cell number of miR-20b between the groups at the 40um-layer (Figure 4.18).

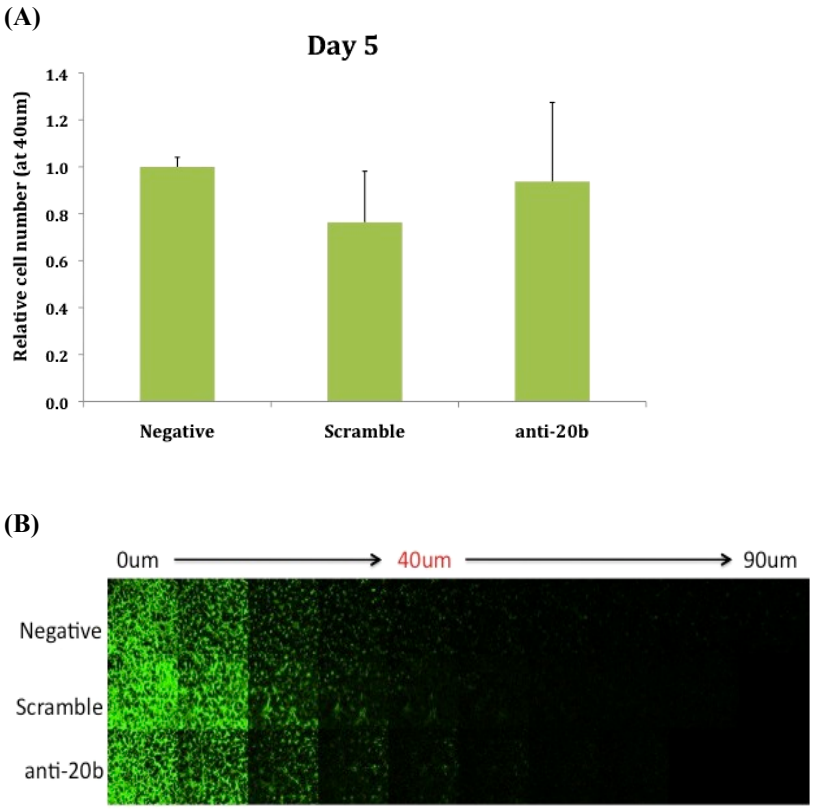

Figure 4.18 Comparison of invasive ability in negative control, scramble and miR-20b inhibitor transfected A375 melanoma cells. The two figures compare the invasive ability using the transwell inverse invasive assay. (A) Cells migrating through matrigel after 5 days were quantified at the 40um-layer. The relative cell number was measured for each group using the ratio of the cell number at the 40um-layer/ that at the bottom layer (0um). Results represent average ratios ± SEM of five microscope fields of one individual experiment. The ratio for each group was normalized to the negative control group. (B) Stacked pictures are confocal microscopic pictures from the bottom layer (0um) to the tenth layer (90um). Each layer is 10um thick. The 40um-layer indicated in red was used to quantify relative cell number. The experiment was repeated twice with the same result. The above result is from one experiment.

4.2.6.5 Methylcellulose colony formation assay

The colony forming ability in methylcellulose was also assayed in anti-20b experiment. Colony size was used to evaluate the capacity for colony formation and was measured on Day1, Day3, Day6.

Colony size measured on Day1, Day3 and Day6 is shown in Figure 4.19 (A-C). It is clear that from Figure 4.19-A, where each group on Day 1 contains mainly single cells that all groups were equivalent at the start. There was no difference of colony size on both Day3 and on Day6 between the groups (Figure 4.19-B, C).

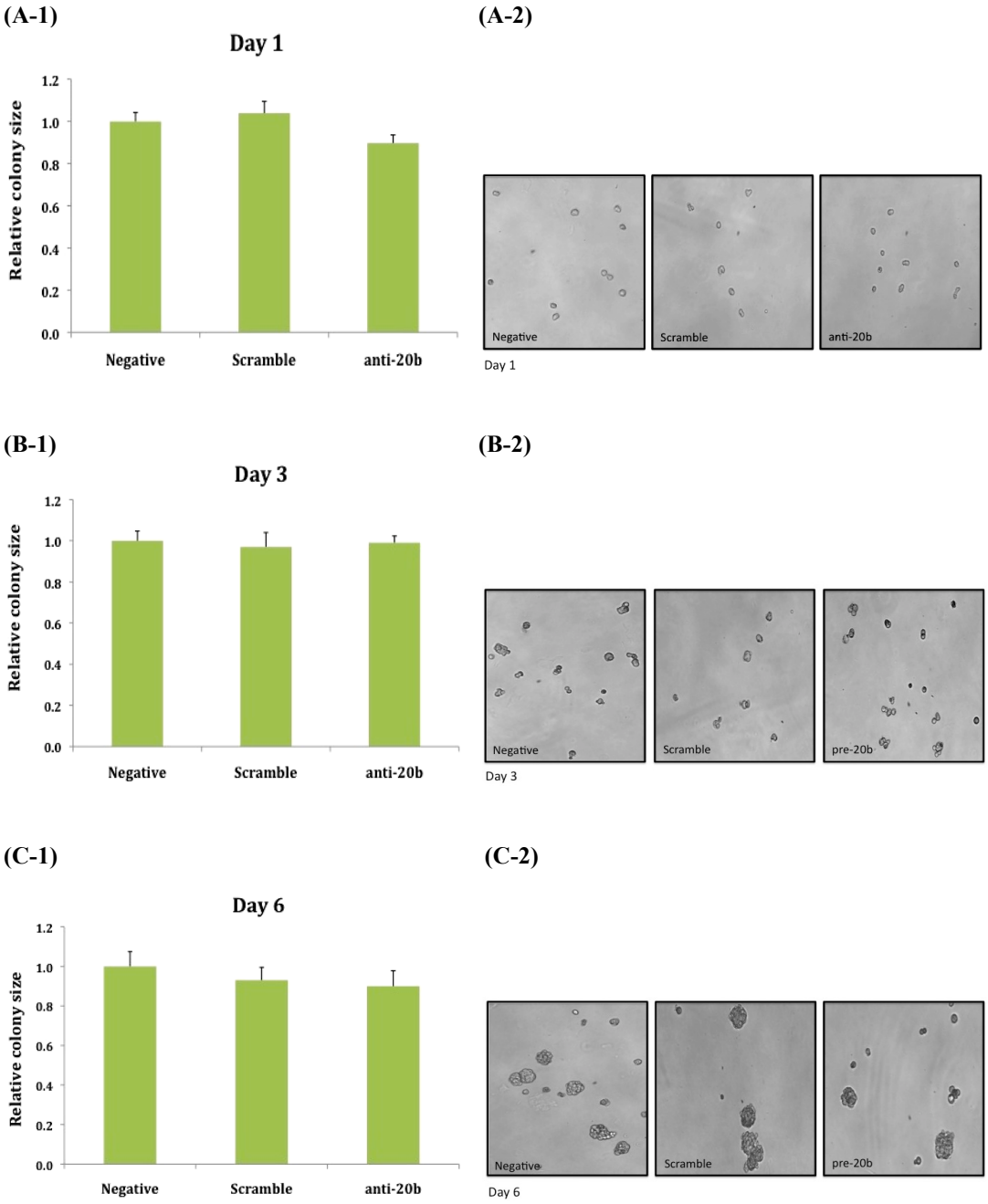

Figure 4.19 Comparison of colony formation in negative control, scramble and miR-20b inhibitor transfected A375 melanoma cells. The three histograms compare the average colony size in the methylcellulose assay on Day 1, Day 3 and Day 6 (A-1, B-1, C-1). Results represent the average

colony size ± SEM of 30 colonies and each group was normalized to the negative control group. Images of colony size of each group are also shown (A-2, B-2, C-2). The experiment was repeated twice with the same results. The above result is from one experiment.

4.3 Discussion

It has been identified in my array work that miR-200c was greatly reduced in melanomas relative to benign naevi, which is consistent with the results of two other studies [370, 371]. Moreover, miR-200c was significantly downregulated in metastatic melanoma compared to primary melanoma from the array, although it wasn't in the top list in the metastasis vs. primary comparison. Given the above facts, the role of the miR-200 family in other cancers, and target prediction results for miR-200c from the Diana Lab web source, it was chosen first from the miR-200 family for functional studies.

Many research groups have shown that miR-200 family members inhibit cancer cell migration through inhibiting the EMT process rather than influencing cell growth [399, 400, 403, 404]. In my study, there were no changes in cell proliferation, cell cycle status or apoptosis in melanoma cells with upregulated miR-200c. However, there was a significant reduction in both colony size and number in the methylcellulose assay, which is an *in vitro* surrogate assay for tumourigenecity. Migration inhibition was not observed in my transwell migration assay, but a good explanation for this comes from other studies on the invasive behaviour of melanoma cells. It has been discovered that melanoma cell invasion *in vivo* is affected by cell morphology and switching between different modes of invasion [421, 422]. The assays of migration on rigid 2D substrates, or transwell migration assays as used in my study, cannot reproduce the rounded "amoeboid" form of movement seen *in vivo* [423, 424]. Interestingly, it was found that expression of miR-200c in melanoma cells drives the rounded-amoeboid form of cell migration, while miR-200a drives the elongated form or mesenchymal-type of invasion using a refined 3D assay with a thick deformable collagen-I matrix [425]. They found both miR-200a and miR-200c

can enhance invasion in some melanoma cell lines using the 3D assay. Thus, the failure to see inhibition of migration in melanoma cells with increased levels of miR-200c in my transwell migration assay is consistent with recent published results.

For the miR-200c target study, I took advantage of the report that the miR-200 family directly target ZEB1 and ZEB2 in other cancers. Therefore, I detected expression of ZEB2 without using a luciferase report system. I detected significant ZEB2 repression at the transcriptional level one day after transfection with the miR-200c precursor and this was accompanied by a significant increase of E-cadherin gene expression. Both effects reduced over time, most likely because the miR-200c upregulating effect was transient. The expression of N-cadherin was not changed, perhaps because the observation time was not long enough, or the increased E-cadherin level was not sufficient to trigger the changes of N-cadherin. I conclude that elevating expression of miR-200c in melanoma cells can inhibit tumourigenicity through repressing colony forming ability in methylcellulose. Further studies would be needed to see if this results in smaller melanoma size *in vivo*. Additionally, although I was not able to evaluate E-cadherin protein level changes in miR-200c increased melanoma cells, it is possible that EMT in melanoma may be reversed to MET through upregulating miR-200c.

As mentioned in the introduction of this Chapter, miR-200c could sensitize NSCLC cells to cisplatin treatment [419]. To investigate whether miR-200c expression is correlated to chemoresistance in melanoma cells, a cell survival assay following cisplatin treatment was performed. No significant change in the IC50 for cisplatin was observed in miR-200c increased melanoma cells. On the contrary, a recent paper has shown significantly increased miR-200c expression in cisplatin-resistant oesophageal cancer cells compared with their parent cells [426]. Knockdown of miR-200c expression resulted in reduced phosphorylation of AKT, indicating overexpression of miR-200c induces cisplatin resistance through activating the AKT signalling pathway. The above results indicate that the relationship between miR-200c and chemoresistance is complicated and may be tissue-specific.

For miR-205, the results of functional studies were quite similar to miR-200c. No

changes occurred in cell proliferation or apoptosis post-transfection of the miR-205 precursor. Melanoma cells with overexpressed miR-205 showed slight inhibition in migration assay, although the inhibition was not significant. Whether miR-205 has the same effects on invasive behaviour as that of miR-200c needs to be studied. Likewise, increased expression of miR-205 may also decrease melanoma size *in vivo* as there was a significant reduction of colony size and colony number in the methylcellulose assay. miR-205 and the miR-200 family share the common targets, ZEB1 and ZEB2. However, unlike the inhibition of ZEB2 mRNA observed in melanoma cells with increased miR-200c, no inhibition was observed in cells with elevated miR-205. Moreover, upregulating miR-205 and miR-200c simultaneously did not have a stronger effect than miR-200c alone, indicating that they do not cooperate with each other. A very recent study identified that E2F1 and E2F5 were direct targets of miR-205. It also elucidated that miR-205 negatively regulates the AKT pathway through targeting these two transcription factors in C8161.9 melanoma cells [427]. Moreover, miR-205 were also involved in inhibiting cell proliferation, inducing apoptosis and reducing colony formation in both transient and stable miR-205 elevated C8161.9 melanoma cells. The inconsistency between the results of the above study and my work is probably because of the different melanoma cell lines used.

Another important miRNA—miR-211, showed a significant reduction in melanomas compared to naevi. Notably, it also showed a thousand fold decrease in most of the melanoma cell lines examined compared to immortalised melanocytes. In my functional studies of miR-211, I found that ectopic expression of miR-211 significantly decreased colony forming ability in methylcellulose and inhibited cell migration in melanoma cells. However, cell proliferation changes in normal media were not observed. Three papers have been published recently that discussed the role of miR-211 in melanomagenesis. There are both consistencies and inconsistencies with my results.

The consistency is that the same expression pattern in both cells and tissues implies miR-211 definitely acts as a tumour suppressor. The question is how? Mazer *et al.*

revealed that miR-211 inversely regulates KCNMA1 at both transcription and protein levels. KCNMA1 encodes a component of a K^+ exporting channel whose function is modulated by Ca^{2+}. It has been linked to tumour cell proliferation in prostate cancer [428], cell migration in glioma [429], and antineoplastic drug resistance in melanoma cells [430]. Levy *et al.* found that transforming growth factor receptor II (TGFBR2) and nuclear factor of activated T-cells 5 (NFAT5) are the direct targets of miR-211. Boyle *et al.* reported that BRN2 is the direct target of miR-211. However, the discrepancy is that in Mazer *et al.*'s study, overexpression of miR-211 inhibited both cell proliferation and migration of melanoma cells, while the other two groups only showed changes in migration, which is consistent with my results.

Intriguingly, miR-211 is encoded within the sixth intron of TRPM1 (melastatin), a candidate suppressor of melanoma metastasis. MITF is the transcription factor for TRPM1. MITF coodinately regulates both miR-211 and TRPM1 expression [381]. High levels of MITF inhibit melanoma invasiveness and this is likely due to its effects on miR-211 independent of melastatin, indicating that TRPM1 is not itself a tumour suppressor, but is rather a marker of expression of the true melanoma tumour suppressor at this locus, miR-211 [382, 383].

miR-20b was upregulated in melanoma tissues compared to the other three miRNAs that I also conducted functional studies on. It has been reported to accumulate in tumour cells and act as an oncogene in human T-cell leukemia and mouse breast tumours [379, 431]. My functional studies for miR-20b did not show any changes in melanoma cells with reduced miR-20b levels. A possible explanation could be that the miR-20b reduction was too small to show significant functional differences, or miR-20b functions in other carcinogenetic processes that were not assayed in my work.

The roles of miR-20b in tumourigenesis are quite complicated. Two papers discussed the role of miRNAs in angiogenesis under hypoxic condition, whereas none of my studies were relevant to tumour angiogenesis. miR-20b was confirmed to regulate oxygenation and two angiogenesis related regulators (hypoxia inducible factor 1 α

subunit—HIF-1α and vascular endothelial growth factor—VEGF) in several mouse tumour cell lines, including a melanoma mouse cell line—B16 [432]. Both HIF-1α and VEGF are the direct targets of miR-20b [432, 433] and HIF-1α can also inversely regulate miR-20b expression [432]. Furthermore, VEGF can be transcriptionally activated by HIF-1α [434]. Zhang *et al.* found differentially low expression of miR-20b in hypoxia compared to the normoxic condition. Combined with the fact that overexpression of HIF-1α leads to a decrease in the level of miR-20b, it could explain why upregulation of miR-20b was established in my melanoma tissues but the inhibition of cell growth was not seen after downregulation of miR-20b in my cell based study. My hypothesis is: when tumour cells proliferate in normoxia, the low level of HIF-1α regulates miR-20b and upregulation of miR-20b is seen. When tumour cell proliferation reaches a hypoxic condition, HIF-1α becomes upregulated and thus miR-20b becomes downregulated and low miR-20b keeps high levels of HIF-1α until VEGF is upregulated to continue tumour progression. The multiple relationship among miR-20b, HIF-1α and VEGF implies their reciprocal action in allowing tumour cells to adapt to different oxygen concentration and angiogenesis for survival. Therefore, oxygen condition should be taken into account in functional studies on miR-20b.

Four miRNAs of the miRNA microarray profile were further studied through functional assays. In this Chapter, it was found that expression of both miR-200c and miR-205 reduced colony forming ability in methylcellulose. This Chapter also first reported that miR-200c negatively regulated expression of ZEB2 and resulted in upregulated E-cadherin at the transcriptional level in melanoma, indicating miR-200c may contribute to the MET process through overexpression of E-cadherin. For miR-211, ectopic expression inhibited colony formation and tumour cell migration. None of these miRNAs influenced cell growth in normal culture conditions. To conclude, miR-200c, miR-205 and miR-211 act as tumour suppressors in melanoma pathogenesis. The functions of miR-20b need further investigation.

Chapter 5: Role of the BRAF V600E mutation in melanomagenesis

5.1 Introduction

Cutaneous melanoma is 10 times more frequently seen in white populations than in black individuals, which indicates a protective role for melanin pigment [435]. The major role of melanin is to protect against the harmful actions of solar radiation. UVR represents a fraction of the solar radiation but it is responsible for the majority of its carcinogenic effect. UVR is divided into UVC (200-280nm), UVB (280-320nm) and UVA (320-400nm) [436]. The UVC spectrum rarely reaches the earth's surface while UVA and UVB wavelength represent 95% and 5% of the UV spectrum reaching the earth's surface. UVB is more efficiently absorbed by cellular molecules, although it is about 20-fold less abundant than UVA [435]. The interaction of UVB with DNA results in 6-4PP and CPD between adjacent pyrimidine sites. If 6-4PPs and CPDs are not repaired, they can induce mutations in many genes. The most abundant mutations after UVB are C to T and CC to TT transitions at bipyrimidine sites or pyrimidine runs, called "UVB fingerprint mutations" [437]. UVB can also induce reactive oxygen species (ROS). Recent studies reported that UVA is also an important factor involved in photocarcinogenesis but through different mechanisms to UVB [437]. UVA induces DNA damage indirectly through the absorption of UVA photons by other cellular structures, such as chromophores, with formation of ROS (H_2O_2). This can transfer the UVA energy to DNA via mutagenic oxidative intermediates, such as 8-hydroxydeoxyguanosine. DNA damage by UVA radiation typically consists of T to G transversions, called "UVA fingerprints". It was found that irradiation of melanocytes with UVA or UVB leads to alterations of different intracellular proteins, indicating that UVA and UVB may trigger initiation of melanoma via separate intracellular pathways [438].

The BRAF gene is a member of the RAF family which comprises three members: ARAF, BRAF and CRAF. It encodes a serine-threonine protein kinase [439]. RAS is a small G protein that is embedded in the plasma membrane of cells and is activated downstream of growth factor receptor tyrosine kinases, cytokines and hormones. RAF is activated following its recruitment to the plasma membrane by RAS and then triggers the MAPK pathway, which regulates cell proliferation, differentiation,

senescence and survival [439].

BRAF is the only RAF protein to be frequently mutated in cancer. No ARAF mutations have been identified so far [440, 441]. CRAF mutations are only rarely found [440, 442], but the gene is overexpressed in some ovarian and pulmonary carcinomas, indicating that CRAF can act as an oncogene [443]. Besides BRAF mutations, NRAS mutations are found in all subtypes of melanoma, although the overall mutation frequency (15-30%) is lower than that of BRAF. Generally, BRAF and RAS (N, H, or K) mutations are mutually exclusive with only few exceptions. Mutations in cKIT are most common in mucosal, acral or chronically sun-damaged skin melanomas [131, 444, 445]. CCND1 is amplified most commonly in melanomas without BRAF or RAS mutations, whereas melanomas with mutation in either of the latter two genes display elevated Cyclin D1 levels [446, 447]. CDK4 amplifications are more common in acral and mucosal melanomas and are also inversely correlated with BRAF or RAS mutations or CCND1 amplifications [447]. From the above evidence, it is clear that constitutive activation of the RAS/MEK/ERK pathway, by oncogenic lesions in one of the pathway's components, is an important step in melanoma development. However, BRAF mutation is the most common among all these mutations and aberrant gene expressions.

More than 30 different BRAF mutations have been identified in a number of malignancies including thyroid, ovarian, lung and colon cancer as well as melanoma [448]. Among human cancers, BRAF mutations are most common in melanoma. The prevalence of BRAF mutations varies substantially among the different types of melanoma. The highest frequency (50% to 60%) is found in cutaneous melanoma [447]. It is rare in mucosal, acral and conjunctival melanomas, and virtually absent from uveal melanomas. Furthermore, within the group of cutaneous melanomas, BRAF mutations are highest on sites of intermittently sun-exposed skin, rather than on chronically sun-damaged or completely unexposed skin [447]. Cutaneous melanomas on sites of chronically sun-damaged skin harbour wild type BRAF and arise later in life [447, 449]. More intriguingly, the high frequency of BRAF mutations is also seen in melanocytic naevi [450]. Within the BRAF mutations, the

most common one, which accounts for more than 90% of total BRAF mutations [77] corresponds to a T>A transversion at position 1799, resulting in the substitution of Valine by Glutamine at codon 600 (V600E BRAF mutation). The BRAF V600E mutation displays increased kinase activity relative to the wild type protein and has transforming capacity [77]. Cell lines expressing the BRAF V600E are dependent on it for proliferation and survival [451-453] and most do not require RAS for proliferation [77].

Cutaneous melanoma can vary significantly in clinical and histopathological appearance, which has led to the development and refinement of morphologically based classification systems. The standard classification for melanoma uses the current World Health Organization (WHO) classification that distinguishes four main types of melanoma as described in Chapter 1 (See Page 6). These distinctions are related to clinical features such as anatomic site of the primary tumour, pace of tumour evolution and the patient age. However, clinical management based only on the above classifications is difficult. For example, a number of melanomas are differentially classified by different observers, or classified as "ambiguous" because these classifications are defined by multiple criteria [454]. On the other hand, genetic alterations can serve as biomarkers for classification purposes even though the complete profile of genetic factors is still not available. Viros *et al.* described that combining the morphological appearance and the genetic changes could be clinically useful for therapy stratification and for retrospective study of clinical trial data. They found BRAF mutation status is strongly related to some phenotypic features such as pigmentation, cell shape, size, and nesting of primary melanomas, which implies that refined morphological classification of primary melanomas can be used to improve existing melanoma classifications by integrating genetic and morphologic features [455].

In our group, about 150 melanoma samples were available from a TMA panel constructed by Dr Ewan Brown, containing primary and metastatic melanoma samples with clinicopathological records. We have also developed a mature method to genotype the BRAF V600E mutation. Potentially, we are able to perceive new

insights into the role of the BRAF mutation in melanomagenesis and melanoma classifications by investigating the relationship between BRAF mutation status and the clinicopathological signatures in our sample cohort. Moreover, we can also associate BRAF mutation to patient survival.

Therefore, the objectives of this Chapter were: to genotype BRAF V600E mutations in FFPE melanoma tissues from our TMA cohort; to identify the correlation between the BRAF V600E mutation and the clinicopathological features; to assess the prognostic value of the BRAF V600E mutation.

5.2 Results

5.2.1 BRAF V600E mutation frequency in melanoma tissues

5.2.1.1 BRAF V600E mutation assay

Genetic analysis by restriction fragment length polymorphism (RFLP) allows the examination of nucleic acids for the presence of known sequence variants. A segment that is to be searched for a mutation is amplified from genomic DNA, digested by the appropriate restriction enzyme, and then separated by agarose gel electrophoroesis. Although RFLP analysis is highly sensitive and relatively easy to perform, many polymorphisms are the result of single-base substitutions that fail to create or remove a restriction site and therefore cannot be genotyped by simple PCR and RFLP analysis. A mismatch PCR primer can be used to overcome this as it artificially creates a restriction site in the amplified product to allow the detection of the presence of a base substitution by RFLP.

In order to associate the presence of the BRAF V600E mutation with history of UV exposure and other available clinicopathological characteristics, an assay was developed for detection of this mutation in melanoma samples. The assay used PCR with a mismatch PCR primer and an XbaI RFLP, which is a method originally

reported by Hayashida *et al.* [456]. DNA extracted from FFPE specimens is often fragmented and PCR is difficult when amplifying products greater than 100bp in length. In order to increase the efficiency of the PCR on DNA isolated from FFPE tissues, a nested PCR was also used which was developed by Dr Jim Selfridge. Figure 5.1 shows the genotyping assay schematically.

(A)

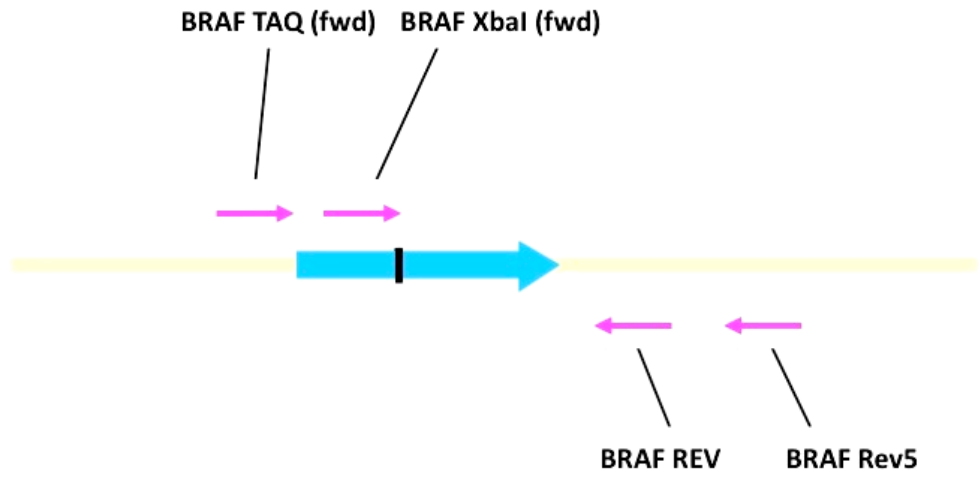

(B)

```
  1 ATTGACTCTA AGAGGAAAGA TGAAGTACTA TGTTTTAAAG AATATTATAT TACAGAATTA TAGAAATTAG ATCTCTTACC TAAACTCTTC ATAATGCTTG
    TAACTGAGAT TCTCCTTTCT ACTTCATGAT ACAAAATTTC TTATAATATA ATGTCTTAAT ATCTTTAATC TAGAGAATGG ATTTGAGAAG TATTACGAAC

                                BRAF TAQ (fwd)                                                  BRAF XbaI (fwd)
101 CTCTGATAGG AAAATGAGAT CTACTGTTTT CCTTTACTTA CTACACCTCA GATATATTTC TTCATGAAGA CCTCACAGTA AAAATAGGTG ATTTTGGTCT
    GAGACTATCC TTTTACTCTA GATGACAAAA GGAAATGAAT GATGTGGAGT CTATATAAAG AAGTACTTCT GGAGTGTCAT TTTTATCCAC TAAAACCAGA

201 AGCTACAGTG AAATCTCGAT GGAGTGGGTC CCATCAGTTT GAACAGTTGT CTGGATCCAT TTTGTGGATG GTAAGAATTG AGGCTATTTT TCCACTGATT
    TCGATGTCAC TTTAGAGCTA CCTCACCCAG GGTAGTCAAA CTTGTCAACA GACCTAGGTA AAACACCTAC CATTCTTAAC TCCGATAAAA AGGTGACTAA

301 AAATTTTTGG CCCTGAGATG CTGCTGAGTT ACTAGAAAGT CATTGAAGGT CTCAACTATA GTATTTTCAT AGTTCCCAGT ATTCACAAAA ATCAGTGTTC
    TTTAAAAACC GGGACTCTAC GACGACTCAA TGATCTTTCA GTAACTTCCA GAGTTGATAT CATAAAAGTA TCAAGGGTCA TAAGTGTTTT TAGTCACAAG
      BRAF REV                                                                                  BRAF Rev5
401 TTATTTTTTA TGTAAATAGA TTTTTTAACT TTTTTCTTTA CCCTTAAAAC GAATATTTTG AAACCAGTTT CAGTGTATTT CAAACAAAAA TATATGTCTT
    AATAAAAAAT ACATTTATCT AAAAAATTGA AAAAAGAAAT GGGAATTTTG CTTATAAAAC TTTGGTCAAA GTCACATAAA GTTTGTTTTT ATATACAGAA
```

XbaI (fwd): TAAAAATAGGTGATTTTGGTCTAGCTCTAG

(C)

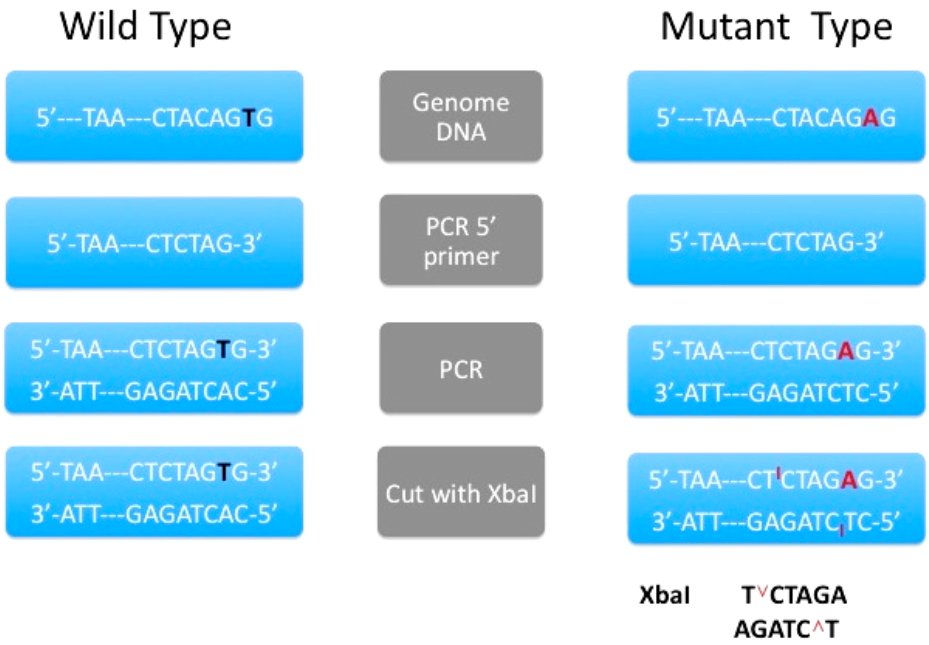

Fig 5.1 BRAF PCR RFLP analysis. (A) Schematic diagram showing position of primers used for BRAF nested PCR. The site of the transversion mutation T1799A is marked with a black bar. (B) Sequence of genomic DNA (exon 15) containing coding sequence in blue and primers indicated with red line and black texts. Mismatched primer nucleotides are in bold and underlined in blue. The site of the T1799A mutation is in red bold. The nested PCR primers are: BRAF TAQ (fwd) and BRAF Rev5 (Nested 1); BRAF XbaI (fwd) and BRAF REV (Nested 2). (C) Strategy underlying the PCR-RFLP method for detection of BRAF T1799A mutation. DNA was amplified by PCR using a mismatched forward primer AC to CT (where the wildtype AC was changed to CT). The Amplified products were digested with XbaI. In this case only mutant DNA products can be cut by XbaI, as shown in red.

5.2.1.2 Sensitivity of genotyping method

Although the TMA cores were taken from areas that were rich in tumour cells it was likely that the cores still contained some non-tumour material. So heterozygous BRAF mutant and wild type cultured cells were used to elucidate the sensitivity of the assay, by determining the lowest frequency of mutant cells that could be detected in the presence of wild type cells in the TMA core samples. Different ratios of mutant and non-mutant containing DNA were made up and subjected to PCR and digestion as described above. The sensitivity results are shown in Figure 5.2. A band

of 105bp identified the presence of the BRAF V600E mutation. In this figure, a very faint band at 105bp is seen in Lane 3, indicating that the sensitivity of the assay is 10%. This suggested that the assay could detect mutant BRAF V600E if it was present in at least 10% of cells isolated from the TMA cores. Moreover, heterozygous and homozygous BRAF mutant samples of primary melanoma tissues can also been seen in Lane 7 and Lane 8, respectively.

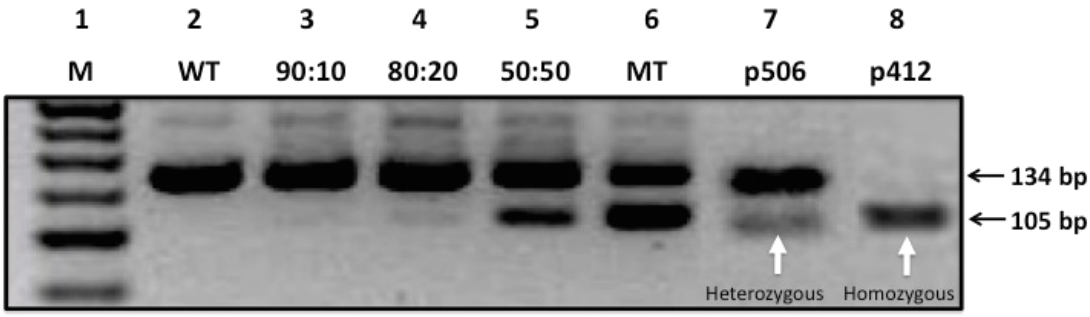

Figure 5.2 BRAF V600E RFLP assay. Lanes 2 to 6 are sample mixtures of BRAF V600E wild type (WT) and mutant type (MT) of DNA in the indicated ratios. In each case the total amount of DNA used for PCR was the same (1ug). Lane 7 and Lane 8 are two individual primary melanoma samples with heterozygous and homozygous BRAF V600E mutations, respectively. M: Marker, WT: Wild type, MT: Mutant. The assay used nested PCR for BRAF exon 15. 134bp is the size of the nested PCR product, while 105bp is this size if the PCR product contains the mutation and is restricted by XbaI.

5.2.1.3 Frequency of the BRAF V600E mutation in melanoma samples

Cores were available from 115 primary and 29 metastatic melanoma tissues and BRAF V600E mutation results were observed from all of them. The frequency of BRAF V600E mutation was 20% in primary melanoma tissues, and 69% in metastases (Table 5.1). In addition, examples of homozygous mutants were also seen in both primary and metastatic melanoma samples.

	Primary Melanoma	Metastatic Melanoma
BRAF V600E Heterozygous MT	21	17
BRAF V600E Homozygous MT	2	3
Wild type	92	9
BRAF mutation frequency (%)	23/115 (20%)	20/29 (69%)

Table 5.1 BRAF V600E mutational status in melanoma samples. The table shows the frequency of the BRAF V600E mutation in tumour samples from both primary and metastatic melanoma patients and the status of heterozygous and homozygous mutant types. MT: Mutant type.

5.2.2 Statistical analysis of the BRAF V600E mutation in primary melanoma

I have correlated the BRAF V600E mutation to age, gender, Breslow thickness, ulceration, solar elastosis (SE) and pigmentation using either Chi-square or Fisher's exact test.

Two sets of available records were not analysed statistically: anatomic sites (sun-exposed, sun-protected, acral) and histo-type. For site records, patients with BRAF mutations accounted for 6.7% (1/15) sun-exposed, 20.6% (20/97) sun-protected and 66.7% (2/3) acral samples. However, the numbers in some subgroups were too small for analysis and SE was a better indicator to quantify UV exposure. For histo-type records of the cohort, 25% LLM (2/8), 20% SSM (17/87), 16.7% NM (3/18) and 50% (1/2) ALM patients had BRAF V600E mutations. Sample size of some of the subgroups was also too small and so multivariate analysis was not used in this study.

5.2.2.1 BRAF V600E mutation and age

In 115 primary melanoma patients, the median and mean ages at diagnosis were 54.8yrs and 54.87yrs. Previous studies of the correlation between BRAF mutation and age have used different age cutoffs. So far, three common age cutoffs were used (45yrs [457], 55yrs [455], 60yrs [458]) and it was found that BRAF mutations were

more common in the younger age group. However, there was no correlation between BRAF mutation and age in our cohort using any of the three cutoffs.

(A)

	Age ≤ 45	**Age > 45**	**Total**
BRAF (+)	7 (6.1%)	16 (13.9%)	23 (20%)
BRAF (-)	31 (27.0%)	61 (53.0%)	92 (80%)
Total	38 (33.1%)	77 (66.9%)	115 (100%)
p value	**p=0.77**		

(B)

	Age ≤ 55	**Age > 55**	**Total**
BRAF (+)	11 (9.6%)	12 (10.4%)	23 (20%)
BRAF (-)	47 (40.9%)	45 (39.1%)	92 (80%)
Total	58 (50.5%)	57 (49.5%)	115 (100%)
p value	**p=0.78**		

(C)

	Age ≤ 60	**Age > 60**	**Total**
BRAF (+)	13 (11.3%)	10 (8.7%)	23 (20%)
BRAF (-)	55 (47.8%)	37 (32.2%)	92 (80%)
Total	68 (59.1%)	47 (40.9%)	115 (100%)
p value	**p=0.78**		

Table 5.2 Comparison of the BRAF V600E mutation and age in primary melanoma patients. Patients were divided into young and old groups. The Chi-square test was used for all three tables. Numbers in brackets in this and in the following tables in this chapter, represent the percentage of patients in each category.

5.2.2.2 BRAF V600E mutation and gender

In the cohort, males and females accounted for 44.3% and 55.7%, respectively. 29.4% male patients possessed the BRAF V600E mutation, whereas only 12.5%

females had the mutation. The statistical test that showed the mutation was present at significantly higher frequency in male relative to female patients (Table 5.3).

	Male	Female	Total
BRAF (+)	15 (13.0%)	8 (7.0%)	23 (20%)
BRAF (-)	36 (31.3%)	56 (48.7%)	92 (80%)
Total	51 (44.3%)	64 (55.7%)	115 (100%)
p value	**p=0.024**		

Table 5.3 Comparison of the BRAF V600E mutation and gender in primary melanoma patients. The Chi-square test was used.

5.2.2.3 BRAF V600E mutation and Breslow thickness

When correlating to Breslow thickness, BRAF V600E mutation frequencies of 13.5%, 17.4%, 44.4% and 20% were identified in the four subgroups of the Breslow system, respectively (Table 5.4, A). When the subgroups were combined into bigger groups, the results were interesting. In Table 5.4-B, the data were divided into thin and thick groups with a cutoff at 1mm thick. This result did not reach statistical significance for correlating BRAF mutation and tumour thickness. However, when the cutoff was set at 2mm thick, the BRAF V600E mutation was significantly correlated to thicker tumour lesions (Table 5.4, C). The correlation was significant when the Bonferroni correlation for multiple tests was applied. (In this case the significance cutoff was 0.05/2 = 0.025).

(A)

	≤ 1mm	1.01-2.0mm	2.01-4.0mm	> 4.0mm	Total
BRAF (+)	8	4	8	3	23
BRAF (-)	51	19	10	12	92
Total	59	23	18	15	115

(B)

	≤ 1mm	> 1mm	Total
BRAF (+)	8 (7.0%)	15 (13.0%)	23 (20%)
BRAF (-)	51 (44.3%)	41 (35.7%)	92 (80%)
Total	59 (51.3%)	56 (48.7%)	115 (100%)
p value		**p=0.076**	

(C)

	≤ 2mm	> 2mm	Total
BRAF (+)	12 (10.4%)	11 (9.6%)	23 (20%)
BRAF (-)	70 (60.9%)	22 (19.1%)	92 (80%)
Total	82 (71.3%)	33 (28.7%)	115 (100%)
p value		**p=0.023**	

Table 5.4 Comparison of the BRAF V600E mutation and melanoma lesion thickness in primary melanoma patients. Melanoma lesion thickness was evaluated using the Breslow system. Table (A) shows number of BRAF V600E positive and negative tumours in different melanoma lesion thickness groups according to the Breslow thickness. Table (B) correlates BRAF mutation status with thin lesion (≤ 1mm) or thick lesion (>1mm) groups. Table (C) correlates BRAF mutation status with thin lesion (≤ 2mm) or thick lesion (>2mm) groups. The Chi-square test was used.

5.2.2.4 BRAF V600E mutation and ulceration

For correlation analysis between the BRAF V600E mutation and ulceration, the Ulceration unknown group was removed. The Incipient group, which represents those tissues with very early signs of ulceration, was added to the Yes group. In this cohort, there was no correlation between the BRAF V600E mutation and ulceration (Table 5.5).

(A)

	Yes	No	Incipient	Unknown	Total
BRAF (+)	10	10	2	1	23
BRAF (-)	26	49	13	4	92
Total	36	59	15	5	115

(B)

	Yes	No	Total
BRAF (+)	12 (10.9%)	10 (9.1%)	22 (20%)
BRAF (-)	39 (35.5%)	49 (44.5%)	88 (80%)
Total	51 (46.4%)	59 (53.6%)	110 (100%)
p value	**p=0.39**		

Table 5.5 Comparison of the BRAF V600E mutation and ulceration in primary melanoma patients. Ulceration was divided into four groups as shown in table (A). The Incipient group was added into the Yes group and the Unknown group was removed for analysis. Table (B) analyzed the correlation between the BRAF V600E mutation and ulceration. The Chi-square test was used.

5.2.2.5 BRAF V600E mutation and solar elastosis

Solar elastosis (SE) is a histological indicator of chronic sun-induced damage (CSD). The degree of SE in the dermis of each primary melanoma sample was scored according to a method reported by Landi *et al.* [459]. The aim was to provide a quantitative assessment of sun damage in the skin in which the melanoma arose. The scores (0-11) took account of both amount and distribution of the elastosis seen. The SE scoring was performed on H&E stained sections by Dr Tamasin Doig. It was divided into two groups: low group (score 0-6) and high group (score 7-11). 10 samples had no SE records. The frequency of BRAF mutation patients in the low SE group was 21.7%, with only 7.7% in the high SE group. However, the statistical result did not reach significance for correlating BRAF mutation and low SE (Table 5.6).

	SE ≤ 6	SE > 6	Total
BRAF (+)	20 (19.0%)	1 (1.0%)	21 (20%)
BRAF (-)	72 (68.6%)	12 (11.4%)	84 (80%)
Total	92 (87.6%)	13 (12.4%)	105 (100%)
p value	**p=0.46**		

Table 5.6 Comparison of the BRAF V600E mutation and solar elastosis in primary melanoma patients. SE scores were divided into low (0-6) or high (7-11) [459]. Fisher's exact test was used.

5.2.2.6 BRAF V600E mutation and pigmentation

Pigmentation was scored according to a described method [455]. It was defined as the degree of melanin accumulation within the constituent melanocytes and was scored on a five-point scale (0-4). The scoring method was: 0, (absent) no pigment discernible even at high power; 1, (faint) pigmentation barely visible at low power. At high power, melanocytes showed a faint diffuse melanin pigment or a few pigment granules. 2, (moderate) pigmentation visible at low power with translucent cytoplasm that is significantly lighter than the hematoxylin stained nuclei; 3, (high) pigmentation easily visible at low power with the cytoplasmic pigmentation reaching an intensity approximating that of the nucleus; 4, (very high) cytoplasm strikingly pigmented making it difficult to identify nuclei.

Scores 0-2 were put into the low pigment group, while scores 3-4 were put into the high pigment group. The H&E slide of one primary sample was not available for scoring. A 14.7% BRAF mutation frequency was seen in the low pigment group while 47.4% was seen in the high pigment group. The Fisher's exact test showed significant correlation (p=0.003) between the BRAF V600E mutation and pigmentation, indicating that the presence of BRAF V600E mutation was associated with pigmentation.

	Pigmentation ≤ 2	**Pigmentation > 2**	**Total**
BRAF (+)	14 (12.3%)	9 (7.9%)	23 (20.2%)
BRAF (-)	81 (71.0%)	10 (8.8%)	91 (79.8%)
Total	95 (83.3%)	19 (16.7%)	114 (100%)
p value	**p=0.003**		

Table 5.7 Comparison of the BRAF V600E mutation and pigmentation in primary melanoma patients. Pigmentation scores were divided into low (0-2) or high (3-4) [455]. Fisher's exact test was used.

5.2.3 Prognostic evaluation of the BRAF V600E mutation

In assessing whether the BRAF V600E mutation affects patient survival and melanoma relapse, two cases were excluded as they had no follow-up records. For two survival analyses, the endpoint was death. For time to melanoma relapse, the endpoint was relapse. Table 5.8 summarises the number of cases that were put into the analyses. The following three Kaplan-Meier analyses were based on the data in this table.

	Overall Survival		Melanoma Specific Survival		Relapse	
	Yes	No	Yes	No	Yes	No
BRAF (+)	14	9	17	6	9	14
BRAF (-)	68	22	76	14	15	75
Total	82	31	93	20	24	89

Table 5.8 Data for survival and time to relapse analysis.

5.2.3.1 Survival analysis

To evaluate whether the BRAF V600E mutation correlated with prognosis in patients with primary melanoma, Kaplan-Meier survival curves were constructed using overall and melanoma-specific survival (Figure 5.3 and Figure 5.4). Patients with the BRAF V600E mutation had no significant difference in overall and melanoma-specific survival (log-rank test =0.1981 and 0.25, respectively) compared to patients without the mutation. The hazard ratios were 1.65 and 1.74, respectively.

5.2.3.2 Time to melanoma relapse

Using Kaplan Meier analyses, the BRAF V600E mutation was found to correlate with time to melanoma relapse in our cohort, although the presence of the BRAF V600E mutation seems to be having no effect on overall and melanoma-specific survival (Figure 5.5). The result suggested that patients with BRAF V600E mutation would have melanoma relapse earlier than those without this mutation. The hazard ratio was 2.62.

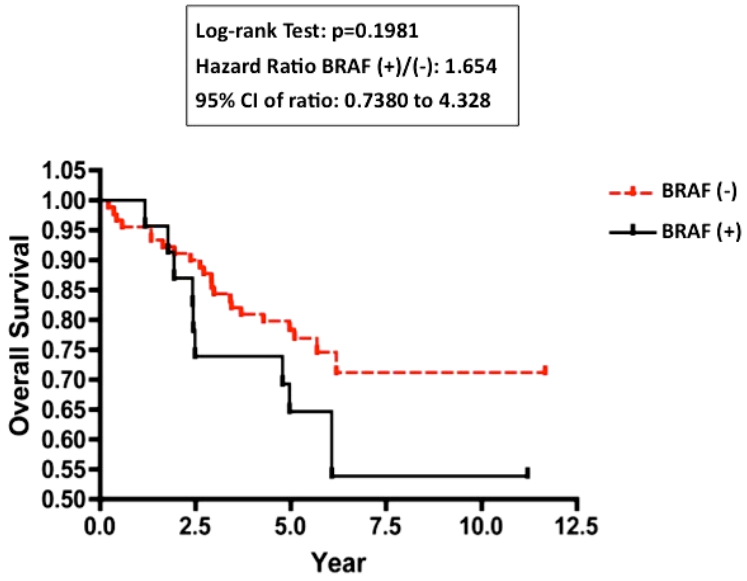

Figure 5.3 Comparison of the BRAF V600E mutation and overall survival in melanoma patients. The Kaplan-Meier survival analysis shows the relationship between the BRAF V600E mutation and overall survival in melanoma patients (year since diagnosis). The key in the graph includes p value, hazard ratio and 95% CI of hazard ratio.

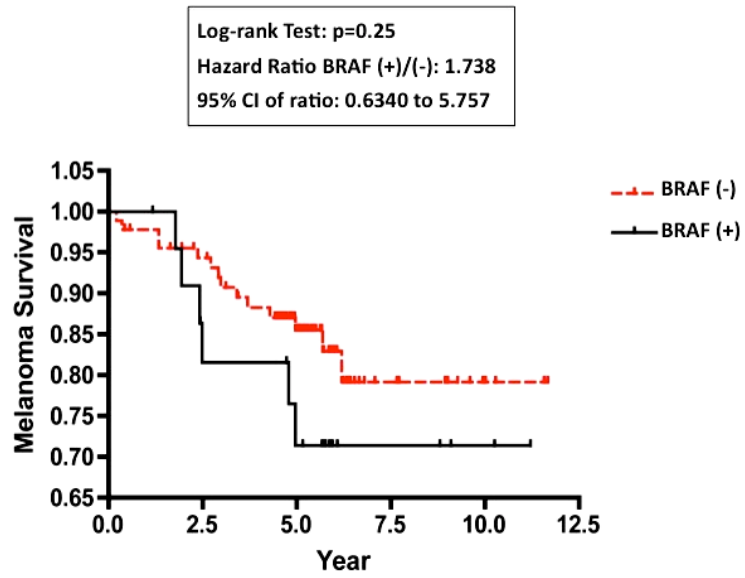

Figure 5.4 Comparison of the BRAF V600E mutation and melanoma specific survival in melanoma patients. The Kaplan-Meier survival analysis shows the relationship between the BRAF V600E mutation and melanoma specific survival in melanoma patients (year since diagnosis). The key in the graph includes p value, hazard ratio and 95% CI of hazard ratio.

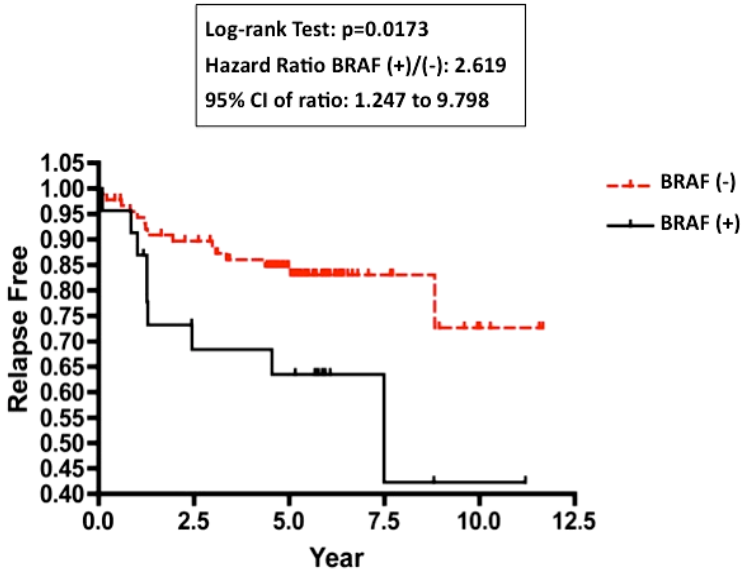

Figure 5.5 Comparison of the BRAF V600E mutation and melanoma relapse. The Kaplan-Meier melanoma relapse analysis shows the relationship between the BRAF V600E mutation and time to melanoma relapse in melanoma patients (year since diagnosis). The key in the graph includes p value, hazard ratio and 95% CI of hazard ratio.

5.3 Discussion

In this Chapter, I showed that the frequency of the BRAF V600E mutation was 20% using nested PCR-RFLP method in a 115-case primary melanoma cohort. The frequency was 69% in metastatic melanoma samples. The presence of the BRAF mutation was associated with gender and pigmentation. It was related to Breslow thickness when the lesion was thicker than 2mm. In assessing the BRAF mutation's prognostic value, patients with BRAF V600E mutations seem to have melanoma relapse earlier than those without the mutation. However, there was no evidence that there was a correlation between the BRAF mutation and overall and melanoma-specific survival in our sample panel.

To compare my results to others, I summarised the frequencies of the BRAF V600E mutation in primary melanoma tissues from a number of published papers (Table 5.9). The prevalence of the BRAF V600E mutation observed in this study in metastatic melanoma is consistent with reported frequencies in Pollock's study [460], while the frequency in primary melanomas was lower than in many published reports, but was similar to that in most other large sample number studies (No.5, 12, 14 in Table 5.9). The reported incidence of the BRAF V600E mutation varies between 20-80% in primary melanoma samples. The reasons why it varies so greatly probably depend on the different types of samples analysed, the sample size and the genotyping method used. BRAF mutations are more prevalent in superficial spreading and nodular melanoma than in other types. Most of the published papers did not mention the sensitivity of the genotyping assay. However, I showed that our assay sensitivity is able to detect the mutation in small tumours when the cores contain up to 90% non-tumour tissue.

Interestingly, there were two examples of homozygous BRAF mutation in primary samples which is rare and has not been reported in other papers, although there is one report of a possible homozygous mutation of BRAF in melanocytic lesions (benign and atypical naevi) [461] .

No.	Frequency (%)	Detection method	Sensitivity	Reference
1	6/9 (66.7%)	Sequencing	ND	Davies H, 2002
2	37/71 (52.1%)	SSCP/Sequencing	ND	Omholt K, 2003
3	4/5 (80.0%)	AS-PCR	ND	Pollock PM, 2003
4	14/25 (56%)	PCR-RFLP/Sequencing	ND	Uribe P, 2003
5	28/97 (28.9%)	Sequencing	ND	Yazdi AS, 2003
6	24/32 (75.0%)	Sequencing	ND	Maldonado JL, 2003
7	10/35 (28.6%)	SSCP/Sequencing	ND	Kumar R, 2003
8	17/59 (28.8%)	SSCP/Sequencing	ND	Masaru S, 2004
9	13/51 (25.5%)	SSCP/Sequencing	ND	Akslen L, 2005
10	20/36 (55.6%)	PCR/RFLP	ND	Goydos JS, 2005
11	33/58 (56.9%)	AS-PCR	ND	Goel VK, 2006
12	19/81 (23.5%)	ND	ND	Poynter JN, 2006
13	112/251 (44.6%)	AS-PCR	2%	Liu W, 2007
14	60/214 (28.0%)	SSCP/Sequencing	ND	Thomas NE, 2007
15	30/69 (43.4%)	Sequencing	ND	Kannengiesser C, 2008
16	4/18 (22.2%)	Sequencing	ND	Dadzie OE, 2008
17	23/115 (20.0%)	PCR-RFLP	10%	This thesis

Table 5.9 Summary of primary melanoma BRAF V600E mutation frequencies in publications. The table summarizes published data of BRAF V600E mutation frequencies for the last ten years with detection method and sensitivity of the assay. ND: Not described. AS-PCR: Allele specific PCR; SSCP: Single-strand conformational polymorphism.

In correlation analyses of BRAF mutation and clinicopathological signatures, there seems no agreement either. Although the age cutoff may be not the same, some

research results showed that the BRAF mutation was more common in younger patients [455, 457, 458, 462]. In Viros' paper, age at diagnosis < 55yrs was described as the single most predictive factor for BRAF mutation and the mutation showed a significant decrease in survival when stratified by this age cutoff. However, this was not seen in my study. BRAF mutation was correlated to male patients in our cohort, which is consistent with the report from Uribe *et al*, indicating that mutation frequencies may be related to hormonal influences in melanocyte biology [461]. Generally, the presence of the BRAF mutation has not been correlated to the key prognostic indicator, Breslow thickness, except for Liu's study that reported a correlation with lower thickness [462]. However, my data indicated that BRAF mutation was related to higher thickness when the cutoff was 2mm, which is opposite to their results. Interestingly, both of our results showed significant correlation between BRAF mutation and more frequent pigment production, which was also seen in Viros's study [455]. This evidence supports the finding that mutant BRAF V600E activates the MAPK pathway and modulates MITF function and melanocytes' differentiation [462]. A relationship between BRAF mutation and ulceration is rarely seen, but Akslen *et al.* reported that primary tumours with BRAF mutation were more often ulcerated than wild type tumours [463].

Solar elastosis (SE) reflects cumulative UV exposure. Many studies showed an inverse relationship between BRAF mutation and SE [449, 455, 457, 459, 462]. However, there was no correlation between SE and BRAF mutation in my study, perhaps due to the small sample size. It still needs to be determined whether UVR causes BRAF mutations since there are both arguments against and for this association.

The arguments against the association are: first, the most common BRAF V600E mutation results from a single base-pair substitution (T>A) while the typical mutations caused by UVR are C>T/CC>TT; secondly, the BRAF mutation also occurs frequently in other cancers, such as thyroid, ovarian and colon cancer, which arise in the absence of UVR [448].

On the other hand, there are arguments that support the association that the BRAF mutation is the result of UVR. It was proposed that T>A mutation could arise from error-prone replication of UV-damaged DNA [458]. BRAF mutation is often seen in cutaneous melanoma but not in uveal and mucosal melanomas indicating that it is related to UVR. Moreover, BRAF mutation is common in sites that receive intermittent UVR (trunk and extremities), whereas it is rarely seen in locations that receive the lowest (mucosa) and highest (face) sun exposure. Other theories are: BRAF mutations may result from reactive oxygen species, which may be produced as a by-product of melanomagenesis or by pheomelanin absorption of UVA [458]; BRAF mutation is linked to inflammation that may result from sunburn; the fact that melanocytic lesions have a high frequency of BRAF mutation may be explained by UVR triggering a stronger proliferative response in melanocytes with an activating BRAF mutation than in neighbouring cells with wild type BRAF, further promoting melanoma progression in UV-exposed sites [464, 465].

Prior to my study, some studies correlated BRAF mutation to Clark level, a previous prognostic marker. However, there was no evidence showing that the presence of BRAF mutation affects survival [461, 466]. Using Kaplan Meier survival analysis, my results showed melanoma patients with BRAF mutation had shorter trends of overall survival and melanoma survival compared to patients without BRAF mutation, although the difference was not significant. The analysis also showed that patients with BRAF V600E mutation had significantly shorter melanoma-recurrence free times than patients without BRAF mutation. However, if the patient survival had been monitored over a longer period then the presence of the BRAF mutation may have become significant.

As mentioned in Chapter 1, personalised therapy has become the hope for curing cancer. Several strategies for inhibiting MAPK signalling, including RAF kinase inhibitors and MEK inhibitors, are now being evaluated clinically in melanoma therapy. The limited activity of sorafenib in tumours with BRAF mutation prompted the development of second-generation RAF inhibitors with greater selectivity for mutant BRAF. Vemurafinib (PLX4032) is a potent inhibitor of mutated BRAF. It has

marked antitumour effects against melanoma cell lines with the BRAF V600E mutation, but not against cells with wild type BRAF [467]. Phase 1 and 2 clinical trials with Vemurafinib have shown response rates of more than 50% in patients with metastatic melanoma with the BRAF V600E mutation. A very recent report of the drug in a Phase 3 trial showed that Vemurafinib improved rates of overall and progression-free survival in patients with previously untreated melanoma with BRAF V600E mutation compared to the Dacarbazine group [467]. Besides the most common adverse events such as arthralgia, fatigue and photosensitive skin reactions of grade 2 or 3 that were seen in 12% of the patients, 18% of patients developed at least one squamous cell carcinoma of the skin or keratoacanthoma. One of the suggested mechanisms was linked to the observation that drugs that selectively inhibit BRAF drive RAS-dependent BRAF binding to CRAF and CRAF activation and MEK-ERK signalling when BRAF is inhibited in the presence of oncogenic RAS. Another problem that needs to be clarified is that melanomas become resistant to Vemurafinib. Studies from several groups have indicated that the MAPK pathway can be reactivated in resistant tumours, although the precise mechanisms of reactivation are still being investigated.

Chapter 6: Summary

6.1 General discussion

My work presented in this thesis focused on two types of molecules: melanoma-specific miRNAs and oncogenic BRAF. In Chapter 3, a melanoma-specific miRNA expression profile was established and miRNA biomarker candidates were verified. Studies in Chapter 4 identified three miRNAs acting as tumour suppressors in melanomagenesis. The work in Chapter 5 determined the prevalence of BRAF mutation based on our TMA panel and correlated it with clinicopathological signatures and melanoma patient survival. The investigation of these key non-coding and coding genes improves our understanding of the molecular pathogenesis of cutaneous melanoma, identifies novel miRNA biomarker candidates in both diagnosis and prognosis, and may help us to develop more effective therapeutic interventions for cutaneous melanoma.

miRNAs are highly conserved, indicating their important roles in basic cellular processes. miRNA alterations have been observed in all forms of cancer. High throughput analyses identified specific miRNA expression patterns in various cancers, suggesting that miRNA expression profiles are tissue-specific and possess diagnostic value. Additionally, miRNA expression profiling can be utilized to determine cancer prognosis. More importantly for studies on melanoma where access to fresh frozen tissue is limited, reproducible miRNA expression profiles from FFPE samples can be obtained that are comparable to those from fresh frozen samples. Against this background, I carried out a miRNA microarray study. I consider my miRNA profiling study to be the best melanoma-specific miRNA profile so far because it detects the most miRNA probes, has the most FFPE samples, contains complete stages in melanoma progression and is verified by qPCR. Through this, I obtained a melanoma-specific miRNA expression profile based on FFPE samples. This profile established a number of miRNAs that were differentially expressed between benign naevi and melanomas and showed high potential in melanoma diagnosis, where morphological separation is particularly difficult for certain types of melanocytic lesion. Therefore, in a further study of miRNA diagnostic roles in melanoma, expression of five miRNAs was determined using qRT-PCR in FFPE

samples of additional types of these melanocytic lesions, including Blue naevus, Spitz naevus and dysplastic naevus. Possibly due to the limitation of very small sample size, I did not identify a miRNA that can separate the different melanocytic lesions clearly. However, I believe that such an approach could still be helpful diagnostically if large sample numbers are used and the use of miRNA *in-situ* hybridization (ISH) for miRNA detection can be developed to eliminate the need for RNA extraction from very small lesions such as *in-situ* melanoma. Moreover, in an attempt to identify miRNAs with prognostic value, a comparison between non-recurrent and recurrent primary melanoma was performed. Again, increasing sample numbers will be needed to identify differentially expressed miRNAs. In addition, retrieving the detailed survival records of the primary melanoma patients would be needed for further analysis to correlate differentially expressed miRNAs with patient survival.

One of the most important mechanisms of miRNA action is to stimulate mRNA cleavage resulting in mRNA degradation. miRNAs have been shown to target both tumour suppressors and oncogenes to influence cancer development. Some miRNAs can have opposite effects in different cancers, or can switch between these two functions and act as a tumour suppressor at one time and an oncogene at another time. Thus, altering miRNA expression could to be a novel treatment for cancers.

23 miRNAs were identified as candidates for follow on functional studies from the differentially expressed miRNAs between benign naevi and malignancies. Nine miRNAs from the 23 candidates were verified by qRT-PCR and four of them were taken on into functional assays. Interestingly, ectopic overexpression of miR-200c and miR-205 in melanoma cells inhibited anchorage independent colony forming ability. Moreover, elevation of miR-200c resulted in increased expression levels of E-cadherin through negative regulation of the ZEB2 gene. Ectopic overexpression of miR-211 in melanoma cells repressed both colony formation and migratory ability. These findings indicate that miR-200c, miR-205 and miR-211 may act as tumour suppressors in melanomagenesis, which could make these miRNAs potential targets for melanoma therapy. Further studies, such as investigating more melanoma cell

lines, constructing stable cell lines with ectopic expression of these miRNAs, and animal models would be needed to confirm the above association between these miRNAs and melanomagenesis, and would be useful to address additional questions that I have not been able to answer. For example, in my transient expression assays, mRNA level changes of N-cadherin were not observed and there was difficulty in detecting a change in E-cadherin protein levels. However, using miR-200c precursor transfected stable cell lines it may be possible to see decreased mRNA and protein levels of N-cadherin, which would suggest that miR-200c influences the EMT process through both mRNA and protein level changes of E-cadherin.

Oncogenic BRAF, which activates the MAPK pathway and results in tumour development, has been well studied in recent years. BRAF mutations are common in benign melanocytic naevi, primary and metastatic melanomas. The BRAF V600E mutation accounts for the majority of BRAF mutations. Based on the samples from our TMA panel, 20% and 69% BRAF V600E mutations were found in primary and metastatic melanoma, respectively. The correlation between BRAF mutation and clinicopathological features varies according to different reports. In our study, the presence of BRAF mutation was associated with gender and pigmentation. It was related to Breslow thickness when the lesion was thicker than 2mm. In assessing the BRAF mutation's prognostic value, patients with BRAF V600E mutations have melanoma relapse earlier than those without the mutation. However, no evidence showing that there was correlation between BRAF mutations and overall survival and melanoma-specific survival was found in our sample panel. This additional study is a useful supplement to further understanding of the role of the BRAF mutation in melanoma.

In Caramuta's study, miRNA expression profiles were associated with clinical characteristics, patient survival, and mutational status for BRAF and NRAS [358]. Therefore, it would have been interesting to investigate whether there were expression level differences for the melanoma-specific miRNAs I identified between patients with mutated BRAF and patients with wild type BRAF and whether such differences affected survival. However, there were only a very few samples in

common between the miRNA and BRAF project and so no such analysis was possible. This did not reflect bad experimental design, but rather that insufficient material was available from the large number of thin primary melanomas in the TMA study to also extract RNA for miRNA analysis and DNA for BRAF mutation detection.

6.2 Future work

Following on from the work described in the thesis, especially for the miRNA project, there remains a need for further research. First is to develop and use miRNA ISH on our melanoma TMA panel. miRCURY LNA™ detection probes have been successfully used in various types of samples, including FFPE tissues [468], although it is a difficult work technically. I believe that miRNAs can be used in conjunction with conventional histology to facilitate the diagnosis of melanocytic lesions. Applying ISH on conventional FFPE patient samples to the best miRNA markers I have identified by microarray and qRT-PCR is a feasible approach to achieve the goal. Using miRNA ISH, it may be able to answer the questions: whether the miRNA expression patterns I obtained by microarray and verified by qPCR are supported by miRNA ISH expression patterns; whether using miRNA ISH can discriminate between various type of melanocytic lesions; whether the best miRNA biomarker candidates detected by miRNA ISH can be used as a routine diagnostic tool clinically.

Secondly, functional studies using stable cell lines and research experiments *in vivo* are necessary. The tumour suppressor functions of the two most interesting miRNAs, miR-200c and miR-211, can be verified and further investigated using stable cell lines transfected with miR-200c and miR-211 vectors. Long-term observations can be made using the anchorage independent colony formation assay. Moreover, tumour growth can be measured after stable cells are injected subcutaneously into nude mice. miRNA target studies at both the mRNA and protein level can also be carried out for longer time courses with a coupled luciferase assay that can confirm direct targets.

The above work would be valuable and necessary to establish the case for using miRNAs as future treatments for melanoma.

The studies I presented in the thesis were mostly directed to the downstream effects of miRNAs. However, miRNA regulation is an important topic, which is crucial in carcinogenesis. Epigenetic alterations are widely described as essential players in cancer progression. Such epigenetic modification mainly results in aberrant gene expression due to DNA methylation or histone deacetylation. Mis-expression of miRNAs is partially dependent on epigenetic regulation. Therefore, it would be essential to study methylation or histone deacetylation status of the miRNA gene candidates from my miRNA expression profile. A most recent paper reported that the miR-200 family, especially miR-200c and miR-205 loci, are specifically silenced and gain promoter hypermethylation and repressive chromatin marks in muscle invasive bladder tumours and undifferentiated bladder cell lines [469]. The questions of whether these miRNA genes are silenced and methylated in melanoma and whether correcting this is required for cure of melanoma need to be answered.

Other work would involve: target studies of aberrant miRNAs using gene expression array or protein array on cells with ectopic miRNA expression; functional studies of miR-675, miR-203 or other differentially expressed miRNAs; and further study on miR-20b under different oxygen conditions. Moreover, it was found that miRNAs are present in the circulation of humans and other animals [470]. miRNAs can be used as biomarkers in blood and other biofluids, and the potential role of detecting miRNA expression in body fluids could be an important non-invasive tool for early cancer detection [471].

In conclusion, the investigation of both non-coding and coding genes improves our understanding in cutaneous melanomagenesis. Established miRNA biomarker candidates would be useful clinically in both diagnosis and prognosis. Finally, the functional miRNA candidates may be the basis for future treatments for cutaneous melanoma.

References

1. Vancoillie, G., J. Lambert, and J.M. Nayaert, *Melanocyte biology and its implications for the clinician.* Eur J Dermatol, 1999. **9**(3): p. 241-51.

2. Duband, J.L. and J.P. Thiery, *Appearance and distribution of fibronectin during chick embryo gastrulation and neurulation.* Dev Biol, 1982. **94**(2): p. 337-50.

3. Prota, G., *Recent advances in the chemistry of melanogenesis in mammals.* J Invest Dermatol, 1980. **75**(1): p. 122-7.

4. Land, E.J. and P.A. Riley, *Spontaneous redox reactions of dopaquinone and the balance between the eumelanic and phaeomelanic pathways.* Pigment Cell Res, 2000. **13**(4): p. 273-7.

5. Poh Agin, P., R.M. Sayre, and M.R. Chedekel, *Photodegradation of phaeomelanin: an in vitro model.* Photochem Photobiol, 1980. **31**(4): p. 359-62.

6. Persad, S., I.A. Menon, and H.F. Haberman, *Comparison of the effects of UV-visible irradiation of melanins and melanin-hematoporphyrin complexes from human black and red hair.* Photochem Photobiol, 1983. **37**(1): p. 63-8.

7. Scott, M.C., et al., *Human melanocortin 1 receptor variants, receptor function and melanocyte response to UV radiation.* J Cell Sci, 2002. **115**(Pt 11): p. 2349-55.

8. Wenczl, E., et al., *(Pheo)melanin photosensitizes UVA-induced DNA damage in cultured human melanocytes.* J Invest Dermatol, 1998. **111**(4): p. 678-82.

9. Rees, J.L., *Genetics of hair and skin color.* Annu Rev Genet, 2003. **37**: p. 67-90.

10. Kennedy, C., et al., *Melanocortin 1 receptor (MC1R) gene variants are associated with an increased risk for cutaneous melanoma which is largely independent of skin type and hair color.* J Invest Dermatol, 2001. **117**(2): p. 294-300.

11. Ananthaswamy, H.N., et al., *Sunlight and skin cancer: inhibition of p53 mutations in UV-irradiated mouse skin by sunscreens.* Nat Med, 1997. **3**(5): p. 510-4.

12. Soehnge, H., A. Ouhtit, and O.N. Ananthaswamy, *Mechanisms of induction of skin cancer by UV radiation.* Front Biosci, 1997. **2**: p. d538-51.

13. el-Deiry, W.S., et al., *WAF1, a potential mediator of p53 tumor suppression.* Cell, 1993. **75**(4): p. 817-25.

14. Hermeking, H., et al., *14-3-3 sigma is a p53-regulated inhibitor of G2/M progression.* Mol Cell, 1997. **1**(1): p. 3-11.

15. Hill, L.L., et al., *Fas ligand: a sensor for DNA damage critical in skin cancer etiology.* Science, 1999. **285**(5429): p. 898-900.

16. Lo, H.L., et al., *Differential biologic effects of CPD and 6-4PP UV-induced DNA damage on the induction of apoptosis and cell-cycle arrest.* BMC Cancer, 2005. **5**: p. 135.

17. You, Y.H., et al., *Cyclobutane pyrimidine dimers are responsible for the vast majority of mutations induced by UVB irradiation in mammalian cells.* J Biol Chem, 2001. **276**(48): p. 44688-94.

18. de Boer, J. and J.H. Hoeijmakers, *Nucleotide excision repair and human syndromes.* Carcinogenesis, 2000. **21**(3): p. 453-60.

19. Wood, R.D., *DNA damage recognition during nucleotide excision repair in mammalian cells.* Biochimie, 1999. **81**(1-2): p. 39-44.

20. Kraemer, K.H., et al., *The role of sunlight and DNA repair in melanoma and nonmelanoma skin cancer. The xeroderma pigmentosum paradigm.* Arch Dermatol, 1994. **130**(8): p. 1018-21.

21. Stary, A. and A. Sarasin, *The genetics of the hereditary xeroderma pigmentosum syndrome.* Biochimie, 2002. **84**(1): p. 49-60.

22. Spatz, A., et al., *Association between DNA repair-deficiency and high level of p53 mutations in melanoma of Xeroderma pigmentosum.* Cancer Res, 2001. **61**(6): p. 2480-6.

23. Thompson, J.F., R.A. Scolyer, and R.F. Kefford, *Cutaneous melanoma.* Lancet, 2005. **365**(9460): p. 687-701.

24. Gilchrest, B.A., et al., *The pathogenesis of melanoma induced by ultraviolet radiation.* N Engl J Med, 1999. **340**(17): p. 1341-8.

25. Opdecamp, K., et al., *Melanocyte development in vivo and in neural crest cell cultures: crucial dependence on the Mitf basic-helix-loop-helix-zipper transcription factor.* Development, 1997. **124**(12): p. 2377-86.

26. Sasaki, M., et al., *Up-regulation of tyrosinase gene by nitric oxide in human melanocytes.* Pigment Cell Res, 2000. **13**(4): p. 248-52.

27. Suzuki, I., et al., *Participation of the melanocortin-1 receptor in the UV control of pigmentation.* J Investig Dermatol Symp Proc, 1999. **4**(1): p. 29-34.

28. Ivanova, K., et al., *Effect of nitric oxide on the adhesion of human melanocytes to extracellular matrix components.* J Pathol, 1997. **183**(4): p. 469-76.

29. Karim-Kos, H.E., et al., *Recent trends of cancer in Europe: a combined approach of incidence, survival and mortality for 17 cancer sites since the 1990s.* Eur J Cancer, 2008. **44**(10): p. 1345-89.

30. Coory, M., et al., *Trends for in situ and invasive melanoma in Queensland, Australia, 1982-2002.* Cancer Causes Control, 2006. **17**(1): p. 21-7.

31. *About melanoma skin cancer- A Quick guide* 2011, Cancer Research UK.

32. Cancer Research UK cancer stats, 2008.

33. *Surveillance epidemiology and end results. Faststats*. Available from: http://seer.cancer.gov/faststats.

34. Fecher, L.A., et al., *Toward a molecular classification of melanoma.* J Clin Oncol, 2007. **25**(12): p. 1606-20.

35. Harrison, S.L., R.M. MacKie, and R. MacLennan, *Development of melanocytic nevi in the first three years of life.* J Natl Cancer Inst, 2000. **92**(17): p. 1436-8.

36. Gandini, S., et al., *Meta-analysis of risk factors for cutaneous melanoma: II. Sun exposure.* Eur J Cancer, 2005. **41**(1): p. 45-60.

37. Armstrong, B.K. and A. Kricker, *The epidemiology of UV induced skin cancer.* J Photochem Photobiol B, 2001. **63**(1-3): p. 8-18.

38. Holly, E.A., et al., *Cutaneous melanoma in women. I. Exposure to sunlight, ability to tan, and other risk factors related to ultraviolet light.* Am J Epidemiol, 1995. **141**(10): p. 923-33.

39. Westerdahl, J., et al., *Use of sunbeds or sunlamps and malignant melanoma in southern Sweden.* Am J Epidemiol, 1994. **140**(8): p. 691-9.

40. Bataille, V., et al., *A multicentre epidemiological study on sunbed use and cutaneous melanoma in Europe.* Eur J Cancer, 2005. **41**(14): p. 2141-9.

41. Autier, P., *Cutaneous malignant melanoma: facts about sunbeds and sunscreen.* Expert Rev Anticancer Ther, 2005. **5**(5): p. 821-33.

42. Palmer, J.S., et al., *Melanocortin-1 receptor polymorphisms and risk of melanoma: is the association explained solely by pigmentation phenotype?* Am J Hum Genet, 2000. **66**(1): p. 176-86.

43. Mossner, R., et al., *Variations of the melanocortin-1 receptor and the glutathione-S transferase T1 and M1 genes in cutaneous malignant melanoma.* Arch Dermatol Res, 2007. **298**(8): p. 371-9.

44. Gandini, S., et al., *Meta-analysis of risk factors for cutaneous melanoma: I. Common and atypical naevi.* Eur J Cancer, 2005. **41**(1): p. 28-44.

45. Bataille, V. and E. de Vries, *Melanoma--Part 1: epidemiology, risk factors, and prevention.* BMJ, 2008. **337**: p. a2249.

46. Aitken, J., et al., *CDKN2A variants in a population-based sample of Queensland families with melanoma.* J Natl Cancer Inst, 1999. **91**(5): p. 446-52.

47. Roberts, D.L., et al., *U.K. guidelines for the management of cutaneous melanoma.* Br J Dermatol, 2002. **146**(1): p. 7-17.

48. Balch, C.M., et al., *Final version of 2009 AJCC melanoma staging and classification.* J Clin Oncol, 2009. **27**(36): p. 6199-206.

49. Balch, C.M., et al., *Prognostic factors analysis of 17,600 melanoma patients: validation of the American Joint Committee on Cancer melanoma staging system.* J Clin Oncol, 2001. **19**(16): p. 3622-34.

50. Rousseau, D.L., Jr., et al., *Revised American Joint Committee on Cancer staging criteria accurately predict sentinel lymph node positivity in clinically node-negative melanoma patients.* Ann Surg Oncol, 2003. **10**(5): p. 569-74.

51. Balch, C.M., et al., *An evidence-based staging system for cutaneous melanoma.* CA Cancer J Clin, 2004. **54**(3): p. 131-49; quiz 182-4.

52. Carlson, J.A., et al., *Molecular diagnostics in melanoma.* J Am Acad Dermatol, 2005. **52**(5): p. 743-75; quiz 775-8.

53. Lodha, S., et al., *Discordance in the histopathologic diagnosis of difficult melanocytic neoplasms in the clinical setting.* J Cutan Pathol, 2008. **35**(4): p. 349-52.

54. Blokx, W.A., M.C. van Dijk, and D.J. Ruiter, *Molecular cytogenetics of cutaneous melanocytic lesions - diagnostic, prognostic and therapeutic aspects.* Histopathology. **56**(1): p. 121-32.

55. Balch, C.M., et al., *Final version of the American Joint Committee on Cancer staging system for cutaneous melanoma.* J Clin Oncol, 2001. **19**(16): p. 3635-48.

56. Friedman, R.J., D.S. Rigel, and A.W. Kopf, *Early detection of malignant melanoma: the role of physician examination and self-examination of the skin.* CA Cancer J Clin, 1985. **35**(3): p. 130-51.

57. Hersey, P., *Adjuvant therapy for high-risk primary and resected metastatic melanoma.* Intern Med J, 2003. **33**(1-2): p. 33-43.

58. Eggermont, A., et al. *EORTC 18991: Long-term adjuvant pegylated interferon-alpha2b (PEG-IFN) compared to observation in resected stage III*

melanoma, final results of a randomized phase III trial in *ASCO* 2007 Journal of Clinical oncology.

59. Thirlwell, C. and P. Nathan, *Melanoma--part 2: management.* BMJ, 2008. **337**: p. a2488.

60. http://www.cancerhelp.org.uk/type/melanoma/treatment/melanoma-statistics-and-outlook.

61. Davies, M.A. and Y. Samuels, *Analysis of the genome to personalize therapy for melanoma.* Oncogene, 2010. **29**(41): p. 5545-55.

62. Atkins, M.B., et al., *High-dose recombinant interleukin 2 therapy for patients with metastatic melanoma: analysis of 270 patients treated between 1985 and 1993.* J Clin Oncol, 1999. **17**(7): p. 2105-16.

63. Phan, G.Q., et al., *Factors associated with response to high-dose interleukin-2 in patients with metastatic melanoma.* J Clin Oncol, 2001. **19**(15): p. 3477-82.

64. Tsao, H., M.B. Atkins, and A.J. Sober, *Management of cutaneous melanoma.* N Engl J Med, 2004. **351**(10): p. 998-1012.

65. Clark, W.H., Jr., et al., *A study of tumor progression: the precursor lesions of superficial spreading and nodular melanoma.* Hum Pathol, 1984. **15**(12): p. 1147-65.

66. Michaloglou, C., et al., *BRAFE600-associated senescence-like cell cycle arrest of human naevi.* Nature, 2005. **436**(7051): p. 720-4.

67. Braig, M. and C.A. Schmitt, *Oncogene-induced senescence: putting the brakes on tumor development.* Cancer Res, 2006. **66**(6): p. 2881-4.

68. Robinson, M.J. and M.H. Cobb, *Mitogen-activated protein kinase pathways.* Curr Opin Cell Biol, 1997. **9**(2): p. 180-6.

69. Crews, C.M., A. Alessandrini, and R.L. Erikson, *The primary structure of MEK, a protein kinase that phosphorylates the ERK gene product.* Science, 1992. **258**(5081): p. 478-80.

70. Kyriakis, J.M., et al., *Raf-1 activates MAP kinase-kinase.* Nature, 1992. **358**(6385): p. 417-21.

71. Cohen, C., et al., *Mitogen-actived protein kinase activation is an early event in melanoma progression.* Clin Cancer Res, 2002. **8**(12): p. 3728-33.

72. Nesbit, M., et al., *Basic fibroblast growth factor induces a transformed phenotype in normal human melanocytes.* Oncogene, 1999. **18**(47): p. 6469-76.

73. Li, G., K. Satyamoorthy, and M. Herlyn, *N-cadherin-mediated intercellular interactions promote survival and migration of melanoma cells.* Cancer Res, 2001. **61**(9): p. 3819-25.

74. Padua, R.A., N.C. Barrass, and G.A. Currie, *Activation of N-ras in a human melanoma cell line.* Mol Cell Biol, 1985. **5**(3): p. 582-5.

75. Hocker, T. and H. Tsao, *Ultraviolet radiation and melanoma: a systematic review and analysis of reported sequence variants.* Hum Mutat, 2007. **28**(6): p. 578-88.

76. Brose, M.S., et al., *BRAF and RAS mutations in human lung cancer and melanoma.* Cancer Res, 2002. **62**(23): p. 6997-7000.

77. Davies, H., et al., *Mutations of the BRAF gene in human cancer.* Nature, 2002. **417**(6892): p. 949-54.

78. Smalley, K.S., *Understanding melanoma signaling networks as the basis for molecular targeted therapy.* J Invest Dermatol, 2010. **130**(1): p. 28-37.

79. Garnett, M.J. and R. Marais, *Guilty as charged: B-RAF is a human oncogene.* Cancer Cell, 2004. **6**(4): p. 313-9.

80. Wan, P.T., et al., *Mechanism of activation of the RAF-ERK signaling pathway by oncogenic mutations of B-RAF.* Cell, 2004. **116**(6): p. 855-67.

81. Bhatt, K.V., et al., *Adhesion control of cyclin D1 and p27Kip1 levels is deregulated in melanoma cells through BRAF-MEK-ERK signaling.* Oncogene, 2005. **24**(21): p. 3459-71.

82. Zhang, X.D., et al., *Activation of ERK1/2 protects melanoma cells from TRAIL-induced apoptosis by inhibiting Smac/DIABLO release from mitochondria.* Oncogene, 2003. **22**(19): p. 2869-81.

83. Eisenmann, K.M., et al., *Mitogen-activated protein kinase pathway-dependent tumor-specific survival signaling in melanoma cells through inactivation of the proapoptotic protein bad.* Cancer Res, 2003. **63**(23): p. 8330-7.

84. Cartlidge, R.A., et al., *Oncogenic BRAF(V600E) inhibits BIM expression to promote melanoma cell survival.* Pigment Cell Melanoma Res, 2008. **21**(5): p. 534-44.

85. Kumar, S.M., et al., *Mutant V600E BRAF increases hypoxia inducible factor-1alpha expression in melanoma.* Cancer Res, 2007. **67**(7): p. 3177-84.

86. Woods, D., et al., *Induction of beta3-integrin gene expression by sustained activation of the Ras-regulated Raf-MEK-extracellular signal-regulated kinase signaling pathway.* Mol Cell Biol, 2001. **21**(9): p. 3192-205.

87. Benbow, U., et al., *High levels of MMP-1 expression in the absence of the 2G single nucleotide polymorphism is mediated by p38 and ERK1/2 mitogen-activated protein kinases in VMM5 melanoma cells.* J Cell Biochem, 2002. **86**(2): p. 307-19.

88. Ge, X., Y.M. Fu, and G.G. Meadows, *U0126, a mitogen-activated protein kinase kinase inhibitor, inhibits the invasion of human A375 melanoma cells.* Cancer Lett, 2002. **179**(2): p. 133-40.

89. Huntington, J.T., et al., *Overexpression of collagenase 1 (MMP-1) is mediated by the ERK pathway in invasive melanoma cells: role of BRAF mutation and fibroblast growth factor signaling.* J Biol Chem, 2004. **279**(32): p. 33168-76.

90. Kono, M., et al., *Role of the mitogen-activated protein kinase signaling pathway in the regulation of human melanocytic antigen expression.* Mol Cancer Res, 2006. **4**(10): p. 779-92.

91. Miller, A.J. and M.C. Mihm, Jr., *Melanoma.* N Engl J Med, 2006. **355**(1): p. 51-65.

92. Stahl, J.M., et al., *Deregulated Akt3 activity promotes development of malignant melanoma.* Cancer Res, 2004. **64**(19): p. 7002-10.

93. Tsao, H., et al., *Genetic interaction between NRAS and BRAF mutations and PTEN/MMAC1 inactivation in melanoma.* J Invest Dermatol, 2004. **122**(2): p. 337-41.

94. Li, J., et al., *PTEN, a putative protein tyrosine phosphatase gene mutated in human brain, breast, and prostate cancer.* Science, 1997. **275**(5308): p. 1943-7.

95. Steck, P.A., et al., *Identification of a candidate tumour suppressor gene, MMAC1, at chromosome 10q23.3 that is mutated in multiple advanced cancers.* Nat Genet, 1997. **15**(4): p. 356-62.

96. You, M.J., et al., *Genetic analysis of Pten and Ink4a/Arf interactions in the suppression of tumorigenesis in mice.* Proc Natl Acad Sci U S A, 2002. **99**(3): p. 1455-60.

97. Lin, W.M., et al., *Modeling genomic diversity and tumor dependency in malignant melanoma.* Cancer Res, 2008. **68**(3): p. 664-73.

98. Brazil, D.P., J. Park, and B.A. Hemmings, *PKB binding proteins. Getting in on the Akt.* Cell, 2002. **111**(3): p. 293-303.

99. Wu, H., V. Goel, and F.G. Haluska, *PTEN signaling pathways in melanoma.* Oncogene, 2003. **22**(20): p. 3113-22.

100. Cantley, L.C. and B.G. Neel, *New insights into tumor suppression: PTEN suppresses tumor formation by restraining the phosphoinositide 3-kinase/AKT pathway.* Proc Natl Acad Sci U S A, 1999. **96**(8): p. 4240-5.

101. Datta, S.R., et al., *Akt phosphorylation of BAD couples survival signals to the cell-intrinsic death machinery.* Cell, 1997. **91**(2): p. 231-41.

102. Robertson, G.P., *Functional and therapeutic significance of Akt deregulation in malignant melanoma.* Cancer Metastasis Rev, 2005. **24**(2): p. 273-85.

103. Bedogni, B., et al., *The hypoxic microenvironment of the skin contributes to Akt-mediated melanocyte transformation.* Cancer Cell, 2005. **8**(6): p. 443-54.

104. Bedogni, B., et al., *Notch1 is an effector of Akt and hypoxia in melanoma development.* J Clin Invest, 2008. **118**(11): p. 3660-70.

105. Hodgkinson, C.A., et al., *Mutations at the mouse microphthalmia locus are associated with defects in a gene encoding a novel basic-helix-loop-helix-zipper protein.* Cell, 1993. **74**(2): p. 395-404.

106. Nishimura, E.K., S.R. Granter, and D.E. Fisher, *Mechanisms of hair graying: incomplete melanocyte stem cell maintenance in the niche.* Science, 2005. **307**(5710): p. 720-4.

107. Widlund, H.R. and D.E. Fisher, *Microphthalamia-associated transcription factor: a critical regulator of pigment cell development and survival.* Oncogene, 2003. **22**(20): p. 3035-41.

108. Loercher, A.E., et al., *MITF links differentiation with cell cycle arrest in melanocytes by transcriptional activation of INK4A.* J Cell Biol, 2005. **168**(1): p. 35-40.

109. Carreira, S., et al., *Mitf cooperates with Rb1 and activates p21Cip1 expression to regulate cell cycle progression.* Nature, 2005. **433**(7027): p. 764-9.

110. Wellbrock, C. and R. Marais, *Elevated expression of MITF counteracts B-RAF-stimulated melanocyte and melanoma cell proliferation.* J Cell Biol, 2005. **170**(5): p. 703-8.

111. Hoek, K.S., et al., *In vivo switching of human melanoma cells between proliferative and invasive states.* Cancer Res, 2008. **68**(3): p. 650-6.

112. McGill, G.G., et al., *Bcl2 regulation by the melanocyte master regulator Mitf modulates lineage survival and melanoma cell viability.* Cell, 2002. **109**(6): p. 707-18.

113. Du, J., et al., *Critical role of CDK2 for melanoma growth linked to its melanocyte-specific transcriptional regulation by MITF.* Cancer Cell, 2004. **6**(6): p. 565-76.

114. Goding, C.R., *Mitf from neural crest to melanoma: signal transduction and transcription in the melanocyte lineage.* Genes Dev, 2000. **14**(14): p. 1712-28.

115. Garraway, L.A., et al., *Integrative genomic analyses identify MITF as a lineage survival oncogene amplified in malignant melanoma.* Nature, 2005. **436**(7047): p. 117-22.

116. Wellbrock, C., et al., *Oncogenic BRAF regulates melanoma proliferation through the lineage specific factor MITF.* PLoS One, 2008. **3**(7): p. e2734.

117. Haass, N.K., et al., *Adhesion, migration and communication in melanocytes and melanoma.* Pigment Cell Res, 2005. **18**(3): p. 150-9.

118. Johnson, J.P., *Cell adhesion molecules in the development and progression of malignant melanoma.* Cancer Metastasis Rev, 1999. **18**(3): p. 345-57.

119. Danen, E.H., et al., *E-cadherin expression in human melanoma.* Melanoma Res, 1996. **6**(2): p. 127-31.

120. Hsu, M.Y., et al., *Shifts in cadherin profiles between human normal melanocytes and melanomas.* J Investig Dermatol Symp Proc, 1996. **1**(2): p. 188-94.

121. Gottardi, C.J., E. Wong, and B.M. Gumbiner, *E-cadherin suppresses cellular transformation by inhibiting beta-catenin signaling in an adhesion-independent manner.* J Cell Biol, 2001. **153**(5): p. 1049-60.

122. Qi, J., et al., *Transendothelial migration of melanoma cells involves N-cadherin-mediated adhesion and activation of the beta-catenin signaling pathway.* Mol Biol Cell, 2005. **16**(9): p. 4386-97.

123. Danen, E.H., et al., *Emergence of alpha 5 beta 1 fibronectin- and alpha v beta 3 vitronectin-receptor expression in melanocytic tumour progression.* Histopathology, 1994. **24**(3): p. 249-56.

124. Brooks, P.C., et al., *Localization of matrix metalloproteinase MMP-2 to the surface of invasive cells by interaction with integrin alpha v beta 3.* Cell, 1996. **85**(5): p. 683-93.

125. Felding-Habermann, B., et al., *Involvement of tumor cell integrin alpha v beta 3 in hematogenous metastasis of human melanoma cells.* Clin Exp Metastasis, 2002. **19**(5): p. 427-36.

126. Hofmann, U.B., et al., *Coexpression of integrin alpha(v)beta3 and matrix metalloproteinase-2 (MMP-2) coincides with MMP-2 activation: correlation with melanoma progression.* J Invest Dermatol, 2000. **115**(4): p. 625-32.

127. Sharpless, E. and L. Chin, *The INK4a/ARF locus and melanoma.* Oncogene, 2003. **22**(20): p. 3092-8.

128. Sharpless, N.E., et al., *The differential impact of p16(INK4a) or p19(ARF) deficiency on cell growth and tumorigenesis.* Oncogene, 2004. **23**(2): p. 379-85.

129. Kamijo, T., et al., *Tumor suppression at the mouse INK4a locus mediated by the alternative reading frame product p19ARF.* Cell, 1997. **91**(5): p. 649-59.

130. Recio, J.A., et al., *Ink4a/arf deficiency promotes ultraviolet radiation-induced melanomagenesis.* Cancer Res, 2002. **62**(22): p. 6724-30.

131. Curtin, J.A., et al., *Somatic activation of KIT in distinct subtypes of melanoma.* J Clin Oncol, 2006. **24**(26): p. 4340-6.

132. Jiang, X., et al., *Imatinib targeting of KIT-mutant oncoprotein in melanoma.* Clin Cancer Res, 2008. **14**(23): p. 7726-32.

133. Ashida, A., et al., *Pathological activation of KIT in metastatic tumors of acral and mucosal melanomas.* Int J Cancer, 2009. **124**(4): p. 862-8.

134. Yang, J. and A. Richmond, *Constitutive IkappaB kinase activity correlates with nuclear factor-kappaB activation in human melanoma cells.* Cancer Res, 2001. **61**(12): p. 4901-9.

135. Stecca, B., et al., *Melanomas require HEDGEHOG-GLI signaling regulated by interactions between GLI1 and the RAS-MEK/AKT pathways.* Proc Natl Acad Sci U S A, 2007. **104**(14): p. 5895-900.

136. Niu, G., et al., *Roles of activated Src and Stat3 signaling in melanoma tumor cell growth.* Oncogene, 2002. **21**(46): p. 7001-10.

137. Balint, K., et al., *Activation of Notch1 signaling is required for beta-catenin-mediated human primary melanoma progression.* J Clin Invest, 2005. **115**(11): p. 3166-76.

138. Carracedo, A., et al., *Inhibition of mTORC1 leads to MAPK pathway activation through a PI3K-dependent feedback loop in human cancer.* J Clin Invest, 2008. **118**(9): p. 3065-74.

139. Davies, M., B. Hennessy, and G.B. Mills, *Point mutations of protein kinases and individualised cancer therapy.* Expert Opin Pharmacother, 2006. **7**(16): p. 2243-61.

140. Karasarides, M., et al., *B-RAF is a therapeutic target in melanoma.* Oncogene, 2004. **23**(37): p. 6292-8.

141. Hauschild, A., et al., *Results of a phase III, randomized, placebo-controlled study of sorafenib in combination with carboplatin and paclitaxel as second-line treatment in patients with unresectable stage III or stage IV melanoma.* J Clin Oncol, 2009. **27**(17): p. 2823-30.

142. Flaherty, K.T., et al., *A phase I trial of the oral, multikinase inhibitor sorafenib in combination with carboplatin and paclitaxel.* Clin Cancer Res, 2008. **14**(15): p. 4836-42.

143. Fisher, D.E., et al., *Melanoma from bench to bedside: meeting report from the 6th international melanoma congress.* Pigment Cell Melanoma Res, 2010. **23**(1): p. 14-26.

144. Antonescu, C.R., et al., *L576P KIT mutation in anal melanomas correlates with KIT protein expression and is sensitive to specific kinase inhibition.* Int J Cancer, 2007. **121**(2): p. 257-64.

145. Hodi, F.S., et al., *Major response to imatinib mesylate in KIT-mutated melanoma.* J Clin Oncol, 2008. **26**(12): p. 2046-51.

146. Quintas-Cardama, A., et al., *Complete response of stage IV anal mucosal melanoma expressing KIT Val560Asp to the multikinase inhibitor sorafenib.* Nat Clin Pract Oncol, 2008. **5**(12): p. 737-40.

147. Woodman, S.E., et al., *Activity of dasatinib against L576P KIT mutant melanoma: molecular, cellular, and clinical correlates.* Mol Cancer Ther, 2009. **8**(8): p. 2079-85.

148. Taft, R.J., M. Pheasant, and J.S. Mattick, *The relationship between non-protein-coding DNA and eukaryotic complexity.* Bioessays, 2007. **29**(3): p. 288-99.

149. Taft, R.J., et al., *Non-coding RNAs: regulators of disease.* J Pathol. **220**(2): p. 126-39.

150. Saito, K., et al., *Specific association of Piwi with rasiRNAs derived from retrotransposon and heterochromatic regions in the Drosophila genome.* Genes Dev, 2006. **20**(16): p. 2214-22.

151. Kapranov, P., et al., *RNA maps reveal new RNA classes and a possible function for pervasive transcription.* Science, 2007. **316**(5830): p. 1484-8.

152. Taft, R.J., et al., *Tiny RNAs associated with transcription start sites in animals.* Nat Genet, 2009. **41**(5): p. 572-8.

153. Fire, A., et al., *Potent and specific genetic interference by double-stranded RNA in Caenorhabditis elegans.* Nature, 1998. **391**(6669): p. 806-11.

154. Grishok, A., H. Tabara, and C.C. Mello, *Genetic requirements for inheritance of RNAi in C. elegans.* Science, 2000. **287**(5462): p. 2494-7.

155. Voinnet, O., *Non-cell autonomous RNA silencing.* FEBS Lett, 2005. **579**(26): p. 5858-71.

156. Voinnet, O., *Origin, biogenesis, and activity of plant microRNAs.* Cell, 2009. **136**(4): p. 669-87.

157. Malone, C.D. and G.J. Hannon, *Small RNAs as guardians of the genome.* Cell, 2009. **136**(4): p. 656-68.

158. Carthew, R.W. and E.J. Sontheimer, *Origins and Mechanisms of miRNAs and siRNAs.* Cell, 2009. **136**(4): p. 642-55.

159. Ghildiyal, M. and P.D. Zamore, *Small silencing RNAs: an expanding universe.* Nat Rev Genet, 2009. **10**(2): p. 94-108.

160. Hamilton, A.J. and D.C. Baulcombe, *A species of small antisense RNA in posttranscriptional gene silencing in plants.* Science, 1999. **286**(5441): p. 950-2.

161. Hammond, S.M., et al., *An RNA-directed nuclease mediates post-transcriptional gene silencing in Drosophila cells.* Nature, 2000. **404**(6775): p. 293-6.

162. Pal-Bhadra, M., U. Bhadra, and J.A. Birchler, *RNAi related mechanisms affect both transcriptional and posttranscriptional transgene silencing in Drosophila.* Mol Cell, 2002. **9**(2): p. 315-27.

163. Loh, Y.H., et al., *The Oct4 and Nanog transcription network regulates pluripotency in mouse embryonic stem cells.* Nat Genet, 2006. **38**(4): p. 431-40.

164. Impey, S., et al., *Defining the CREB regulon: a genome-wide analysis of transcription factor regulatory regions.* Cell, 2004. **119**(7): p. 1041-54.

165. Cawley, S., et al., *Unbiased mapping of transcription factor binding sites along human chromosomes 21 and 22 points to widespread regulation of noncoding RNAs.* Cell, 2004. **116**(4): p. 499-509.

166. Guttman, M., et al., *Chromatin signature reveals over a thousand highly conserved large non-coding RNAs in mammals.* Nature, 2009. **458**(7235): p. 223-7.

167. Taft, R.J., et al., *Non-coding RNAs: regulators of disease.* J Pathol, 2010. **220**(2): p. 126-39.

168. Lee, R.C., R.L. Feinbaum, and V. Ambros, *The C. elegans heterochronic gene lin-4 encodes small RNAs with antisense complementarity to lin-14.* Cell, 1993. **75**(5): p. 843-54.

169. Pasquinelli, A.E., et al., *Conservation of the sequence and temporal expression of let-7 heterochronic regulatory RNA.* Nature, 2000. **408**(6808): p. 86-9.

170. Johnson, C.D., et al., *The let-7 microRNA represses cell proliferation pathways in human cells.* Cancer Res, 2007. **67**(16): p. 7713-22.

171. Johnson, S.M., et al., *RAS is regulated by the let-7 microRNA family.* Cell, 2005. **120**(5): p. 635-47.

172. Sato, F., et al., *MicroRNAs and epigenetics.* FEBS J, 2011. **278**(10): p. 1598-609.

173. Bartel, D.P., *MicroRNAs: genomics, biogenesis, mechanism, and function.* Cell, 2004. **116**(2): p. 281-97.

174. Ibanez-Ventoso, C., M. Vora, and M. Driscoll, *Sequence relationships among C. elegans, D. melanogaster and human microRNAs highlight the extensive conservation of microRNAs in biology.* PLoS One, 2008. **3**(7): p. e2818.

175. Chapman, E.J. and J.C. Carrington, *Specialization and evolution of endogenous small RNA pathways.* Nat Rev Genet, 2007. **8**(11): p. 884-96.

176. Lee, Y., et al., *MicroRNA genes are transcribed by RNA polymerase II.* EMBO J, 2004. **23**(20): p. 4051-60.

177. Cai, X., C.H. Hagedorn, and B.R. Cullen, *Human microRNAs are processed from capped, polyadenylated transcripts that can also function as mRNAs.* RNA, 2004. **10**(12): p. 1957-66.

178. Borchert, G.M., W. Lanier, and B.L. Davidson, *RNA polymerase III transcribes human microRNAs.* Nat Struct Mol Biol, 2006. **13**(12): p. 1097-101.

179. Winter, J., et al., *Many roads to maturity: microRNA biogenesis pathways and their regulation.* Nat Cell Biol, 2009. **11**(3): p. 228-34.

180. Song, G. and L. Wang, *MiR-433 and miR-127 arise from independent overlapping primary transcripts encoded by the miR-433-127 locus.* PLoS One, 2008. **3**(10): p. e3574.

181. Akbari, M.R., et al., *Germline RAP80 mutations and susceptibility to breast cancer.* Breast Cancer Res Treat, 2009. **113**(2): p. 377-81.

182. Han, J., et al., *The Drosha-DGCR8 complex in primary microRNA processing.* Genes Dev, 2004. **18**(24): p. 3016-27.

183. Han, J., et al., *Molecular basis for the recognition of primary microRNAs by the Drosha-DGCR8 complex.* Cell, 2006. **125**(5): p. 887-901.

184. Yi, R., et al., *Exportin-5 mediates the nuclear export of pre-microRNAs and short hairpin RNAs.* Genes Dev, 2003. **17**(24): p. 3011-6.

185. Bohnsack, M.T., K. Czaplinski, and D. Gorlich, *Exportin 5 is a RanGTP-dependent dsRNA-binding protein that mediates nuclear export of pre-miRNAs.* RNA, 2004. **10**(2): p. 185-91.

186. Lund, E., et al., *Nuclear export of microRNA precursors.* Science, 2004. **303**(5654): p. 95-8.

187. Lund, E. and J.E. Dahlberg, *Substrate selectivity of exportin 5 and Dicer in the biogenesis of microRNAs.* Cold Spring Harb Symp Quant Biol, 2006. **71**: p. 59-66.

188. Zeng, Y. and B.R. Cullen, *Structural requirements for pre-microRNA binding and nuclear export by Exportin 5.* Nucleic Acids Res, 2004. **32**(16): p. 4776-85.

189. Maniataki, E. and Z. Mourelatos, *A human, ATP-independent, RISC assembly machine fueled by pre-miRNA.* Genes Dev, 2005. **19**(24): p. 2979-90.

190. Gregory, R.I., et al., *Human RISC couples microRNA biogenesis and posttranscriptional gene silencing.* Cell, 2005. **123**(4): p. 631-40.

191. Haase, A.D., et al., *TRBP, a regulator of cellular PKR and HIV-1 virus expression, interacts with Dicer and functions in RNA silencing.* EMBO Rep, 2005. **6**(10): p. 961-7.

192. Lee, Y., et al., *The role of PACT in the RNA silencing pathway.* EMBO J, 2006. **25**(3): p. 522-32.

193. MacRae, I.J., et al., *In vitro reconstitution of the human RISC-loading complex.* Proc Natl Acad Sci U S A, 2008. **105**(2): p. 512-7.

194. Diederichs, S. and D.A. Haber, *Dual role for argonautes in microRNA processing and posttranscriptional regulation of microRNA expression.* Cell, 2007. **131**(6): p. 1097-108.

195. Carmell, M.A. and G.J. Hannon, *RNase III enzymes and the initiation of gene silencing.* Nat Struct Mol Biol, 2004. **11**(3): p. 214-8.

196. Bernstein, E., et al., *Role for a bidentate ribonuclease in the initiation step of RNA interference.* Nature, 2001. **409**(6818): p. 363-6.

197. Grishok, A., et al., *Genes and mechanisms related to RNA interference regulate expression of the small temporal RNAs that control C. elegans developmental timing.* Cell, 2001. **106**(1): p. 23-34.

198. Schwarz, D.S., et al., *Asymmetry in the assembly of the RNAi enzyme complex.* Cell, 2003. **115**(2): p. 199-208.

199. Khvorova, A., A. Reynolds, and S.D. Jayasena, *Functional siRNAs and miRNAs exhibit strand bias.* Cell, 2003. **115**(2): p. 209-16.

200. Filipowicz, W., S.N. Bhattacharyya, and N. Sonenberg, *Mechanisms of post-transcriptional regulation by microRNAs: are the answers in sight?* Nat Rev Genet, 2008. **9**(2): p. 102-14.

201. Eulalio, A., E. Huntzinger, and E. Izaurralde, *Getting to the root of miRNA-mediated gene silencing.* Cell, 2008. **132**(1): p. 9-14.

202. Yekta, S., I.H. Shih, and D.P. Bartel, *MicroRNA-directed cleavage of HOXB8 mRNA.* Science, 2004. **304**(5670): p. 594-6.

203. Kiriakidou, M., et al., *An mRNA m7G cap binding-like motif within human Ago2 represses translation.* Cell, 2007. **129**(6): p. 1141-51.

204. Chendrimada, T.P., et al., *MicroRNA silencing through RISC recruitment of eIF6.* Nature, 2007. **447**(7146): p. 823-8.

205. Maroney, P.A., Y. Yu, and T.W. Nilsen, *MicroRNAs, mRNAs, and translation.* Cold Spring Harb Symp Quant Biol, 2006. **71**: p. 531-5.

206. Ozsolak, F., et al., *Chromatin structure analyses identify miRNA promoters.* Genes Dev, 2008. **22**(22): p. 3172-83.

207. Wang, X., et al., *High-resolution human core-promoter prediction with CoreBoost_HM.* Genome Res, 2009. **19**(2): p. 266-75.

208. Zhou, X., et al., *Characterization and identification of microRNA core promoters in four model species.* PLoS Comput Biol, 2007. **3**(3): p. e37.

209. Corcoran, D.L., et al., *Features of mammalian microRNA promoters emerge from polymerase II chromatin immunoprecipitation data.* PLoS One, 2009. **4**(4): p. e5279.

210. Luciano, D.J., et al., *RNA editing of a miRNA precursor.* RNA, 2004. **10**(8): p. 1174-7.

211. Blow, M.J., et al., *RNA editing of human microRNAs.* Genome Biol, 2006. **7**(4): p. R27.

212. Yang, W., et al., *Modulation of microRNA processing and expression through RNA editing by ADAR deaminases.* Nat Struct Mol Biol, 2006. **13**(1): p. 13-21.

213. Scadden, A.D., *The RISC subunit Tudor-SN binds to hyper-edited double-stranded RNA and promotes its cleavage.* Nat Struct Mol Biol, 2005. **12**(6): p. 489-96.

214. Kawahara, Y., et al., *RNA editing of the microRNA-151 precursor blocks cleavage by the Dicer-TRBP complex.* EMBO Rep, 2007. **8**(8): p. 763-9.

215. Kawahara, Y., et al., *Redirection of silencing targets by adenosine-to-inosine editing of miRNAs.* Science, 2007. **315**(5815): p. 1137-40.

216. Abelson, J.F., et al., *Sequence variants in SLITRK1 are associated with Tourette's syndrome.* Science, 2005. **310**(5746): p. 317-20.

217. Saunders, M.A., H. Liang, and W.H. Li, *Human polymorphism at microRNAs and microRNA target sites.* Proc Natl Acad Sci U S A, 2007. **104**(9): p. 3300-5.

218. Duan, R., C. Pak, and P. Jin, *Single nucleotide polymorphism associated with mature miR-125a alters the processing of pri-miRNA.* Hum Mol Genet, 2007. **16**(9): p. 1124-31.

219. Wu, M., et al., *Genetic variations of microRNAs in human cancer and their effects on the expression of miRNAs.* Carcinogenesis, 2008. **29**(9): p. 1710-6.

220. Saito, Y., et al., *Specific activation of microRNA-127 with downregulation of the proto-oncogene BCL6 by chromatin-modifying drugs in human cancer cells.* Cancer Cell, 2006. **9**(6): p. 435-43.

221. Lewis, B.P., C.B. Burge, and D.P. Bartel, *Conserved seed pairing, often flanked by adenosines, indicates that thousands of human genes are microRNA targets.* Cell, 2005. **120**(1): p. 15-20.

222. Baek, D., et al., *The impact of microRNAs on protein output.* Nature, 2008. **455**(7209): p. 64-71.

223. Selbach, M., et al., *Widespread changes in protein synthesis induced by microRNAs.* Nature, 2008. **455**(7209): p. 58-63.

224. Carthew, R.W., *Gene regulation by microRNAs.* Curr Opin Genet Dev, 2006. **16**(2): p. 203-8.

225. Jiang, Q., et al., *miR2Disease: a manually curated database for microRNA deregulation in human disease.* Nucleic Acids Res, 2009. **37**(Database issue): p. D98-104.

226. Barbato, C., et al., *Thinking about RNA? MicroRNAs in the brain.* Mamm Genome, 2008. **19**(7-8): p. 541-51.

227. Hennessy, E. and L. O'Driscoll, *Molecular medicine of microRNAs: structure, function and implications for diabetes.* Expert Rev Mol Med, 2008. **10**: p. e24.

228. Medina, P.P. and F.J. Slack, *microRNAs and cancer: an overview.* Cell Cycle, 2008. **7**(16): p. 2485-92.

229. Vasudevan, S., Y. Tong, and J.A. Steitz, *Switching from repression to activation: microRNAs can up-regulate translation.* Science, 2007. **318**(5858): p. 1931-4.

230. Kloosterman, W.P., et al., *In situ detection of miRNAs in animal embryos using LNA-modified oligonucleotide probes.* Nat Methods, 2006. **3**(1): p. 27-9.

231. You, Y., et al., *Design of LNA probes that improve mismatch discrimination.* Nucleic Acids Res, 2006. **34**(8): p. e60.

232. Denys, B., et al., *A real-time polymerase chain reaction assay for rapid, sensitive, and specific quantification of the JAK2V617F mutation using a locked nucleic acid-modified oligonucleotide.* J Mol Diagn, 2010. **12**(4): p. 512-9.

233. Yamamichi, N., et al., *Locked nucleic acid in situ hybridization analysis of miR-21 expression during colorectal cancer development.* Clin Cancer Res, 2009. **15**(12): p. 4009-16.

234. Pena, J.T., et al., *miRNA in situ hybridization in formaldehyde and EDC-fixed tissues.* Nat Methods, 2009. **6**(2): p. 139-41.

235. John, B., et al., *Human MicroRNA targets.* PLoS Biol, 2004. **2**(11): p. e363.

236. Ruby, J.G., et al., *Evolution, biogenesis, expression, and target predictions of a substantially expanded set of Drosophila microRNAs.* Genome Res, 2007. **17**(12): p. 1850-64.

237. Lall, S., et al., *A genome-wide map of conserved microRNA targets in C. elegans.* Curr Biol, 2006. **16**(5): p. 460-71.

238. Kertesz, M., et al., *The role of site accessibility in microRNA target recognition.* Nat Genet, 2007. **39**(10): p. 1278-84.

239. Miranda, K.C., et al., *A pattern-based method for the identification of MicroRNA binding sites and their corresponding heteroduplexes.* Cell, 2006. **126**(6): p. 1203-17.

240. Maragkakis, M., et al., *DIANA-microT web server: elucidating microRNA functions through target prediction.* Nucleic Acids Res, 2009. **37**(Web Server issue): p. W273-6.

241. Papadopoulos, G.L., et al., *DIANA-mirPath: Integrating human and mouse microRNAs in pathways.* Bioinformatics, 2009. **25**(15): p. 1991-3.

242. Kanehisa, M., *The KEGG database.* Novartis Found Symp, 2002. **247**: p. 91-101; discussion 101-3, 119-28, 244-52.

243. Kanehisa, M., et al., *From genomics to chemical genomics: new developments in KEGG.* Nucleic Acids Res, 2006. **34**(Database issue): p. D354-7.

244. Care, A., et al., *MicroRNA-133 controls cardiac hypertrophy.* Nat Med, 2007. **13**(5): p. 613-8.

245. Chang, J., et al., *Liver-specific microRNA miR-122 enhances the replication of hepatitis C virus in nonhepatic cells.* J Virol, 2008. **82**(16): p. 8215-23.

246. Mehler, M.F. and J.S. Mattick, *Non-coding RNAs in the nervous system.* J Physiol, 2006. **575**(Pt 2): p. 333-41.

247. Esau, C., et al., *miR-122 regulation of lipid metabolism revealed by in vivo antisense targeting.* Cell Metab, 2006. **3**(2): p. 87-98.

248. Krutzfeldt, J., et al., *Silencing of microRNAs in vivo with 'antagomirs'.* Nature, 2005. **438**(7068): p. 685-9.

249. Calin, G.A., et al., *Frequent deletions and down-regulation of micro- RNA genes miR15 and miR16 at 13q14 in chronic lymphocytic leukemia.* Proc Natl Acad Sci U S A, 2002. **99**(24): p. 15524-9.

250. Calin, G.A., et al., *Human microRNA genes are frequently located at fragile sites and genomic regions involved in cancers.* Proc Natl Acad Sci U S A, 2004. **101**(9): p. 2999-3004.

251. Sevignani, C., et al., *MicroRNA genes are frequently located near mouse cancer susceptibility loci.* Proc Natl Acad Sci U S A, 2007. **104**(19): p. 8017-22.

252. Tagawa, H. and M. Seto, *A microRNA cluster as a target of genomic amplification in malignant lymphoma.* Leukemia, 2005. **19**(11): p. 2013-6.

253. Mavrakis, K.J., et al., *Genome-wide RNA-mediated interference screen identifies miR-19 targets in Notch-induced T-cell acute lymphoblastic leukaemia.* Nat Cell Biol, 2010. **12**(4): p. 372-9.

254. Huse, J.T., et al., *The PTEN-regulating microRNA miR-26a is amplified in high-grade glioma and facilitates gliomagenesis in vivo.* Genes Dev, 2009. **23**(11): p. 1327-37.

255. Zhang, L., et al., *microRNAs exhibit high frequency genomic alterations in human cancer.* Proc Natl Acad Sci U S A, 2006. **103**(24): p. 9136-41.

256. Ryan, B.M., A.I. Robles, and C.C. Harris, *Genetic variation in microRNA networks: the implications for cancer research.* Nat Rev Cancer, 2010. **10**(6): p. 389-402.

257. Yang, R., et al., *Polymorphisms in BRCA2 resulting in aberrant codon-usage and their analysis on familial breast cancer risk.* Breast Cancer Res Treat, 2009. **118**(2): p. 407-13.

258. Jazdzewski, K., et al., *Common SNP in pre-miR-146a decreases mature miR expression and predisposes to papillary thyroid carcinoma.* Proc Natl Acad Sci U S A, 2008. **105**(20): p. 7269-74.

259. Chin, L.J., et al., *A SNP in a let-7 microRNA complementary site in the KRAS 3' untranslated region increases non-small cell lung cancer risk.* Cancer Res, 2008. **68**(20): p. 8535-40.

260. Merritt, W.M., et al., *Dicer, Drosha, and outcomes in patients with ovarian cancer.* N Engl J Med, 2008. **359**(25): p. 2641-50.

261. Chiosea, S., et al., *Overexpression of Dicer in precursor lesions of lung adenocarcinoma.* Cancer Res, 2007. **67**(5): p. 2345-50.

262. Chiosea, S., et al., *Up-regulation of dicer, a component of the MicroRNA machinery, in prostate adenocarcinoma.* Am J Pathol, 2006. **169**(5): p. 1812-20.

263. Egger, G., et al., *Epigenetics in human disease and prospects for epigenetic therapy.* Nature, 2004. **429**(6990): p. 457-63.

264. Lujambio, A. and M. Esteller, *CpG island hypermethylation of tumor suppressor microRNAs in human cancer.* Cell Cycle, 2007. **6**(12): p. 1455-9.

265. Lujambio, A., et al., *Genetic unmasking of an epigenetically silenced microRNA in human cancer cells.* Cancer Res, 2007. **67**(4): p. 1424-9.

266. Lujambio, A. and M. Esteller, *How epigenetics can explain human metastasis: a new role for microRNAs.* Cell Cycle, 2009. **8**(3): p. 377-82.

267. Brueckner, B., et al., *The human let-7a-3 locus contains an epigenetically regulated microRNA gene with oncogenic function.* Cancer Res, 2007. **67**(4): p. 1419-23.

268. Lopez-Serra, L. and M. Esteller, *Proteins that bind methylated DNA and human cancer: reading the wrong words.* Br J Cancer, 2008. **98**(12): p. 1881-5.

269. Hayashita, Y., et al., *A polycistronic microRNA cluster, miR-17-92, is overexpressed in human lung cancers and enhances cell proliferation.* Cancer Res, 2005. **65**(21): p. 9628-32.

270. Takamizawa, J., et al., *Reduced expression of the let-7 microRNAs in human lung cancers in association with shortened postoperative survival.* Cancer Res, 2004. **64**(11): p. 3753-6.

271. Stahlhut Espinosa, C.E. and F.J. Slack, *The role of microRNAs in cancer.* Yale J Biol Med, 2006. **79**(3-4): p. 131-40.

272. Kluiver, J., et al., *BIC and miR-155 are highly expressed in Hodgkin, primary mediastinal and diffuse large B cell lymphomas.* J Pathol, 2005. **207**(2): p. 243-9.

273. Eis, P.S., et al., *Accumulation of miR-155 and BIC RNA in human B cell lymphomas.* Proc Natl Acad Sci U S A, 2005. **102**(10): p. 3627-32.

274. He, H., et al., *The role of microRNA genes in papillary thyroid carcinoma.* Proc Natl Acad Sci U S A, 2005. **102**(52): p. 19075-80.

275. Volinia, S., et al., *A microRNA expression signature of human solid tumors defines cancer gene targets.* Proc Natl Acad Sci U S A, 2006. **103**(7): p. 2257-61.

276. Ciafre, S.A., et al., *Extensive modulation of a set of microRNAs in primary glioblastoma.* Biochem Biophys Res Commun, 2005. **334**(4): p. 1351-8.

277. He, L., et al., *microRNAs join the p53 network--another piece in the tumour-suppression puzzle.* Nat Rev Cancer, 2007. **7**(11): p. 819-22.

278. Michael, M.Z., et al., *Reduced accumulation of specific microRNAs in colorectal neoplasia.* Mol Cancer Res, 2003. **1**(12): p. 882-91.

279. Hurst, D.R., M.D. Edmonds, and D.R. Welch, *Metastamir: the field of metastasis-regulatory microRNA is spreading.* Cancer Res, 2009. **69**(19): p. 7495-8.

280. Hirohashi, S., *Inactivation of the E-cadherin-mediated cell adhesion system in human cancers.* Am J Pathol, 1998. **153**(2): p. 333-9.

281. Iorio, M.V., et al., *MicroRNA gene expression deregulation in human breast cancer.* Cancer Res, 2005. **65**(16): p. 7065-70.

282. Hood, J.D. and D.A. Cheresh, *Role of integrins in cell invasion and migration.* Nat Rev Cancer, 2002. **2**(2): p. 91-100.

283. Yanaihara, N., et al., *Unique microRNA molecular profiles in lung cancer diagnosis and prognosis.* Cancer Cell, 2006. **9**(3): p. 189-98.

284. Lim, L.P., et al., *Microarray analysis shows that some microRNAs downregulate large numbers of target mRNAs.* Nature, 2005. **433**(7027): p. 769-73.

285. Dalmay, T. and D.R. Edwards, *MicroRNAs and the hallmarks of cancer.* Oncogene, 2006. **25**(46): p. 6170-5.

286. Baker, A.H., D.R. Edwards, and G. Murphy, *Metalloproteinase inhibitors: biological actions and therapeutic opportunities.* J Cell Sci, 2002. **115**(Pt 19): p. 3719-27.

287. Qi, J.H., et al., *A novel function for tissue inhibitor of metalloproteinases-3 (TIMP3): inhibition of angiogenesis by blockage of VEGF binding to VEGF receptor-2.* Nat Med, 2003. **9**(4): p. 407-15.

288. Chan, J.A., A.M. Krichevsky, and K.S. Kosik, *MicroRNA-21 is an antiapoptotic factor in human glioblastoma cells.* Cancer Res, 2005. **65**(14): p. 6029-33.

289. Bernstein, E., et al., *Dicer is essential for mouse development.* Nat Genet, 2003. **35**(3): p. 215-7.

290. Wienholds, E., et al., *The microRNA-producing enzyme Dicer1 is essential for zebrafish development.* Nat Genet, 2003. **35**(3): p. 217-8.

291. Shcherbata, H.R., et al., *The MicroRNA pathway plays a regulatory role in stem cell division.* Cell Cycle, 2006. **5**(2): p. 172-5.

292. Calin, G.A., et al., *MicroRNA profiling reveals distinct signatures in B cell chronic lymphocytic leukemias.* Proc Natl Acad Sci U S A, 2004. **101**(32): p. 11755-60.

293. Calin, G.A., et al., *A MicroRNA signature associated with prognosis and progression in chronic lymphocytic leukemia.* N Engl J Med, 2005. **353**(17): p. 1793-801.

294. Metzler, M., et al., *High expression of precursor microRNA-155/BIC RNA in children with Burkitt lymphoma.* Genes Chromosomes Cancer, 2004. **39**(2): p. 167-9.

295. Calin, G.A. and C.M. Croce, *MicroRNA signatures in human cancers.* Nat Rev Cancer, 2006. **6**(11): p. 857-66.

296. Blenkiron, C. and E.A. Miska, *miRNAs in cancer: approaches, aetiology, diagnostics and therapy.* Hum Mol Genet, 2007. **16 Spec No 1**: p. R106-13.

297. Hoshida, Y., et al., *Gene expression in fixed tissues and outcome in hepatocellular carcinoma.* N Engl J Med, 2008. **359**(19): p. 1995-2004.

298. Lawrie, C.H., et al., *Detection of elevated levels of tumour-associated microRNAs in serum of patients with diffuse large B-cell lymphoma.* Br J Haematol, 2008. **141**(5): p. 672-5.

299. Mitchell, P.S., et al., *Circulating microRNAs as stable blood-based markers for cancer detection.* Proc Natl Acad Sci U S A, 2008. **105**(30): p. 10513-8.

300. Schetter, A.J., et al., *MicroRNA expression profiles associated with prognosis and therapeutic outcome in colon adenocarcinoma.* JAMA, 2008. **299**(4): p. 425-36.

301. Jiang, J., et al., *Association of MicroRNA expression in hepatocellular carcinomas with hepatitis infection, cirrhosis, and patient survival.* Clin Cancer Res, 2008. **14**(2): p. 419-27.

302. Ji, J., et al., *MicroRNA expression, survival, and response to interferon in liver cancer.* N Engl J Med, 2009. **361**(15): p. 1437-47.

303. Si, M.L., et al., *miR-21-mediated tumor growth.* Oncogene, 2007. **26**(19): p. 2799-803.

304. Ebert, M.S., J.R. Neilson, and P.A. Sharp, *MicroRNA sponges: competitive inhibitors of small RNAs in mammalian cells.* Nat Methods, 2007. **4**(9): p. 721-6.

305. Chung, K.H., et al., *Polycistronic RNA polymerase II expression vectors for RNA interference based on BIC/miR-155.* Nucleic Acids Res, 2006. **34**(7): p. e53.

306. Stegmeier, F., et al., *A lentiviral microRNA-based system for single-copy polymerase II-regulated RNA interference in mammalian cells.* Proc Natl Acad Sci U S A, 2005. **102**(37): p. 13212-7.

307. Kota, J., et al., *Therapeutic microRNA delivery suppresses tumorigenesis in a murine liver cancer model.* Cell, 2009. **137**(6): p. 1005-17.

308. Bhardwaj, A., S. Singh, and A.P. Singh, *MicroRNA-based Cancer Therapeutics: Big Hope from Small RNAs.* Mol Cell Pharmacol, 2011. **2**(5): p. 213-219.

309. Cochrane, D.R., et al., *MicroRNA-200c mitigates invasiveness and restores sensitivity to microtubule-targeting chemotherapeutic agents.* Mol Cancer Ther, 2009. **8**(5): p. 1055-66.

310. Weidhaas, J.B., et al., *MicroRNAs as potential agents to alter resistance to cytotoxic anticancer therapy.* Cancer Res, 2007. **67**(23): p. 11111-6.

311. Xi, Y., et al., *Systematic analysis of microRNA expression of RNA extracted from fresh frozen and formalin-fixed paraffin-embedded samples.* RNA, 2007. **13**(10): p. 1668-74.

312. Li, J., et al., *Comparison of miRNA expression patterns using total RNA extracted from matched samples of formalin-fixed paraffin-embedded (FFPE) cells and snap frozen cells.* BMC Biotechnol, 2007. **7**: p. 36.

313. Lu, J., et al., *MicroRNA expression profiles classify human cancers.* Nature, 2005. **435**(7043): p. 834-8.

314. Gray-Schopfer, V.C., et al., *Cellular senescence in naevi and immortalisation in melanoma: a role for p16?* Br J Cancer, 2006. **95**(4): p. 496-505.

315. Langdon, S.P., et al., *Characterization and properties of nine human ovarian adenocarcinoma cell lines.* Cancer Res, 1988. **48**(21): p. 6166-72.

316. *User Bulletin #2--ABI PRISM 7700 Sequence Detection System*.

317. Towbin, H., T. Staehelin, and J. Gordon, *Electrophoretic transfer of proteins from polyacrylamide gels to nitrocellulose sheets: procedure and some applications.* Proc Natl Acad Sci U S A, 1979. **76**(9): p. 4350-4.

318. *Ambion TechNotes 12 (1) Optimizing siRNA for RNAi*.

319. Hennigan, R.F., K.L. Hawker, and B.W. Ozanne, *Fos-transformation activates genes associated with invasion.* Oncogene, 1994. **9**(12): p. 3591-600.

320. Scott, L.A., et al., *Invasion of normal human fibroblasts induced by v-Fos is independent of proliferation, immortalization, and the tumor suppressors p16INK4a and p53.* Mol Cell Biol, 2004. **24**(4): p. 1540-59.

321. Neumann, H.A., G.W. Lohr, and A.A. Fauser, *Tumor colony formation from human spontaneous tumors in a methylcellulose monolayer system.* Res Exp Med (Berl), 1984. **184**(3): p. 137-43.

322. Rosenfeld, N., et al., *MicroRNAs accurately identify cancer tissue origin.* Nat Biotechnol, 2008. **26**(4): p. 462-9.

323. Bargaje, R., et al., *Consensus miRNA expression profiles derived from interplatform normalization of microarray data.* RNA, 2010. **16**(1): p. 16-25.

324. Dahiya, N., et al., *MicroRNA expression and identification of putative miRNA targets in ovarian cancer.* PLoS One, 2008. **3**(6): p. e2436.

325. Gaur, A., et al., *Characterization of microRNA expression levels and their biological correlates in human cancer cell lines.* Cancer Res, 2007. **67**(6): p. 2456-68.

326. Blower, P.E., et al., *MicroRNA expression profiles for the NCI-60 cancer cell panel.* Mol Cancer Ther, 2007. **6**(5): p. 1483-91.

327. Mueller, D.W., M. Rehli, and A.K. Bosserhoff, *miRNA expression profiling in melanocytes and melanoma cell lines reveals miRNAs associated with formation and progression of malignant melanoma.* J Invest Dermatol, 2009. **129**(7): p. 1740-51.

328. *Illumina miRNA Expression Profiling Version2 panel guide*, Illumina.

329. Fan, J.B., et al., *A versatile assay for high-throughput gene expression profiling on universal array matrices.* Genome Res, 2004. **14**(5): p. 878-85.

330. Berezikov, E., et al., *Many novel mammalian microRNA candidates identified by extensive cloning and RAKE analysis.* Genome Res, 2006. **16**(10): p. 1289-98.

331. Berezikov, E., et al., *Diversity of microRNAs in human and chimpanzee brain.* Nat Genet, 2006. **38**(12): p. 1375-7.

332. Chen, J., et al., *Highly sensitive and specific microRNA expression profiling using BeadArray technology.* Nucleic Acids Res, 2008. **36**(14): p. e87.

333. Zhang, W., J.E. Dahlberg, and W. Tam, *MicroRNAs in tumorigenesis: a primer.* Am J Pathol, 2007. **171**(3): p. 728-38.

334. Molnar, V., et al., *Changes in miRNA expression in solid tumors: an miRNA profiling in melanomas.* Semin Cancer Biol, 2008. **18**(2): p. 111-22.

335. Castoldi, M., et al., *A sensitive array for microRNA expression profiling (miChip) based on locked nucleic acids (LNA).* RNA, 2006. **12**(5): p. 913-20.

336. *TaqMan MicroRNA Assay protocol*.

337. Nelson, P.T., et al., *Microarray-based, high-throughput gene expression profiling of microRNAs.* Nat Methods, 2004. **1**(2): p. 155-61.

338. Szafranska, A.E., et al., *Accurate molecular characterization of formalin-fixed, paraffin-embedded tissues by microRNA expression profiling.* J Mol Diagn, 2008. **10**(5): p. 415-23.

339. Glud, M., et al., *MicroRNA expression in melanocytic nevi: the usefulness of formalin-fixed, paraffin-embedded material for miRNA microarray profiling.* J Invest Dermatol, 2009. **129**(5): p. 1219-24.

340. Massi, G., *Melanocytic nevi simulant of melanoma with medicolegal relevance.* Virchows Arch, 2007. **451**(3): p. 623-47.

341. Elder, D.E., *Precursors to melanoma and their mimics: nevi of special sites.* Mod Pathol, 2006. **19 Suppl 2**: p. S4-20.

342. Blokx, W.A., M.C. van Dijk, and D.J. Ruiter, *Molecular cytogenetics of cutaneous melanocytic lesions - diagnostic, prognostic and therapeutic aspects.* Histopathology, 2010. **56**(1): p. 121-32.

343. Schultz, J., et al., *MicroRNA let-7b targets important cell cycle molecules in malignant melanoma cells and interferes with anchorage-independent growth.* Cell Res, 2008. **18**(5): p. 549-57.

344. Worley, L.A., et al., *Micro-RNAs associated with metastasis in uveal melanoma identified by multiplexed microarray profiling.* Melanoma Res, 2008. **18**(3): p. 184-90.

345. Bemis, L.T., et al., *MicroRNA-137 targets microphthalmia-associated transcription factor in melanoma cell lines.* Cancer Res, 2008. **68**(5): p. 1362-8.

346. *MicroRNA Expression Profiling Assay guide*, Illumina.

347. *A Comparison of Normalization Techniques for MicroRNA Microarray Data*. 2008, Berkeley electronic press.

348. Baskerville, S. and D.P. Bartel, *Microarray profiling of microRNAs reveals frequent coexpression with neighboring miRNAs and host genes.* RNA, 2005. **11**(3): p. 241-7.

349. Farh, K.K., et al., *The widespread impact of mammalian MicroRNAs on mRNA repression and evolution.* Science, 2005. **310**(5755): p. 1817-21.

350. Landgraf, P., et al., *A mammalian microRNA expression atlas based on small RNA library sequencing.* Cell, 2007. **129**(7): p. 1401-14.

351. He, L., et al., *A microRNA polycistron as a potential human oncogene.* Nature, 2005. **435**(7043): p. 828-33.

352. Git, A., et al., *Systematic comparison of microarray profiling, real-time PCR, and next-generation sequencing technologies for measuring differential microRNA expression.* RNA, 2010. **16**(5): p. 991-1006.

353. Wightman, B., I. Ha, and G. Ruvkun, *Posttranscriptional regulation of the heterochronic gene lin-14 by lin-4 mediates temporal pattern formation in C. elegans.* Cell, 1993. **75**(5): p. 855-62.

354. *Endogenous Controls for Real-Time Quantitation of miRNA Using TaqMan® MicroRNA Assays*. 2008/2010, Applied Biosystems.

355. Drakaki, A. and D. Iliopoulos, *MicroRNA Gene Networks in Oncogenesis.* Curr Genomics, 2009. **10**(1): p. 35-41.

356. Tong, A.W., et al., *MicroRNA profile analysis of human prostate cancers.* Cancer Gene Ther, 2009. **16**(3): p. 206-16.

357. Segura, M.F., et al., *Melanoma MicroRNA signature predicts post-recurrence survival.* Clin Cancer Res, 2010. **16**(5): p. 1577-86.

358. Caramuta, S., et al., *MicroRNA expression profiles associated with mutational status and survival in malignant melanoma.* J Invest Dermatol, 2010. **130**(8): p. 2062-70.

359. Friedman, R.C., et al., *Most mammalian mRNAs are conserved targets of microRNAs.* Genome Res, 2009. **19**(1): p. 92-105.

360. Krutzfeldt, J. and M. Stoffel, *MicroRNAs: a new class of regulatory genes affecting metabolism.* Cell Metab, 2006. **4**(1): p. 9-12.

361. Bueno, M.J., I. Perez de Castro, and M. Malumbres, *Control of cell proliferation pathways by microRNAs.* Cell Cycle, 2008. **7**(20): p. 3143-8.

362. Jovanovic, M. and M.O. Hengartner, *miRNAs and apoptosis: RNAs to die for.* Oncogene, 2006. **25**(46): p. 6176-87.

363. Stefani, G. and F.J. Slack, *Small non-coding RNAs in animal development.* Nat Rev Mol Cell Biol, 2008. **9**(3): p. 219-30.

364. He, X., J.K. Eberhart, and J.H. Postlethwait, *MicroRNAs and micromanaging the skeleton in disease, development and evolution.* J Cell Mol Med, 2009. **13**(4): p. 606-18.

365. Shi, L., et al., *The MicroArray Quality Control (MAQC) project shows inter- and intraplatform reproducibility of gene expression measurements.* Nat Biotechnol, 2006. **24**(9): p. 1151-61.

366. Khew-Goodall, Y. and G.J. Goodall, *Myc-modulated miR-9 makes more metastases.* Nat Cell Biol, 2010. **12**(3): p. 209-11.

367. Kong, W., et al., *MicroRNA-155 regulates cell survival, growth, and chemosensitivity by targeting FOXO3a in breast cancer.* J Biol Chem, 2010. **285**(23): p. 17869-79.

368. Shimizu, S., et al., *The let-7 family of microRNAs inhibits Bcl-xL expression and potentiates sorafenib-induced apoptosis in human hepatocellular carcinoma.* J Hepatol, 2010. **52**(5): p. 698-704.

369. Wang, Y., et al., *Profiling microRNA expression in hepatocellular carcinoma reveals microRNA-224 up-regulation and apoptosis inhibitor-5 as a microRNA-224-specific target.* J Biol Chem, 2008. **283**(19): p. 13205-15.

370. Chen, J., et al., *MicroRNA-193b represses cell proliferation and regulates cyclin D1 in melanoma.* Am J Pathol, 2010. **176**(5): p. 2520-9.

371. Philippidou, D., et al., *Signatures of microRNAs and selected microRNA target genes in human melanoma.* Cancer Res, 2010. **70**(10): p. 4163-73.

372. Kong, D., et al., *miR-200 regulates PDGF-D-mediated epithelial-mesenchymal transition, adhesion, and invasion of prostate cancer cells.* Stem Cells, 2009. **27**(8): p. 1712-21.

373. Korpal, M. and Y. Kang, *The emerging role of miR-200 family of microRNAs in epithelial-mesenchymal transition and cancer metastasis.* RNA Biol, 2008. **5**(3): p. 115-9.

374. Gregory, P.A., et al., *MicroRNAs as regulators of epithelial-mesenchymal transition.* Cell Cycle, 2008. **7**(20): p. 3112-8.

375. Viticchie, G., et al., *MiR-203 controls proliferation, migration and invasive potential of prostate cancer cell lines.* Cell Cycle, 2011. **10**(7): p. 1121-31.

376. Bo, J., et al., *microRNA-203 suppresses bladder cancer development by repressing bcl-w expression.* FEBS J, 2011. **278**(5): p. 786-92.

377. Chiang, Y., et al., *Aberrant expression of miR-203 and its clinical significance in gastric and colorectal cancers.* J Gastrointest Surg, 2011. **15**(1): p. 63-70.

378. Li, J., et al., *miR-203 reverses chemoresistance in p53-mutated colon cancer cells through downregulation of Akt2 expression.* Cancer Lett, 2011. **304**(1): p. 52-9.

379. Sun, Y., et al., *Expression profile of microRNAs in c-Myc induced mouse mammary tumors.* Breast Cancer Res Treat, 2009. **118**(1): p. 185-96.

380. Tsang, W.P., et al., *Oncofetal H19-derived miR-675 regulates tumor suppressor RB in human colorectal cancer.* Carcinogenesis, 2010. **31**(3): p. 350-8.

381. Mazar, J., et al., *The regulation of miRNA-211 expression and its role in melanoma cell invasiveness.* PLoS One, 2010. **5**(11): p. e13779.

382. Levy, C., et al., *Intronic miR-211 assumes the tumor suppressive function of its host gene in melanoma.* Mol Cell, 2010. **40**(5): p. 841-9.

383. Boyle, G.M., et al., *Melanoma cell invasiveness is regulated by miR-211 suppression of the BRN2 transcription factor.* Pigment Cell Melanoma Res, 2011. **24**(3): p. 525-537.

384. Chang, K.W., et al., *Association between high miR-211 microRNA expression and the poor prognosis of oral carcinoma.* J Dent Res, 2008. **87**(11): p. 1063-8.

385. Segura, M.F., et al., *Aberrant miR-182 expression promotes melanoma metastasis by repressing FOXO3 and microphthalmia-associated transcription factor.* Proc Natl Acad Sci U S A, 2009. **106**(6): p. 1814-9.

386. Sherr, C.J. and J.M. Roberts, *CDK inhibitors: positive and negative regulators of G1-phase progression.* Genes Dev, 1999. **13**(12): p. 1501-12.

387. Kim, Y.K., et al., *Functional links between clustered microRNAs: suppression of cell-cycle inhibitors by microRNA clusters in gastric cancer.* Nucleic Acids Res, 2009. **37**(5): p. 1672-81.

388. Xia, L., et al., *miR-15b and miR-16 modulate multidrug resistance by targeting BCL2 in human gastric cancer cells.* Int J Cancer, 2008. **123**(2): p. 372-9.

389. Zhu, W., et al., *miR-181b modulates multidrug resistance by targeting BCL2 in human cancer cell lines.* Int J Cancer, 2010. **127**(11): p. 2520-9.

390. Liu, A.M., R.T. Poon, and J.M. Luk, *MicroRNA-375 targets Hippo-signaling effector YAP in liver cancer and inhibits tumor properties.* Biochem Biophys Res Commun, 2010. **394**(3): p. 623-7.

391. Gramantieri, L., et al., *Cyclin G1 is a target of miR-122a, a microRNA frequently down-regulated in human hepatocellular carcinoma.* Cancer Res, 2007. **67**(13): p. 6092-9.

392. Fornari, F., et al., *MiR-122/cyclin G1 interaction modulates p53 activity and affects doxorubicin sensitivity of human hepatocarcinoma cells.* Cancer Res, 2009. **69**(14): p. 5761-7.

393. Ivanovska, I., et al., *MicroRNAs in the miR-106b family regulate p21/CDKN1A and promote cell cycle progression.* Mol Cell Biol, 2008. **28**(7): p. 2167-74.

394. le Sage, C., et al., *Regulation of the p27(Kip1) tumor suppressor by miR-221 and miR-222 promotes cancer cell proliferation.* EMBO J, 2007. **26**(15): p. 3699-708.

395. Fornari, F., et al., *MiR-221 controls CDKN1C/p57 and CDKN1B/p27 expression in human hepatocellular carcinoma.* Oncogene, 2008. **27**(43): p. 5651-61.

396. Huang, S. and X. He, *The role of microRNAs in liver cancer progression.* Br J Cancer, 2011. **104**(2): p. 235-40.

397. Eccles, S.A. and D.R. Welch, *Metastasis: recent discoveries and novel treatment strategies.* Lancet, 2007. **369**(9574): p. 1742-57.

398. Ma, L., J. Teruya-Feldstein, and R.A. Weinberg, *Tumour invasion and metastasis initiated by microRNA-10b in breast cancer.* Nature, 2007. **449**(7163): p. 682-8.

399. Gregory, P.A., et al., *The miR-200 family and miR-205 regulate epithelial to mesenchymal transition by targeting ZEB1 and SIP1.* Nat Cell Biol, 2008. **10**(5): p. 593-601.

400. Korpal, M., et al., *The miR-200 family inhibits epithelial-mesenchymal transition and cancer cell migration by direct targeting of E-cadherin transcriptional repressors ZEB1 and ZEB2.* J Biol Chem, 2008. **283**(22): p. 14910-4.

401. Bracken, C.P., et al., *A double-negative feedback loop between ZEB1-SIP1 and the microRNA-200 family regulates epithelial-mesenchymal transition.* Cancer Res, 2008. **68**(19): p. 7846-54.

402. Hurteau, G.J., et al., *Overexpression of the microRNA hsa-miR-200c leads to reduced expression of transcription factor 8 and increased expression of E-cadherin.* Cancer Res, 2007. **67**(17): p. 7972-6.

403. Burk, U., et al., *A reciprocal repression between ZEB1 and members of the miR-200 family promotes EMT and invasion in cancer cells.* EMBO Rep, 2008. **9**(6): p. 582-9.

404. Park, S.M., et al., *The miR-200 family determines the epithelial phenotype of cancer cells by targeting the E-cadherin repressors ZEB1 and ZEB2.* Genes Dev, 2008. **22**(7): p. 894-907.

405. Savagner, P., *Leaving the neighborhood: molecular mechanisms involved during epithelial-mesenchymal transition.* Bioessays, 2001. **23**(10): p. 912-23.

406. Fuchs, I.B., et al., *The prognostic significance of epithelial-mesenchymal transition in breast cancer.* Anticancer Res, 2002. **22**(6A): p. 3415-9.

407. Eger, A., et al., *DeltaEF1 is a transcriptional repressor of E-cadherin and regulates epithelial plasticity in breast cancer cells.* Oncogene, 2005. **24**(14): p. 2375-85.

408. Comijn, J., et al., *The two-handed E box binding zinc finger protein SIP1 downregulates E-cadherin and induces invasion.* Mol Cell, 2001. **7**(6): p. 1267-78.

409. Shirakihara, T., M. Saitoh, and K. Miyazono, *Differential regulation of epithelial and mesenchymal markers by deltaEF1 proteins in epithelial mesenchymal transition induced by TGF-beta.* Mol Biol Cell, 2007. **18**(9): p. 3533-44.

410. Ross, D.T., et al., *Systematic variation in gene expression patterns in human cancer cell lines.* Nat Genet, 2000. **24**(3): p. 227-35.

411. Moretti, S., et al., *Immunohistochemical evidence of cytokine networks during progression of human melanocytic lesions.* Int J Cancer, 1999. **84**(2): p. 160-8.

412. Herlyn, M., et al., *Lessons from melanocyte development for understanding the biological events in naevus and melanoma formation.* Melanoma Res, 2000. **10**(4): p. 303-12.

413. Kuphal, S. and A.K. Bosserhoff, *Influence of the cytoplasmic domain of E-cadherin on endogenous N-cadherin expression in malignant melanoma.* Oncogene, 2006. **25**(2): p. 248-59.

414. Alonso, S.R., et al., *A high-throughput study in melanoma identifies epithelial-mesenchymal transition as a major determinant of metastasis.* Cancer Res, 2007. **67**(7): p. 3450-60.

415. Shimoyama, Y., et al., *Identification of three human type-II classic cadherins and frequent heterophilic interactions between different subclasses of type-II classic cadherins.* Biochem J, 2000. **349**(Pt 1): p. 159-67.

416. Tang, A., et al., *E-cadherin is the major mediator of human melanocyte adhesion to keratinocytes in vitro.* J Cell Sci, 1994. **107 (Pt 4)**: p. 983-92.

417. Mikesh, L.M., et al., *Evaluation of molecular markers of mesenchymal phenotype in melanoma.* Melanoma Res, 2010. **20**(6): p. 485-95.

418. Seve, P. and C. Dumontet, *Chemoresistance in non-small cell lung cancer.* Curr Med Chem Anticancer Agents, 2005. **5**(1): p. 73-88.

419. Ceppi, P., et al., *Loss of miR-200c expression induces an aggressive, invasive, and chemoresistant phenotype in non-small cell lung cancer.* Mol Cancer Res, 2010. **8**(9): p. 1207-16.

420. Gandellini, P., et al., *miR-205 Exerts tumor-suppressive functions in human prostate through down-regulation of protein kinase Cepsilon.* Cancer Res, 2009. **69**(6): p. 2287-95.

421. Sanz-Moreno, V., et al., *Rac activation and inactivation control plasticity of tumor cell movement.* Cell, 2008. **135**(3): p. 510-23.

422. Pinner, S. and E. Sahai, *PDK1 regulates cancer cell motility by antagonising inhibition of ROCK1 by RhoE.* Nat Cell Biol, 2008. **10**(2): p. 127-37.

423. Sahai, E. and C.J. Marshall, *Differing modes of tumour cell invasion have distinct requirements for Rho/ROCK signalling and extracellular proteolysis.* Nat Cell Biol, 2003. **5**(8): p. 711-9.

424. Wolf, K., et al., *Compensation mechanism in tumor cell migration: mesenchymal-amoeboid transition after blocking of pericellular proteolysis.* J Cell Biol, 2003. **160**(2): p. 267-77.

425. Elson-Schwab, I., A. Lorentzen, and C.J. Marshall, *MicroRNA-200 family members differentially regulate morphological plasticity and mode of melanoma cell invasion.* PLoS One, 2010. **5**(10).

426. Hamano, R., et al., *Overexpression of miR-200c Induces Chemoresistance in Esophageal Cancers Mediated Through Activation of the Akt Signaling Pathway.* Clin Cancer Res, 2011. **17**(9): p. 3029-38.

427. Dar, A.A., et al., *miRNA-205 Suppresses Melanoma Cell Proliferation and Induces Senescence via Regulation of E2F1 Protein.* J Biol Chem, 2011. **286**(19): p. 16606-14.

428. Bloch, M., et al., *KCNMA1 gene amplification promotes tumor cell proliferation in human prostate cancer.* Oncogene, 2007. **26**(17): p. 2525-34.

429. Aubert, B., et al., *Observation of a new Ds meson decaying to DK at a mass of 2.86 GeV/c2.* Phys Rev Lett, 2006. **97**(22): p. 222001.

430. Gyorffy, B., et al., *Analysis of gene expression profiles in melanoma cells with acquired resistance against antineoplastic drugs.* Melanoma Res, 2006. **16**(2): p. 147-55.

431. Landais, S., et al., *Oncogenic potential of the miR-106-363 cluster and its implication in human T-cell leukemia.* Cancer Res, 2007. **67**(12): p. 5699-707.

432. Lei, Z., et al., *Regulation of HIF-1alpha and VEGF by miR-20b tunes tumor cells to adapt to the alteration of oxygen concentration.* PLoS One, 2009. **4**(10): p. e7629.

433. Hua, Z., et al., *MiRNA-directed regulation of VEGF and other angiogenic factors under hypoxia.* PLoS One, 2006. **1**: p. e116.

434. Forsythe, J.A., et al., *Activation of vascular endothelial growth factor gene transcription by hypoxia-inducible factor 1.* Mol Cell Biol, 1996. **16**(9): p. 4604-13.

435. Slominski, A., et al., *Melanin pigmentation in mammalian skin and its hormonal regulation.* Physiol Rev, 2004. **84**(4): p. 1155-228.

436. Slominski, A. and J. Pawelek, *Animals under the sun: effects of ultraviolet radiation on mammalian skin.* Clin Dermatol, 1998. **16**(4): p. 503-15.

437. Agar, N.S., et al., *The basal layer in human squamous tumors harbors more UVA than UVB fingerprint mutations: a role for UVA in human skin carcinogenesis.* Proc Natl Acad Sci U S A, 2004. **101**(14): p. 4954-9.

438. Zhang, H. and I. Rosdahl, *Ultraviolet A and B differently induce intracellular protein expression in human skin melanocytes--a speculation of separate pathways in initiation of melanoma.* Carcinogenesis, 2003. **24**(12): p. 1929-34.

439. Gray-Schopfer, V.C., et al., *Tumor necrosis factor-alpha blocks apoptosis in melanoma cells when BRAF signaling is inhibited.* Cancer Res, 2007. **67**(1): p. 122-9.

440. Emuss, V., et al., *Mutations of C-RAF are rare in human cancer because C-RAF has a low basal kinase activity compared with B-RAF.* Cancer Res, 2005. **65**(21): p. 9719-26.

441. Lee, J.W., et al., *Mutational analysis of the ARAF gene in human cancers.* APMIS, 2005. **113**(1): p. 54-7.

442. Zebisch, A., et al., *Two transforming C-RAF germ-line mutations identified in patients with therapy-related acute myeloid leukemia.* Cancer Res, 2006. **66**(7): p. 3401-8.

443. McPhillips, F., et al., *Raf-1 is the predominant Raf isoform that mediates growth factor-stimulated growth in ovarian cancer cells.* Carcinogenesis, 2006. **27**(4): p. 729-39.

444. Willmore-Payne, C., et al., *Human malignant melanoma: detection of BRAF- and c-kit-activating mutations by high-resolution amplicon melting analysis.* Hum Pathol, 2005. **36**(5): p. 486-93.

445. Willmore-Payne, C., et al., *BRAF and c-kit gene copy number in mutation-positive malignant melanoma.* Hum Pathol, 2006. **37**(5): p. 520-7.

446. Errico, M.E., et al., *Expression of cyclin-D1 in uveal malignant melanoma.* Anticancer Res, 2003. **23**(3B): p. 2701-6.

447. Curtin, J.A., et al., *Distinct sets of genetic alterations in melanoma.* N Engl J Med, 2005. **353**(20): p. 2135-47.

448. Anna, B., et al., *Mechanism of UV-related carcinogenesis and its contribution to nevi/melanoma.* Expert Rev Dermatol, 2007. **2**(4): p. 451-469.

449. Maldonado, J.L., et al., *Determinants of BRAF mutations in primary melanomas.* J Natl Cancer Inst, 2003. **95**(24): p. 1878-90.

450. Thomas, N.E., et al., *Number of nevi and early-life ambient UV exposure are associated with BRAF-mutant melanoma.* Cancer Epidemiol Biomarkers Prev, 2007. **16**(5): p. 991-7.

451. Calipel, A., et al., *Mutation of B-Raf in human choroidal melanoma cells mediates cell proliferation and transformation through the MEK/ERK pathway.* J Biol Chem, 2003. **278**(43): p. 42409-18.

452. Hingorani, S.R., et al., *Suppression of BRAF(V599E) in human melanoma abrogates transformation.* Cancer Res, 2003. **63**(17): p. 5198-202.

453. Brummer, T., et al., *Functional analysis of the regulatory requirements of B-Raf and the B-Raf(V600E) oncoprotein.* Oncogene, 2006. **25**(47): p. 6262-76.

454. Weyers, W., et al., *Classification of cutaneous malignant melanoma: a reassessment of histopathologic criteria for the distinction of different types.* Cancer, 1999. **86**(2): p. 288-99.

455. Viros, A., et al., *Improving melanoma classification by integrating genetic and morphologic features.* PLoS Med, 2008. **5**(6): p. e120.

456. Hayashida, N., et al., *A rapid and simple detection method for the BRAF(T1796A) mutation in fine-needle aspirated thyroid carcinoma cells.* Thyroid, 2004. **14**(11): p. 910-5.

457. Bauer, J., et al., *BRAF mutations in cutaneous melanoma are independently associated with age, anatomic site of the primary tumor, and the degree of solar elastosis at the primary tumor site.* Pigment Cell Melanoma Res, 2011. **24**(2): p. 345-51.

458. Thomas, N.E., M. Berwick, and M. Cordeiro-Stone, *Could BRAF mutations in melanocytic lesions arise from DNA damage induced by ultraviolet radiation?* J Invest Dermatol, 2006. **126**(8): p. 1693-6.

459. Landi, M.T., et al., *MC1R germline variants confer risk for BRAF-mutant melanoma.* Science, 2006. **313**(5786): p. 521-2.

460. Pollock, P.M., et al., *High frequency of BRAF mutations in nevi.* Nat Genet, 2003. **33**(1): p. 19-20.

461. Uribe, P., Wistuba, II, and S. Gonzalez, *BRAF mutation: a frequent event in benign, atypical, and malignant melanocytic lesions of the skin.* Am J Dermatopathol, 2003. **25**(5): p. 365-70.

462. Liu, W., et al., *Distinct clinical and pathological features are associated with the BRAF(T1799A(V600E)) mutation in primary melanoma.* J Invest Dermatol, 2007. **127**(4): p. 900-5.

463. Akslen, L.A., et al., *BRAF and NRAS mutations are frequent in nodular melanoma but are not associated with tumor cell proliferation or patient survival.* J Invest Dermatol, 2005. **125**(2): p. 312-7.

464. Lang, J. and R.M. MacKie, *Prevalence of exon 15 BRAF mutations in primary melanoma of the superficial spreading, nodular, acral, and lentigo maligna subtypes.* J Invest Dermatol, 2005. **125**(3): p. 575-9.

465. Papp, T., et al., *Mutational analysis of the BRAF gene in human congenital and dysplastic melanocytic naevi.* Melanoma Res, 2005. **15**(5): p. 401-7.

466. Saldanha, G., et al., *Cutaneous melanoma subtypes show different BRAF and NRAS mutation frequencies.* Clin Cancer Res, 2006. **12**(15): p. 4499-505.

467. Chapman, P.B., et al., *Improved survival with vemurafenib in melanoma with BRAF V600E mutation.* N Engl J Med. **364**(26): p. 2507-16.

468. Nuovo, G.J., et al., *A methodology for the combined in situ analyses of the precursor and mature forms of microRNAs and correlation with their putative targets.* Nat Protoc, 2009. **4**(1): p. 107-15.

469. Wiklund, E.D., et al., *Coordinated epigenetic repression of the miR-200 family and miR-205 in invasive bladder cancer.* Int J Cancer, 2011. **128**(6): p. 1327-34.

470. Weber, J.A., et al., *The microRNA spectrum in 12 body fluids.* Clin Chem, 2010. **56**(11): p. 1733-41.

471. Edward R. Sauter, N.P., *Body fluid micro(mi)RNAs as biomarkers for human cancer*. 2011, Journal of Nucleic Acids Investigation

Appendix 1

(A)

Naevus ID	Yield (ng)	260/280 Ratio
67955	1287	1.90
70975	996	1.78
67936	2176	1.91
68519	2838	2.06
68641	2285	2.02
59981	5748	2.06
68554	512	1.58
68555	698	1.88
67773	775	2.00
68623	944	1.85
64554	1350	1.59
64337	1453	1.82
64403	1215	1.88
64196	1361	1.90
64240	1876	1.85
64878	2967	1.91
64880	1148	1.81
64442	1576	1.88

(B)

Primary ID		Yield (ng)	260/280 Ratio
Non	RG1	818	2.06
	RG2	1973	2.03
	RG3	2185	2.03
	RG4	1831	2.03
	RG5	727	2.02
	RG6	1167	2.08
	RG7	2305	1.87
	RG8	1822	2.05
	RG9	1275	1.97
	RG10	1162	1.96
Re	RG11	1916	2.07
	RG12	1949	2.04
	RG13	1224	2.00
	RG14	1403	2.00
	RG15	567	2.07
	RG16	1647	2.06
	RG17	2169	2.01
	RG18	1633	2.06

	RG19	2188	2.07
	RG20	1768	2.05

(C)

Metastatic ID	Yield (ng)	260/280 Ratio
07117	2297	2.00
M4	6008	1.91
M5	5428	2.02
M6	1670	2.04
M7	1133	2.01
M11	1190	1.82
M17	2407	2.01
M29	5607	2.04
M31	1612	1.89
M33	657.5	1.75
M34	4915	1.96
M36	4970	1.96
M38	833	1.86
M39	690	1.59
M41	1185	1.94
M42	1340	1.73
M44	2095	1.98
M48	4050	1.96
M53	2608	1.78
M54	2020	1.93
M57	1423	1.93

(D)

Other naevus ID	Yield (ng)	260/280 Ratio
Blue-07619	350	1.98
Blue-03401	216	1.76
Blue-03390	484	1.73
Blue-18434	359	1.88
Spitz-08007	437	1.59
Spitz-27937	1563	1.75
Dysplastic-14013	1381	1.71
Dysplastic-14568	1116	1.73

The FFPE samples used in microarray and qPCR. The four tables list the yields and 260/280 ratios of all FFPE tissues: (A) Naevi; (B) Primary melanomas (Non: non-recurrent melanoma, Re: recurrent primary melanoma); (C) Metastatic melanomas; (D) Blues, spitz and dysplastic naevi.

Appendix 2

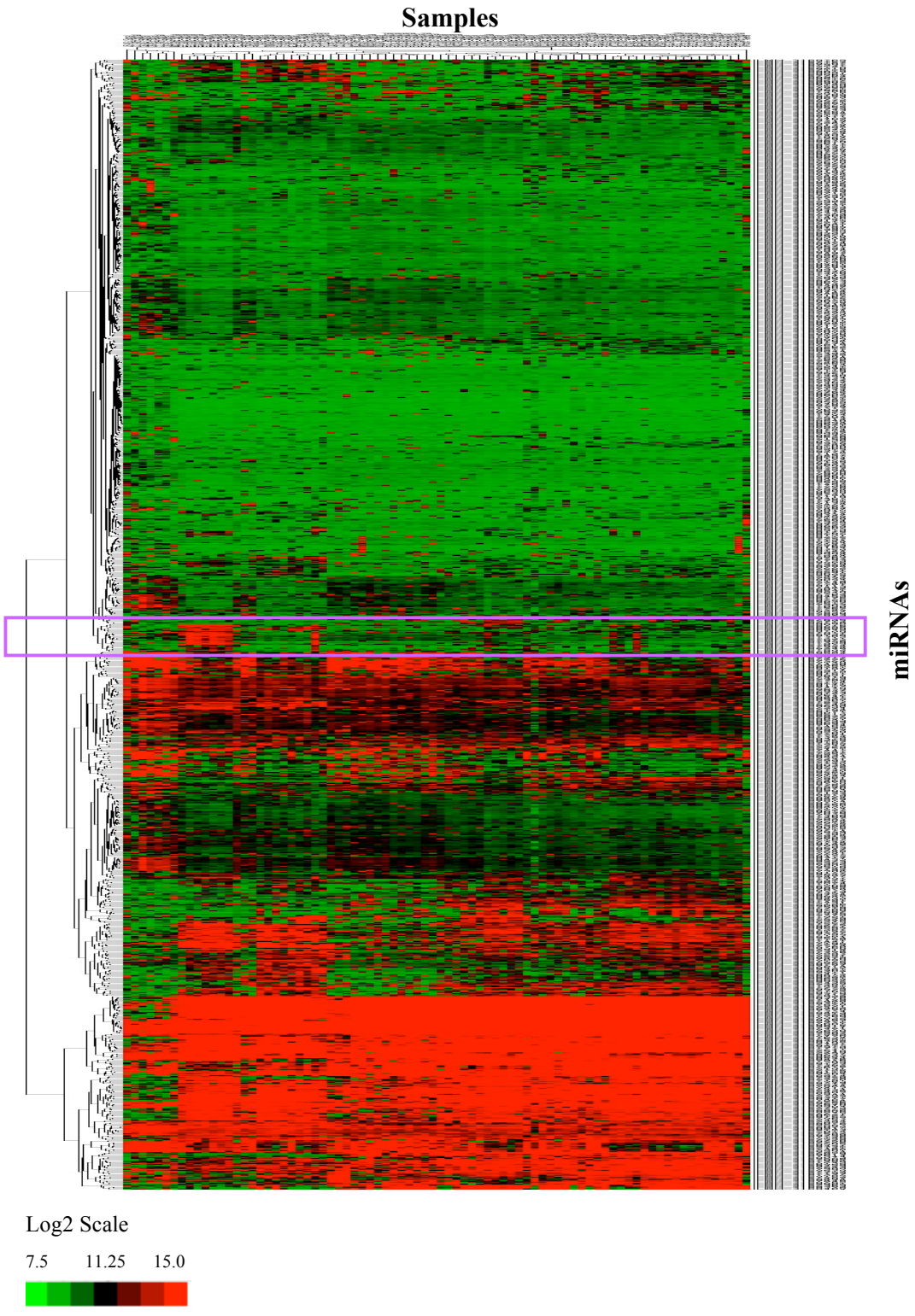

The clustering heatmap for all the microRNAs on all the samples on the microarray. Horizontal: Samples; Vertical: miRNAs. The purple square indicates the part of heatmap shown in Figure 3.5.

Appendix 3

(A) Comparison between primary melanoma and naevi

No	miR	Adjusted P	P value	Log_2 FC	Log_2 Average Intensity
1	solexa-2580-353	3.52E-13	4.08E-16	-2.67	8.51
2	solexa-8048-104	1.45E-12	4.51E-15	3.72	13.27
3	hsa-miR-603	1.45E-12	5.06E-15	2.79	11.71
4	solexa-2683-338	5.33E-12	2.47E-14	4.05	11.83
5	HS_29	9.76E-11	5.66E-13	3.86	12.90
6	hsa-miR-663b	7.04E-10	4.90E-12	3.43	12.22
7	hsa-miR-1826	8.69E-10	7.06E-12	2.23	13.60
8	hsa-miR-200b*	1.26E-09	1.17E-11	-3.52	9.32
9	hsa-miR-1308	1.69E-09	1.76E-11	0.81	14.56
10	solexa-578-1915	2.47E-09	3.10E-11	3.50	11.78
11	hsa-miR-183	2.47E-09	3.15E-11	-3.06	8.96
12	hsa-miR-149	5.13E-07	7.15E-09	-2.41	9.12
13	hsa-miR-200a	1.55E-06	2.34E-08	-2.79	9.52
14	hsa-miR-205	2.49E-06	4.05E-08	-2.44	11.34
15	HS_22.1	4.35E-06	7.57E-08	2.28	13.07
16	hsa-miR-675	4.87E-06	9.04E-08	3.06	11.11
17	hsa-miR-99a	6.97E-06	1.39E-07	-2.03	11.84
18	hsa-miR-200b	6.97E-06	1.46E-07	-3.04	11.83
19	HS_33	7.20E-06	1.59E-07	1.87	10.44
20	hsa-miR-455-5p	8.39E-06	1.95E-07	-2.45	9.60
21	HS_263.1	1.10E-05	2.68E-07	1.12	13.78
22	hsa-miR-182	1.76E-05	4.48E-07	-2.82	9.69
23	hsa-miR-203	2.91E-05	7.75E-07	-2.62	10.88
24	hsa-miR-494	4.99E-05	1.39E-06	2.91	11.36
25	hsa-miR-145	8.96E-05	2.60E-06	-0.91	13.85
26	HS_35	1.42E-04	4.27E-06	2.76	9.23
27	hsa-miR-455-3p	1.93E-04	6.03E-06	-2.13	12.51
28	hsa-miR-20b	2.55E-04	8.28E-06	2.43	11.16
29	hsa-miR-95	3.54E-04	1.19E-05	1.40	13.50
30	hsa-miR-888	3.97E-04	1.38E-05	-1.86	8.85
31	hsa-miR-891b	4.72E-04	1.70E-05	-1.34	8.12
32	hsa-miR-141	5.14E-04	1.91E-05	-2.16	10.03
33	hsa-miR-519e*	6.76E-04	2.59E-05	1.88	8.92
34	hsa-miR-198	7.98E-04	3.15E-05	2.45	9.09
35	hsa-miR-195	9.29E-04	3.77E-05	-1.80	12.92
36	hsa-miR-923	9.86E-04	4.16E-05	0.88	14.11
37	hsa-miR-224	9.86E-04	4.23E-05	-2.54	10.13
38	hsa-miR-378	1.02E-03	4.50E-05	-2.02	12.21
39	HS_43.1	1.30E-03	5.86E-05	1.09	8.92
40	hsa-miR-1285	1.32E-03	6.12E-05	2.65	12.37
41	hsa-miR-1273	1.41E-03	6.72E-05	2.89	11.67
42	HS_143	1.48E-03	7.21E-05	2.05	10.69
43	hsa-miR-154	1.98E-03	9.87E-05	-1.63	8.58
44	hsa-miR-200c	2.12E-03	1.08E-04	-1.41	13.04
45	hsa-miR-30c-1*	2.55E-03	1.33E-04	1.76	13.84
46	hsa-miR-876-3p	2.68E-03	1.43E-04	-1.90	9.48

47	solexa-3927-221	2.97E-03	1.62E-04	0.58	14.29
48	hsa-miR-139-5p	3.85E-03	2.14E-04	-1.79	10.41
49	hsa-miR-1274a	4.02E-03	2.34E-04	0.47	14.65
50	hsa-miR-429	4.02E-03	2.34E-04	-1.75	9.14
51	hsa-miR-1248	4.02E-03	2.38E-04	2.36	10.94
52	hsa-miR-497	4.65E-03	2.81E-04	-1.78	10.14
53	hsa-miR-29b-2*	5.05E-03	3.11E-04	-1.07	8.39
54	HS_78	5.06E-03	3.20E-04	0.99	9.33
55	HS_40	5.06E-03	3.29E-04	-0.87	9.59
56	hsa-miR-125b	5.06E-03	3.29E-04	-0.59	14.39
57	hsa-miR-885-5p	5.42E-03	3.58E-04	-1.07	8.25
58	hsa-miR-27b*	5.53E-03	3.72E-04	-1.18	9.94
59	hsa-miR-204	5.58E-03	3.82E-04	-1.52	11.18
60	HS_100	5.69E-03	3.96E-04	0.26	14.55
61	hsa-miR-140-3p	6.57E-03	4.69E-04	-1.19	12.83
62	hsa-miR-1300	6.57E-03	4.73E-04	1.51	9.77
63	hsa-miR-27a*	7.44E-03	5.44E-04	-1.09	9.41
64	hsa-miR-1249	8.38E-03	6.22E-04	-1.59	11.76
65	hsa-miR-431	8.51E-03	6.41E-04	-1.15	8.85
66	hsa-miR-1290	8.66E-03	6.63E-04	-1.82	10.12
67	hsa-miR-189:9.1	8.71E-03	6.77E-04	-1.14	10.82
68	hsa-miR-365	8.91E-03	7.03E-04	-1.15	11.23
69	solexa-2952-306	1.12E-02	9.02E-04	0.32	14.28
70	solexa-5620-151	1.12E-02	9.07E-04	1.67	9.22
71	hsa-miR-567	1.16E-02	9.67E-04	-0.52	8.39
72	solexa-826-1288	1.16E-02	9.72E-04	1.90	10.26
73	solexa-15-44487	1.34E-02	1.14E-03	0.92	10.32
74	solexa-8211-102	1.36E-02	1.17E-03	1.47	13.46
75	solexa-555-1991	1.37E-02	1.19E-03	0.74	13.34
76	hsa-miR-127-3p	1.84E-02	1.63E-03	-1.06	8.74
77	hsa-miR-639	1.84E-02	1.64E-03	1.38	8.60
78	hsa-miR-565:9.1	1.88E-02	1.70E-03	0.63	14.07
79	HS_112	2.16E-02	1.98E-03	1.03	8.29
80	hsa-miR-576-3p	2.19E-02	2.03E-03	1.12	9.11
81	HS_241.1	2.34E-02	2.20E-03	1.47	10.45
82	hsa-miR-125b-2*	2.38E-02	2.26E-03	-1.25	8.51
83	hsa-miR-199a*:9.1	2.43E-02	2.34E-03	-0.89	13.36
84	hsa-miR-9*	2.67E-02	2.60E-03	1.33	10.89
85	HS_126	2.82E-02	2.78E-03	0.96	8.61
86	hsa-miR-1228*	2.89E-02	2.89E-03	0.48	13.89
87	solexa-4793-177	3.15E-02	3.21E-03	1.16	12.26
88	hsa-miR-140-5p	3.15E-02	3.22E-03	-1.53	10.87
89	HS_186	3.21E-02	3.31E-03	-0.82	9.65
90	hsa-miR-25*	3.29E-02	3.43E-03	0.80	9.97
91	hsa-miR-9	3.59E-02	3.85E-03	1.87	10.76
92	hsa-miR-218	3.59E-02	3.85E-03	-1.49	10.61
93	hsa-miR-342-5p	3.59E-02	3.87E-03	-1.25	11.40
94	hsa-miR-591	3.86E-02	4.24E-03	0.81	9.49
95	HS_196.1	3.86E-02	4.26E-03	1.11	8.55
96	HS_188	4.15E-02	4.70E-03	1.42	10.95
97	hsa-miR-100	4.15E-02	4.71E-03	-0.86	13.64
98	hsa-miR-335	4.15E-02	4.72E-03	0.90	11.76
99	hsa-miR-196a*	4.29E-02	4.95E-03	0.83	8.34
100	hsa-miR-28-3p	4.29E-02	4.97E-03	-1.03	12.42

101	HS_31.1	4.40E-02	5.19E-03	1.05	9.40
102	hsa-miR-181a-2*	4.40E-02	5.20E-03	-1.44	10.97
103	hsa-miR-139-3p	4.60E-02	5.52E-03	-0.69	8.42
104	hsa-miR-744*	4.60E-02	5.55E-03	-0.36	8.34
105	hsa-miR-921	4.91E-02	6.10E-03	-0.73	8.46
106	hsa-miR-875-5p	4.91E-02	6.11E-03	-0.56	8.87
107	hsa-miR-664	4.91E-02	6.11E-03	0.65	13.49
108	hsa-miR-767-5p	4.91E-02	6.19E-03	1.21	10.43
109	HS_116	4.91E-02	6.30E-03	1.66	10.65
111	hsa-miR-147b	4.91E-02	6.33E-03	-0.99	9.06
112	hsa-miR-335*	4.91E-02	6.35E-03	-1.13	8.90
113	hsa-miR-873	4.91E-02	6.40E-03	-1.31	9.33

(B) Comparison between metastatic melanoma and naevi

No	**miR**	**Adjusted P**	**P value**	**Log_2 FC**	**Log_2 Average Intensity**
1	hsa-miR-205	3.88E-16	4.50E-19	-5.23	11.34
2	solexa-2580-353	8.42E-16	1.95E-18	-3.03	8.51
3	hsa-miR-203	2.06E-15	7.18E-18	-6.00	10.88
4	hsa-miR-183	6.41E-11	2.98E-13	-3.52	8.96
5	solexa-2683-338	1.19E-10	6.93E-13	3.65	11.83
6	hsa-miR-200b*	1.27E-10	9.28E-13	-3.78	9.32
7	hsa-miR-200c	1.27E-10	1.03E-12	-3.13	13.04
8	hsa-miR-603	1.26E-09	1.17E-11	2.20	11.71
9	solexa-8048-104	4.64E-09	4.85E-11	2.78	13.27
10	hsa-miR-1308	2.38E-08	2.76E-10	0.73	14.56
11	hsa-miR-200b	8.86E-08	1.14E-09	-3.67	11.83
12	hsa-miR-200a	8.86E-08	1.23E-09	-3.11	9.52
13	hsa-miR-663b	9.07E-08	1.37E-09	2.81	12.22
14	HS_29	1.03E-07	1.67E-09	2.93	12.90
15	solexa-578-1915	4.56E-07	7.94E-09	2.84	11.78
16	hsa-miR-1826	6.26E-07	1.16E-08	1.70	13.60
17	hsa-miR-141	2.24E-06	4.42E-08	-2.92	10.03
18	hsa-miR-149	4.38E-06	9.14E-08	-2.15	9.12
19	solexa-555-1991	9.09E-06	2.00E-07	1.28	13.34
20	hsa-miR-95	9.86E-06	2.29E-07	1.71	13.50
21	hsa-miR-429	1.91E-05	4.66E-07	-2.53	9.14
22	hsa-miR-21*	2.42E-05	6.17E-07	2.12	9.86
23	hsa-miR-224	3.06E-05	8.23E-07	-3.16	10.13
24	hsa-miR-182	3.06E-05	8.52E-07	-2.71	9.69
25	hsa-miR-142-5p	1.02E-04	2.96E-06	2.26	9.50
26	hsa-miR-923	2.11E-04	6.36E-06	0.98	14.11
27	hsa-miR-20b	2.26E-04	7.09E-06	2.43	11.16
28	hsa-miR-675	2.90E-04	9.43E-06	2.40	11.11
29	hsa-miR-891b	4.47E-04	1.54E-05	-1.33	8.12
30	hsa-miR-888	4.47E-04	1.56E-05	-1.83	8.85
31	hsa-miR-9	5.51E-04	1.98E-05	2.88	10.76
32	hsa-miR-455-5p	6.04E-04	2.24E-05	-1.89	9.60
33	hsa-let-7c	8.37E-04	3.21E-05	-0.90	13.81
34	hsa-miR-9*	1.02E-03	4.00E-05	1.88	10.89
35	hsa-miR-155	1.02E-03	4.14E-05	1.31	13.28

36	HS_100	1.46E-03	6.21E-05	0.29	14.55
37	hsa-miR-455-3p	1.46E-03	6.44E-05	-1.82	12.51
38	hsa-miR-873	1.46E-03	6.46E-05	-1.99	9.33
39	hsa-miR-876-3p	1.57E-03	7.12E-05	-1.98	9.48
40	hsa-miR-139-5p	1.92E-03	8.90E-05	-1.89	10.41
41	hsa-miR-548d-5p	2.01E-03	9.58E-05	-1.08	9.71
42	hsa-miR-1300	2.29E-03	1.12E-04	1.67	9.77
43	hsa-miR-204	2.58E-03	1.29E-04	-1.64	11.18
44	HS_264.1	2.85E-03	1.45E-04	0.76	8.56
45	hsa-miR-567	3.21E-03	1.67E-04	-0.60	8.39
46	solexa-3927-221	3.42E-03	1.82E-04	0.57	14.29
47	hsa-miR-1274a	3.45E-03	1.89E-04	0.47	14.65
48	hsa-miR-365	3.45E-03	1.92E-04	-1.27	11.23
49	hsa-miR-1321	4.05E-03	2.30E-04	0.45	8.41
50	HS_108.1	4.26E-03	2.47E-04	-2.18	11.17
51	hsa-miR-1248	4.67E-03	2.77E-04	2.32	10.94
52	solexa-826-1288	4.71E-03	2.84E-04	2.09	10.26
53	hsa-miR-193b	4.96E-03	3.05E-04	-1.62	12.93
54	solexa-15-44487	6.83E-03	4.28E-04	1.00	10.32
55	HS_33	7.55E-03	4.87E-04	1.14	10.44
56	HS_114	7.55E-03	4.90E-04	-0.62	8.94
57	hsa-miR-1290	8.11E-03	5.51E-04	-1.84	10.12
58	hsa-miR-142-3p	8.11E-03	5.52E-04	1.55	12.74
59	hsa-miR-508-3p	8.11E-03	5.55E-04	-2.56	12.66
60	hsa-miR-99a	8.14E-03	5.67E-04	-1.21	11.84
61	hsa-miR-10a*	8.14E-03	5.76E-04	1.32	10.40
62	hsa-miR-211	8.75E-03	6.29E-04	-2.37	12.93
63	hsa-miR-23b*	9.27E-03	6.77E-04	-1.40	8.93
64	HS_75.1	9.70E-03	7.20E-04	-1.07	8.69
65	hsa-miR-767-5p	9.91E-03	7.47E-04	1.51	10.43
66	HS_93	1.02E-02	7.84E-04	0.77	8.81
67	HS_43.1	1.02E-02	7.94E-04	0.88	8.92
68	HS_78	1.02E-02	8.07E-04	0.91	9.33
69	hsa-miR-449a	1.02E-02	8.20E-04	-1.69	8.93
70	hsa-miR-513:9.1	1.16E-02	9.46E-04	-2.10	9.97
71	hsa-miR-509-3p	1.24E-02	1.02E-03	-2.31	13.39
72	hsa-miR-27a*	1.24E-02	1.04E-03	-1.02	9.41
73	HS_194	1.25E-02	1.06E-03	-1.00	8.20
74	hsa-miR-154	1.30E-02	1.12E-03	-1.32	8.58
75	hsa-miR-506	1.32E-02	1.15E-03	-2.39	12.17
76	hsa-miR-542-3p	1.37E-02	1.21E-03	1.12	9.52
77	hsa-miR-137	1.38E-02	1.23E-03	0.95	10.32
78	HS_263.1	1.39E-02	1.26E-03	0.64	13.78
79	hsa-miR-618	1.41E-02	1.29E-03	0.76	9.33
80	HS_40	1.46E-02	1.35E-03	-0.76	9.59
81	HS_22.1	1.57E-02	1.47E-03	1.21	13.07
82	hsa-miR-146b-3p	1.62E-02	1.54E-03	0.50	8.71
83	hsa-miR-105	1.63E-02	1.57E-03	1.14	10.81
84	hsa-miR-189:9.1	1.70E-02	1.66E-03	-1.04	10.82
85	hsa-miR-513a-5p	1.95E-02	1.92E-03	-1.55	11.46
86	hsa-miR-196a	2.03E-02	2.03E-03	1.43	13.41
87	hsa-miR-1249	2.11E-02	2.14E-03	-1.40	11.76
88	hsa-miR-27b	2.11E-02	2.16E-03	-0.86	13.49
89	hsa-miR-664	2.79E-02	2.88E-03	0.71	13.49
90	hsa-miR-885-5p	3.13E-02	3.28E-03	-0.86	8.25

91	hsa-miR-1202	3.13E-02	3.31E-03	0.44	8.40
92	HS_241.1	3.24E-02	3.46E-03	1.39	10.45
93	hsa-miR-16-1*	3.38E-02	3.65E-03	0.83	10.12
94	hsa-miR-801:9.1	3.81E-02	4.15E-03	0.70	8.69
95	hsa-miR-513c	4.08E-02	4.50E-03	-1.58	9.62
96	hsa-miR-199a*:9.1	4.17E-02	4.64E-03	-0.81	13.36
97	hsa-miR-147b	4.94E-02	5.56E-03	-0.99	9.06

(C) Comparison between metastatic and primary melanoma

No	**miR**	**Adjusted P**	**P value**	**Log_2 FC**	**Log_2 Average Intensity**
1	hsa-miR-205	4.42E-09	6.64E-12	-2.79	11.34
2	hsa-miR-203	4.42E-09	1.03E-11	-3.38	10.88
3	hsa-miR-145	4.16E-06	1.45E-08	0.97	13.85
4	hsa-miR-200c	2.71E-05	1.26E-07	-1.72	13.04
5	hsa-miR-142-5p	7.14E-04	4.14E-06	1.86	9.50
6	hsa-miR-519e*	2.11E-03	1.47E-05	-1.62	8.92
7	hsa-miR-198	5.06E-03	4.11E-05	-2.00	9.09
8	hsa-miR-21*	1.22E-02	1.19E-04	1.30	9.86
9	hsa-miR-452	1.22E-02	1.27E-04	-1.24	9.52
10	hsa-miR-1296	1.96E-02	2.28E-04	1.77	9.60
11	hsa-miR-509-3p	2.11E-02	2.76E-04	-2.17	13.39
12	hsa-miR-150	2.11E-02	3.10E-04	1.01	14.05
13	hsa-miR-19a	2.11E-02	3.19E-04	1.41	10.40
14	hsa-miR-22	3.42E-02	5.55E-04	0.74	12.69
15	hsa-miR-506	4.46E-02	7.76E-04	-2.09	12.17
16	hsa-miR-542-5p	4.49E-02	8.77E-04	1.53	9.70
17	HS_22.1	4.49E-02	8.95E-04	-1.07	13.07
18	HS_143	4.49E-02	9.39E-04	-1.39	10.69
19	hsa-miR-558	4.79E-02	1.15E-03	1.31	9.80
20	hsa-miR-29c	4.79E-02	1.22E-03	1.14	13.03
21	hsa-miR-28-3p	4.79E-02	1.27E-03	0.99	12.42
22	HS_132.1	4.79E-02	1.32E-03	-1.28	9.60
23	hsa-miR-514	4.79E-02	1.32E-03	-2.47	12.60
24	hsa-miR-494	4.79E-02	1.33E-03	-1.51	11.36
25	hsa-miR-140-3p	4.79E-02	1.39E-03	0.89	12.83

Differentially expressed miRNAs in three comparisons. The three tables list all the differentially expressed miRNAs: (A) Primary melanoma versus naevi; (B) Metastatic melanoma versus naevi; (C) Metastatic versus primary melanoma. P value: from t-test. Adjusted P: adjusted P value is the way to correct for multiple testing. Log_2 FC: Log_2 Fold Changes (In X vs. Y comparison, when Y>X, log_2 FC is negative, when Y<X, log_2 FC is positive. Average Intensity: stands for the average signal intensity of all samples on the array for the particular miRNA.

Appendix 4

(A)

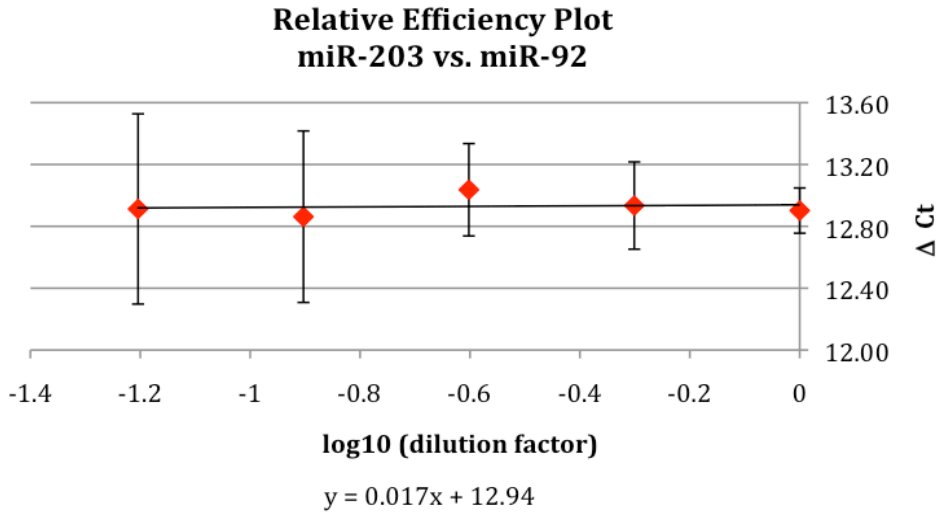

(B)

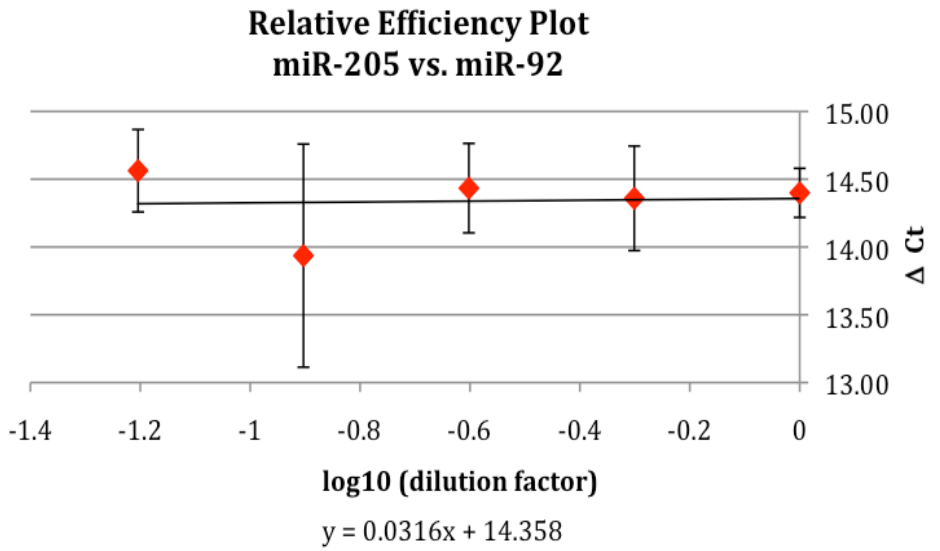

(C)

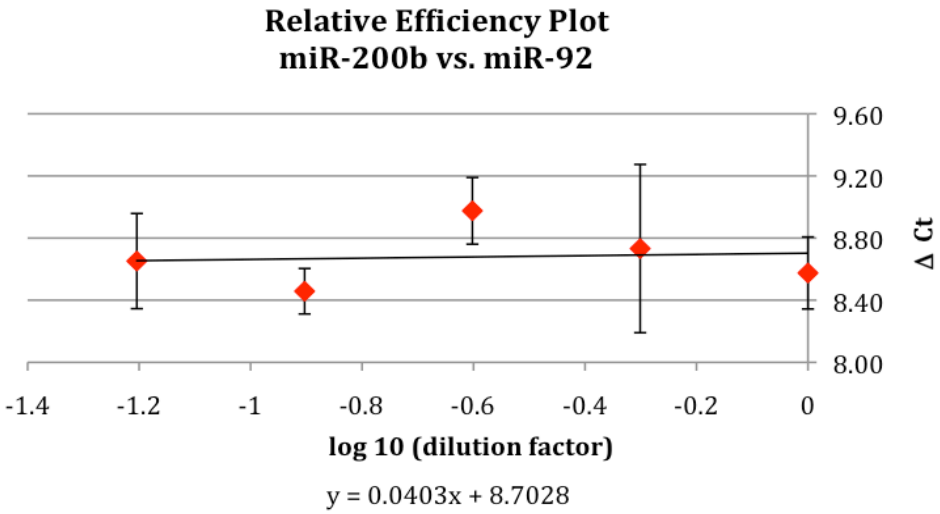
Relative Efficiency Plot
miR-200b vs. miR-92
9.60
9.20
8.80
8.40
8.00
Δ Ct
-1.4
-1.2
-1
-0.8
-0.6
-0.4
-0.2
0
log 10 (dilution factor)
y = 0.0403x + 8.7028

(D)

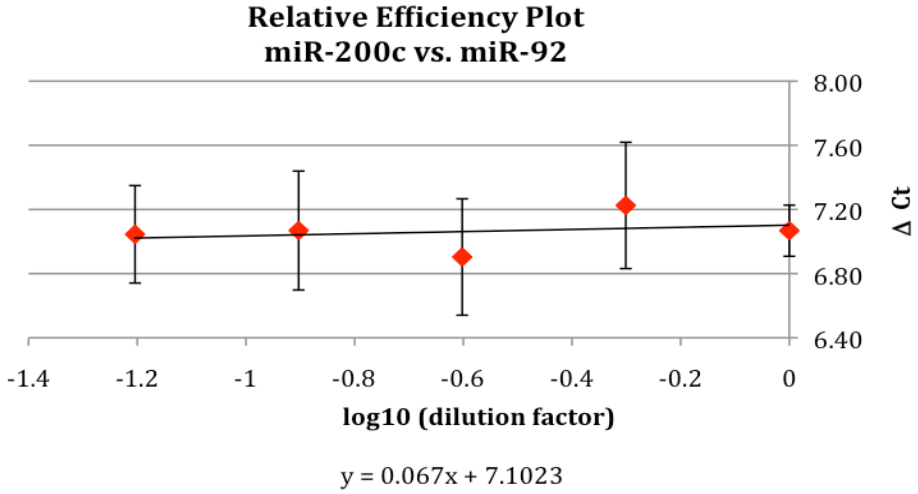
Relative Efficiency Plot
miR-200c vs. miR-92
8.00
7.60
7.20
6.80
6.40
Δ Ct
-1.4
-1.2
-1
-0.8
-0.6
-0.4
-0.2
0
log10 (dilution factor)
y = 0.067x + 7.1023

(E)

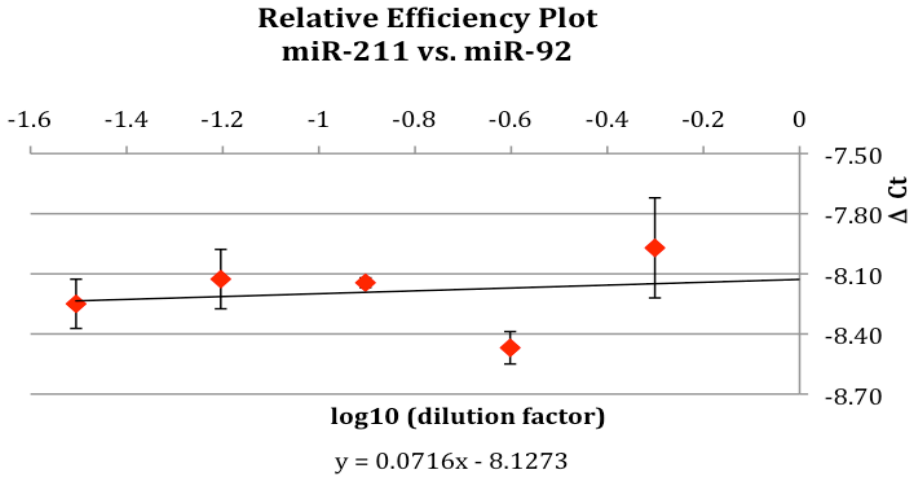
Relative Efficiency Plot
miR-211 vs. miR-92
-1.6
-1.4
-1.2
-1
-0.8
-0.6
-0.4
-0.2
0
-7.50
-7.80
-8.10
-8.40
-8.70
Δ Ct
log10 (dilution factor)
y = 0.0716x - 8.1273

(F)

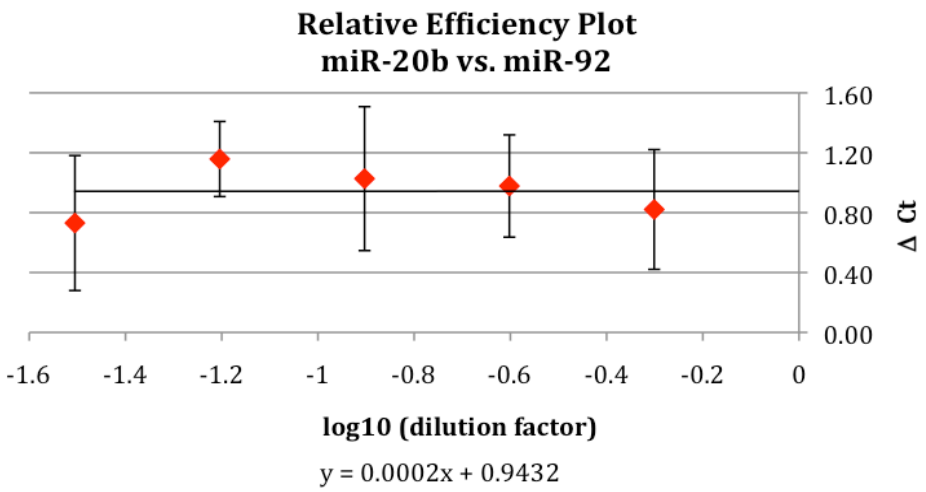

(G)

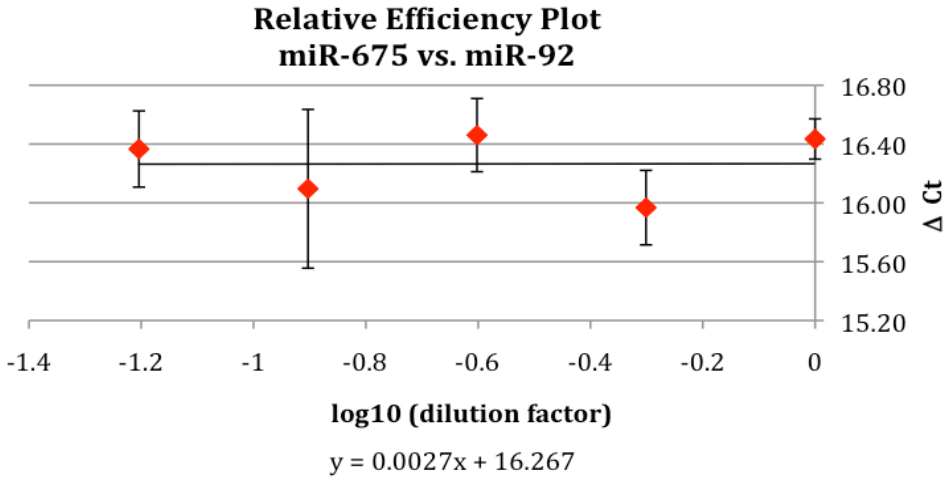

Validation of ΔΔCt method for miRNA expression relative to miR-92 as endogenous control. Relative efficiency plots: (A) miR-203 vs. miR-92; (B) miR-205 vs. miR-92; (C) miR-200b vs. miR-92; (D) miR-200c vs. miR-92; (E) miR-211 vs. miR-92; (F) miR-20b vs. miR-92; (G) miR-675 vs. miR-92. Using the ΔΔCt method for quantification, a validation experiment was performed on RNA extracted from either A375 or HER1 to demonstrate that the PCR efficiencies of target and reference were approximately equal. The approach is considered valid if the absolute value of the slope of log (dilution factor) vs. ΔCt is <0.1. The slopes obtained for each miRNA indicate that the method used to quantify and compare miRNA expression relative to the miR-92 control is valid. X-axis: log10 of dilution factor, Y-axis: value of ΔCt ± STDEV. The standard deviation (STDEV) of the quotient here is calculated from the standard deviations of target miRNA values and internal control miR-92 values using the following formula: $STDEV_C = \sqrt{STDEV_T{}^2 + STDEV_R{}^2}$ (C: Comparative Method, T: Target, R: Reference) [316].

Appendix 5

(A)

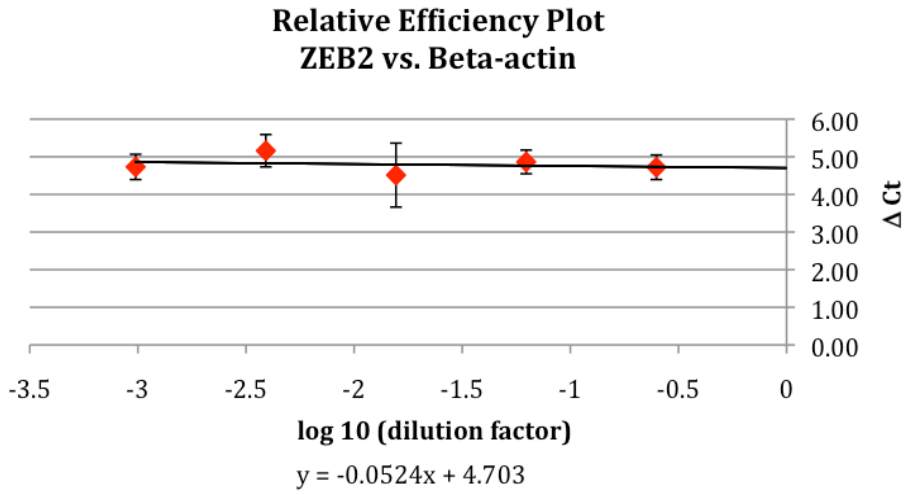

(B)

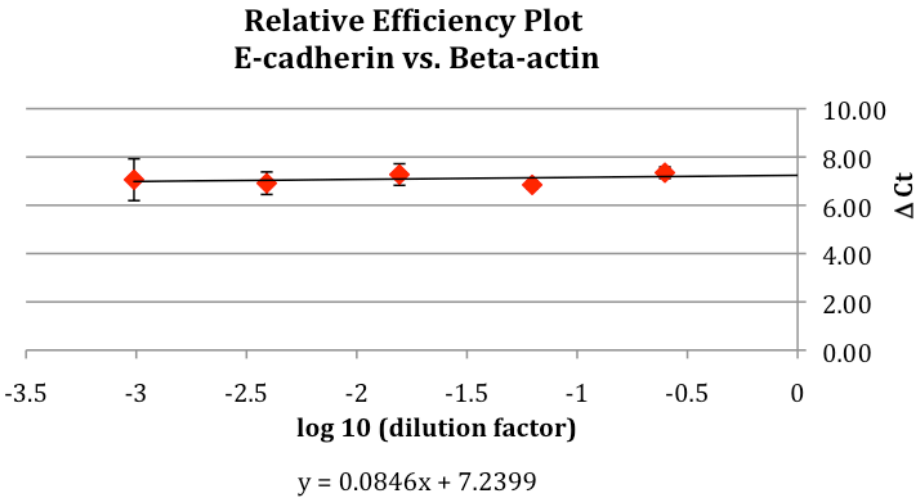

(C)

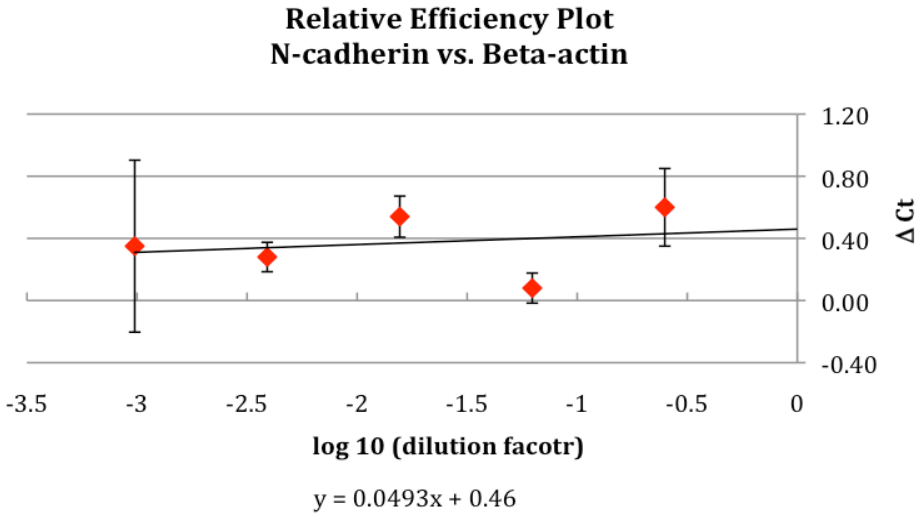

Validation of the ΔΔCt method for mRNA expression relative to beta-actin. Relative efficiency plots: (A) ZEB2 vs. Beta-actin; (B) E-cadherin vs. Beta-actin and (C) N-cadherin vs. Beta-actin. Using the ΔΔCt method for quantification, a validation experiment was performed on RNA extracted from A375 melanoma cells to demonstrate that the PCR efficiencies of target and reference were approximately equal. The approach is considered valid if the absolute value of the slope of log10 (dilution factor) vs. ΔCt is <0.1. X-axis: log10 of dilution factor, Y-axis: value of ΔCt ± STDEV. The STDEV of the quotient here is calculated from the standard deviations of mRNA values and internal control beta-actin values using the following formula: $STDEV_C = \sqrt{STDEV_T^2 + STDEV_R^2}$ (C: Comparative Method, T: Target, R: Reference) [316].